IDENTIFYING THE SYMMETRY CLASS AND DETERMINING THE CLOSEST SYMMETRY CLASS OF AN ELASTICITY TENSOR

CAĞRI DINER


CENTRE FOR NFLD. STUDIES
MEMORIAL UNIVERSITY
OF NEWFOUNDLAND

IDENTIFYING THE SYMMETRY CLASS AND DETERMINING THE CLOSEST SYMMETRY CLASS OF AN ELASTICITY TENSOR

by

Çağrı Diner

A Thesis Submitted to the School of
Graduate Studies in partial fulfillment of
the requirement for the degree of
Doctor of Philosophy

Department of Earth Sciences
Memorial University of Newfoundland

May 2009

St. John's Newfoundland

Abstract

In this thesis, two main problems are solved and then applied to a geophysical problem. First, we identify the symmetry class of an elasticity tensor, if it exhibits a symmetry. Second, if the tensor is generally anisotropic, we find the closest symmetric elasticity tensor of a given class among all possible orientations of the coordinate systems. Using these results, we suggest a method to find the symmetry class that is the "best" choice to represent the given anisotropic elasticity tensor.

For an application of these methods and results, we investigate the closest symmetry class of a medium that is obtained by combining two differently oriented planar structures. More precisely, we combine two transversely isotropic (TI) media that may correspond to layering and cracks in a subsurface, and whose rotation axes are neither parallel nor perpendicular to each other. Then, we find the closest symmetry class of the combined medium as the angle varies between their orientations. We give several examples for the case of two TI media where the angle between their rotation axes are small ($< 15°$), intermediate ($40° - 65°$) and large ($> 75°$). We see that if the angle is large enough ($> 75°$), then the combination can be approximated as an orthotropic medium. If the angle is small ($< 15°$) then the resultant medium is close to TI symmetry. However, intermediate angles between the structures may or may not give the symmetry of the combined medium close to a higher symmetry class than monoclinic.

Moreover, we investigate the velocities of the waves propagating in a combined

medium that has more than one planar structure. We find that the fastest velocity direction of the waves is not aligned with any of the orientations of the TI media that composes the medium.

To measure closeness in the space of elasticity tensors, we use the Euclidean norm for defining a distance function. The nonlinearity and existence of several extrema makes it difficult to find the absolute minimum of the distance function among all coordinate systems. Fortunately, in the case of monoclinic and TI symmetry, the parameters of the distance function reduce to two; there are three for other symmetry classes. Thus, one can plot the monoclinic- and TI-distance functions on the surface of the two-dimensional sphere.

We prove that the symmetry of the elasticity tensor is also a symmetry of the monoclinic-distance function and vice versa. Furthermore, we show that the monoclinic-distance function vanishes along the normals of the mirror planes of the medium. Therefore, by observing the plot one can infer the symmetry of a given elasticity tensor. The plot also allows us to guide a search for finding the absolute minimum of the monoclinic-distance function.

We prove that the value of the orthotropic-distance function for any coordinate system is half of the value of the sum of monoclinic-distance functions along particular directions. These directions correspond to three mutually perpendicular vectors that are the normals of the mirror planes of orthotropic symmetry. This relation allows us to use the plot of the monoclinic-distance function to determine the closest orthotropic elasticity tensor.

Furthermore, we present examples of other symmetry classes, namely trigonal, tetragonal and cubic. We see that the orientations of the closest tetragonal, trigonal and cubic elasticity tensors are either the same as, or as close as 1°, to the orientation of the minimum of the sum of monoclinic-distance functions along some particular directions. These particular directions are aligned with the normals of the

mirror planes of the corresponding symmetry class. Thus, one can use the plot of the monoclinic-distance function to infer about the closeness to any symmetry class.

Acknowledgements

First and foremost, I would like to express my gratitude to my supervisor, Dr. Michael Slawinski, for giving me the opportunity and motivation to undertake this work. Dr. Slawinski's perpetual energy, enthusiasm, guidance and encouragement during this research were a beneficial contribution to this thesis. I also appreciate Dr. Slawinski's confidence and the responsibility granted to me throughout this work.

I wish to express my warm and sincere thanks to my former cosupervisors, Dr. Andrej Bóna and Dr. Nelu Bucataru, for their theoretical advice and sharing their experience. I would like to thank Dr. Mikhail Kochetov for our discussions and for sharing his insightful comments.

I am grateful to Dr. Jeremy Hall and Dr. Tom Calon for providing their valuable time and expert opinions. I would like to thank them for answering my endless questions with patience. Our various meetings and courses have given me invaluable geological insights.

Very special thanks go to my friend, David Dalton, for editing and discussing every part of this thesis during our regular meetings. His help, support, interest, valuable discussions and suggestions played a key role in writing this thesis. I would also like to thank Leslie McNab for her help in editing the thesis.

I also want to thank Rob, Oktay, Canan, Ron, Chris, Burcu, Bursin and Bora Abi for their friendship during my years in St. John's. Many thanks to my family and my wife, Öznur, for her continued support and love.

List of Figures

Nomenclature

$\bar{A}$	rotation in 6D, namely $\bar{A} \in SO(6)$
$\bar{X}$	rotation in 6D with unknown variables
ϵ_{ij}	strain tensor
$\mathbf{e_1}$	unit vector in the direction of x-axis, namely $\mathbf{e_1} = (1, 0, 0)$
$\mathbf{e_2}$	unit vector in the direction of y-axis, namely $\mathbf{e_2} = (0, 1, 0)$
$\mathbf{e_3}$	unit vector in the direction of z-axis, namely $\mathbf{e_3} = (0, 0, 1)$
$\mathcal{L}^{sym}$	the set of all elasticity matrices which are represented in their natural coordinate axes and belonging to the symmetry class denoted by sym
σ_{ij}	stress tensor
A	rotation in 3D, namely $A \in SO(3)$
C	elasticity tensor represented by a 6×6 matrix
C^{sym}	the projection of C onto $\mathcal{L}^{sym}$
c_{ijkl}	elasticity tensor in 3D
$d(\bar{X}^T C \bar{X}, \mathcal{L}^{sym})$	distance function of C to $\mathcal{L}^{sym}$ in all coordinate systems

$d(C, \mathcal{L}^{sym})$ distance function of C to $\mathcal{L}^{sym}$ in the coordinate system where C is expressed in

G_C the symmetry group of elasticity matrix C

I identity element in the set of orthogonal transformations in 3D

$M_{\mathbf{v}}$ reflection transformation around a plane whose normal is the vector $\mathbf{v}$

$O(3)$ the set of orthogonal transformations in 3D

$R_{\theta,\mathbf{v}}$ rotation transformation around the vector $\mathbf{v}$ by θ degrees.

$SO(3)$ the set of rotations, which is a subgroup of $O(3)$ in 3D

TI transversely isotropic symmetry class

X rotation in 3D with unknown variables

Contents

Chapter 1

Introduction

The branch of mechanics in which materials are treated as continuous is known as continuum mechanics. In this theory a body, or a medium, is composed of infinitesimal volumes that are referred to as material points. While studying a material's response to seismic waves, we use the continuum mechanics approach. According to this approach a medium is composed of sufficiently closely spaced material points so that its descriptive functions, such as position, displacement, velocity or temperature can be considered as continuous. In other words, we choose to disregard the atomic structure of matter and the explicit interactions among the atoms; this approximation simplifies the mathematical description of the medium and the motion within it.

Elastic behavior, or a response of a material to stress that may be caused by wave propagation, is described by its elasticity tensor, under the assumption that deformation is small and the material returns to its original position after the stress is removed.

The main focus of this thesis is on the symmetries of the elasticity tensor that characterizes a given material. Since the elasticity tensor finds applications in different branches of physics, geophysics, mineralogy and engineering, the methods described in the thesis can be used in many applications regardless of the way that the tensor

is obtained. Within earth sciences, the elasticity tensor can represent a subsurface region of Earth studied seismically. It can also represent a crustal or a mantle rock or a mineral. Symmetry of a medium provides information about its structure, and its elasticity tensor allows us to obtain quantitative description for studying the symmetry.

In this chapter, we first introduce previous work done on identifying the symmetry of an elasticity tensor and on determining the closest tensor belonging to a particular symmetry class. Then, we give basic tensor notations that are used throughout the text. Finally, we present the eight symmetry classes of elasticity tensors by introducing the symmetry group of each class and the form of the elasticity matrix when both are introduced in their natural coordinate systems.

1.1 Literature Review

Identifying the symmetry classes of elastic media is studied by many researchers, such as Lord Kelvin [34], Love [35], Voigt [47], Fedorov [19], Backus [4], Rychlewski [42], Walpole [48], Cowin and Mehrabadi [13], Sutcliffe [45], Slawinski et al. [8, 9], Helbig [26], Forte and Vianello [20] and Chadwick et al. [12]. In practice, it is important to identify the symmetry class of a given medium because its symmetries and orientations are generally not known before the experiment takes place.

There are several ways to solve the problem of identifying the symmetry class of the medium and the orientation of its symmetry axes. The harmonic decomposition of an elasticity tensor is one of the methods. The necessary coordinate-free conditions in using this method are discussed by Backus [4], Boehler [6], Forte and Vianello [21], Baerheim [5] and Rychlewski [43]. The two associated second-rank tensors, namely dilatation and Voigt tensors, are also used for finding these conditions. This approach is used by Cowin and Mehrabadi [13], Helbig [26], Chadwick et al. [12] and Bóna et

al. [9].

Studying the eigensystems of a given elasticity tensor is another approach for identifying its symmetry class. This approach was used by Fedorov [19], Walpole [48], Rychlewski [13], Cowin and Mehrabadi [36], Sutcliffe [45], Helbig [26], and Yang et al. [49]. These authors find the necessary conditions for identifying the symmetry class of an elasticity tensor by considering the eigenvalues and eigenspaces of the dilatation and Voigt tensors. Thus, their method is coordinate independent. Rychlewski [41] provides sufficient conditions to check whether or not an elasticity tensor belongs to the transversely isotropic class, given that the rotation axis is known. Cowin and Mehrabadi [36] discuss the monoclinic symmetry in a coordinate-independent way. Sutcliffe [45] focuses on the spectral decomposition of elasticity tensors for all symmetry classes. Yang et al. [49] identify the symmetry classes of an elastic materials by considering numerical examples. Bóna et al. [8] follow the eigensystem approach to formulate both the necessary and sufficient coordinate-free conditions for identifying the symmetry class of a given elasticity tensor and to find the symmetry axes of the medium.

In this thesis, we use a new approach for identifying the symmetry of a medium. We plot the distance function of an elasticity tensor to the monoclinic symmetry class and determine its symmetry by observing the plot. We also find the orientations of the normal of the symmetry planes of the medium. There are several advantages to this method. First, the computations are more straightforward, as compared to other methods. Since calculations are guided by the plot, they are easier to follow and check. Prior to this work, there had been no computer programme to identify symmetries of a medium by tensor-algebra method mentioned above. Thus, we provide for the first time a complete algorithm for calculating the symmetry class of a given set of elastic moduli.

The second advantage of the visualizing method is that it may suggest to which

symmetry class a given elasticity tensor is the closest. If an elasticity tensor is obtained without an a priori assumption of any symmetry, then it is evaluated as generally anisotropic. Hence, it becomes important to ask about the closeness, rather than belonging, to a particular symmetry class.

The third chapter is a continuation of the work of Cowin, Gazis et al., Fedorov, Moakher et.al., Norris et.al., Slawinski et.al. and Voigt [14, 23, 19, 38, 37, 32, 33, 47]. These researchers have examined the notion of an effective tensor and distance in the space of elasticity tensors. In general, the problem is solved if the projection is restricted to one coordinate system. However, in applications, it is more desirable to find the orientation of the coordinate system that gives the closest tensor, which is the "effective" tensor of a given symmetry class. For all symmetry classes except TI and monoclinic, searching for the best orientation is a nonlinear minimization problem in a three-dimensional manifold. This problem can be reduced to a two-dimensional minimization problem for monoclinic and TI symmetries. Reducing by one parameter allows us to plot the distance function. In this way, one can use the plot of distance function to guide the search for the minimum. Slawinski et al. [32, 33] used a similar method; namely, using the plot of the distance functions, for solving the orientation of the closest TI and monoclinic tensors. Then, they suggest an orientation to search for the minimum of orthotropic-distance function by considering the plot of TI- and monoclinic-distance functions. The authors state that their method works for the elasticity tensors that are close to orthotropic symmetry. In this thesis, we introduce a theorem that states a relation between an orthotropic-distance function and sum of monoclinic-distance functions for three perpendicular directions. Thus, the theorem shows where to achieve the minimum of orthotropic-distance function by considering its monoclinic plot whether the given tensor is close or not close to the orthotropic symmetry. Then, we generalize this approach for finding the minimum of other distance functions, namely trigonal-, tetragonal- and cubic-distance functions.

Dellinger [17] suggests a discrete search algorithm for finding the minimum of transversely isotropic-distance function among all coordinate system. The author admits that the result is not guaranteed to be the absolute minimum. Kochetov and Slawinski [32] formulated the minimization problem in terms of polynomial functions on the unit sphere in the three-dimensional space. With this, they plot the transversely isotropic and monoclinic-distance functions and examine the local extrema on the projected sphere. However, their formulation permits finding the orientation of the closest orthotropic elasticity tensor if the given anisotropic tensor is close to orthotropic symmetry.

Arts et al. [2] use the transversely isotropic and monoclinic symmetries to search for the orientation of the closest orthotropic tensor. However, they are not using a distance function; instead they consider the average of the closest eigenvectors of the dilatation and Voigt tensors as the x_3-axis that describes the orientation of the orthotropic approximation of an elasticity tensor. In general, the orientation they find does not give the minimum of the distance between the elasticity tensor and its orthotropic approximation. Kochetov and Slawinski [33] propose to use the mirror-plane normal of the closest monoclinic tensor or the rotation-symmetry axis of the closest transversely isotropic tensor as an initial guess for the search of the closest orthotropic tensor. They also prove that if an elasticity tensor is a small perturbation of an orthotropic one, then the mirror plane normal of the closest monoclinic tensor is in a neighbourhood of one of the axes of the closest orthotropic tensor.

1.2 Tensor Notation

In continuum mechanics, a seismic wave is assumed to propagate in a continuous medium which is called a **continuum**. A continuum is formulated mathematically in terms of continuous functions representing the average properties of many microscopic

objects forming the actual material. In this context, all the associated quantities become scalar, vector or tensor [44]. Examples of these physical quantities are the stress tensor, which is used for describing the state of stress in the medium; the strain tensor, which is a measure of deformation occuring during the passage of a seismic wave; the elasticity tensor, which describes the elastic response of the medium; and the wave vector, which indicates the direction of the wave propagating in the continuum. In fact, scalars and vectors can be regarded as zero- and first-rank tensors, respectively. Thus, we begin the thesis by defining and introducing the basic properties of a tensor which is the mathematical structure of the concepts listed above. The notation of the tensors introduced in this section will be used throughout the text.

Definition 1 *An n-th rank tensor in Euclidean space of dimension d is a collection of real numbers*

$$T_{i_1 i_2 \ldots i_n}, \text{ where } i_1 \ldots i_n \in \{1, 2, .., d\},$$

assigned to each orthonormal coordinate system. The collections of numbers representing the same tensor in different coordinate systems are related as follows:

$$T'_{i_1 i_2 \ldots i_n} = \sum_{j_1 \ldots j_n}^{d} T_{j_1 \ldots j_n} A_{j_1 i_1} \ldots A_{j_n i_n}, \tag{1.1}$$

where A is any orthogonal transformation that transforms a coordinate system to another one and $T'_{i_1 i_2 \ldots i_n}$ is the tensor represented in the transformed coordinate system.

Now, we introduce the summation convention, i.e., whenever an index is repeated, it is a dummy index indicating a summation running through the integral numbers $1, 2, ..., d$. This convention is known as **Einstein's summation convention**. Thus, we can write Equation 1.1 by using Einstein's summation convention as

$$T'_{i_1 i_2 \ldots i_n} = T_{j_1 \ldots j_n} A_{j_1 i_1} \ldots A_{j_n i_n}.$$

From now on, whenever an index is repeated in one side of the equation, it should imply that Einstein's summation convention is used. In this thesis, we shall always

let $d = 3$.

A second-rank tensor can be regarded as a linear transformation on the space of vectors. Let T be a transformation map, which transforms any vector in 3D to another vector in 3D. If T transforms $\mathbf{a_1}$ into $\mathbf{b_1}$, then we write

$$T(\mathbf{a_1}) = \mathbf{b_1}.$$

If T has the following properties, called linear properties,

$$\begin{aligned} T(\mathbf{a_1} + \mathbf{a_2}) &= T(\mathbf{a_1}) + T(\mathbf{a_2}), \\ T(\alpha \mathbf{a_1}) &= \alpha T(\mathbf{a_1}), \end{aligned}$$

where $\mathbf{a_1}$ and $\mathbf{a_2}$ are any two vectors in 3D and α is any scalar, then T is called a **linear transformation**. It is also called a **second-rank tensor**.

Let $\mathbf{e_1}$, $\mathbf{e_2}$ and $\mathbf{e_3}$ be unit vectors in the direction of the x-, y- and z-axes, respectively, of a rectangular Cartesian coordinate system. In this system,

$$\begin{aligned} \mathbf{e_1} &= (1, 0, 0), \\ \mathbf{e_2} &= (0, 1, 0), \\ \mathbf{e_3} &= (0, 0, 1). \end{aligned}$$

Then, the Cartesian components of a vector $\mathbf{a}$ are given by

$$\begin{aligned} a_1 &= \mathbf{e_1} \cdot \mathbf{a}, \\ a_2 &= \mathbf{e_2} \cdot \mathbf{a}, \\ a_3 &= \mathbf{e_3} \cdot \mathbf{a}, \end{aligned}$$

where $\cdot$ corresponds to dot product. In short, one can write the above equations as

$$a_i = \mathbf{e_i} \cdot \mathbf{a} \text{ for all } i \in \{1, 2, 3\}.$$

Equivalently, the vector $\mathbf{a}$ may be represented in terms of its components as

$$\mathbf{a} = a_1 \mathbf{e_1} + a_2 \mathbf{e_2} + a_3 \mathbf{e_3}, \tag{1.2}$$

and in short, this equation can be expressed as

$$\mathbf{a} = a_i \mathbf{e}_i, \tag{1.3}$$

where we use the Einstein's summation convention.

Now, we consider a linear transformation T and show how to represent it in a matrix form. Namely, we will define the tensor components denoted by T_{ij}. For a vector $\mathbf{a}$, assume that T maps it to $\mathbf{b}$. Thus

$$\mathbf{b} = T(\mathbf{a}) = a_1 T(\mathbf{e_1}) + a_2 T(\mathbf{e_2}) + a_3 T(\mathbf{e_3}) = a_i T(\mathbf{e_i}),$$

where the summation convention is used in the last equality and the second equality is due to the linearity of T. Then, we can write the components of $\mathbf{b}$ as

$$\begin{aligned} b_1 &= \mathbf{b} \cdot \mathbf{e_1} = a_1 \mathbf{e_1} \cdot T(\mathbf{e_1}) + a_2 \mathbf{e_1} \cdot T(\mathbf{e_2}) + a_3 \mathbf{e_1} \cdot T(\mathbf{e_3}), \\ b_2 &= \mathbf{b} \cdot \mathbf{e_2} = a_1 \mathbf{e_2} \cdot T(\mathbf{e_1}) + a_2 \mathbf{e_2} \cdot T(\mathbf{e_2}) + a_3 \mathbf{e_2} \cdot T(\mathbf{e_3}), \\ b_3 &= \mathbf{b} \cdot \mathbf{e_3} = a_1 \mathbf{e_3} \cdot T(\mathbf{e_1}) + a_2 \mathbf{e_3} \cdot T(\mathbf{e_2}) + a_3 \mathbf{e_3} \cdot T(\mathbf{e_3}), \end{aligned}$$

or by using the summation convention, we can express these three equalities by the following equation:

$$b_i = a_j \mathbf{e_i} \cdot T(\mathbf{e_j}) \text{ for } i \in \{1, 2, 3\}. \tag{1.4}$$

We shall agree to write the dot product, $\mathbf{e_i} \cdot T(\mathbf{e_j})$, as components of tensor T, formally defining

$$T_{ij} := \mathbf{e_i} \cdot T(\mathbf{e_j}). \tag{1.5}$$

Then Equation 1.4 can be written in component form as

$$b_i = T_{ij} a_j \text{ for } i \in \{1, 2, 3\}. \tag{1.6}$$

The above equations, namely 1.6, can be written in matrix form as

$$\begin{bmatrix} b_1 \\ b_2 \\ b_3 \end{bmatrix} = \begin{bmatrix} T_{11} & T_{12} & T_{13} \\ T_{21} & T_{22} & T_{23} \\ T_{31} & T_{32} & T_{33} \end{bmatrix} \begin{bmatrix} a_1 \\ a_2 \\ a_3 \end{bmatrix}. \tag{1.7}$$

Here, the matrix

$$\begin{bmatrix} T_{11} & T_{12} & T_{13} \\ T_{21} & T_{22} & T_{23} \\ T_{31} & T_{32} & T_{33} \end{bmatrix}$$

is called the **matrix of the tensor T** with respect to the orthogonal coordinate system $\{\mathbf{e_1}, \mathbf{e_2}, \mathbf{e_3}\}$.

In the view of the definition of the tensor components expressed in Equation 1.5, it is obvious that the components of T, namely T_{ij}, depend on the coordinate system $\{\mathbf{e_1}, \mathbf{e_2}, \mathbf{e_3}\}$ in which T is expressed. This is analogous to how the components of a vector change with the different coordinate systems. A vector does not depend on any coordinate system, even though its components do. Similarly a tensor does not depend on any coordinate system even though its components do. Thus, a tensor has infinitely many matrix representations— one for each set of unit base vectors. If $\{\mathbf{e_1}, \mathbf{e_2}, \mathbf{e_3}\}$ and $\{\mathbf{e'_1}, \mathbf{e'_2}, \mathbf{e'_3}\}$ are two different bases, then we denote the components of tensor T by T_{ij} and T'_{ij} for each of the basis vectors, respectively.

Now, we show how to obtain an orthogonal transformation, A, for rotating the coordinate systems. Suppose $\{\mathbf{e_1}, \mathbf{e_2}, \mathbf{e_3}\}$ and $\{\mathbf{e'_1}, \mathbf{e'_2}, \mathbf{e'_3}\}$ are unit vectors corresponding to two Cartesian coordinate systems. Then, $\{\mathbf{e'_1}, \mathbf{e'_2}, \mathbf{e'_3}\}$ can be obtained from $\{\mathbf{e_1}, \mathbf{e_2}, \mathbf{e_3}\}$ by a rigid rotation if both systems are same handed. That is, $\{\mathbf{e_1}, \mathbf{e_2}, \mathbf{e_3}\}$ and $\{\mathbf{e'_1}, \mathbf{e'_2}, \mathbf{e'_3}\}$ are related by an orthogonal transformation tensor, denoted by A, through the equations

$$\mathbf{e'_i} = A(\mathbf{e_i}) = A_{mi}\mathbf{e}_m, \text{ for any } i \in \{1, 2, 3\}. \tag{1.8}$$

More precisely,

$$\begin{aligned}
\mathbf{e}_1' &= A_{11}\mathbf{e}_1 + A_{21}\mathbf{e}_2 + A_{31}\mathbf{e}_3 \\
\mathbf{e}_2' &= A_{12}\mathbf{e}_1 + A_{22}\mathbf{e}_2 + A_{32}\mathbf{e}_3 \\
\mathbf{e}_3' &= A_{13}\mathbf{e}_1 + A_{23}\mathbf{e}_2 + A_{33}\mathbf{e}_3,
\end{aligned}$$

where the components of A can be obtained by using the definition of the components of a tensor, expressed in Equation 1.5. Explicitly,

$$A_{mi} = \mathbf{e_m} \cdot A(\mathbf{e_i}) = \mathbf{e_m} \cdot \mathbf{e_i}' = \cos\gamma, \tag{1.9}$$

where γ is the angle between $\mathbf{e_i}'$ and $\mathbf{e_m}$. Note that an orthogonal transformation is a linear transformation for which the transformed vectors preserve their lengths and the angle between them. This property of the orthogonal tensors gives the following equation:

$$A^T A = AA^T = I, \text{ for any } A \in O(3), \tag{1.10}$$

where $O(3)$ is the **space of orthogonal transformation tensors** in 3D and $\mathbf{I}$ denotes the 3×3 **identity matrix**. The **space of rotation tensors** will be denoted by $SO(3)$ which is a subgroup of $O(3)$.

Euler's rotation theorem states that a rotation matrix can be decomposed as a product of three elementary rotations. By using this theorem, one can find the rotation matrix that transforms the coordinate system, $\{\mathbf{e_1}, \mathbf{e_2}, \mathbf{e_3}\}$, to the coordinate system $\{\mathbf{e_1}', \mathbf{e_2}', \mathbf{e_3}'\}$. One may define three sets of coordinate axes with their origin in common in such a way that each one of them differs from the previous frame by an elementary rotation. See Figure 1.1. In these conditions, any target can be reached by performing three simple rotations. The first two rotations determine the new $\mathbf{e_3}$-axis, namely $\mathbf{e_3}'$, and the third rotation will obtain all the orientation possibilities that $\mathbf{e_3}'$ allows. To obtain $\mathbf{e_3}'$, firstly one applies a rotation around the $\mathbf{e_3}$-axis of the original

reference frame, that is

$$Z_1 = \begin{bmatrix} \cos\psi & -\sin\psi & 0 \\ \sin\psi & \cos\psi & 0 \\ 0 & 0 & 1 \end{bmatrix}. \tag{1.11}$$

This rotation is followed by a rotation around the rotated $\mathbf{e_1}$-axis, namely

$$Z_2 = \begin{bmatrix} 1 & 0 & 0 \\ 0 & \cos\phi & -\sin\phi \\ 0 & \sin\phi & \cos\phi \end{bmatrix}. \tag{1.12}$$

Thus, $Z_1 Z_2$ rotates the $\mathbf{e_3}$-axis to $\mathbf{e_3}'$-axis. Now, it remains to rotate intermediate $\mathbf{e_1}$- and $\mathbf{e_2}$-axes to their final configuration, namely $\mathbf{e_1}'$- and $\mathbf{e_2}'$-axes. The last elementary rotation matrix is around $\mathbf{e_3}'$-axis and in the form

$$Z_3 = \begin{bmatrix} \cos\theta & -\sin\theta & 0 \\ \sin\theta & \cos\theta & 0 \\ 0 & 0 & 1 \end{bmatrix}. \tag{1.13}$$

Thus, the rotation matrix $A \in SO(3)$ that rotates the coordinate system $\{\mathbf{e_1}, \mathbf{e_2}, \mathbf{e_3}\}$ to the coordinate system $\{\mathbf{e}'_1, \mathbf{e}'_2, \mathbf{e}'_3\}$ is achieved by three elementary rotations:

$$\begin{aligned} A &= Z_1 Z_2 Z_3 \qquad (1.14) \\ &= \begin{bmatrix} \cos\psi\cos\theta - \sin\psi\cos\phi\sin\theta & -\cos\psi\sin\theta - \sin\psi\cos\phi\cos\theta & \sin\psi\sin\phi \\ \sin\psi\cos\theta + \cos\psi\cos\phi\sin\theta & -\sin\psi\sin\theta + \cos\psi\cos\phi\cos\theta & -\cos\psi\sin\phi \\ \sin\phi\sin\theta & \sin\phi\cos\theta & \cos\phi \end{bmatrix}. \end{aligned}$$

The geometry of the transformation A can be seen in Figure 1.1. Note that the rotation matrix A, which is expressed in Equation 1.14, is in accordance with Equation 1.9, namely

$$A_{ij} = \mathbf{e_i} \cdot A(\mathbf{e_j}) = \mathbf{e_i} \cdot \mathbf{e}'_j.$$

For example, consider $\mathbf{e}'_2$. It is possible to observe from Figure 1.1 that

$$\mathbf{e}'_2 = (-\cos\psi\sin\theta - \sin\psi\cos\phi\cos\theta, -\sin\psi\sin\theta + \cos\psi\cos\phi\cos\theta, \sin\phi\cos\theta).$$

Then

$$A_{12} = \mathbf{e_1} \cdot \mathbf{e_2'} = -\cos\psi \sin\theta - \sin\psi \cos\phi \cos\theta.$$

Now, consider a vector $\mathbf{v}$. The components of $\mathbf{v}$ with respect to $\{\mathbf{e_1}, \mathbf{e_2}, \mathbf{e_3}\}$ and $\{\mathbf{e_1'}, \mathbf{e_2'}, \mathbf{e_3'}\}$ are $v_i = \mathbf{e_1} \cdot \mathbf{v}$ and $v_i' = \mathbf{e_1}' \cdot \mathbf{v}$, respectively. Since

$$v_i' = \mathbf{e_1}' \cdot \mathbf{v} = A_{mi}\mathbf{e_m} \cdot \mathbf{v},$$

we have

$$v_i' = A_{mi}v_m. \tag{1.15}$$

In matrix form, the above expression 1.15 can be written

$$\begin{bmatrix} v_1' \\ v_2' \\ v_3' \end{bmatrix} = \begin{bmatrix} A_{11} & A_{21} & A_{31} \\ A_{12} & A_{22} & A_{32} \\ A_{13} & A_{23} & A_{33} \end{bmatrix} \begin{bmatrix} v_1 \\ v_2 \\ v_3 \end{bmatrix} \tag{1.16}$$

or, in short,

$$\mathbf{v}' = A^T(\mathbf{v}). \tag{1.17}$$

Equations 1.15 and 1.17 are the **transformation laws**. The former is expressed in tensor form and the latter in matrix form, relating the components of the same vector with respect to different coordinate systems.

Next, consider a linear transformation T. The components of T with respect to $\{\mathbf{e_1}, \mathbf{e_2}, \mathbf{e_3}\}$ and $\{\mathbf{e_1'}, \mathbf{e_2'}, \mathbf{e_3'}\}$ are $T_{ij} = \mathbf{e_i} \cdot T(\mathbf{e_j})$ and $T_{ij}' = \mathbf{e_i}' \cdot T(\mathbf{e_j}')$, respectively. Since

$$T_{ij}' = \mathbf{e_i}' \cdot T(\mathbf{e_j}') = A_{mi}\mathbf{e_m} \cdot T(A_{nj}\mathbf{e_n}) = A_{mi}A_{nj}(\mathbf{e_m} \cdot T(\mathbf{e_n})),$$

we obtain

$$T_{ij}' = A_{mi}A_{nj}T_{mn}. \tag{1.18}$$

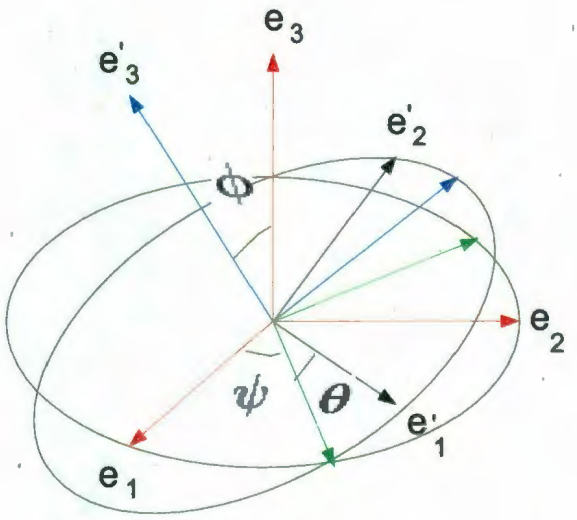

Figure 1.1: Three elementary transformations are applied to rotate the coordinate system $\{\mathbf{e_1}, \mathbf{e_2}, \mathbf{e_3}\}$ to $\{\mathbf{e'_1}, \mathbf{e'_2}, \mathbf{e'_3}\}$. The first transformation is a rotation of ψ degrees around $\mathbf{e_3}$-axis and rotates the red coordinate system to the green one. Note that since $\mathbf{e_3}$ remains the same, so does its color. The second transformation is around the rotated $\mathbf{e_1}$-axis for ϕ degrees and it transforms the green to the blue coordinate system. These two transformations determine the location of $\mathbf{e'_3}$-axis. The last one is around $\mathbf{e'_3}$-axis for θ degrees. It determines the locations of $\mathbf{e'_1}$- and $\mathbf{e'_2}$-axes.

The transformation rule for second-rank tensors, expressed in Equation 1.18, can be written in matrix form as

$$\begin{bmatrix} T'_{11} & T'_{12} & T'_{13} \\ T'_{21} & T'_{22} & T'_{23} \\ T'_{31} & T'_{32} & T'_{33} \end{bmatrix} = \begin{bmatrix} A_{11} & A_{21} & A_{31} \\ A_{12} & A_{22} & A_{32} \\ A_{13} & A_{23} & A_{33} \end{bmatrix} \begin{bmatrix} T_{11} & T_{12} & T_{13} \\ T_{21} & T_{22} & T_{23} \\ T_{31} & T_{32} & T_{33} \end{bmatrix} \begin{bmatrix} A_{11} & A_{12} & A_{13} \\ A_{21} & A_{22} & A_{23} \\ A_{31} & A_{32} & A_{33} \end{bmatrix}, \quad (1.19)$$

or, in short,

$$T' = A^T T A.$$

Notice that in Equation 1.18, there are two components of the orthogonal transformation matrix A appearing in every term of the summation. This is due to the fact that two subindices are associated with the tensor T. Thus each A is transforming one of the subindices. These subindices correspond to directions when a tensor represents a physical quantity.

Similarly, one can show the transformation rule for a higher-order tensor, in particular for the elasticity tensor. Generalizing Equation 1.18, the transformation rule for the fourth-rank elasticity tensor is

$$c'_{ijkl} := A_{mi} A_{nj} A_{pk} A_{ql} c_{mnpq}, \quad (1.20)$$

where $A \in O(3)$ is an orthogonal transformation and c is the elasticity tensor expressed in the coordinate system $\{\mathbf{e_1}, \mathbf{e_2}, \mathbf{e_3}\}$. Then, c' is expressed in the rotated coordinate system, namely $\{A(\mathbf{e_1}), A(\mathbf{e_2}), A(\mathbf{e_3})\}$. A fourth-rank tensor is associated with four directions. The number of directions needed for defining a tensor determines its rank. Thus, one uses four rotation matrices to express a fourth-rank tensor in a different coordinate system.

The second chapter of the thesis solves the problem of recognizing if a given elasticity tensor, which is represented in any coordinate system, belongs to a particular symmetry class. More precisely, the problem is to determine the rotation matrix that transforms the coordinate system of the given elasticity tensor into another coordinate

system so that one can identify to which symmetry class it belongs by considering the form of the tensor.

1.3 Eight Material-Symmetry Classes of Elasticity Tensor

An important property of tensors is the transformation law under rotations which is expressed in Equation 1.1. Due to this property a tensor can be described in any coordinate system. Although it is the same tensor, its parameters depend on the orientation of the coordinate system in which it is expressed.

Observe that in Equation 1.20, the rule is expressed in fourth-rank tensor notation, not in the matrix notation. In Appendix A.3.3, we show how a fourth-rank tensor in 3D is represented as a second-rank tensor in 6D. Thus, in order to use the transformation rule for 6×6 matrices, we convert the orthogonal transformation matrix from 3D to a matrix in 6D. To do so we use the Kelvin notation of the elasticity matrix and 6D vectors of stress and strain expressed in Equation A.45. Refer to Appendix A.3.4 for how to obtain the 6D-orthogonal transformation matrix. In the rest of the thesis, we use the notation, e.g. A, for denoting the orthogonal transformations in 3D. The transformations in 6D that rotate the coordinate system of an elasticity matrix C will be denoted with a bar, e.g. $\bar{A} \in SO(6)$.

In Appendix A.3.2, we see that there are twenty-one independent parameters of the elasticity tensor because of the symmetries expressed in Equations A.33, A.34 and A.37. All these symmetries result from physical laws like balance of angular momentum and existence of strain-energy function. Thus, any elasticity tensor possesses these symmetries. In this section, we show that an elasticity tensor, representing a particular material, can be more symmetric and therefore it has fewer independent parameters depending on the intrinsic symmetries of the material. For example,

bedding, or other layers in the sedimentary rocks, introduce an orientation in the structure. Then, the medium is approximated as transversely isotropic. Likewise, any oriented feature in a subsurface and their combinations affect the symmetry of the medium, e.g. cracks, faults and minerals with preferred orientations that persist over long distances.

We say that an elasticity tensor is **symmetric with respect to an orthogonal transformation** A if one rotates the tensor by A and gets the same elasticity tensor. We call the orthogonal transformation matrix $A \in SO(3)$ a **symmetry element** of C if C is symmetric with respect to A. This is mathematically expressed as: C is symmetric with respect to an orthogonal transformation A if

$$C' = \bar{A}^T C \bar{A} = C, \tag{1.21}$$

where A and $\bar{A}$ are 3×3 and 6×6 orthogonal transformation matrices, respectively. Thus, C' and C are the elasticity matrices represented in the transformed and the original coordinates, respectively.

The set of all symmetry elements of an elasticity tensor C is called the **symmetry group of C** and denoted by G_C. Thus

$$G_C = \{A \in O(3) \mid C = \bar{A}^T C \bar{A}\}, \tag{1.22}$$

where $O(3)$ denotes the set of all orthogonal transformations in 3D.

Now, we define an equivalance relation in the space of elasticity tensors. According to this definition, two elasticity tensors, C_1 and C_2, are in the same class if their symmetry groups, G_{C_1} and G_{C_2}, are conjugate. The conjugacy means that there exists a rotation $A \in SO(3)$ such that

$$G_{C_2} = A^T G_{C_1} A.$$

Geometrically, the conjugate of a symmetry group G_{C_1} corresponds to representing it in a different coordinate system. For example; consider a rotated elasticity tensor

$\bar{A}^T C \bar{A}$, for some rotation tensor $A \in SO(3)$. Then the symmetry group of $G_{\bar{A}^T C \bar{A}}$ is conjugate of G_C. More precisely,

$$G_{\bar{A}^T C \bar{A}} = A^T G_C A.$$

Since we represent $\bar{A}^T C \bar{A}$ in a rotated coordinate system, namely in $\{A(\mathbf{e_1}), A(\mathbf{e_2}), A(\mathbf{e_3})\}$, the symmetry elements of the tensor are also expressed in the rotated coordinate system.

In the literature, there are several nonequivalent definitions of the symmetries of the elasticity tensor. In accordance with the definition of conjugate symmetry groups, there are eight symmetry classes as shown by Forte and Vianello [20], Chadwick et al. [12] and Bóna et al. [9]. These eight symmetry classes of elasticity tensor are isotropic, cubic, transversely isotropic, tetragonal, trigonal, orthotropic, monoclinic and generally anisotropic. Now, we present the form of elasticity tensor belonging to each symmetry class. These forms are the matrix representations of the elasticity tensor with respect to its natural basis.

Definition 2 *We call the basis* $\{\mathbf{e_1}, \mathbf{e_2}, \mathbf{e_3}\}$ *the* ***natural coordinate axes*** *for the elasticity tensor* C *if the symmetry directions of* C*, like its rotation axis and normal of symmetry planes, are either aligned with the directions* $\mathbf{e_1}, \mathbf{e_2}, \mathbf{e_3}$ *or lie in any of the coordinate planes, e.g.* $\mathbf{e_1 e_2}$*-plane.*

The isotropic elasticity tensor is of the form

$$C = \begin{bmatrix} C_{44}+C_{12} & C_{12} & C_{12} & 0 & 0 & 0 \\ C_{12} & C_{44}+C_{12} & C_{23} & 0 & 0 & 0 \\ C_{12} & C_{12} & C_{44}+C_{12} & 0 & 0 & 0 \\ 0 & 0 & 0 & C_{44} & 0 & 0 \\ 0 & 0 & 0 & 0 & C_{44} & 0 \\ 0 & 0 & 0 & 0 & 0 & C_{44} \end{bmatrix}.$$

The symmetry group of an isotropic elasticity tensor is $G_C = O(3)$. Note that the form of the isotropic tensor does not change for any coordinate system since its symmetry group is all orthogonal transformations. Thus, any coordinate system is natural for isotropy.

For cubic symmetry, the natural basis for the elasticity tensor is the coordinate axes which are aligned with 4-fold rotation axes of the cube. Moreover, the diagonals should be aligned with the three-fold rotation axes. With respect to that coordinate system, the symmetry group of a cubic elasticity tensor is

$$G^{Cubic} = \{A \in O(3) \mid A(e_i) = \pm e_j, \text{ for any } i, j \in \{1, 2, 3\}\}.$$

The matrix representation of this tensor with respect to the natural coordinate axes is

$$C = \begin{bmatrix} C_{11} & C_{12} & C_{12} & 0 & 0 & 0 \\ C_{12} & C_{11} & C_{12} & 0 & 0 & 0 \\ C_{12} & C_{12} & C_{11} & 0 & 0 & 0 \\ 0 & 0 & 0 & C_{44} & 0 & 0 \\ 0 & 0 & 0 & 0 & C_{44} & 0 \\ 0 & 0 & 0 & 0 & 0 & C_{44} \end{bmatrix}.$$

Note that there are three independent parameters for cubic elasticity tensors whereas there are two for isotropic media.

An elasticity tensor has a transversely isotropic (TI) symmetry if it is invariant under an n-fold rotation, where $n > 4$. Herman [28] showed that this is equivalent to the invariance under any rotation around a fixed axis. If $\mathbf{e_3}$ is parallel to the axis of rotation, then $\{\mathbf{e_1}, \mathbf{e_2}, \mathbf{e_3}\}$ is the natural coordinate axes for a TI elasticity tensor. Note that the orientations of $\mathbf{e_1}$ and $\mathbf{e_2}$ do not matter. The symmetry group with respect to this coordinate system is

$$G^{TI} = \{\pm I, \pm R_{\theta,\mathbf{e_3}}, \pm M_{\mathbf{v}} \mid \theta \in [0, 2\pi), \text{ for all } \mathbf{v} \text{ lying in } \mathbf{e_1 e_2}\text{-plane}\},$$

where I is the identity element of O(3), $R_{\theta,\mathbf{e_3}}$ denotes a rotation by θ around $\mathbf{e_3}$-axis and $M_{\mathbf{v}}$ denotes reflection about the planes whose normal is any $\mathbf{v}$ in the $\mathbf{e_1e_2}$-plane. Note that we have not written down $M_{\mathbf{e_3}}$ as an element of G^{TI} although it is, because of the fact that

$$-R_{\theta,\mathbf{e_3}} = M_{\mathbf{e_3}}.$$

Since $-R_{\theta,\mathbf{e_3}} \in G^{TI}$ so is $M_{\mathbf{e_3}}$.

We choose the notation $\mathbf{M}$ for reflection transformation because this plane is also called a **mirror plane**. The subscript of M shows the normal direction of the mirror plane.

The matrix representation of a tensor with TI symmetry with respect to a natural basis is

$$C = \begin{bmatrix} C_{11} & C_{12} & C_{13} & 0 & 0 & 0 \\ C_{12} & C_{11} & C_{13} & 0 & 0 & 0 \\ C_{13} & C_{13} & C_{33} & 0 & 0 & 0 \\ 0 & 0 & 0 & C_{44} & 0 & 0 \\ 0 & 0 & 0 & 0 & C_{44} & 0 \\ 0 & 0 & 0 & 0 & 0 & C_{11} - C_{12} \end{bmatrix}. \tag{1.23}$$

An elasticity tensor, C, has a tetragonal symmetry if it is invariant under a four-fold rotation. If $\mathbf{e_3}$ is parallel to the axis of rotation, then there exists a natural basis, $\{\mathbf{e_1}, \mathbf{e_2}, \mathbf{e_3}\}$, of C where $\mathbf{e_1}$ and $\mathbf{e_2}$ are parallel to the normal of any two orthogonal symmetry planes. The symmetry group with respect to this basis is

$$G^{Tetra} = \{\pm I, \pm R_{\frac{\pi}{2},\mathbf{e_3}}, \pm R_{-\frac{\pi}{2},\mathbf{e_3}}, \pm M_{\mathbf{e_i}}, \pm M_{(1,1,0)}, \pm M_{(1,-1,0)} \mid i \in \{1,2,3\}\}. \tag{1.24}$$

Here, $M_{\mathbf{e_1}}, M_{\mathbf{e_2}}, M_{(1,1,0)}$ and $M_{(1,-1,0)}$ are reflections about four planes that contain $\mathbf{e_3}$-axis and the angle between any two planes is either $\frac{\pi}{2}$ or $\frac{\pi}{4}$. $M_{\mathbf{e_3}}$ is perpendicular to all of these planes.

The matrix representation of a tetragonal elasticity tensor with respect to the natural basis is

$$C = \begin{bmatrix} C_{11} & C_{12} & C_{13} & 0 & 0 & 0 \\ C_{12} & C_{11} & C_{13} & 0 & 0 & 0 \\ C_{13} & C_{13} & C_{33} & 0 & 0 & 0 \\ 0 & 0 & 0 & C_{44} & 0 & 0 \\ 0 & 0 & 0 & 0 & C_{44} & 0 \\ 0 & 0 & 0 & 0 & 0 & C_{66} \end{bmatrix}. \tag{1.25}$$

An elasticity tensor, C, has trigonal symmetry if it is invariant under a three-fold rotation. If $\mathbf{e_3}$ is parallel to the axis of rotation, then there exists a natural basis of C, namely $\{\mathbf{e_1}, \mathbf{e_2}, \mathbf{e_3}\}$, where either $\mathbf{e_1}$ or $\mathbf{e_2}$ is aligned with a normal of one of the symmetry planes. Its symmetry group is

$$G^{Trigo} = \{\pm I, \pm R_{\frac{2\pi}{3},\mathbf{e_3}}, \pm R_{-\frac{2\pi}{3},\mathbf{e_3}}, \pm M_{\mathbf{e_1}}, \pm M_{(\cos\frac{\pi}{6},\sin\frac{\pi}{6},0)}, \pm M_{(\cos\frac{5\pi}{6},\sin\frac{5\pi}{6},0)}\}. \tag{1.26}$$

Here, $M_{\mathbf{e_1}}$, $M_{(\cos\frac{\pi}{6},\sin\frac{\pi}{6},0)}$ and $M_{(\cos\frac{5\pi}{6},\sin\frac{5\pi}{6},0)}$ are reflections about three planes that contain $\mathbf{e_3}$-axis and the angle between any two planes is $\frac{\pi}{3}$.

The matrix representation of an trigonal elasticity tensor with respect to the natural basis is

$$C = \begin{bmatrix} C_{11} & C_{12} & C_{13} & C_{14} & 0 & 0 \\ C_{12} & C_{11} & C_{13} & -C_{14} & 0 & 0 \\ C_{13} & C_{13} & C_{33} & 0 & 0 & 0 \\ C_{14} & -C_{14} & 0 & C_{44} & 0 & 0 \\ 0 & 0 & 0 & 0 & C_{44} & \sqrt{2}C_{14} \\ 0 & 0 & 0 & 0 & \sqrt{2}C_{14} & C_{11} - C_{12} \end{bmatrix}. \tag{1.27}$$

An elasticity tensor, C, has orthotropic symmetry if it is invariant under three reflections around three mutually orthogonal planes. Note that if a tensor is symmetric with respect to any two mirror planes orthogonal to each other, then it must

be symmetric around another plane which is perpendicular to the first two planes. The natural coordinate system of C is obtained whenever the normals of the mirror planes are aligned with $\mathbf{e_1}$, $\mathbf{e_2}$ and $\mathbf{e_3}$. Its symmetry group with respect to this basis is

$$G^{Ortho} = \{\pm I, \pm M_{\mathbf{e_1}}, \pm M_{\mathbf{e_2}}, \pm M_{\mathbf{e_3}}\}. \tag{1.28}$$

The matrix representation of an orthotropic elasticity tensor with respect to its natural basis is

$$C = \begin{bmatrix} C_{11} & C_{12} & C_{13} & 0 & 0 & 0 \\ C_{12} & C_{22} & C_{23} & 0 & 0 & 0 \\ C_{13} & C_{23} & C_{33} & 0 & 0 & 0 \\ 0 & 0 & 0 & C_{44} & 0 & 0 \\ 0 & 0 & 0 & 0 & C_{55} & 0 \\ 0 & 0 & 0 & 0 & 0 & C_{66} \end{bmatrix}. \tag{1.29}$$

An elasticity tensor, C, has monoclinic symmetry if it is invariant under a reflection around a plane. The natural coordinate system of C is obtained whenever $\mathbf{e_3}$ is aligned with the normal of the mirror plane. We can choose any two orthonormal vectors for the $\mathbf{e_1}$- and $\mathbf{e_2}$-axis. Its symmetry group is

$$G^{Mono} = \{\pm I, \pm M_{\mathbf{e_3}}\}.$$

Then the matrix representation of a monoclinic elasticity tensor is

$$C = \begin{bmatrix} C_{11} & C_{12} & C_{13} & 0 & 0 & C_{16} \\ C_{12} & C_{22} & C_{23} & 0 & 0 & C_{26} \\ C_{13} & C_{13} & C_{33} & 0 & 0 & C_{36} \\ C_{16} & C_{26} & C_{36} & C_{44} & C_{45} & 0 \\ 0 & 0 & 0 & C_{45} & C_{55} & 0 \\ 0 & 0 & 0 & 0 & 0 & C_{66} \end{bmatrix}.$$

According to the symmetry groups presented above, we can put an order among the symmetry classes of elasticity tensors by considering their subgroup relationships. For example, the symmetry group of monoclinic, $G^{Mono} = \{\pm I, \pm M_{\mathbf{e}_3}\}$, is a subgroup of the orthotropic group, $G^{Ortho} = \{\pm I, \pm M_{\mathbf{e}_1}, \pm M_{\mathbf{e}_2}, \pm M_{\mathbf{e}_3}\}$. All the subgroup relations are shown in Figure 1.2. The lines between the symmetry classes imply that the symmetry group of the corresponding class is a subgroup of the class which lies above. As shown in Figure 1.2, there is no order relation between the trigonal and the orthotropic groups. Observing the symmetry group of the trigonal class, expressed in Equation 1.26, the symmetry planes of a trigonal elasticity tensor contain no three planes that are mutually orthogonal to each other. However, the symmetry planes of the orthotropic group, expressed in Equation 1.28, are three mutually orthogonal planes. Thus, one is not a subgroup of the other group. An important feature of the order relation referred from Figure 1.2 is that monoclinic symmetry class is the subgroup of all symmetry classes except generally anisotropic symmetry.

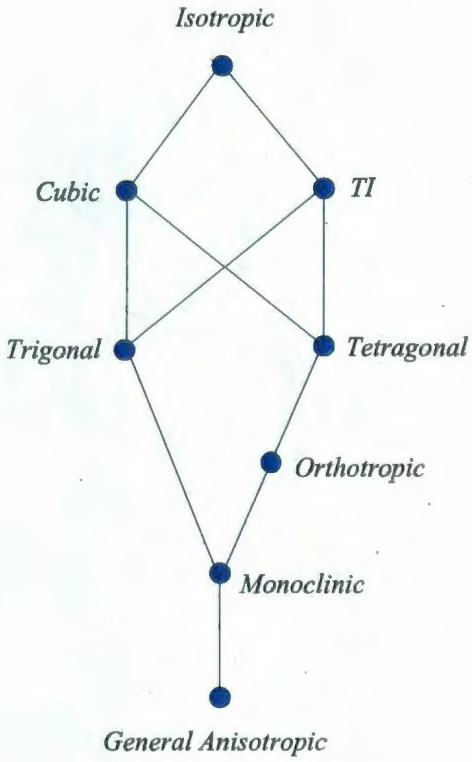

Figure 1.2: Order Relation of the Eight Symmetry Classes of Elasticity Tensors

Chapter 2

Identifying the Symmetry Class of an Elasticity Tensor

In this chapter, we solve the problem of identifying the symmetry of a medium, if it has any. The medium, that its elasticity tensor is measured, can be different materials depending on the application. It may be a mineral, a rock or a region of earth. If it is a mineral, one generally assumes the symmetry of the tensor before measuring its components. However, if the medium is a rock or a subsurface region of Earth, then, in general, there is no a priori assumption about the symmetry of the medium. Thus, the directions in which the measurements are done generally do not align with the symmetry directions of the medium. Therefore, the resulting elasticity tensor is expressed in some coordinate system other than its natural coordinate axes. Unlike the form of elasticity tensor whenever it is represented in its natural coordinate system, the elasticity matrix hides the symmetry of the medium whenever it is represented in an arbitrary coordinate system. Therefore, a method is needed for identifying the symmetry of the tensor. We propose a method to determine the symmetry class of an elasticity tensor which is represented in an orthogonal coordinate system of arbitrary orientation.

Previously, the identification of the symmetry of the elasticity tensor was done by finding its eigenvalues and eigenvectors in the work of Cowin et al., Slawinski et al. and Helbig [8, 13, 25]. According to their method, each symmetry class is characterized by relationships among its eigenvectors and eigenvalues should be satisfied for a given tensor. However, checking these relationships is a vast amount of work and involves nontrivial relations. Refer to Section 1.1 for reference to the previous works done on identifying the symmetry of a given elasticity tensor.

In this chapter, we present a more efficient method for recognizing the symmetry class of an elasticity tensor. Our method is based on plotting the distance function of the tensor to the monoclinic symmetry class. Based on the observations made in the plot, the symmetry of the tensor can be determined.

In Section 2.1, we introduce basic definitions and formulations of the distance function. We present theorems about the symmetry classes for which their distance functions can be plotted. We also state properties of the plot of distance functions. In the rest of the sections of this chapter, we give examples for each symmetry class on how to determine the transformation matrix that rotates the tensor to its natural coordinate so that its symmetry becomes apparent.

2.1 Formulation of the Distance Function

The problem of representing a region or a material with fewer parameters gives rise to the question of how to find the "closest" elasticity tensor with a higher symmetry than the measured one. As we pointed out previously, the elasticity tensor, which is obtained by inverting geophysical data, is found to be generally anisotropic. This implies that there are 21 independent parameters to represent the medium. However, seismic modeling generally requires fewer parameters. Equivalently, it requires higher symmetry of the medium. Thus, a distance function is needed by which one can

find the closest elasticity tensor that belongs to a given symmetry class. We use this function to determine the closest symmetric tensor in the next chapter. However, in this chapter we use the distance function to determine which symmetry class does the medium belongs to. In other words, we are looking for an orientation where the distance function vanishes. Thus, all the examples presented in this chapter does belong to one of the symmetry classes of elasticity tensor.

A natural definition for distance is achieved by defining Euclidean norm in the space of elasticity tensors. We define the norm of an elasticity tensor as

$$||c_{ijkl}||^2 := c_{ijkl}c_{ijkl}, \tag{2.1}$$

where the summation convention is used. The norm can be defined in the matrix form as

$$||C||^2 := Tr(C^T C), \tag{2.2}$$

where Tr is the trace of a 6×6 matrix and C^T denotes the transpose of the elasticity matrix C.

Note that the definition of the norm of an elasticity tensor is analogous to the norm defined in the three-dimensional vector space. In other words, the concept of norm defined in the space of one-rank tensors is generalized to the space of fourth-rank tensors.

After we define the norm, a natural definition of distance in the space of elasticity tensors can be generalized from the three-dimensional vector space, too. Recall that the distance between a vector, v, and a linear subspace in 3D, denoted by $\mathcal{L}$, is achieved by considering the orthogonal projection of the vector, $pr(v)$, onto the linear subspace $\mathcal{L}$. See Figure 2.1. The orthogonality of the projection guarantees minimization of the distance between the vector and the linear subspace. In the space of elasticity tensors, a similar definition is used for the distance between a given elasticity tensor C and a linear subspace of elasticity tensors. We denote the

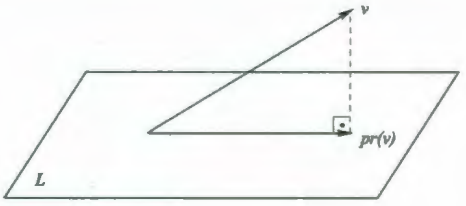

Figure 2.1: The projection of $\mathbf{v}$ onto the linear space $\mathcal{L}$ in 3D. Note that the difference of $\mathbf{v} - pr(\mathbf{v})$ is perpendicular to $pr(\mathbf{v})$.

linear subspace of elasticity tensors which are expressed in the coordinate system $\{\mathbf{e_1}, \mathbf{e_2}, \mathbf{e_3}\}$ and belong to a particular symmetry class by $\mathcal{L}^{\mathbf{sym}}$, where *sym* is one of the seven symmetry classes. Herein, we exclude the generally anisotropic symmetry class since all the elasticity tensors belong to that class. Then, the distance between C and $\mathcal{L}^{sym}$ is defined by the following minimization process:

$$\min_{C' \in \mathcal{L}^{sym}} \| C - C' \| . \tag{2.3}$$

The subspace of elasticity tensors $\mathcal{L}^{sym}$ being linear guarantees the uniqueness of this minimization process. Thus, the minimum value of $\| C - C' \|$ for all $C' \in \mathcal{L}^{sym}$ gives the distance between C and $\mathcal{L}^{sym}$.

Moreover, this unique point, where the minimum is attained, is a projection. Gazis et al. [23] prove that the orthogonal projection of an elasticity tensor C onto the linear space $\mathcal{L}^{sym}$, is expressed as the average given by

$$pr_{sym}(C) := \int_{G \in G^{sym}} \bar{G}^T C \bar{G}, \tag{2.4}$$

where $pr_{sym}(C)$ is the projection of C onto the subspace $\mathcal{L}^{sym}$ and G^{sym} is the symmetry group of $\mathcal{L}^{sym}$. The symbol $\int_{G \in G^{sym}}$ denotes the averaging over the group G^{sym}, i.e. summation and/or integration divided by the volume of the group. It is proved in [23] that the projected elasticity tensor, $pr_{sym}(C)$, is closest to the tensor C among

all the tensors in the subspace $\mathcal{L}^{sym}$. Herein, the closest refers to the minimum of the norms of the difference between C and any tensor in $\mathcal{L}^{sym}$. This minimum is achieved for $pr_{sym}(C) \in \mathcal{L}^{sym}$. We formally state this as

$$\min_{C' \in \mathcal{L}^{sym}} \| C - C' \| = \| C - pr_{sym}(C) \| . \tag{2.5}$$

Note that the closest elasticity tensor to C in the subspace $\mathcal{L}^{sym}$, namely $pr_{sym}(C)$, is expressed in its natural coordinate system, namely $\{\mathbf{e_1}, \mathbf{e_2}, \mathbf{e_3}\}$. This is because in Equation 2.4, the average is taken over the symmetry group G^{sym} which is defined in its natural coordinate system. Thus, the tensor $pr_{sym}(C)$ is evaluated on the coordinate system $\{\mathbf{e_1}, \mathbf{e_2}, \mathbf{e_3}\}$. If the projection is taken in any other coordinate system, then it is not equal to the $pr_{sym}(C)$ expressed in Equation 2.4.

The integral above reduces to a finite sum for the symmetry classes whose symmetry groups are finite; that is, for all classes except isotropy and TI. However, one can always find a finite subgroup of isotropy and TI such that the projection can be evaluated on this finite subgroups which is showed by Kochetov and Slawinski [32]. Furthermore, it is shown by Gazis et al. [23] that if C is positive definite then $pr_{sym}(C)$ is also positive-definite, which is required for elasticity tensors representing real media due to the existence of the strain-energy function. From now on, we will denote $pr_{sym}(C)$ by C^{sym}.

One drawback of this approach is that while it minimizes the Euclidean distance between the original and projected elasticity tensor, it does not give the same distance for the original and projected compliance tensor (the inverse of elasticity tensor). A medium can be equivalently represented by either its elasticity tensor or the inverse of it, namely compliance tensor. In physics, it is generally expected that the distance of a tensor to a particular symmetry class remains the same for the inverse of the tensor as well. Some papers consider another formulation of a distance function based on non-Euclidean norms such as the Riemannian or log-Euclidean metrics which do not have this deficiency [1, 38]. More precisely, these distance functions provide a unique

projection for the value of the distance whether one uses the elasticity tensor or the compliance tensor [40].

However, using the Euclidean projection is physically appealing since it seeks to approximate acoustical properties of the material. As it is proven by Norris [40], the question of which elasticity tensor, belonging to a particular symmetry class, is the best acoustic fit to a given anisotropic material is equivalent to finding the Euclidean projection of C onto $\mathcal{L}^{sym}$. This provides a well-grounded acoustical basis for using the Euclidean projection as a natural way to simplify ultrasonic or acoustic data.

Acoustic wave speeds and polarizations of the waves are primarily related by the Christoffel Matrix which is not linear with respect to the components of the wave vector. However, the Christoffel Matrix can be written in a form such that it becomes linear in the components of the wave vector. To do so, the related fourth-rank tensor, C^*, is defined by Norris and Slawinski [40, 7] by

$$c^*_{ijkl} := \frac{1}{2}(c_{ikjl} + c_{iljk}). \tag{2.6}$$

Then, the Christoffel matrix can be introduced as a second-rank tensor with respect to the wave vector $\mathbf{n}$ as

$$Q_{ij} := c^*_{ijkl} n_k n_l. \tag{2.7}$$

Fedorov's approach to get the best fitting isotropic elastic moduli to a given C is to find the minimum of the difference between $Q(C, \mathbf{n})$ and $Q(C', \mathbf{n})$ for all directions $n \in \mathbb{R}^3$ where C' represents isotropic elasticity tensors. This approach is generalized to any symmetry class by Norris in [40]. More precisely, he considers the acoustical distance function f:

$$f(C, C') := \frac{1}{4\pi} \int_0^{2\pi} d\psi \int_0^{\pi} \sin\phi \;\; ||Q(C, \mathbf{n}) - Q(C', \mathbf{n})||^2 d\phi, \tag{2.8}$$

where $\mathbf{n} = (\cos\psi \sin\phi, \sin\psi \sin\phi, \cos\phi)$. The function f gives the distance between the acoustical tensors $Q(C, \mathbf{n})$ and $Q(C', \mathbf{n})$ which is averaged over all orientations $\mathbf{n}$.

Thus, the minimum of f is the best fit in the sense that it minimizes the orientation-averaged squared difference of the acoustical tensors. The main result in [40] is the proof of the equivalence of the following minimization problems:

$$\min_{C' \in \mathcal{L}^{sym}} f(C, C') = \min_{C' \in \mathcal{L}^{sym}} ||C - C'|| = ||C - C^{sym}||,$$

for a given elasticity tensor C. Hence, it is concluded that the Euclidean projection is identical to Fedorov's approach.

As far as applications are concerned, the Euclidean Projection Method is one of the most common methods used to determine the closest elasticity tensor as it is used by Helbig, Browaeys et al. and Gangi [27, 10, 22]. The theoretical background of how to calculate the closest elasticity tensor is introduced by Gazis et al. [23] and by Fedorov [19] using a different approach. However, Norris [40] has showed that these two approaches are equivalent.

In the papers cited in above paragraph, the projection of a given elasticity tensor, which is expressed in Equation 2.4, is calculated in the coordinate system that the tensor is expressed in. Thus, the closest symmetric elasticity tensor is found in the coordinate system $\{\mathbf{e_1}, \mathbf{e_2}, \mathbf{e_3}\}$. However, restricting the projection to only one coordinate system, namely to $\{\mathbf{e_1}, \mathbf{e_2}, \mathbf{e_3}\}$, has a major drawback. Even if a tensor C belongs to a particular symmetry class, say transversely isotropic (TI), and is expressed in a different coordinate system than its natural coordinate system, then the distance of C to $\mathcal{L}^{TI}$ does not vanish. In other words, the value of the distance between C and $\mathcal{L}^{TI}$ is non-zero whenever C is expressed in a coordinate-system other than its natural coordinate system. This undesirable result is due to restricting the projection to the coordinate system $\{\mathbf{e_1}, \mathbf{e_2}, \mathbf{e_3}\}$. In order to resolve this, in this thesis we examine the closest elasticity tensor in all possible orientations of the coordinate systems.

Before generalizing the distance function to all coordinate systems, we state the explicit forms of the projected tensors to some symmetry classes. Recall that for the

coordinate system $\{\mathbf{e_1}, \mathbf{e_2}, \mathbf{e_3}\}$, the closest tensor belonging to a particular symmetry class is given by the projection operator defined in Equation 2.4. Explicit expressions for the projections in all symmetry classes are obtained by applying Equation 2.4 in [23, 37] and for the monoclinic, TI and orthotropic symmetry classes in [32, 33]. Then, the projection of C onto $\mathcal{L}^{mono}$, namely C^{mono}, is found as

$$C^{mono} = \begin{bmatrix} C_{11} & C_{12} & C_{13} & 0 & 0 & C_{16} \\ C_{12} & C_{22} & C_{23} & 0 & 0 & C_{26} \\ C_{13} & C_{23} & C_{33} & 0 & 0 & C_{36} \\ 0 & 0 & 0 & C_{44} & C_{45} & 0 \\ 0 & 0 & 0 & C_{45} & C_{55} & 0 \\ C_{16} & C_{26} & C_{36} & 0 & 0 & C_{66} \end{bmatrix}. \tag{2.9}$$

C^{mono} is the closest monoclinic elasticity tensor to C in the coordinate system $\{\mathbf{e_1}, \mathbf{e_2}, \mathbf{e_3}\}$ and the normal of the symmetry plane of C^{mono} is parallel to $\mathbf{e_3}$.

Similarly, the projection of C onto $\mathcal{L}^{TI}$, namely C^{TI}, is given in [37, 32] as

$$C^{TI} = \begin{bmatrix} C_{11}^{TI} & C_{12}^{TI} & C_{13}^{TI} & 0 & 0 & 0 \\ C_{12}^{TI} & C_{11}^{TI} & C_{13}^{TI} & 0 & 0 & 0 \\ C_{13}^{TI} & C_{13}^{TI} & C_{33}^{TI} & 0 & 0 & 0 \\ 0 & 0 & 0 & C_{44}^{TI} & 0 & 0 \\ 0 & 0 & 0 & 0 & C_{44}^{TI} & 0 \\ 0 & 0 & 0 & 0 & 0 & C_{11}^{TI} - C_{12}^{TI} \end{bmatrix}, \tag{2.10}$$

where

$$\begin{aligned} C_{11}^{TI} &= \frac{1}{8}(3C_{11} + 3C_{22} + 2C_{12} + 2C_{66}), \\ C_{12}^{TI} &= \frac{1}{8}(C_{11} + C_{22} + 6C_{12} - 2C_{66}), \\ C_{13}^{TI} &= \frac{1}{2}(C_{13} + C_{23}), \\ C_{33}^{TI} &= C_{33}, \\ C_{44}^{TI} &= \frac{1}{2}(C_{44} + C_{55}). \end{aligned} \tag{2.11}$$

C^{TI} is the closest TI elasticity tensor to C in the coordinate system $\{\mathbf{e_1}, \mathbf{e_2}, \mathbf{e_3}\}$ and the normal of the symmetry plane of C^{TI} is parallel to $\mathbf{e_3}$.

Since C^{sym} is the Euclidean projection of C onto the linear subspace $\mathcal{L}^{sym}$, $C - C^{sym}$ and C^{sym} are perpendicular to each other. Then, we have the following equality which is by Moakher and Norris [37]

$$||C - C^{sym}||^2 = ||C||^2 - ||C^{sym}||^2. \tag{2.12}$$

Note that Equation 2.12 is analogous to Pythagoras theorem in 3D.

Based on the Equation 2.12, we can redefine the distance, which is expressed in Equation 2.5, of an elasticity tensor to the space of tensors belonging to a particular symmetry class as

Definition 3 *The distance of C to $\mathcal{L}^{sym}$ is*

$$d(C, \mathcal{L}^{sym}) := ||C||^2 - ||C^{sym}||^2, \tag{2.13}$$

where $C^{sym} \in \mathcal{L}^{sym}$ is the projection of C onto $\mathcal{L}^{sym}$ and sym is one of the seven symmetry classes of elasticity tensors.

Note that we choose to consider the square of the Expression 2.5 for the definition of distance. Using Definition 3 and the projected matrix C^{mono} in Expression 2.9 , we can write the distance to monoclinic symmetry in the coordinate system $\{\mathbf{e_1}, \mathbf{e_2}, \mathbf{e_3}\}$ in terms of the components of a general anisotropic tensor C as

$$d(C, \mathcal{L}^{mono}) = 2(C_{14}^2 + C_{24}^2 + C_{34}^2 + C_{15}^2 + C_{25}^2 + C_{35}^2 + C_{46}^2 + C_{56}^2). \tag{2.14}$$

Similarly, we obtain the distance to TI as

$$\begin{aligned} d(C, \mathcal{L}^{TI}) \;=\; & C_{13}^2 + C_{23}^2 + C_{12}C_{66} - C_{44}C_{55} + 2(C_{45}^2 + C_{14}^2 \\ & + C_{34}^2 + C_{25}^2 + C_{36}^2 + C_{15}^2 + C_{56}^2 + C_{24}^2 + C_{16}^2 + C_{35}^2 + C_{46}^2 \\ & + C_{26}^2 - C_{13}C_{23}) + \frac{1}{2}(C_{12}^2 + C_{44}^2 + C_{55}^2 + C_{66}^2 - C_{22}C_{66} \\ & - C_{11}C_{12} - C_{11}C_{66} - C_{12}C_{22}) + \frac{5}{8}(C_{11}^2 + C_{22}^2) - \frac{3}{4}C_{11}C_{22}. \end{aligned} \tag{2.15}$$

In this thesis, we define the distance function in such a way that it becomes a function of the rotation matrix so that it gives the value of the distance of the rotated C, namely $\bar{X}^T C \bar{X}$, to $\mathcal{L}^{sym}$, where $X \in SO(3)$. More precisely, we generalize the definition of the distance as follows:

Definition 4 *The distance function of X maps $\bar{X}^T C \bar{X}$ to $\mathcal{L}^{sym}$ by the following equation:*

$$\begin{aligned} d(\bar{X}^T C \bar{X}, \mathcal{L}^{sym}) : &= ||\bar{X}^T C \bar{X}||^2 - ||(\bar{X}^T C \bar{X})^{sym}||^2, \\ &= ||C||^2 - ||(\bar{X}^T C \bar{X})^{sym}||^2 \text{ since } ||C|| = ||\bar{X}^T C \bar{X}||, \end{aligned} \quad (2.16)$$

where $X \in SO(3)$ and $\bar{X} \in SO(6)$.

Note that $\bar{X}^T C \bar{X}$ is expressed in the coordinate system $\{X(\mathbf{e_1}), X(\mathbf{e_2}), X(\mathbf{e_3})\}$. It is important to note that the norm of the projected C, namely $||C^{sym}||$, is not invariant whenever C is expressed in a rotated coordinate system. In other words, in general, $||C^{sym}|| \neq ||(\bar{X}^T C \bar{X})^{sym}||$ for any $\bar{X}$, where $\bar{X}$ is not a symmetry element of C. Therefore, the value of the expression for the distance in Definition 4 changes as $\bar{X}$ changes.

To find the best approximation for C in the space of monoclinic tensors, we minimize the value of $d(\bar{X}^T C \bar{X}, \mathcal{L}^{mono})$ over all rotation tensors $X \in SO(3)$. To do so, firstly we calculate $C' = \bar{X} C \bar{X}^T$ as a function of $X \in SO(3)$ and find the projection of C' by substituting the resulting entries of C' in Equation 2.14. Then, we minimize the resulting expression. It is a very long expression and highly nonlinear. Thus, even for a computer programme, it is difficult to compute the absolute minimum of it because of many local extrema.

However, the distance function to monoclinic and transversely isotropic symmetries are special cases among other distance functions. Both of the distance functions,

namely $d(C, \mathcal{L}^{mono})$ and $d(C, \mathcal{L}^{TI})$, are invariant under the rotations around the $\mathbf{e_3}$-axis. This is formally stated as

Theorem 1 *Let C be an elasticity matrix. Let $A \in SO(3)$ such that its rotation axis is $\mathbf{e_3}$. Then*

$$d(C, \mathcal{L}^{sym}) = d(\bar{A}^T C \bar{A}, \mathcal{L}^{sym}),$$

where *sym* is either monoclinic or TI.

Before proving Theorem 1, we will state some lemmas that are used in the proof of the theorem.

Lemma 2 *Let C be an elasticity matrix and let $A \in SO(3)$ be any orthogonal transformation. Then we have the following equality:*

$$d(\bar{A}^T C \bar{A}, \mathcal{L}^{sym}) = d(C, \bar{A}\mathcal{L}^{sym}\bar{A}^T), \tag{2.17}$$

where sym is one of the seven symmetry classes.

PROOF. Note that $\bar{A}\mathcal{L}^{sym}\bar{A}^T$ is the space of elasticity tensors which belong to the symmetry class, *sym*, but are expressed in the coordinate system $\{A^T(\mathbf{e_1}), A^T(\mathbf{e_2}), A^T(\mathbf{e_3})\}$. Thus, the closest tensor to C in that coordinate system is found by averaging over the group $AG^{sym}A^T$, where G^{sym} is the group expressed in the basis $\{\mathbf{e_1}, \mathbf{e_2}, \mathbf{e_3}\}$. In formal terms, the closest tensor to C in the linear space $\bar{A}\mathcal{L}^{sym}\bar{A}^T$, which we denote by $C^{\overline{sym}}$, is found by the following equations:

$$\begin{aligned} C^{\overline{sym}} &= \int_{X \in AG^{sym}A^T} \bar{X}^T C \bar{X} \\ &= \int_{G \in G^{sym}} (\bar{A}\bar{G}\bar{A}^T)^T C (\bar{A}\bar{G}\bar{A}^T) \\ &= \int_{G \in G^{sym}} \bar{A}\bar{G}^T\bar{A}^T C \bar{A}\bar{G}\bar{A}^T \\ &= \bar{A}\left(\int_{G \in G^{sym}} \bar{G}^T\bar{A}^T C \bar{A}\bar{G}\right)\bar{A}^T. \end{aligned} \tag{2.18}$$

Now, the left-hand side of Equation 2.17 can be written as

$$\begin{aligned} d(\bar{A}^T C \bar{A}, \mathcal{L}^{sym}) &= ||\bar{A}^T C \bar{A}||^2 - ||(\bar{A}^T C \bar{A})^{sym}||^2 \\ &= ||C||^2 - ||(\bar{A}^T C \bar{A})^{sym}||^2 \text{ since } ||C|| = ||(\bar{A}^T C \bar{A})||^2 \\ &= ||C||^2 - ||\int_{G \in G^{sym}} G^T \bar{A}^T C \bar{A} G||^2. \end{aligned} \tag{2.19}$$

In order to find the right-hand side of Equation 2.17, namely $d(C, \bar{A}\mathcal{L}^{sym}\bar{A}^T)$, one should consider the norm of the closest elasticity tensor to C in the linear space $\bar{A}\mathcal{L}^{sym}\bar{A}^T$. Thus, by using Equation 2.18, we get

$$\begin{aligned} d(C, \bar{A}\mathcal{L}^{sym}\bar{A}^T) &= ||C||^2 - ||C^{\overline{sym}}||^2 \\ &= ||C||^2 - ||\bar{A}\left(\int_{G \in G^{sym}} \bar{G}^T \bar{A}^T C \bar{A} \bar{G}\right)\bar{A}^T|| \\ &= ||C||^2 - ||\int_{G \in G^{sym}} \bar{G}^T \bar{A}^T C \bar{A} \bar{G}||. \end{aligned} \tag{2.20}$$

Since expressions 2.20 and 2.19 are equal, we have the desired result.

■

Lemma 3 *Let $A \in SO(3)$ be any orthogonal transformation such that its rotation axis is $\mathbf{e_3}$. Then*

$$\bar{A}\mathcal{L}^{mono}\bar{A}^T = \mathcal{L}^{mono}, \tag{2.21}$$

where $\bar{A} \in SO(6)$ is the 6D orthogonal transformation of $A \in SO(3)$.

PROOF. Note that $C \in \bar{A}\mathcal{L}^{mono}\bar{A}^T$ means that if $X \in AG^{mono}A^T$ then $\bar{X}^T C \bar{X} = C$, where

$$A = \begin{bmatrix} \cos\theta & -\sin\theta & 0 \\ \sin\theta & \cos\theta & 0 \\ 0 & 0 & 1 \end{bmatrix}, \text{ for any } \theta \in [0, 2\pi) \tag{2.22}$$

and $G^{Mono} = \{\pm I, \pm M_{\mathbf{e_3}}\}$, where

$$M_{\mathbf{e_3}} = \begin{bmatrix} 1 & 0 & 0 \\ 0 & 1 & 0 \\ 0 & 0 & -1 \end{bmatrix}. \tag{2.23}$$

In order to show $\mathcal{L}^{mono} = \bar{A}\mathcal{L}^{mono}\bar{A}^T$, assume that $C \in \mathcal{L}^{mono}$. Then we get the following logical sentences:

$$\begin{aligned} \bar{M}_{\mathbf{e_3}}{}^T C \bar{M}_{\mathbf{e_3}} = C \quad &\Longleftrightarrow \quad (\bar{A}\bar{A}^T)\bar{M}_{\mathbf{e_3}}{}^T C \bar{M}_{\mathbf{e_3}}(\bar{A}\bar{A}^T) = C \text{ since } \bar{A}\bar{A}^T = I \\ &\Longleftrightarrow \quad \bar{A}\bar{M}_{\mathbf{e_3}}{}^T \bar{A}^T C \bar{A}\bar{M}_{\mathbf{e_3}}\bar{A}^T = C \end{aligned}$$

since A and $M_{\mathbf{e_3}}$ commutes so does $\bar{A}$ and $\bar{M}_{\mathbf{e_3}}$.

$$\Longleftrightarrow \quad (\bar{A}\bar{M}_{\mathbf{e_3}}\bar{A}^T)^T C (\bar{A}\bar{M}_{\mathbf{e_3}}\bar{A}^T) = C. \tag{2.24}$$

Thus, $C \in \bar{A}\mathcal{L}^{mono}\bar{A}^T$ since $AM_{\mathbf{e_3}}A^T \in AG^{mono}A^T$ and similar relations hold for the other symmetry elements of G^{mono}, namely $-M_{\mathbf{e_3}}, \pm I$. The inverse also follows because of the if and only if statements in Expressions 2.24. ■

Now, we can prove Theorem 1 by using the above lemmas.

PROOF. Note that the result of Lemma 3 trivially holds for TI symmetry. More precisely, we have

$$\bar{A}\mathcal{L}^{TI}\bar{A}^T = \mathcal{L}^{TI}, \tag{2.25}$$

where $A \in SO(3)$ be any orthogonal transformation such that its rotation axis is $\mathbf{e_3}$. That is because $A \in G^{TI}$.

Now, consider the following equations:

$$\begin{aligned} d(\bar{A}^T C \bar{A}, \mathcal{L}^{sym}) &= d(C, \bar{A}\mathcal{L}^{sym}\bar{A}^T) \text{ by Lemma 2} && (2.26) \\ &= d(C, \mathcal{L}^{sym}) \text{ by Lemma 3} && (2.27) \end{aligned}$$

Thus, we get the equalities that we want to show, namely $d(\bar{A}^T C \bar{A}, \mathcal{L}^{sym}) = d(C, \mathcal{L}^{sym})$ where sym is either monoclinic or TI. ■

Theorem 1 leads to the following corollary.

Corollary 4 *Let C be an elasticity tensor and $A \in SO(3)$ be any rotation matrix such that $A = Z_1 Z_2 Z_3$ where Z_1, Z_2 and Z_3 are defined in Equations 1.11, 1.12 and 1.13, respectively. Then,*

$$d(\bar{A}^T C \bar{A}, \mathcal{L}^{sym}) = d((\bar{Z}_1 \bar{Z}_2 \bar{Z}_3)^T C (\bar{Z}_1 \bar{Z}_2 \bar{Z}_3), \mathcal{L}^{sym}) = d((\bar{Z}_1 \bar{Z}_2)^T C (\bar{Z}_1 \bar{Z}_2), \mathcal{L}^{sym}), \tag{2.28}$$

where sym is either TI or monoclinic.

In Corollary 4, Z_3 is the orthogonal transformation whose rotation axis is $\mathbf{e_3}$. This property of monoclinic and TI symmetries allows us to reduce one parameter in the formulation of $d(\bar{A}^T C \bar{A}, \mathcal{L}^{sym})$. This reduction is due to the omission of one of the Euler angles that is used to express the rotation tensor A. As mentioned in Section 1.2, according to Euler's rotation theorem any rotation tensor in 3D can be decomposed as a product of three elementary rotations, namely around $\mathbf{e_3}$-, $\mathbf{e_1}$- and $\mathbf{e_3}$-axes. The two first elementary rotations determine the new $\mathbf{e_3}$-axis, namely $\mathbf{e_3'}$-axis, and the third elementary rotation will obtain all the orientation possibilities that this $\mathbf{e_3'}$-axis allows. Due to the Corollary 4, one can omit the third elementary rotation since it does not change the values of $d(\bar{A}^T C \bar{A}, \mathcal{L}^{mono})$ and $d(\bar{A}^T C \bar{A}, \mathcal{L}^{TI})$. Then, the rotation tensor A has one fewer parameter, as do the distance functions $d(\bar{A}^T C \bar{A}, \mathcal{L}^{mono})$ and $d(\bar{A}^T C \bar{A}, \mathcal{L}^{TI})$.

The reduction of a parameter for monoclinic and TI symmetry allows us to plot the distance function $d(\bar{X}^T C \bar{X}, \mathcal{L}^{sym})$ on a two-dimensional sphere in 3D, namely onto the surface of the sphere. Points on the unit-sphere represent a vector in 3D, more precisely each point is the vector $X(\mathbf{e_3})$, which is the z-axis of $\bar{X}^T C \bar{X}$. The color associated with the vector $X(\mathbf{e_3})$ represents the value of the distance function of $\bar{X}^T C \bar{X}$ to monoclinic or TI symmetry class. Note that the spherical coordinates of the vector $X(\mathbf{e_3})$, where X is in the form 1.14, can be written as

$$X(\mathbf{e_3}) = \left(\cos(\psi - \frac{\pi}{2}) \sin\phi, \sin(\psi - \frac{\pi}{2}) \sin\phi, \cos\phi\right). \tag{2.29}$$

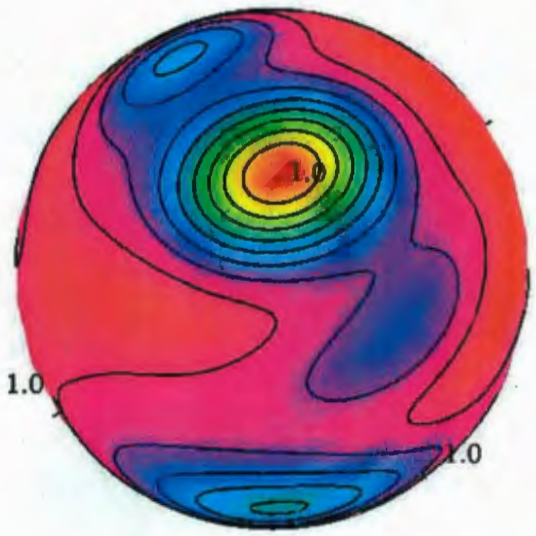

Figure 2.2: The plot of the distance function $d(\bar{X}^T C \bar{X}, \mathcal{L}^{TI})$ for a generally anisotropic C. The orange spot locates the orientation of the z-axis of the elasticity tensor where it is closest to TI symmetry, in other words, it is the orientation where the minimum of TI-distance function achieved. 1.0 locates the orientation of the coordinate system $(\mathbf{e_1}, \mathbf{e_2}, \mathbf{e_3})$.

Refer to Figure 2.2 to examine the plot of a distance function. The scale of the colors are shown in Figure 2.3. We will examine the applications of plotting in the next sections.

Note that the distance function takes equal values at antipodal points on the sphere. Thus, three views of a plot show all there is to see without distortion near boundary of projection.

Plotting the distance functions makes the minimization problem of the nonlinear expression, namely $d(\bar{X}^T C \bar{X}, \mathcal{L}^{mono})$ and $d(\bar{X}^T C \bar{X}, \mathcal{L}^{TI})$ solvable. This is because, after observing the plot, one restricts the search for the minimum to a subset of the two-dimensional sphere. Then, a computer programme can calculate the minimum of the distance function. In this restricted region, not only the value of the distance of

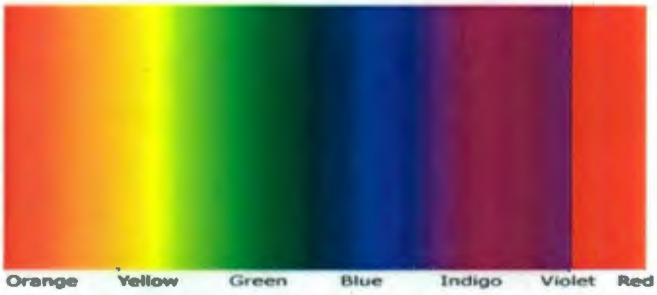

Figure 2.3: The scale of colours in the plot of monoclinic- and TI-distance functions. Orange indicates the minimum and red indicates the maximum of the function.

C to monoclinic or TI is calculated, but also the orientation of the closest monoclinic or TI tensor is achieved. For example, to obtain the exact value of the distance function of TI, one first determines the orientation of the orange region from Figure 2.2. It is possible to do that by using the plotting options of the computer programme in which the plot is drawn. Then, one can use the minimization command for the distance function $d(\bar{X}^T C \bar{X}, \mathcal{L}^{TI})$ around the orange region.

The fundamental reason for the reduction of the parameters in the case of monoclinic and TI symmetry is that both of the symmetry classes are represented by one symmetry plane. Hence their natural-coordinate system can be represented by one axis, namely the normal of the symmetry plane. Thus, two Euler angles of a rotation tensor is enough to rotate the coordinate system of C to any other orientation since z-axis of C determines the coordinate system.

2.2 Identifying Symmetries of Elasticity Tensor

In this section, we show how the plotting of the distance function $d(\bar{X}^T C \bar{X}, \mathcal{L}^{mono})$ can help us to identify the symmetries of an elasticity tensor.

The plots of the distance functions to monoclinic and TI, namely $d(\bar{X}^T C \bar{X}, \mathcal{L}^{mono})$ and $d(\bar{X}^T C \bar{X}, \mathcal{L}^{TI})$, reflect the symmetry of the medium. Thus, if the tensor has a tetragonal symmetry, one observes that the plot has a four-fold symmetry, five symmetry planes where four of them contain the rotation axis and they are 45 degrees apart from each other and the other symmetry plane is perpendicular to the rotation axis. Furthermore, the monoclinic-distance function vanishes in the directions of the normal of each symmetry plane. Hence, one can determine the orientations of the normals of the symmetry planes by determining the zeros of the distance function. Now, we will prove these statements.

Theorem 5 *Let C be an elasticity tensor which is expressed in any coordinate system and assume that C belongs to one of the seven symmetry classes. Then, the distance function, namely $d(\bar{X}^T C \bar{X}, \mathcal{L}^{sym})$, is symmetric with respect to any elements of G_C. More precisely,*

$$d(\bar{X}^T C \bar{X}, \mathcal{L}^{sym}) = d((\bar{A}\bar{X})^T C (\bar{A}\bar{X}), \mathcal{L}^{sym}) \tag{2.30}$$

for any $X \in SO(3)$ and A any symmetry element of C.

PROOF. Since $A \in G_C$, we have $C = \bar{A}^T C \bar{A}$. Then

$$\begin{aligned} d((\bar{A}\bar{X})^T C (\bar{A}\bar{X}), \mathcal{L}^{sym}) &= d(\bar{X}^T \bar{A}^T C \bar{A} \bar{X}), \mathcal{L}^{sym}) \\ &= d(\bar{X}^T C \bar{X}), \mathcal{L}^{sym}). \end{aligned}$$

■

Since the distance functions are symmetric so are their plots. Thus, plots reflect the symmetry of a tensor if it has any. Another important theorem that we use to determine the symmetry class of C from the monoclinic plot is the following:

Theorem 6 *Let C be an elasticity tensor and assume that C has a mirror symmetry with respect to a plane whose normal is* $\mathbf{n}$. *Then the distance function of C to monoclinic symmetry vanishes whenever C is represented in a coordinate system where its z-axis is aligned with* $\mathbf{n}$. *In other words,*

$$d(\bar{A}^T C \bar{A}, \mathcal{L}^{mono}) = 0, \tag{2.31}$$

for $\{A \in SO(3) \mid A(\mathbf{e_3}) = \mathbf{n}\}$.

PROOF. Since C has one symmetry plane then it is at least monoclinic. Thus, the monoclinic-distance function of C vanishes whenever C is expressed in a coordinate system where z-axis is aligned with the normal of the symmetry plane. Thus, $d(\bar{A}^T C \bar{A}, \mathcal{L}^{mono}) = 0$ for $A \in SO(3)$ such that $A(\mathbf{e_3}) = \mathbf{n}$. ■

By using Theorem 6, we determine the orientations of the normals of the mirror planes by locating the zeros of the monoclinic-distance function from its plot. Theorem 5 implies that one can determine the symmetry of the elasticity tensor by recognizing the symmetric pattern of the plot of its distance function.

2.2.1 Identifying TI Symmetry

Now, we introduce examples of elasticity tensors belonging to different symmetry classes. These tensors can be represented in any coordinate system and we show how to identify their symmetry class by using the plot of their distance functions. For an isotropic medium, any coordinate axes is a natural coordinate system for its elasticity tensor. In other words, the form of the tensor is invariant under any orthogonal transformation. Thus, the problem of identifying the symmetry class of an isotropic tensor is trivial.

We start with TI elasticity tensor. The form of TI tensor is presented in Equation 1.23 whenever it is expressed in its natural-coordinate system, namely $\mathbf{e_3}$ is parallel to the rotation axis of C. Figure 2.4 shows the plot of the TI-distance function,

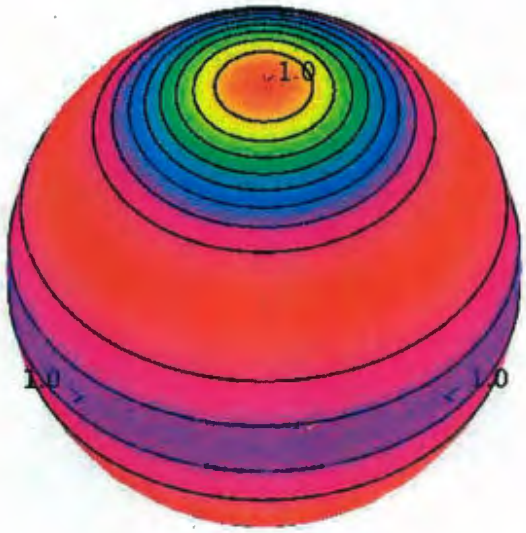

Figure 2.4: The plot of the distance function $d(\bar{X}^T C \bar{X}, \mathcal{L}^{TI})$ for C expressed in Equation 2.32. Three coordinate axes intersects the sphere at points 1.0 seen on the plot. The rotation axis of C is aligned with $\mathbf{e_3}$. The graph has infinitely-fold rotation around its rotation axis. The TI-distance function vanishes along $\mathbf{e_3}$-direction, namely $d(C, \mathcal{L}^{TI}) = 0$.

$d(\bar{X}^T C \bar{X}, \mathcal{L}^{TI})$ for all $X \in SO(3)$, for the elasticity tensor C expressed in the following matrix.

$$C = \begin{bmatrix} 104.12 & 31.09 & 36.62 & 0 & 0 & 0 \\ 31.09 & 104.12 & 36.62 & 0 & 0 & 0 \\ 36.62 & 36.62 & 82.49 & 0 & 0 & 0 \\ 0 & 0 & 0 & 52.84 & 0 & 0 \\ 0 & 0 & 0 & 0 & 52.84 & 0 \\ 0 & 0 & 0 & 0 & 0 & 73.02 \end{bmatrix}. \tag{2.32}$$

Observe that just as C has the infinite-fold rotation symmetry about the $\mathbf{e_3}$-

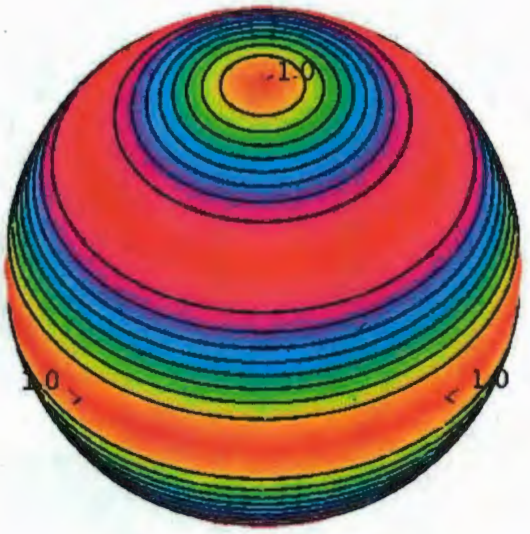

Figure 2.5: The plot of the distance function $d(\bar{X}^T C \bar{X}, \mathcal{L}^{mono})$ for C expressed in Equation 2.32. The function vanishes along $\mathbf{e_3}$-direction and any direction perpendicular to $\mathbf{e_3}$ as can be inferred from the orange color.

axis, so does the plot of its distance function which is a result of Theorem 5. The distance function vanishes for the orientation $\mathbf{e_3}$, namely $d(C, \mathcal{L}^{TI}) = 0$. This is expected because C, which is expressed in Equation 2.32, has TI symmetry. Thus, the distance function must vanish in the direction of the rotation axis of C. However, for any other direction the distance function does not vanish which can be seen from Figure 2.4.

Observe the plot of the distance function of the elasticity matrix, C, to the monoclinic symmetry from Figure 2.5.

As expected, the graph has a TI symmetry. The main difference of this plot from the TI-plot 2.4 is the number of directions where the distance function vanishes. The distance function to TI, namely $d(\bar{X}^T C \bar{X}, \mathcal{L}^{TI})$, vanishes only in the direction of the rotation axis whereas monoclinic distance function, $d(\bar{X}^T C \bar{X}, \mathcal{L}^{mono})$, vanishes in the directions of the normals of the symmetry planes which is a result of Theorem 6.

Recall that in TI symmetry group, there is one symmetry plane whose normal is the rotation axis and infinitely many planes that contain the rotation axis. Thus, monoclinic-distance function vanishes in any direction that is perpendicular to the rotation axis.

One can determine the orientation of the rotation axis of a TI elasticity tensor, which is represented in any coordinate system, by observing the plot of its distance function. Now, let us consider the elasticity tensor C', which is the TI tensor C rotated by an orthogonal transformation $A \in SO(3)$, namely $C' = \bar{A}^T C \bar{A}$. Equation 2.33 is the expression of the elasticity tensor C'.

$$
\begin{aligned}
C' &= \begin{bmatrix}
91.71 & 33.91 & 38.40 & 1.13 & -7.61 & -1.32 \\
33.91 & 103.68 & 33.99 & -1.78 & 3.93 & -1.75 \\
38.40 & 33.99 & 91.38 & -1.32 & -7.53 & 1.13 \\
1.13 & -1.78 & -1.32 & 62.74 & -1.06 & -9.82 \\
-7.61 & 3.93 & -7.53 & -1.06 & 56.87 & -1.11 \\
-1.32 & -1.75 & 1.13 & -9.82 & -1.11 & 63.04
\end{bmatrix}, \qquad (2.33) \\
&= \bar{A}^T \begin{bmatrix}
104.12 & 31.09 & 36.62 & 0 & 0 & 0 \\
31.09 & 104.12 & 36.62 & 0 & 0 & 0 \\
36.62 & 36.62 & 82.49 & 0 & 0 & 0 \\
0 & 0 & 0 & 52.84 & 0 & 0 \\
0 & 0 & 0 & 0 & 52.84 & 0 \\
0 & 0 & 0 & 0 & 0 & 73.02
\end{bmatrix} \bar{A},
\end{aligned}
$$

where $\bar{A}$ is the 6×6 matrix obtained by applying Equation A.51 to the 3D rotation matrix

$$
A = \begin{bmatrix}
-\cos\frac{4\pi}{9} & -\frac{\sqrt{2}}{2}\sin\frac{4\pi}{9} & \frac{\sqrt{2}}{2}\sin\frac{4\pi}{9} \\
\sin\frac{4\pi}{9} & -\frac{\sqrt{2}}{2}\cos\frac{4\pi}{9} & \frac{\sqrt{2}}{2}\cos\frac{4\pi}{9} \\
0 & \frac{\sqrt{2}}{2} & \frac{\sqrt{2}}{2}
\end{bmatrix}.
$$

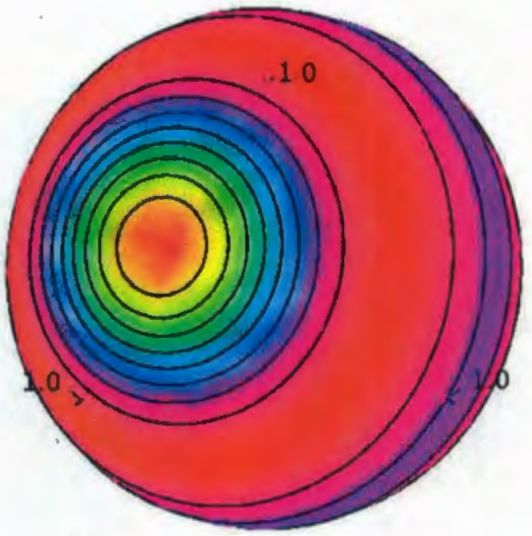

Figure 2.6: The plot of the distance function $d(\bar{X}^T C' \bar{X}, \mathcal{L}^{TI})$ for C' expressed in Equation 2.33. The rotation axis of C' is not aligned with $\mathbf{e_3}$-axis. In other words, it is not expressed in its natural coordinate system. However, the plot reveals the symmetries of C.

The TI symmetry of C' is not obvious because C' is not expressed in its natural coordinate system, namely its rotation axis is not parallel to $\mathbf{e_3}$. Thus, by observing the elasticity matrix it is impossible to understand its symmetry class. However, the plot of its distance function, $d(\bar{X}^T C' \bar{X}, \mathcal{L}^{TI})$, reveals its symmetry class. See Figure 2.6.

Moreover, one can determine the exact orientation of the rotation axis of C' from the plot. Figure 2.6 is the orthogonal projection of the sphere onto the plane whose normal is the vector $(1, 1, 1)$. In other words, the plot is the view of the sphere from $(1, 1, 1)$ direction. Similarly, all the other plots are orthogonal projections onto some plane. The orientation of the rotation axes of the elasticity tensor can be located using the point locater function of the computer program Maple, which is used for plotting the distance function. Thus, one can determine the location of any point on

the sphere by using the point locator option. To view the sphere from different points of view, one can turn the plot in any direction by dragging the mouse. This option of Maple makes the determination of the symmetry of the medium easier.

A more precise method to locate the exact orientation of the rotation axis is that after determining the direction of the axis by using the point locater one makes a restricted search for the minimum of the distance function. By restricted search, we mean to minimize the distance function in a small region around the direction of the rotation axis. As we have mentioned earlier, since the distance function is highly nonlinear the minimization over the unit sphere does not, in general, give the correct value. However, restricting the region for finding the minimum works if there are not several extrema in that region. Observing the graph of the distance function enables us to choose such a region. The direction, where the TI-distance function vanishes, is the orientation of the rotation axis.

2.2.2 Identifying Cubic Symmetry

Now, we consider a cubic elasticity tensor:

$$C^{cubic} = \begin{bmatrix} 3 & 2 & 2 & 0 & 0 & 0 \\ 2 & 3 & 2 & 0 & 0 & 0 \\ 2 & 2 & 3 & 0 & 0 & 0 \\ 0 & 0 & 0 & 8 & 0 & 0 \\ 0 & 0 & 0 & 0 & 8 & 0 \\ 0 & 0 & 0 & 0 & 0 & 8 \end{bmatrix}. \tag{2.34}$$

The plot of the distance function of C^{cubic} to monoclinic symmetry can be seen in Figure 2.7 and 2.8.

Recall that the symmetry group of the cubic elasticity tensor is

$$G^{Cubic} = \{A \in O(3) \mid A(e_i) = \pm e_j \text{ for any } i, j \in \{1, 2, 3\}\}. \tag{2.35}$$

Figure 2.7: The plot of the distance function $d(\bar{X}^T C \bar{X}, \mathcal{L}^{mono})$ for C^{cubic} expressed in Equation 2.34. The three-fold rotation axis can be observed from the diagonal view of the sphere. The function does not vanish along the diagonal-axis since there is no symmetry plane perpendicular to this direction.

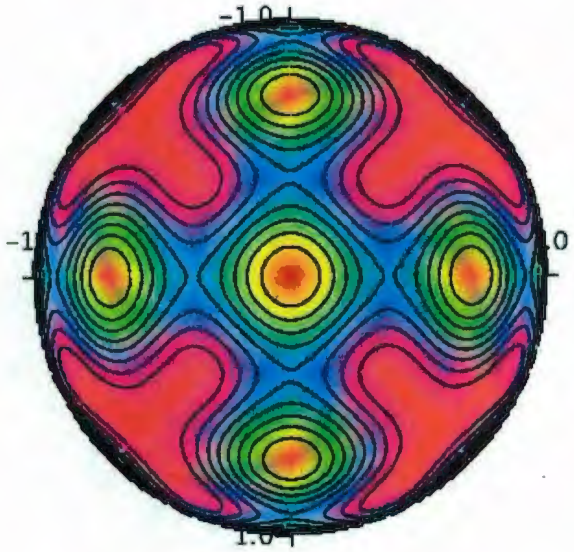

Figure 2.8: The plot of the distance function $d(\bar{X}^T C \bar{X}, \mathcal{L}^{mono})$ for C^{cubic} expressed in 2.34. The four-fold rotation axis can be observed from the $\mathbf{e_3}$-axis view of the sphere. The function vanishes along $\mathbf{e_3}$-axis since there is a symmetry plane perpendicular to this direction. As expected in cubic symmetry, the coordinate axis is aligned with a four-fold rotation axis.

More explicitly, the symmetry elements of the cubic group can be written as

$$G^{Cubic} =< G^{Tetra} \cup G^{Trigo} >, \tag{2.36}$$

which can be inferred from Figure 1.2. Thus, one can observe both tetragonal and trigonal symmetries in a cubic medium. More precisely, there are three four-fold rotation axes in cubic symmetry where they are parallel to the coordinate axes and four three-fold axes which are parallel to the four diagonals of the cube. The relation between the mirror planes and rotation axes in the groups of G^{Tetra} and G^{Trigo} is also valid in the cubic group, namely G^{Cubic}. In other words, to visualize all the symmetry planes in a cubic medium, one first determines the rotation axes and then substitutes the symmetry planes associated with each of the rotation axes. Consider Figure 2.8 which is a view of the distance function plot along $\mathbf{e_3}$-axis. Since $\mathbf{e_3}$-axis is one of the three four-fold rotation axes, it is associated with four symmetry planes that contain the axis and the angle between any two planes is either $\frac{\pi}{4}$ or $\frac{\pi}{2}$. Since the views from other coordinate axes are identical to $\mathbf{e_3}$-axis view one can observe these mirror planes associated with $\mathbf{e_2}$-axis from Figure 2.8. The rotation axis is also associated with a symmetry plane whose normal is $\mathbf{e_3}$. Figure 2.7 is the diagonal view of the sphere. As expected, one can observe one of the four three-fold axes from the figure. The associated symmetry planes of this rotation axis are the mirror planes of a trigonal medium, namely three planes that contains the three-fold rotation axis with angle between any two planes being $\frac{\pi}{3}$. Note that the three-fold symmetry axis is not a normal of a symmetry plane. Thus, we do not observe a minimum along the rotation axis. The other three diagonals have identical views.

Similar to a TI medium, a rotated cubic elastic tensor can be identified from its plot. Let us rotate the cubic tensor C^{cubic}, expressed in Equation 2.34, by any orthogonal transformation $A \in SO(3)$, with $A(\mathbf{e_3}) = (\sin\frac{\pi}{6}\cos\frac{\pi}{9}, \sin\frac{\pi}{6}\sin\frac{\pi}{9}, \cos\frac{\pi}{6})$. Then, the entities of the rotation matrix can be found by applying Equation 1.9 or

Equation 1.14 as

$$A = \begin{bmatrix} -\cos\frac{7\pi}{18} & -\frac{\sqrt{3}}{2}\sin\frac{7\pi}{18} & \frac{1}{2}\sin\frac{7\pi}{18} \\ \sin\frac{7\pi}{18} & -\frac{\sqrt{3}}{2}\cos\frac{7\pi}{18} & \frac{1}{2}\cos\frac{7\pi}{18} \\ 0 & \frac{1}{2} & \frac{\sqrt{3}}{2} \end{bmatrix}.$$

Note that this is not the only A that satisfies $A(\mathbf{e_3}) = (\sin\frac{\pi}{6}\cos\frac{\pi}{9}, \sin\frac{\pi}{6}\sin\frac{\pi}{9}, \cos\frac{\pi}{6})$. After finding the 6×6 rotation matrix which can be obtained by applying Equation A.51 to the 3D rotation matrix A, one rotates the elasticity tensor C^{cubic} to find C':

$$C' = \begin{bmatrix} 6.49 & 0.82 & -0.31 & 0.65 & 1.78 & -1.38 \\ 0.82 & 4.48 & 1.69 & 0.08 & 0.23 & 2.57 \\ -0.31 & 1.69 & 5.62 & -0.73 & -2.01 & -1.19 \\ 0.65 & 0.08 & -0.73 & 7.38 & -1.68 & 0.33 \\ 1.78 & 0.23 & -2.01 & -1.68 & 3.36 & 0.91 \\ -1.38 & 2.57 & -1.19 & 0.33 & 0.91 & 5.65 \end{bmatrix} \tag{2.37}$$

$$= \bar{A}^T \begin{bmatrix} 3.00 & 2.00 & 2.00 & 0 & 0 & 0 \\ 2.00 & 3.00 & 2.00 & 0 & 0 & 0 \\ 2.00 & 2.00 & 3.00 & 0 & 0 & 0 \\ 0 & 0 & 0 & 8.00 & 0 & 0 \\ 0 & 0 & 0 & 0 & 8.00 & 0 \\ 0 & 0 & 0 & 0 & 0 & 8.00 \end{bmatrix} \bar{A}. \tag{2.38}$$

The plot of the distance function of the C' looks similar to C^{cubic} except that it is rotated. See Figure 2.9.

Observing the sphere by dragging the mouse in Maple, one can see the symmetry planes and the rotation axes of the cubic medium. The orientation of these features can be obtained by using the point locater in the Maple Plot and then making a restricted search around those directions.

Figure 2.9: The plot of the distance function $d(\bar{X}^T C' \bar{X}, \mathcal{L}^{mono})$ for C' expressed in Equation 2.37. The four-fold rotation axis can be observed along the direction that is 30° to $\mathbf{e_3}$. Note that the symmetry directions are not aligned with the coordinate axes $\{\mathbf{e_1}, \mathbf{e_2}, \mathbf{e_3}\}$.

Figure 2.10: The plot of the distance function $d(\bar{X}^T C \bar{X}, \mathcal{L}^{mono})$ for C expressed in Equation 2.39. The symmetry directions are not aligned with the coordinate axes $\{\mathbf{e_1}, \mathbf{e_2}, \mathbf{e_3}\}$. The plot suggests that C may have a tetragonal symmetry.

2.2.3 Identifying Tetragonal Symmetry

Now, we consider elasticity tensor C expressed in Equation 2.39:

$$C = \begin{bmatrix} 5.70499 & 1.52344 & 1.62834 & -0.65988 & -1.56095 & 0.91892 \\ 1.52344 & 5.03989 & 1.64179 & -1.18797 & 0.77658 & -1.40593 \\ 1.62834 & 1.64179 & 3.66794 & 0.03736 & 0.01585 & 0.00984 \\ -0.65988 & -1.18797 & 0.03736 & 3.33133 & -0.09854 & 0.91711 \\ -1.56095 & 0.77658 & 0.01585 & -0.09854 & 3.52165 & -1.35995 \\ 0.91892 & -1.40593 & 0.00984 & 0.91711 & -1.35995 & 3.73418 \end{bmatrix}. \quad (2.39)$$

Figures 2.10, 2.11 and 2.12 show the plot of the monoclinic distance function of the above C.

By observing the plots one can see that the elasticity tensor C has a tetragonal

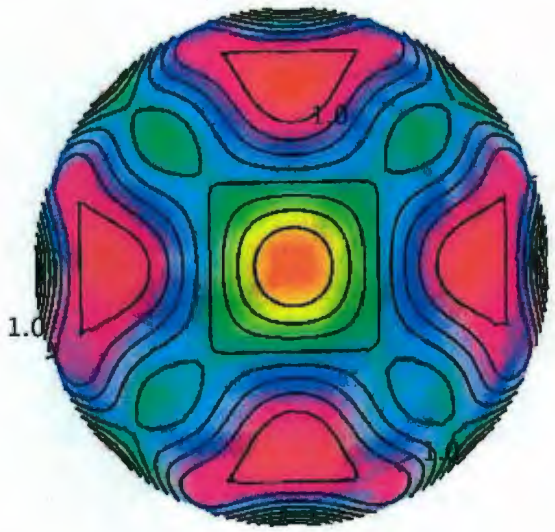

Figure 2.11: The plot of the distance function $d(\bar{X}^T C \bar{X}, \mathcal{L}^{mono})$ for C expressed in Equation 2.39 viewed from the four-fold rotation axis. Existence of a mirror plane, whose normal is along this direction, can be inferred from the orange color which implies a zero of the distance function.

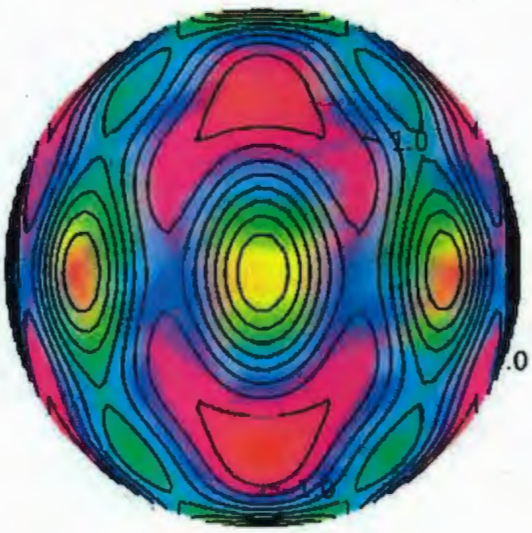

Figure 2.12: The plot of the distance function $d(\bar{X}^T C \bar{X}, \mathcal{L}^{mono})$ for C expressed in Equation 2.39 viewed from a direction perpendicular to the rotation axis. Existence of the mirror planes along this direction and 45° apart in either way from this direction can be observed. These mirror planes are expected in a tetragonal symmetry.

symmetry. By using the point locater in Maple, we roughly determined the location of the rotation axis from the plot as $(\sin\frac{35\pi}{180}\cos\frac{65\pi}{180}, \sin\frac{35\pi}{180}\sin\frac{65\pi}{180}, \cos\frac{35\pi}{180})$. In order to obtain the exact orientation of the rotation axis, we minimize the distance function $d(\bar{X}^T C\bar{X}, \mathcal{L}^{mono})$, around the 10° neighbourhood along this vector. We find that the distance function vanishes along the direction $(\sin\frac{34\pi}{180}\cos\frac{67\pi}{180}, \sin\frac{34\pi}{180}\sin\frac{67\pi}{180}, \cos\frac{34\pi}{180})$. Note that in tetragonal symmetry the four-fold rotation axis is also a normal of one of the symmetry planes which is stated in Equation 1.24. Thus, the distance function vanishes in the direction of the four-fold rotation axis for tetragonal symmetry. In general, this coincidence of the rotation axis being a normal of a symmetry plane holds except for three-fold rotation axes which exist in trigonal and cubic symmetries. We discuss the method of how to locate the three-fold axis in a trigonal symmetry in the next section.

Next, we find the orthogonal transformation that rotates the coordinates of the elasticity matrix C so that the tensor is expressed in its natural coordinate system. More precisely, we are seeking $A \in SO(3)$ such that $C' = \bar{A}^T C\bar{A}$ is in its natural coordinate system, i.e. it has the form of the matrix 1.25. Note that since tetragonal symmetry has two sets of two orthogonal directions where all directions lie in a symmetry plane and orthogonal to the rotation axis, it has two natural coordinate systems. Without loss of generality, we can choose one of the two sets. Although the entities of the elasticity matrix depend on our choice, they both represent the same tetragonal medium.

Figure 2.12 shows the coordinate axes that we have chosen for the tetragonal tensor C. By minimizing the distance function around the region shown in the center of Figure 2.12, it is found that the function vanishes along the direction $\left(\sin\frac{124\pi}{180}\cos\frac{67\pi}{180}, \sin\frac{124\pi}{180}\sin\frac{67\pi}{180}, \cos\frac{124\pi}{180}\right)$. Similarly, the other coordinate axis can be found as $\left(\cos\frac{157\pi}{180}, \sin\frac{157\pi}{180}, 0\right)$. Now, we will find the rotation matrix that transforms the coordinate system formed by the four-fold rotation axis and two directions

which are aligned with the normals of the symmetry planes to the coordinate system $\{\mathbf{e_1}, \mathbf{e_2}, \mathbf{e_3}\}$. We formally write this as

$$\begin{aligned} A(\mathbf{e_1}) &= \left(\sin\frac{124\pi}{180}\cos\frac{67\pi}{180}, \sin\frac{124\pi}{180}\sin\frac{67\pi}{180}, \cos\frac{124\pi}{180}\right), \\ A(\mathbf{e_2}) &= \left(\cos\frac{157\pi}{180}, \sin\frac{157\pi}{180}, 0\right), \\ A(\mathbf{e_3}) &= \left(\sin\frac{34\pi}{180}\cos\frac{67\pi}{180}, \sin\frac{34\pi}{180}\sin\frac{67\pi}{180}, \cos\frac{34\pi}{180}\right), \end{aligned}$$

where $A \in SO(3)$. To find the entries of such an orthogonal transformation A, one can use Equation 1.9 or solve the above linear equations for A. Then, A is obtained by writing the above vectors as the columns of it:

$$A = \begin{bmatrix} \sin\frac{124\pi}{180}\cos\frac{67\pi}{180} & \cos\frac{157\pi}{180} & \sin\frac{34\pi}{180}\cos\frac{67\pi}{180} \\ \sin\frac{124\pi}{180}\sin\frac{67\pi}{180} & \sin\frac{157\pi}{180} & \sin\frac{34\pi}{180}\sin\frac{67\pi}{180} \\ \cos\frac{124\pi}{180} & 0 & \cos\frac{34\pi}{180} \end{bmatrix}. \tag{2.40}$$

After finding the 6D rotational matrix of A by applying equation A.51, we can express C in its natural coordinate system as

$$\begin{aligned} C' &= \bar{A}^T C \bar{A} \\ &= \begin{bmatrix} 5.00000 & 3.00000 & 1.00000 & 0.00000 & 0.00000 & 0.00000 \\ 3.00000 & 5.00000 & 1.00000 & 0.00000 & 0.00000 & 0.00000 \\ 1.00000 & 1.00000 & 4.00000 & 0.00000 & 0.00000 & 0.00000 \\ 0.00000 & 0.00000 & 0.00000 & 2.00000 & 0.00000 & 0.00000 \\ 0.00000 & 0.00000 & 0.00000 & 0.00000 & 2.00000 & 0.00000 \\ 0.00000 & 0.00000 & 0.00000 & 0.00000 & 0.00000 & 7.00000 \end{bmatrix}. \end{aligned} \tag{2.41}$$

where $\bar{A}$ that acts on C in the above equation is a 6D-rotational matrix of A in Equation 2.40. In this example, we consider five decimal points. However, the computations done in a computer, can be made by considering as many digits as possible

depending on how much accuracy is wanted. For the examples that are given in rest of the thesis, the calculations are performed by using eighteen-digit precision mode, even though we write only two decimal points.

Note that one can equivalently choose one of the coordinate axes of C as the vector which is 90° rotated from the one shown in Figure 2.12. Then the orthogonal transformation matrix A', which is used to represent C in its natural coordinate system, will be different than A in Equation 2.40. More precisely, A' is of the form:

$$A' = \begin{bmatrix} -\cos\frac{23\pi}{180} & -\sin\frac{23\pi}{180}\cos\frac{34\pi}{180} & \sin\frac{23\pi}{180}\sin\frac{34\pi}{180} \\ \sin\frac{23\pi}{180} & -\cos\frac{23\pi}{180}\cos\frac{34\pi}{180} & \cos\frac{23\pi}{180}\sin\frac{34\pi}{180} \\ 0 & \sin\frac{34\pi}{180} & \cos\frac{34\pi}{180} \end{bmatrix}. \tag{2.42}$$

However, the elasticity matrix expressed in its natural coordinate system will be the same since C is invariant under 90° rotation around its four-fold rotation axis. This is explicitly stated as

$$\begin{aligned} C'' &= (\bar{A}')^T C \bar{A}' \\ &= \begin{bmatrix} 5.00000 & 3.00000 & 1.00000 & 0.00000 & 0.00000 & 0.00000 \\ 3.00000 & 5.00000 & 1.00000 & 0.00000 & 0.00000 & 0.00000 \\ 1.00000 & 1.00000 & 4.00000 & 0.00000 & 0.00000 & 0.00000 \\ 0.00000 & 0.00000 & 0.00000 & 2.00000 & 0.00000 & 0.00000 \\ 0.00000 & 0.00000 & 0.00000 & 0.00000 & 2.00000 & 0.00000 \\ 0.00000 & 0.00000 & 0.00000 & 0.00000 & 0.00000 & 7.00000 \end{bmatrix}. \end{aligned}$$

Note that one can also express the elasticity tensor in a coordinate system that is 45° rotated around the four-fold rotation axis. Then, it is expressed in its natural coordinate system but the parameters of the tensor will be different than Equation 2.41.

2.2.4 Identifying Trigonal Symmetry

In this example, we introduce a trigonal elasticity tensor. According to the definition of Huo and Del Piero [31], there are ten symmetry classes in the space of elasticity tensors. In their calculations, they divide $SO(3)$ into equivalence classes rather than the space of elasticity tensors. Then, they prove that there are ten such classes [31]. The two additional symmetry classes, according to the definition of Huo and Del Piero, are subgroups of trigonal and tetragonal symmetry. More precisely, they are claiming that there are additional trigonal and tetragonal classes that have no mirror planes but only three- and four-fold rotation axes, respectively. Thus, for trigonal symmetry they introduce another subclass of elasticity tensors which are in the following form:

$$C = \begin{bmatrix} C_{11} & C_{12} & C_{13} & C_{14} & -C_{15} & 0 \\ C_{12} & C_{11} & C_{13} & -C_{14} & C_{15} & 0 \\ C_{13} & C_{13} & C_{33} & 0 & 0 & 0 \\ C_{14} & -C_{14} & 0 & C_{44} & 0 & \sqrt{2}C_{15} \\ -C_{15} & C_{15} & 0 & 0 & C_{44} & \sqrt{2}C_{14} \\ 0 & 0 & 0 & \sqrt{2}C_{15} & \sqrt{2}C_{14} & C_{11} - C_{12} \end{bmatrix}. \tag{2.43}$$

Note that the difference between the above form and the trigonal form that we introduced in Equation 1.27 is the nonzero term C_{15}. They claim that the symmetry group of the above form consists of a three-fold rotation axis aligned with $\mathbf{e_3}$-axis but without the mirror planes $M_{\mathbf{e_1}}$, $M_{(\cos\frac{\pi}{6},\sin\frac{\pi}{6},0)}$, $M_{(\cos\frac{5\pi}{6},\sin\frac{5\pi}{6},0)}$. We are going to give an example of an elasticity tensor having the form of Equation 2.43 and show that it has a trigonal form that has the symmetry group expressed in Equation 1.26 (with mirror planes). However, we will show that the tensor is expressed in a different coordinate system than its natural bases.

Consider the elasticity tensor

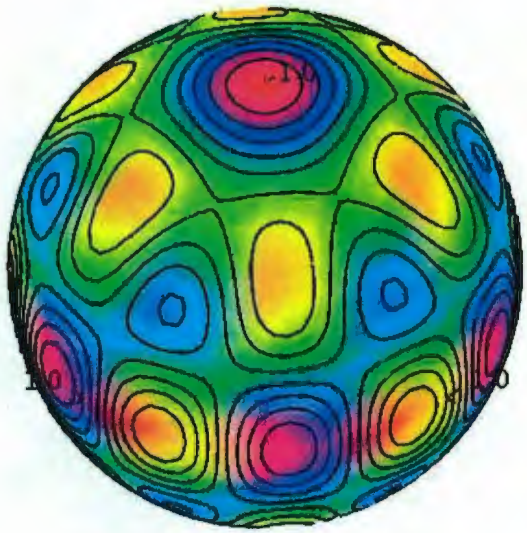

Figure 2.13: The plot of the distance function $d(\bar{X}^T C \bar{X}, \mathcal{L}^{mono})$ for C expressed in Equation 2.44. The symmetry directions are not aligned with the coordinate axes $\{\mathbf{e_1}, \mathbf{e_2}, \mathbf{e_3}\}$. The plot suggests that C may have a trigonal symmetry.

$$C = \begin{bmatrix} 5 & 3 & 1 & \frac{12}{\sqrt{2}} & -\frac{22}{\sqrt{2}} & 0 \\ 3 & 5 & 1 & -\frac{12}{\sqrt{2}} & \frac{22}{\sqrt{2}} & 0 \\ 1 & 1 & 4 & 0 & 0 & 0 \\ \frac{12}{\sqrt{2}} & -\frac{12}{\sqrt{2}} & 0 & 7 & 0 & 22 \\ -\frac{22}{\sqrt{2}} & \frac{22}{\sqrt{2}} & 0 & 0 & 7 & 12 \\ 0 & 0 & 0 & 22 & 12 & 2 \end{bmatrix}. \tag{2.44}$$

Figures 2.13, 2.14 and 2.15 show the plot of the monoclinic-distance function of C which is expressed in Equation 2.44.

In Figure 2.14, one can observe the three-fold symmetry. The existence of the mirror planes in every 60° degrees can be observed from Figure 2.15 which is a view perpendicular to the rotation axis. This suggest that C has a trigonal symmetry. In order to prove it, we minimize the distance function $d(\bar{X}^T C \bar{X}, \mathcal{L}^{mono})$ to find where

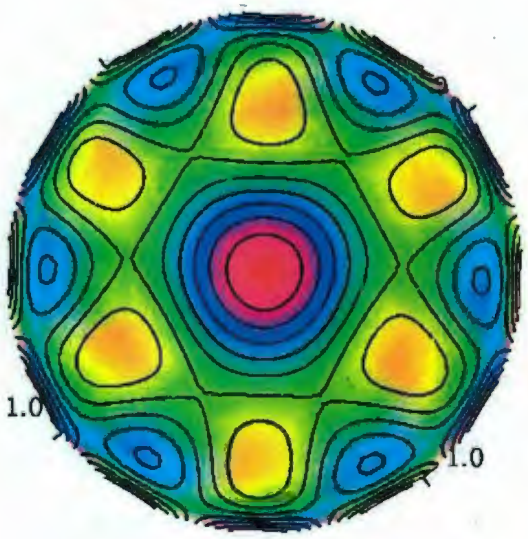

Figure 2.14: The plot of the distance function $d(\bar{X}^T C \bar{X}, \mathcal{L}^{mono})$ for C expressed in Equation 2.44. The plot is viewed from its three-fold rotation axis.

it vanishes, or equivalently, to find the normal of the mirror planes of C. Then we check if the mirror planes are 60° degrees to each other.

An important difference between the infinite-fold (in TI-symmetry), four-fold (in cubic and tetragonal symmetry) rotation axes and the three-fold (in cubic and trigonal symmetry) rotation axis is that three-fold rotation axis is not aligned with a normal of a mirror plane whereas the others are. Thus, the distance function $d(\bar{X}^T C \bar{X}, \mathcal{L}^{mono})$ does not vanish along the three-fold rotation axis as it is seen in Figure 2.14. In order to find it, we first determine the normals of mirror planes and then find a direction which is orthogonal to these normals since three-fold rotation axis is orthogonal to the normals.

Figure 2.15 shows that the normal of mirror planes are neither aligned with $\mathbf{e_1}$ nor $\mathbf{e_2}$. Thus, the elasticity tensor in Equation 2.44 is not expressed in its natural coordinate system.

The roots of the distance function $d(\bar{X}^T C \bar{X}, \mathcal{L}^{mono})$ are found by minimizing the

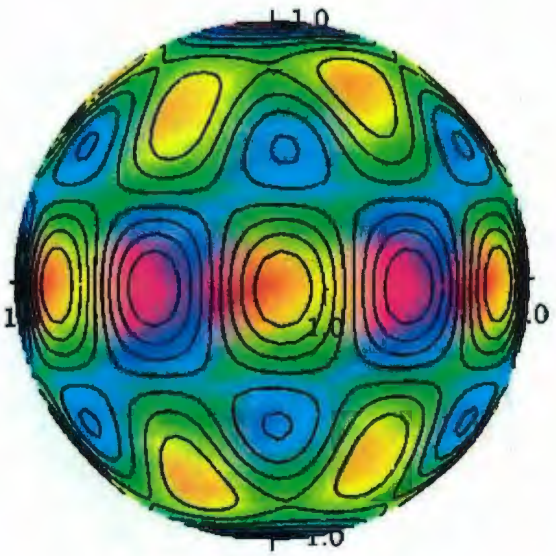

Figure 2.15: The plot of the distance function $d(\bar{X}^T C \bar{X}, \mathcal{L}^{mono})$ where it is viewed from a direction perpendicular to its rotation axis. Three mirror planes, whose locations are characterized by the orange color, are 60° apart. Note that the other minima do not represent mirror planes since $d(\bar{X}^T C \bar{X}, \mathcal{L}^{mono})$ does not vanish along those directions.

function around its extremum directions. These directions are obtained from the monoclinic-plot as: $\left(\cos\frac{20.463\pi}{180}, \sin\frac{20.463\pi}{180}, 0\right)$, $\left(\cos\frac{80.463\pi}{180}, \sin\frac{80.463\pi}{180}, 0\right)$ and $\left(\cos\frac{140.463\pi}{180}, \sin\frac{140.463\pi}{180}, 0\right)$. Thus, the normals lie in the $\mathbf{e_1e_2}$-plane and the difference between them is 60° degrees. Hence the elasticity tensor has trigonal symmetry. In this particular example, it is easy to find that the three-fold rotation axis is along $\mathbf{e_3}$-axis since normals of symmetry planes lie in the $\mathbf{e_1e_2}$-plane.

In order to represent C in its natural coordinate system, it remains to find the orthogonal transformation matrix $A \in SO(3)$ that rotates C to its natural coordinate system. We are looking for $A \in SO(3)$ such that it satisfies the following equations:

$$\begin{aligned} A(\mathbf{e_1}) &= \left(\sin\frac{90\pi}{180}\cos\frac{20.463\pi}{180}, \sin\frac{90\pi}{180}\sin\frac{20.463\pi}{180}, \cos\frac{90\pi}{180}\right), \\ A(\mathbf{e_2}) &= \left(\sin\frac{90\pi}{180}\cos\frac{110.463\pi}{180}, \sin\frac{90\pi}{180}\sin\frac{110.463\pi}{180}, \cos\frac{90\pi}{180}\right), \\ A(\mathbf{e_3}) &= \mathbf{e_3}. \end{aligned} \tag{2.45}$$

The same remarks that we made about choosing the natural coordinate system for tetragonal elasticity tensor can be repeated for trigonal tensor. More precisely, the normal of any mirror plane can be chosen as the $\mathbf{e_1}$-axis to represent C in its natural coordinate system. The representation of C is not going to be same component-wise unless the chosen axes are 120° apart, whereas it is 90° for tetragonal symmetry.

To find the entries of such an orthogonal transformation $A \in SO(3)$ that satisfies 2.45, one can use Equation 1.9, or simply, solve the above linear equations for A. Then, A is obtained as

$$A = \begin{bmatrix} \cos\frac{20.463\pi}{180} & \cos\frac{110.463\pi}{180} & 0 \\ \sin\frac{20.463\pi}{180} & \sin\frac{110.463\pi}{180} & 0 \\ 0 & 0 & 1 \end{bmatrix}.$$

After finding the 6D rotational matrix of $\bar{A}$ by applying equation A.51, we can

express C in its natural coordinate system as

$$C' = \bar{A}^T C \bar{A}$$
$$= \begin{bmatrix} 5 & 3 & 1 & 17.72 & 0 & 0 \\ 3 & 5 & 1 & -17.72 & 0 & 0 \\ 1 & 1 & 4 & 0 & 0 & 0 \\ 17.72 & -17.72 & 0 & 7 & 0 & 0 \\ 0 & 0 & 0 & 0 & 7 & 25.06 \\ 0 & 0 & 0 & 0 & 25.06 & 2 \end{bmatrix}.$$

Thus, we see that the trigonal elasticity tensor C, expressed in Equation 2.44, is not another subgroup of trigonal symmetry but just rotated 20.463° from its natural coordinate system.

2.2.5 Identifying Orthotropic Symmetry

We consider elasticity tensor C expressed in the following equation:

$$C = \begin{bmatrix} 42.03 & 32.49 & 26.42 & 5.79 & 9.94 & 21.33 \\ 32.49 & 36.72 & 34.85 & -5.22 & -35.37 & -23.60 \\ 26.42 & 34.84 & 31.72 & 12.17 & 3.77 & 10.24 \\ 5.79 & -5.22 & 12.17 & 32.84 & 20.98 & 2.36 \\ 9.94 & -35.37 & 3.77 & 20.98 & -22.64 & -9.71 \\ 21.33 & -23.60 & 10.24 & 2.36 & -9.71 & 11.32 \end{bmatrix}. \quad (2.46)$$

Figures 2.16, 2.17 and 2.18 show the plot of the monoclinic-distance function of C, which is expressed above.

By examining the plots one can see that the elasticity tensor C has an orthotropic symmetry since three mutually perpendicular mirror planes are the only observed symmetry elements. By using the point locater in Maple, we roughly determined the

Figure 2.16: The plot of the distance function $d(\bar{X}^T C \bar{X}, \mathcal{L}^{mono})$ for C expressed in Equation 2.46. The symmetry directions are not aligned with the coordinate axes $\{\mathbf{e_1}, \mathbf{e_2}, \mathbf{e_3}\}$. We can observe the normal of a mirror plane from the plot.

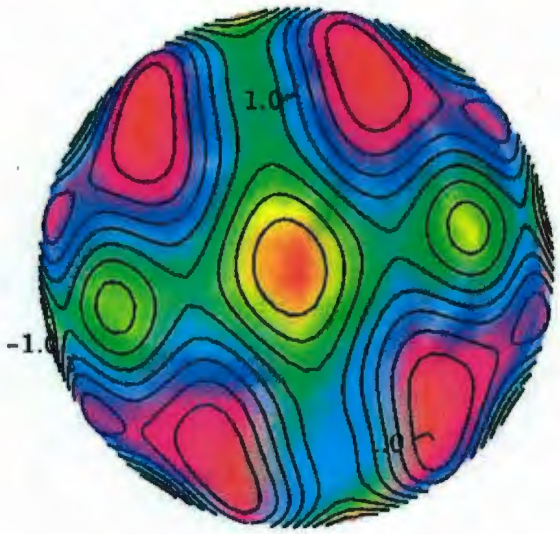

Figure 2.17: The plot of the distance function $d(\bar{X}^T C \bar{X}, \mathcal{L}^{mono})$ for C expressed in Equation 2.46 viewed from a direction perpendicular to a normal of a mirror plane. This normal is also perpendicular to the normal shown in Figure 2.16.

location of the normals of the mirror planes as $\left(\sin\frac{130\pi}{180}\cos\frac{-15\pi}{180}, \sin\frac{130\pi}{180}\sin\frac{-15\pi}{180}, \cos\frac{130\pi}{180}\right)$, $\left(\sin\frac{80\pi}{180}\cos\frac{64\pi}{180}, \sin\frac{80\pi}{180}\sin\frac{64\pi}{180}, \cos\frac{80\pi}{180}\right)$ and $\left(\sin\frac{40\pi}{180}\cos\frac{-34\pi}{180}, \sin\frac{40\pi}{180}\sin\frac{-34\pi}{180}, \cos\frac{40\pi}{180}\right)$. In order to obtain the exact orientation of the normals, we minimize the distance function $d(\bar{X}^T C \bar{X}, \mathcal{L}^{mono})$, around the 10° neighbourhood of the above vectors which are the approximate orientations of the normals. We find that the distance function vanishes along the directions

$$\left(\sin\frac{130.48\pi}{180}\cos\frac{-14.45\pi}{180}, \sin\frac{130.48\pi}{180}\sin\frac{-14.45\pi}{180}, \cos\frac{130.48\pi}{180}\right),$$
$$\left(\sin\frac{80.68\pi}{180}\cos\frac{67.49\pi}{180}, \sin\frac{80.68\pi}{180}\sin\frac{67.49\pi}{180}, \cos\frac{80.68\pi}{180}\right),$$
$$\left(\sin\frac{42\pi}{180}\cos\frac{-33\pi}{180}, \sin\frac{42\pi}{180}\sin\frac{-33\pi}{180}, \cos\frac{42\pi}{180}\right).$$

It is easy to check that these directions are perpendicular to each other since the dot

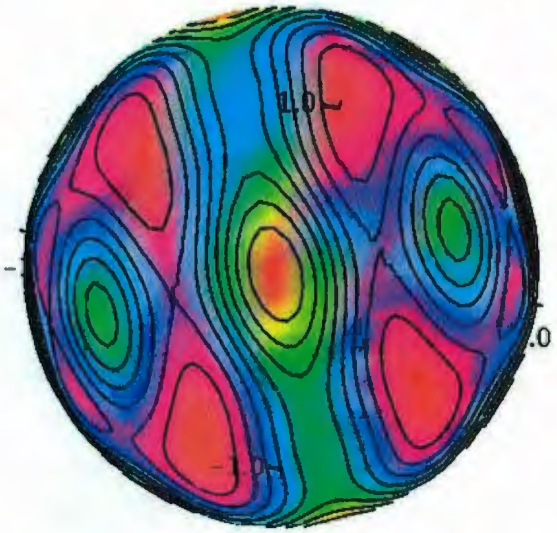

Figure 2.18: The plot of the distance function $d(\bar{X}^T C \bar{X}, \mathcal{L}^{mono})$ for C expressed in Equation 2.46. This normal is also perpendicular to the normal shown in Figure 2.16 and 2.17.

product of any of the two is zero.

Next, we find the orthogonal transformation that rotates the coordinates of the elasticity matrix C so that the tensor is expressed in its natural coordinate system. More precisely, we are seeking $A \in SO(3)$ such that $C' = \bar{A}^T C \bar{A}$ is in its natural coordinate system i.e. it has the form of the matrix 1.29. Note that in order to represent C in its natural coordinate system, one can choose $\{\mathbf{e_1}, \mathbf{e_2}, \mathbf{e_3}\}$ axes as any of the normals of the symmetry planes as long as they form a right-handed system. Although the entities of the elasticity matrix depend on our choice, they all represent the same orthotropic medium.

Figure 2.17 shows the $\mathbf{e_1}$-axis that we have chosen for the orthotropic tensor C. In order to find the rotation matrix that transforms the coordinate system $\{\mathbf{e_1}, \mathbf{e_2}, \mathbf{e_3}\}$ to the coordinate system formed by the three mutually perpendicular normals, one should solve the following linear equations:

$$
\begin{aligned}
A(\mathbf{e_1}) &= \left(\sin\frac{130.48\pi}{180}\cos\frac{-14.45\pi}{180}, \sin\frac{130.48\pi}{180}\sin\frac{-14.45\pi}{180}, \cos\frac{130.48\pi}{180}\right), \\
A(\mathbf{e_2}) &= \left(\sin\frac{80.68\pi}{180}\cos\frac{67.49\pi}{180}, \sin\frac{80.68\pi}{180}\sin\frac{67.49\pi}{180}, \cos\frac{80.68\pi}{180}\right), \\
A(\mathbf{e_3}) &= \left(\sin\frac{42\pi}{180}\cos\frac{-33\pi}{180}, \sin\frac{42\pi}{180}\sin\frac{-33\pi}{180}, \cos\frac{42\pi}{180}\right),
\end{aligned}
$$

where $A \in SO(3)$. Then, A is obtained as

$$
A = \begin{bmatrix}
\sin\frac{130.48\pi}{180}\cos\frac{-14.45\pi}{180} & \sin\frac{80.68\pi}{180}\cos\frac{67.49\pi}{180} & \sin\frac{42\pi}{180}\cos\frac{-33\pi}{180} \\
\sin\frac{130.48\pi}{180}\sin\frac{-14.45\pi}{180} & \sin\frac{80.68\pi}{180}\sin\frac{67.49\pi}{180} & \sin\frac{42\pi}{180}\sin\frac{-33\pi}{180} \\
\cos\frac{130.48\pi}{180} & \cos\frac{80.68\pi}{180} & \cos\frac{42\pi}{180}
\end{bmatrix}. \tag{2.47}
$$

After finding the 6D rotational matrix of $\bar{A}$ by applying Equation A.51, we can express C in its natural coordinate system as

$$
\begin{aligned}
C' &= \bar{A}^T C \bar{A} \\
&= \begin{bmatrix}
5 & 67 & 41 & 0 & 0 & 0 \\
67 & 18 & 23 & 0 & 0 & 0 \\
41 & 23 & 13 & 0 & 0 & 0 \\
0 & 0 & 0 & 57 & 0 & 0 \\
0 & 0 & 0 & 0 & 32 & 0 \\
0 & 0 & 0 & 0 & 0 & 7
\end{bmatrix}.
\end{aligned} \tag{2.48}
$$

We are not going to give an example for identifying a monoclinic elasticity tensor since all of the examples are special cases of monoclinic symmetry. Thus, similar approach should be followed to represent a monoclinic elasticity tensor in its natural coordinate system. Note that in monoclinic symmetry the choice of x- and y- axes changes the parameters of elasticity tensor. However, if $\mathbf{e_3}$ axis is aligned with the

normal of the mirror plane then it is considered to be expressed in its natural coordinate system. This is because the symmetry group of the monoclinic tensor still remains the same, namely $G^{Mono} = \{\pm I, \pm M_{\mathbf{e_3}}\}$.

Chapter 3

Determining the Closest Symmetric Elasticity Tensor

In this chapter, given an elasticity tensor we solve the problem of determining the closest tensor which belongs to a particular symmetry class. The given elasticity tensor may be obtained by inverting the velocities and polarizations of the waves propagating in arbitrary directions through the medium. Since a Hookean solid is an idealization, the elasticity tensor, evaluated without a priori assumption of symmetry, is found to be generally anisotropic. Furthermore, the oriented structures that causes anisotropy are not perfectly symmetric but they might get slightly perturbed or curved as they extend to the deeper parts of the region. Hence, all of these effects, as well as the errors in the measurements make the medium's symmetry generally anisotropic. Therefore, it is important to understand which symmetry class a given elasticity tensor is closest to.

When modeling a subsurface, one needs to know the number of parameters that represents the medium. This number depends on the structure, and thus, the symmetry of the medium. Isotropic models of a subsurface use two parameters, which are called Lamé's parameters. There are five independent parameters for a transversely

isotropic medium. TI-symmetry class generally represents a layering in the medium such as associated with the bedding structure in the sedimentary rocks. Alternatively, planar cracks aligned in a particular direction in an isotropic medium can result in a TI medium [16]. A family of parallel faults, which occur due to tectonic stresses, can also change the symmetry of an isotropic medium to TI. Note that all these examples are planar structures that have particular orientations.

Furthermore, these geological structures generally exist together in a subsurface. Combination of these structures reduces the symmetry of the medium. Thus, several planar elements, whose orientation may be different from each other, can be combined to result in a less symmetric medium. If two TI media whose symmetry axes are perpendicular to each other are combined, then an orthotropic medium results. If they are neither parallel nor perpendicular then the combination is monoclinic. The union of three TI media, where their orientations are not parallel results in generally-anisotropic medium.

In this chapter, we propose a method to determine the closest symmetry class. This method is based on the observations that are made in the plot of the monoclinic-distance function of the elasticity tensor representing the medium. In every section, we present examples illustrating how to find the orientation of the closest tensor belonging to a particular symmetry class and then determine the closest tensor in its natural coordinate system. In each section, a generally anisotropic elasticity tensor is introduced. One of these tensors was obtained from field data; the rest is perturbed from a symmetric elasticity tensor to make it generally anisotropic. It is proved by Kochetov and Slawinski [33] that if an elasticity tensor C is a small perturbation of an orthotropic tensor, then the symmetry directions of the closest orthotropic tensor, namely C^{ortho}, is close to the symmetry directions of the original orthotropic tensor. They do not give a proof for the other symmetry classes, however, they state that it can be achieved similarly for the other symmetry classes. In terms of error

analysis, this result has a practical importance since one may want to know if a measured elasticity tensor falls into one of the seven symmetry classes within a given error range. One can also check by using the method in this chapter, if a measured elasticity tensor can be close to several symmetry classes within the range of error. However, we leave the error issue as a future study, and ignore it in this thesis.

3.1 Determining the Closest TI-Elasticity Tensor

The minimization of the TI-distance function among all orientations solves the problem of finding the symmetry axis of the closest-TI elasticity tensor. More precisely, the minimization process

$$\min_{X \in SO(3)} d(\bar{X}^T C \bar{X}, \mathcal{L}^{TI})$$

gives not only the minimum distance of C to $\mathcal{L}^{TI}$ among all coordinate systems but also finds the Euler angles of $X \in SO(3)$ which transforms the coordinate system to the one where the minimum distance is achieved. In other words, $\bar{X}$ rotates the coordinate system of C in such a way that it becomes closest to TI symmetry in that coordinate system. In Chapter 2, we used this feature of the distance function in order to identify a symmetric elasticity tensor expressed in any coordinate system. In this section, we use the distance function in order to determine the symmetry axis and the parameters of the closest TI tensor.

A geophysical application of this result can be the determination of the orientation of the symmetry axis of a tilted and layered subsurface which is generally close to TI symmetry.

In this section, we propose a method to find whether a given generally-anisotropic elasticity tensor is close to TI symmetry or not. In the literature, there are various ways and methods that evaluate the distance of C to TI symmetry [17, 32, 23, 37]. In some works, the closeness problem is solved by considering a unique coordinate

system [23, 37], whereas in some other works, the closest TI tensor is found among all coordinate systems [17, 32]. In this thesis, by using the plot of the monoclinic-distance function, we seek to find if TI symmetry is a good approximation for a given elasticity tensor. In other words, the method that we propose may suggest if TI symmetry can be chosen to model the medium. If it is not then one can check for the other symmetry classes. This is the content of the next sections.

Now, we introduce an example that is generally anisotropic and calculate how close it is to TI symmetry. Moreover, we will find the elasticity parameters and the orientation of the symmetry axis of the closest-TI elasticity tensor to C. In order to obtain these results, we will consider the plots of the distance functions of C and discuss what kind of information we can obtain from them about the closest symmetry class to C.

Consider the following elasticity tensor:

$$C = \begin{bmatrix} 88.84 & 32.53 & 36.81 & 1.69 & 5.90 & 2.00 \\ 32.53 & 107.86 & 33.29 & -0.79 & -0.42 & 2.70 \\ 36.81 & 33.29 & 99.40 & -0.48 & 6.44 & -0.53 \\ 1.69 & -0.79 & -0.48 & 67.72 & 2.40 & 7.07 \\ 5.90 & -0.42 & 6.44 & 2.40 & 54.50 & -0.54 \\ 2.00 & 2.70 & -0.53 & 7.07 & -0.54 & 58.10 \end{bmatrix}. \tag{3.1}$$

The plot of the TI-distance function of C from different points of views can be seen in Figures 3.1, 3.2, 3.3. After considering the figures, one can observe the symmetry axis of the closest-TI elasticity tensor to C, which is the bullseye. To determine the exact orientation of the bullseye, one can use the same approach that is explained in the last chapter. More precisely, first, the orientation of the bullseye found by the point locater in Maple as $\left(\sin\frac{63\pi}{180}\cos\frac{170\pi}{180}, \sin\frac{63\pi}{180}\sin\frac{170\pi}{180}, \cos\frac{63\pi}{180}\right)$. Then one minimizes the distance function around the 10° neighbourhood of this vector to find the exact orientation of the symmetry axis which is $\left(\sin\frac{62.31\pi}{180}\cos\frac{171.57\pi}{180}, \sin\frac{62.31\pi}{180}\sin\frac{171.57\pi}{180}, \cos\frac{62.31\pi}{180}\right)$.

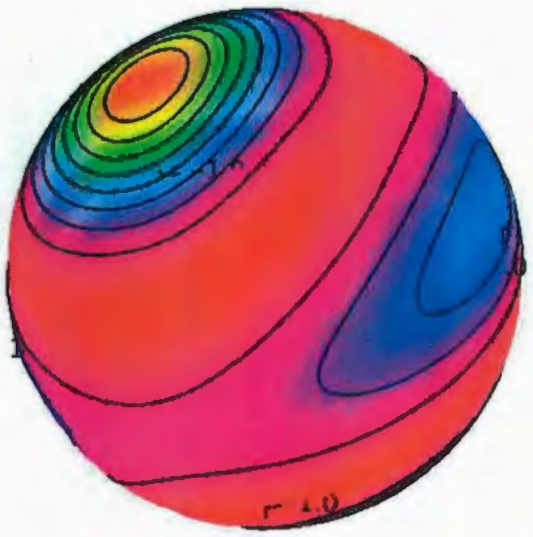

Figure 3.1: The plot of the distance function $d(\bar{X}^T C \bar{X}, \mathcal{L}^{TI})$ of C expressed in Equation 3.1 viewed from a direction where one can observe all the characteristic features of the function. Two extrema can be seen which are almost perpendicular to each other. The minimum which is close to zero is represented by the orange color. The direction of the rotation axis of the closest TI tensor is along the bullseye.

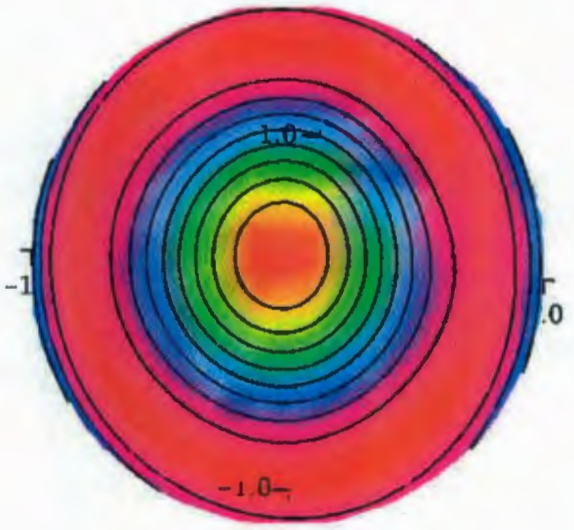

Figure 3.2: The plot of the distance function $d(\bar{X}^T C \bar{X}, \mathcal{L}^{TI})$ of C expressed in Equation 3.1 viewed from a direction of the symmetry axis of the closest TI tensor. The contours are not circular, but perturbed slightly which may suggest that C is close to TI symmetry.

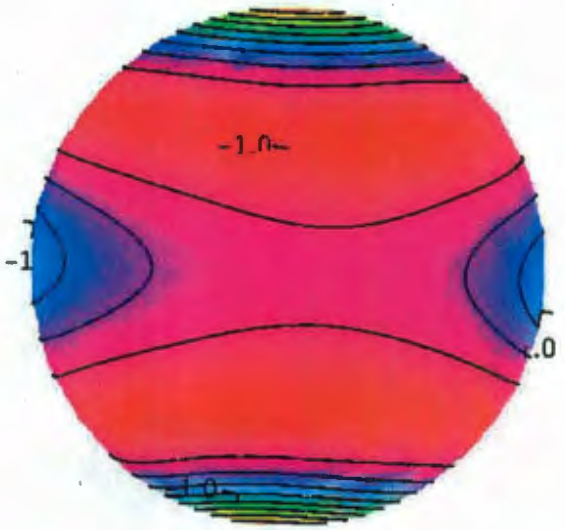

Figure 3.3: The plot of the distance function $d(\bar{X}^T C \bar{X}, \mathcal{L}^{TI})$ of C expressed in Equation 3.1 viewed from a direction perpendicular to the symmetry axis of the closest TI tensor. The noncircularity of the contours are apparent from this direction.

Now, we will determine the rotation matrix, $X_0 \in SO(3)$, that rotates C into the coordinate system where the minimum distance is achieved. The angles that give the minimum value of the distance function are the Euler angles of the rotation matrix $X_0 \in SO(3)$. The minimizing command in Maple gives the Euler angles as follows:

$$\begin{aligned} \phi &= 62.31°, \\ \psi &= 261.57°. \end{aligned} \tag{3.2}$$

To find the rotation matrix, X_0, we substitute these values into Equation 1.14, where $\theta = 0$ since the third rotation does not change the value of the TI distance-

function. Then, we get the following result:

$$X_0 = \begin{bmatrix} -0.146 & 0.459 & -0.875 \\ -0.989 & -0.068 & 0.129 \\ 0 & 0.885 & 0.464 \end{bmatrix}. \tag{3.3}$$

Thus, we can transform C into the coordinate system where the new $\mathbf{e_3}$-axis is the symmetry axis of the closest TI-tensor by $\bar{X}_0^T C \bar{X}_0$. Then, we get

$$\bar{X}_0^T C \bar{X}_0 = \begin{bmatrix} 108.23 & 32.85 & 33.12 & 0.59 & -1.11 & -0.48 \\ 32.85 & 103.33 & 37.58 & 0.86 & -0.09 & -0.87 \\ 33.12 & 37.58 & 82.68 & -1.22 & 0.92 & -1.27 \\ 0.59 & 0.86 & -1.22 & 55.56 & -0.26 & 0.77 \\ -1.11 & -0.09 & 0.92 & -0.26 & 54.55 & -0.18 \\ -0.48 & -0.87 & -1.27 & 0.77 & -0.18 & 72.06 \end{bmatrix}. \tag{3.4}$$

Thus, $\{X_0(\mathbf{e_1}), X_0(\mathbf{e_2}), X_0(\mathbf{e_3})\}$ is the coordinate system that minimizes the distance of C to $\mathcal{L}^{TI}$ whenever C is expressed in that coordinate system. The plot of the TI-distance function of $\bar{X}_0^T C \bar{X}_0$ can be seen in Figure 3.4.

The closest-TI tensor can be achieved for the elasticity tensor $\bar{X}_0^T C \bar{X}_0$ by applying Formula 2.10 as

$$(\bar{X}_0^T C \bar{X}_0)^{TI} = \begin{bmatrix} 105.57 & 33.07 & 35.35 & 0 & 0 & 0 \\ 33.07 & 105.57 & 35.35 & 0 & 0 & 0 \\ 35.35 & 35.35 & 82.68 & 0 & 0 & 0 \\ 0 & 0 & 0 & 55.05 & 0 & 0 \\ 0 & 0 & 0 & 0 & 55.05 & 0 \\ 0 & 0 & 0 & 0 & 0 & 72.50 \end{bmatrix}. \tag{3.5}$$

The tensor $(\bar{X}_0^T C \bar{X}_0)^{TI}$ belongs to the TI symmetry class and it is represented in its natural coordinate system, namely $(\bar{X}_0^T C \bar{X}_0)^{TI} \in \mathcal{L}^{TI}$.

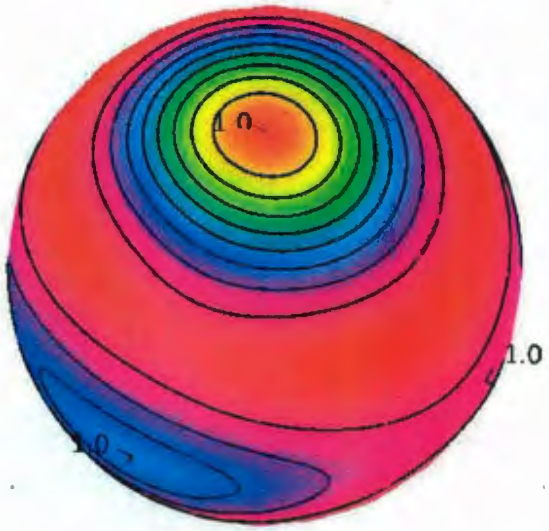

Figure 3.4: The plot of the TI-distance function $d(\bar{X}^T C \bar{X}, \mathcal{L}^{TI})$ of $\bar{X}_0^T C \bar{X}_0$ expressed in Equation 3.4. Note that the symmetry axis of the closest TI-tensor is aligned with $\mathbf{e_3}$-axis.

The distance of the elasticity tensor $\bar{X}_0^T C \bar{X}_0$ to $\mathcal{L}^{TI}$ is

$$\begin{aligned} d(\bar{X}_0^T C \bar{X}_0, \mathcal{L}^{TI}) &= ||\bar{X}_0^T C \bar{X}_0||^2 - ||(\bar{X}_0^T C \bar{X}_0)^{TI}||^2 \\ &= ||C||^2 - ||(\bar{X}_0^T C \bar{X}_0)^{TI}||^2 \\ &= 48.4113, \end{aligned} \tag{3.6}$$

which is the minimum distance of $\bar{X}^T C \bar{X}$ to $\mathcal{L}^{TI}$ among all $X \in SO(3)$.

By considering the distance function, we have found the closest-TI tensor among all coordinate systems. However, one should be careful about choosing the closest symmetry class to a given elasticity tensor. Note that the figures of the TI-distance function of C also suggest that it is close to the orthotropic symmetry class. Indeed, since every TI medium is also orthotropic, a generally-anisotropic medium is closer to the orthotropic class than it is to TI class. Thus, when trying to find which symmetry class is the closest, one should not make the decision upon considering the smallest

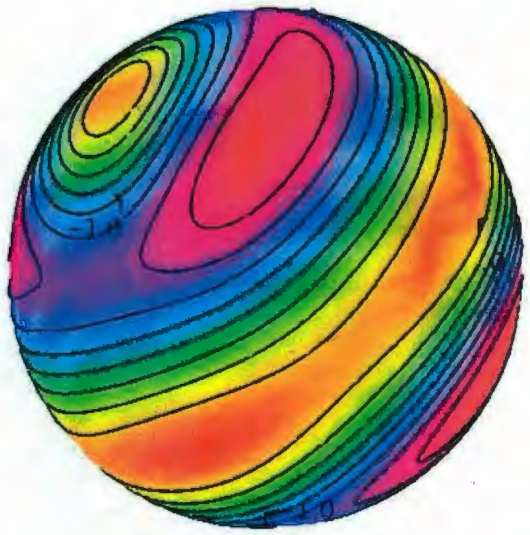

Figure 3.5: The plot of the monoclinic-distance function $d(\bar{X}^T C \bar{X}, \mathcal{L}^{mono})$ of C expressed in Equation 3.1. The existence of the equatorial plane is apparent. The orange color implies that the value of the monoclinic-distance function is close to zero around that plane and along the rotation axis.

value of the distances to $\mathcal{L}^{TI}$ and $\mathcal{L}^{ortho}$. This is because the distance of C to $\mathcal{L}^{ortho}$ will be always smaller than or equal to the distance of C to $\mathcal{L}^{TI}$.

In order to solve this problem, one should consider the plot of the monoclinic-distance function of C. As stated earlier, the monoclinic plot gives more information on the closeness to being a normal of a mirror plane for a particular direction. Thus, if a given generally anisotropic elasticity tensor is close to TI symmetry then it is expected that there exists an equatorial plane appearing in the monoclinic plot. For all orientations lying in the equatorial plane, the distance to $\mathcal{L}^{mono}$ should be almost equivalent and close to zero. This is because in TI symmetry there are infinitely many planes whose normals are perpendicular to its rotation axis.

Figures 3.5, 3.6, 3.7 show the plot of the monoclinic-distance function of C expressed in Equation 3.1.

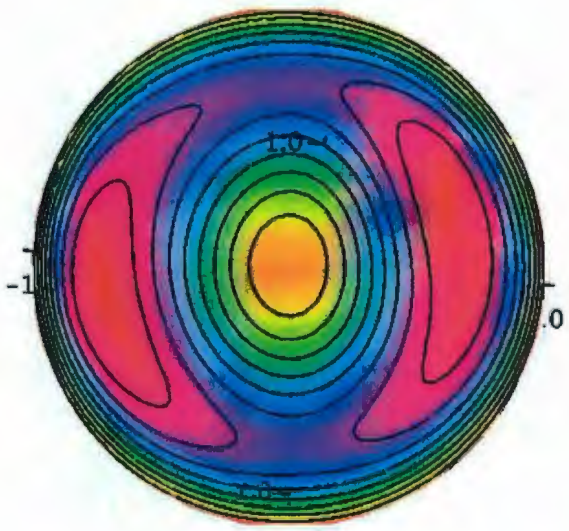

Figure 3.6: The plot of the distance function $d(\bar{X}^T C \bar{X}, \mathcal{L}^{mono})$ for C expressed in Equation 3.1 viewed from a direction of the symmetry axis of the closest-TI tensor. It is apparent that the plot does not have infinite-fold symmetry. Thus, the tensor does not belong to TI-symmetry class. The plot from this view may also suggest that C is close to the orthotropic symmetry.

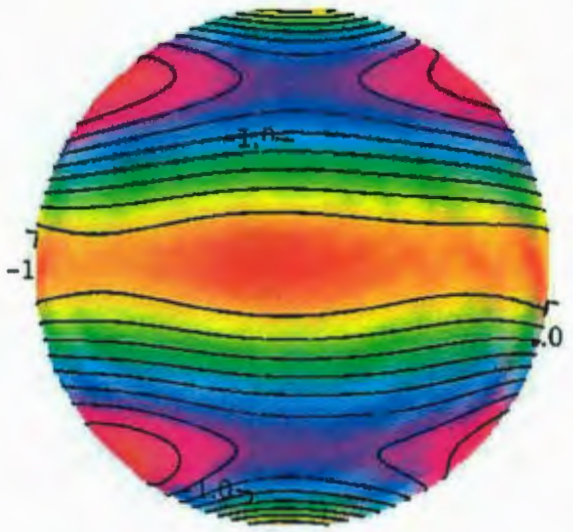

Figure 3.7: The plot of the distance function $d(\bar{X}^T C \bar{X}, \mathcal{L}^{mono})$ of C expressed in Equation 3.1 viewed from a direction perpendicular to the symmetry axis of the closest-TI tensor. This view of the plot suggests that C should be approximated as a TI tensor but not orthotropic. This is because the equatorial plane does not exist for orthotropic medium unless it is close to TI.

Similar to TI plot, monoclinic plot also suggests that C is close to both TI symmetry and orthotropic symmetry. However, there exists an equatorial plane such that any direction in that plane yields almost equal distances to monoclinic symmetry. This can be inferred from the fact that these directions lie between the same contour curves and similar colours. Hence, we conclude that TI symmetry is a better approximation for C, which is expressed in Equation 3.1, than orthotropic symmetry.

3.2 Determining the Closest Monoclinic Elasticity Tensor

In this section, we consider the problem of closeness to monoclinic symmetry class. Since we can plot the distance function to monoclinic symmetry, the method to find the orientation of the closest monoclinic elasticity tensor is similar to the method that we have used in the previous section. Thus, the problem is reduced to finding the absolute minimum of $d(\bar{X}^T C \bar{X}, \mathcal{L}^{mono})$ among all $X \in SO(3)$ from its plot. After determining the orientation of the minimum of $d(\bar{X}^T C \bar{X}, \mathcal{L}^{ortho})$, one rotates the tensor by X_0, where X_0 is the orthogonal transformation for which the minimum is achieved. Then, one evaluates the parameters of the closest monoclinic tensor in the coordinate system whose z-axis is $X_0(\mathbf{e_3})$. To find the parameters of the monoclinic elasticity tensor, one uses Equation 2.9.

To give an example of the procedures that are described in the above paragraph, we will use the same elasticity tensor which is expressed in Equation 3.1. Figures 3.5, 3.6 and 3.7 show the plot of $d(\bar{X}^T C \bar{X}, \mathcal{L}^{mono})$ from different points of views. In order to determine the minimum of the function, we made two searches where the first search is restricted around the closest-TI direction that can be seen in Figure 3.6. The second search is around the equatorial plane which can be observed in Figure 3.7. The minimum distance of C to the monoclinic symmetry around the 20°

neighbourhood of the closest-TI direction is found as

$$\min_{X \in SO(3)} (d(\bar{X}^T C \bar{X}, \mathcal{L}^{mono})) = 10.186, \tag{3.7}$$

where the minimum is attained for the orthogonal transformation A with Euler angles $\phi = 61.50°, \psi = 172.207° + 90°$. Recall from Equation 2.29 that the relation between the Euler angles of the rotation matrix and the new z-axis of the elasticity tensor is that their ψ values have 90° difference. Thus, the direction of the one of the local minimum distance to monoclinic is achieved along the vector

$$\mathbf{v_1} = \left(\sin\frac{61.50\pi}{180} \cos\frac{172.207\pi}{180}, \sin\frac{61.50\pi}{180} \sin\frac{172.207\pi}{180}, \cos\frac{61.50\pi}{180} \right). \tag{3.8}$$

The other search for the minimum distance to the monoclinic symmetry around the equatorial plane gives the minimum as

$$\min_{X \in SO(3)} (d(\bar{X}^T C \bar{X}, \mathcal{L}^{mono})) = 8.286, \tag{3.9}$$

where the minimum is achieved for the orthogonal transformation B eith Euler angles $\phi = 83.81°, \psi = -94.53° + 90°$. Thus, the direction that gives the minimum is achieved along the vector

$$\mathbf{v_2} = \left(\sin\frac{83.81\pi}{180} \cos\frac{-94.53\pi}{180}, \sin\frac{83.81\pi}{180} \sin\frac{-94.53\pi}{180}, \cos\frac{83.81\pi}{180} \right). \tag{3.10}$$

Hence, the closest-monoclinic tensor to C is achieved along $\mathbf{v_2}$ direction since $d(B^T C B, \mathcal{L}^{mono}) < d(\bar{A}^T C \bar{A}, \mathcal{L}^{mono})$. In other words, the normal of the symmetry plane of the closest monoclinic tensor is $\mathbf{v_2}$. To find the parameters of the closest monoclinic tensor, first, we express C in the coordinate system where its z-axis is along $\mathbf{v_2}$, namely we find $B^T C B$. Then, we apply Equation 2.9 to $B^T C B$ and get

$$(B^TCB)^{mono} = \begin{bmatrix} 88.41 & 37.01 & 32.40 & 0 & 0 & 5.99 \\ 37.01 & 99.45 & 33.31 & 0 & 0 & 6.64 \\ 32.40 & 33.31 & 108.09 & 0 & 0 & -0.60 \\ 0 & 0 & 0 & 68.12 & 7.14 & 0 \\ 0 & 0 & 0 & 7.14 & 58.18 & 0 \\ 5.99 & 6.64 & -0.60 & 0 & 0 & 54.16 \end{bmatrix}, \tag{3.11}$$

which is the closest-monoclinic tensor to C.

The closest-monoclinic tensor to C, which is evaluated in a particular coordinate system, is unique for any rotation of C around its z-axis. However, the projected C's do not have the same entities. In other words, they are represented in different coordinate systems but it is the same tensor. More precisely,

$$C^{mono} \neq (\bar{X}^TC\bar{X})^{mono}, \tag{3.12}$$

where the rotation axis of X is $\mathbf{e_3}$, but there exist $\bar{Y} \in SO(3)$ such that

$$\bar{Y}^TC^{mono}\bar{Y} = (\bar{X}^TC\bar{X})^{mono}. \tag{3.13}$$

Thus, Equation 3.13 shows that C^{mono} and $(\bar{X}^TC\bar{X})^{mono}$ are the same tensors but expressed in a different coordinate system. To see that Equation 3.13 holds, take $\bar{Y} = \bar{X}$ and use Equation 2.4 to get the expressions of $(\bar{X}^TC\bar{X})^{mono}$ and C^{mono}.

Hence, Equation 3.13 implies that although the parameters of 3.11 may change if one uses a different transformation than B, it is the same tensor once the orientation of the symmetry plane is fixed.

Note that the z-axis of the closest-TI tensor, which is $\left(\sin\frac{62.31\pi}{180}\cos\frac{171.57\pi}{180}, \sin\frac{62.31\pi}{180}\sin\frac{171.57\pi}{180}, \cos\frac{62.31\pi}{180}\right)$ is not aligned with $\mathbf{v_1}$, but is as close as 2°. This is expected since the minimum direction to monoclinic symmetry measures how far that direction is away from being a normal of a symmetry plane,

whereas the minimum direction to TI symmetry measures its distance to infinite-fold rotation axis.

3.3 Determining the Closest Orthotropic Elasticity Tensor

In this section, we consider the problem of closeness to orthotropic symmetry class. Recall that the distance function can be plotted for only TI and monoclinic symmetries. This is the case because the space of TI-and monoclinic-elasticity tensors, namely $\mathcal{L}^{TI}$ and $\mathcal{L}^{mono}$, are invariant under the rotations around $\mathbf{e_3}$-axis, which is proved in Theorem 1. However, the invariance of the space of orthotropic elasticity tensors, namely $\mathcal{L}^{ortho}$, under all rotations around $\mathbf{e_3}$-axis does not hold. Thus, in order to find the closest orthotropic elasticity tensor among all coordinate systems, we need a different approach. This approach is based on the equality of the orthotropic-distance function to the half of the sum of three monoclinic-distance functions for the directions that are mutually perpendicular to each other.

First, we introduce the closest orthotropic tensor, namely C^{ortho} which is evaluated in its natural coordinate system, to a given elasticity tensor C. Let C be any elasticity tensor,

$$C = \begin{bmatrix} C_{11} & C_{12} & C_{13} & C_{14} & C_{15} & C_{16} \\ C_{12} & C_{22} & C_{23} & C_{24} & C_{25} & C_{26} \\ C_{13} & C_{23} & C_{33} & C_{34} & C_{35} & C_{36} \\ C_{14} & C_{24} & C_{34} & C_{44} & C_{45} & C_{46} \\ C_{15} & C_{25} & C_{35} & C_{45} & C_{55} & C_{56} \\ C_{16} & C_{26} & C_{36} & C_{46} & C_{56} & C_{66} \end{bmatrix}. \tag{3.14}$$

Then, the closest orthotropic elasticity tensor can be found in the coordinate system $\mathbf{e_1}, \mathbf{e_2}, \mathbf{e_3}$ by projecting C onto $\mathcal{L}^{ortho}$. The projection function, which is

defined in Equation 2.4, is

$$C^{ortho} = \frac{1}{4}(C + \bar{M}_{\mathbf{e}_1}^T C \bar{M}_{\mathbf{e}_1} + \bar{M}_{\mathbf{e}_2}^T C \bar{M}_{\mathbf{e}_2} + \bar{M}_{\mathbf{e}_3}^T C \bar{M}_{\mathbf{e}_3}), \tag{3.15}$$

since

$$G^{Ortho} = \{\pm I, \pm M_{\mathbf{e}_1}, \pm M_{\mathbf{e}_2}, \pm M_{\mathbf{e}_3}\},$$

where $M_{\mathbf{e}_i}$ is the reflection around the plane whose normal is $\mathbf{e}_i$ for $i \in \{1,2,3\}$. Hence, C^{ortho} can be found as

$$C^{ortho} = \begin{bmatrix} C_{11} & C_{12} & C_{13} & 0 & 0 & 0 \\ C_{12} & C_{22} & C_{23} & 0 & 0 & 0 \\ C_{13} & C_{23} & C_{33} & 0 & 0 & 0 \\ 0 & 0 & 0 & C_{44} & 0 & 0 \\ 0 & 0 & 0 & 0 & C_{55} & 0 \\ 0 & 0 & 0 & 0 & 0 & C_{66} \end{bmatrix}, \tag{3.16}$$

as it is stated in [33]. It is easy to see that C^{ortho}, expressed in Equation 3.15, is orthotropic since

$$\begin{aligned} \bar{M}_{\mathbf{e}_1}^T C^{ortho} \bar{M}_{\mathbf{e}_1} &= \bar{M}_{\mathbf{e}_1}^T \left(\frac{1}{4}(C + \bar{M}_{\mathbf{e}_1}^T C \bar{M}_{\mathbf{e}_1} + \bar{M}_{\mathbf{e}_2}^T C \bar{M}_{\mathbf{e}_2} + \bar{M}_{\mathbf{e}_3}^T C \bar{M}_{\mathbf{e}_3})\right) \bar{M}_{\mathbf{e}_1} \\ &= \frac{1}{4}(\bar{M}_{\mathbf{e}_1}^T C \bar{M}_{\mathbf{e}_1} + \bar{M}_{\mathbf{e}_1}^T \bar{M}_{\mathbf{e}_1}^T C \bar{M}_{\mathbf{e}_1} \bar{M}_{\mathbf{e}_1} + \bar{M}_{\mathbf{e}_1}^T \bar{M}_{\mathbf{e}_2}^T C \bar{M}_{\mathbf{e}_2} \bar{M}_{\mathbf{e}_1} \\ &\quad + \bar{M}_{\mathbf{e}_1}^T \bar{M}_{\mathbf{e}_3}^T C \bar{M}_{\mathbf{e}_3} \bar{M}_{\mathbf{e}_1}) \\ &= \frac{1}{4}(\bar{M}_{\mathbf{e}_1}^T C \bar{M}_{\mathbf{e}_1} + C + (-\bar{M}_{\mathbf{e}_3})^T C (-\bar{M}_{\mathbf{e}_3}) + (-\bar{M}_{\mathbf{e}_2})^T C (-\bar{M}_{\mathbf{e}_2})) \\ \text{since } \bar{M}_{\mathbf{e}_1} \bar{M}_{\mathbf{e}_1} = I,\ \bar{M}_{\mathbf{e}_2} \bar{M}_{\mathbf{e}_1} = -\bar{M}_{\mathbf{e}_3} &\text{ and } \bar{M}_{\mathbf{e}_3} \bar{M}_{\mathbf{e}_1} = -\bar{M}_{\mathbf{e}_2} \\ &= \frac{1}{4}(\bar{M}_{\mathbf{e}_1}^T C \bar{M}_{\mathbf{e}_1} + C + \bar{M}_{\mathbf{e}_3}^T C \bar{M}_{\mathbf{e}_3} + \bar{M}_{\mathbf{e}_2}^T C \bar{M}_{\mathbf{e}_2}) \\ &= C^{ortho}. \end{aligned} \tag{3.17}$$

Equation 3.17 can be shown for the other symmetry elements of G^{Ortho}, namely for $M_{\mathbf{e}_2}$ and $M_{\mathbf{e}_3}$. Thus, C^{ortho} is orthotropic which is also proved by Gazis et al. [23].

In order to find the distance of a given C to the space of orthotropic elasticity tensors represented in its natural coordinate system, one applies Equation 2.13 to get

$$d(C, \mathcal{L}^{ortho}) := ||C||^2 - ||C^{ortho}||^2. \tag{3.18}$$

If one wants to find the orientation of the closest orthotropic tensor among all coordinate systems, then the distance function should be used which is defined in Definition 4. Applying the definition for the orthotropic symmetry, we get

$$d(\bar{X}^T C \bar{X}, \mathcal{L}^{ortho}) = ||C||^2 - ||(\bar{X}^T C \bar{X})^{ortho}||^2, \text{ for all } X \in SO(3). \tag{3.19}$$

Note that the orientations of the coordinate axes matter for evaluating the projected tensor $(\bar{X}^T C \bar{X})^{ortho}$. More precisely, in orthotropic symmetry, unlike TI and monoclinic symmetry, one axis does not give a unique value for the distance function. The rotation of the elasticity tensor around its z-axis gives different values for the distance function, i.e. Theorem 1 does not hold for orthotropic symmetry. Thus, X is in the form of Equation 1.14, namely $X = Z_1 Z_2 Z_3$. Note that Z_3, which is a function of θ expressed in Equation 1.13, cannot be simplified from Equation 3.19. Hence, one cannot plot the distance function to orthotropic symmetry since its plot is a surface in 4D space, namely three independent variables for expressing the coordinate system and one dependent variable for the value of the distance function. Because we cannot plot the orthotropic-distance function, the minimization of the distance function among all coordinate systems cannot be achieved in the same way as it is done for TI and monoclinic symmetries. Generally, a computer program cannot find the absolute minimum of a highly nonlinear function with several variables.

In order to solve this nonlinear minimization problem and to find the orientation of the closest orthotropic tensor among all coordinate systems, we make use of the monoclinic plot of the elasticity tensor. We already stated that extrema of the monoclinic-distance function show how close a particular direction is to being a normal of a symmetry plane. This may suggest that for finding the orientation of the

closest orthotropic tensor, one should restrict the search around the three almost perpendicular extrema if they exist. If the three almost perpendicular directions do not exist in the monoclinic plot then it can be done around any of the extrema. However, such a case may imply that the tensor under consideration is not close to orthotropic symmetry.

Before giving examples on finding the orientation of the closest orthotropic tensor, we state a theorem which gives a relation between the monoclinic- and orthotropic-distance functions.

Theorem 7 *Let C be an elasticity tensor. Let $R_{\frac{\pi}{2},\mathbf{e_2}} \in SO(3)$ and $R_{\frac{\pi}{2},\mathbf{e_1}} \in SO(3)$ denote the rotation matrices that are around $\mathbf{e_2}$ and $\mathbf{e_1}$ by 90°, respectively. Then the following equation holds:*

$$d(C,\mathcal{L}^{ortho}) = \frac{1}{2}(d(C,\mathcal{L}^{mono}) + d(\bar{R}^T_{\frac{\pi}{2},\mathbf{e_2}} C \bar{R}_{\frac{\pi}{2},\mathbf{e_2}}, \mathcal{L}^{mono}) + d(\bar{R}^T_{\frac{\pi}{2},\mathbf{e_1}} C \bar{R}_{\frac{\pi}{2},\mathbf{e_1}}, \mathcal{L}^{mono})). \tag{3.20}$$

Explicit expressions of $R_{\frac{\pi}{2},\mathbf{e_2}}$ and $R_{\frac{\pi}{2},\mathbf{e_1}}$ are as follows:

$$R_{\frac{\pi}{2},\mathbf{e_2}} = \begin{bmatrix} 0 & 0 & 1 \\ 0 & 1 & 0 \\ -1 & 0 & 0 \end{bmatrix},$$

$$R_{\frac{\pi}{2},\mathbf{e_1}} = \begin{bmatrix} 1 & 0 & 0 \\ 0 & 0 & 1 \\ 0 & -1 & 0 \end{bmatrix}.$$

PROOF. To calculate the left-hand side of Equation 3.20, we substitute Equation 3.15 into Equation 3.18 and obtain

$$d(C,\mathcal{L}^{ortho}) = ||C - \frac{1}{4}(C + \bar{M}^T_{\mathbf{e_1}} C \bar{M}_{\mathbf{e_1}} + \bar{M}^T_{\mathbf{e_2}} C \bar{M}_{\mathbf{e_2}} + \bar{M}^T_{\mathbf{e_3}} C \bar{M}_{\mathbf{e_3}})||^2. \tag{3.21}$$

Simplifying Expression 3.21, we get

$$d(C, \mathcal{L}^{ortho}) = ||\frac{3}{4}C - \frac{1}{4}(\bar{M}_{e_1}^T C \bar{M}_{e_1} + \bar{M}_{e_2}^T C \bar{M}_{e_2} + \bar{M}_{e_3}^T C \bar{M}_{e_3})||^2, \tag{3.22}$$

Similarly, each of the terms in the right-hand side of Equation 3.20 can be written as

$$\begin{aligned} d(C, \mathcal{L}^{mono}) &= ||C - C^{mono}||^2 \\ &= ||C - \frac{1}{2}(C + \bar{M}_{e_3}^T C \bar{M}_{e_3})||^2 \\ &= ||\frac{1}{2}(C - \bar{M}_{e_3}^T C \bar{M}_{e_3})||^2 \end{aligned} \tag{3.23}$$

and

$$\begin{aligned} d(\bar{R}_{\frac{\pi}{2},e_2}^T C \bar{R}_{\frac{\pi}{2},e_2}, \mathcal{L}^{mono}) &= ||\bar{R}_{\frac{\pi}{2},e_2}^T C \bar{R}_{\frac{\pi}{2},e_2} - (\bar{R}_{\frac{\pi}{2},e_2}^T C \bar{R}_{\frac{\pi}{2},e_2})^{mono}||^2 \\ &= ||\bar{R}_{\frac{\pi}{2},e_2}^T C \bar{R}_{\frac{\pi}{2},e_2} - \frac{1}{2}(\bar{R}_{\frac{\pi}{2},e_2}^T C \bar{R}_{\frac{\pi}{2},e_2} + \bar{M}_{e_3}^T (\bar{R}_{\frac{\pi}{2},e_2}^T C \bar{R}_{\frac{\pi}{2},e_2}) \bar{M}_{e_3})||^2 \\ &= ||\bar{R}_{\frac{\pi}{2},e_2}(\bar{R}_{\frac{\pi}{2},e_2}^T C \bar{R}_{\frac{\pi}{2},e_2} - \frac{1}{2}(\bar{R}_{\frac{\pi}{2},e_2}^T C \bar{R}_{\frac{\pi}{2},e_2} + \bar{M}_{e_3}^T (\bar{R}_{\frac{\pi}{2},e_2}^T C \bar{R}_{\frac{\pi}{2},e_2}) \\ &\quad + \bar{M}_{e_3}))\bar{R}_{\frac{\pi}{2},e_2}^T||^2 \end{aligned}$$

since rotating a tensor does not change the value of the norm,

$$\begin{aligned} &= ||\bar{R}_{\frac{\pi}{2},e_2}\bar{R}_{\frac{\pi}{2},e_2}^T C \bar{R}_{\frac{\pi}{2},e_2}\bar{R}_{\frac{\pi}{2},e_2}^T - \frac{1}{2}(\bar{R}_{\frac{\pi}{2},e_2}\bar{R}_{\frac{\pi}{2},e_2}^T C \bar{R}_{\frac{\pi}{2},e_2}\bar{R}_{\frac{\pi}{2},e_2}^T \\ &\quad + \bar{R}_{\frac{\pi}{2},e_2}\bar{M}_{e_3}^T (\bar{R}_{\frac{\pi}{2},e_2}^T C \bar{R}_{\frac{\pi}{2},e_2}) \bar{M}_{e_3} \bar{R}_{\frac{\pi}{2},e_2}^T)||^2 \\ &= ||C - \frac{1}{2}(C + (\bar{R}_{\frac{\pi}{2},e_2}\bar{M}_{e_3}^T \bar{R}_{\frac{\pi}{2},e_2}^T)^T C (\bar{R}_{\frac{\pi}{2},e_2}\bar{M}_{e_3}\bar{R}_{\frac{\pi}{2},e_2}^T))||^2 \\ &= ||C - \frac{1}{2}(C + \bar{M}_{e_2}^T C \bar{M}_{e_2})||^2 \end{aligned}$$

since $\bar{R}_{\frac{\pi}{2},e_2}\bar{M}_{e_3}\bar{R}_{\frac{\pi}{2},e_2}^T = \bar{M}_{e_2}$,

$$= ||\frac{1}{2}(C - \bar{M}_{e_2}^T C \bar{M}_{e_2})||^2 \tag{3.24}$$

Similarly, one can show that

$$d(\bar{R}_{\frac{\pi}{2},e_1}^T C \bar{R}_{\frac{\pi}{2},e_1}, \mathcal{L}^{mono}) = ||\frac{1}{2}(C - \bar{M}_{e_1}^T C \bar{M}_{e_1})||^2.$$

Now, we evaluate the norms of the matrices appearing in Equations 3.23, 3.24 and 3.25. Rotating the coordinate system of C by $\bar{M}_{e_3}$, we get the following equality

$$\bar{M}_{e_3}^T C \bar{M}_{e_3} = \begin{bmatrix} C_{11} & C_{12} & C_{13} & -C_{14} & -C_{15} & C_{16} \\ C_{12} & C_{22} & C_{23} & -C_{24} & -C_{25} & C_{26} \\ C_{13} & C_{23} & C_{33} & -C_{34} & -C_{35} & C_{36} \\ -C_{14} & -C_{24} & -C_{34} & C_{44} & C_{45} & -C_{46} \\ -C_{15} & -C_{25} & -C_{35} & C_{45} & C_{55} & -C_{56} \\ C_{16} & C_{26} & C_{36} & -C_{46} & -C_{56} & C_{66} \end{bmatrix}, \tag{3.25}$$

where C is the matrix expressed in Equation 3.14. Note that a negative sign is introduced for the entries of $\bar{M}_{e_3}^T C \bar{M}_{e_3}$, which has an odd number of 3's in their fourth-rank tensor notation. For example, the entity $C_{14} = c_{1123}$ is multiplied with -1 when $\bar{M}_{e_3}$ acts on C. Then, $\frac{1}{2}(C - \bar{M}_{e_3}^T C \bar{M}_{e_3})$ can be written as

$$\frac{1}{2}(C - \bar{M}_{e_3}^T C \bar{M}_{e_3}) = \begin{bmatrix} 0 & 0 & 0 & C_{14} & C_{15} & 0 \\ 0 & 0 & 0 & C_{24} & C_{25} & 0 \\ 0 & 0 & 0 & C_{34} & C_{35} & 0 \\ C_{14} & C_{24} & C_{34} & 0 & 0 & C_{46} \\ C_{15} & C_{25} & C_{35} & 0 & 0 & C_{56} \\ 0 & 0 & 0 & C_{46} & C_{56} & 0 \end{bmatrix}. \tag{3.26}$$

Similarly, the other matrices can be found as

$$\frac{1}{2}(C - \bar{M}_{\mathbf{e}_2}^T C \bar{M}_{\mathbf{e}_2}) = \begin{bmatrix} 0 & 0 & 0 & C_{14} & 0 & C_{16} \\ 0 & 0 & 0 & C_{24} & 0 & C_{26} \\ 0 & 0 & 0 & C_{34} & 0 & C_{36} \\ C_{14} & C_{24} & C_{34} & 0 & C_{45} & 0 \\ 0 & 0 & 0 & C_{45} & 0 & C_{56} \\ C_{16} & C_{26} & C_{36} & 0 & C_{56} & 0 \end{bmatrix}, \tag{3.27}$$

$$\frac{1}{2}(C - \bar{M}_{\mathbf{e}_1}^T C \bar{M}_{\mathbf{e}_1}) = \begin{bmatrix} 0 & 0 & 0 & 0 & C_{15} & C_{16} \\ 0 & 0 & 0 & 0 & C_{25} & C_{26} \\ 0 & 0 & 0 & 0 & C_{35} & C_{36} \\ 0 & 0 & 0 & 0 & C_{45} & C_{46} \\ C_{15} & C_{25} & C_{35} & C_{45} & 0 & 0 \\ C_{16} & C_{26} & C_{36} & C_{46} & 0 & 0 \end{bmatrix}. \tag{3.28}$$

The matrix appearing in Equation 3.22, namely

$$\frac{3}{4}C - \frac{1}{4}(\bar{M}_{\mathbf{e}_1}^T C \bar{M}_{\mathbf{e}_1} + \bar{M}_{\mathbf{e}_2}^T C \bar{M}_{\mathbf{e}_2} + \bar{M}_{\mathbf{e}_3}^T C \bar{M}_{\mathbf{e}_3}),$$

can be evaluated by summing Equations 3.26, 3.27, 3.28 and then dividing the sum by 2 as

$$\begin{bmatrix} 0 & 0 & 0 & C_{14} & C_{15} & C_{16} \\ 0 & 0 & 0 & C_{24} & C_{25} & C_{26} \\ 0 & 0 & 0 & C_{34} & C_{35} & C_{36} \\ C_{14} & C_{24} & C_{34} & 0 & C_{45} & C_{46} \\ C_{15} & C_{25} & C_{35} & C_{45} & 0 & C_{56} \\ C_{16} & C_{26} & C_{36} & C_{46} & C_{56} & 0 \end{bmatrix}. \tag{3.29}$$

Then, the square of its norm, namely $d(C, \mathcal{L}^{ortho})$, is equal to

$$2(C_{14}^2 + C_{15}^2 + C_{16}^2 + C_{24}^2 + C_{25}^2 + C_{26}^2 + C_{34}^2 + C_{35}^2 + C_{36}^2 + C_{45}^2 + C_{46}^2 + C_{56}^2). \tag{3.30}$$

The sum of the square of the norms appearing in the right-hand side of Equation 3.20 can be achieved by summing the square of the norms of the matrices in Equations 3.28, 3.27, 3.26 and we get

$$\begin{aligned} & 2(C_{14}^2 + C_{15}^2 + C_{24}^2 + C_{25}^2 + C_{34}^2 + C_{35}^2 + C_{46}^2 + C_{56}^2) \\ & +2(C_{14}^2 + C_{16}^2 + C_{24}^2 + C_{26}^2 + C_{34}^2 + C_{36}^2 + C_{45}^2 + C_{56}^2) \\ & +2(C_{15}^2 + C_{16}^2 + C_{25}^2 + C_{26}^2 + C_{35}^2 + C_{36}^2 + C_{45}^2 + C_{46}^2) \\ = \; & 4(C_{14}^2 + C_{15}^2 + C_{16}^2 + C_{24}^2 + C_{25}^2 + C_{26}^2 + C_{34}^2 + C_{35}^2 + C_{36}^2 \\ & +C_{45}^2 + C_{46}^2 + C_{56}^2). \end{aligned} \tag{3.31}$$

Note that the above expression, which is

$$d(C, \mathcal{L}^{mono}) + d(\bar{R}^T_{\frac{\pi}{2},\mathbf{e_2}} C \bar{R}_{\frac{\pi}{2},\mathbf{e_2}}, \mathcal{L}^{mono}) + d(\bar{R}^T_{\frac{\pi}{2},\mathbf{e_1}} C \bar{R}_{\frac{\pi}{2},\mathbf{e_1}}, \mathcal{L}^{mono}),$$

is twice the expression $d(C, \mathcal{L}^{ortho})$ expressed in Equation 3.30. Hence, Equation 3.20 holds. ■

Theorem 7 enables us to determine the orientation of the closest orthotropic tensor from the plot of a monoclinic-distance function. To determine the distance of C to orthotropic symmetry class for any orientation of the coordinate system, one should sum three monoclinic-distance functions directed along the axes of the coordinate system and divide the sum by two.

Now, we introduce a field data example where the medium's elasticity tensor is evaluated by inverting the phase velocities and polarizations for some directions, which are not necessarily aligned with symmetry axes or planes. The evaluation of the elasticity tensor is explained in [18].

The elasticity tensor in [18] is inverted from a multiazimuth, multicomponent VSP data set acquired in Vacuum field, New Mexico. There was no a priori assumption about the symmetry of the medium when the geophysical data was inverted to find the elasticity matrix C. The elasticity matrix in [18] is represented in the following

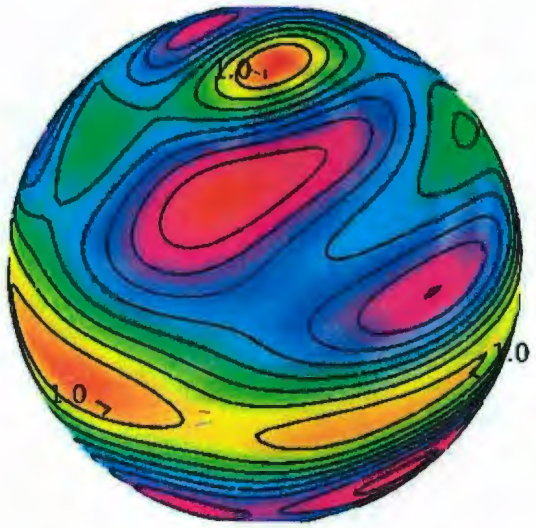

Figure 3.8: The plot of the distance function $d(\bar{X}^T C \bar{X}, \mathcal{L}^{mono})$ for C expressed in Equation 3.32. There is no apparent symmetry observed from the plot. This suggests that C is generally anisotropic. However, three minimum extrema near to the coordinate axes may imply that C is close to the orthotropic symmetry since those extrema are mutually perpendicular.

equation:

$$C = \begin{bmatrix} 7.82 & 3.45 & 2.57 & 0.19 & 0.08 & 0.17 \\ 3.45 & 8.13 & 2.36 & 0.11 & 0.10 & 0.24 \\ 2.57 & 2.36 & 7.09 & -0.13 & 0.40 & 0.23 \\ 0.19 & 0.11 & -0.13 & 3.33 & -0.15 & 0.21 \\ 0.08 & 0.10 & 0.40 & -0.15 & 4.13 & -0.30 \\ 0.17 & 0.24 & 0.23 & 0.21 & -0.30 & 4.85 \end{bmatrix}. \tag{3.32}$$

The plot of the monoclinic-distance function of the generally anisotropic elasticity tensor C is shown in Figures 3.8, 3.9, 3.10, 3.11.

From the plot of the monoclinic-distance function of C, one can determine the

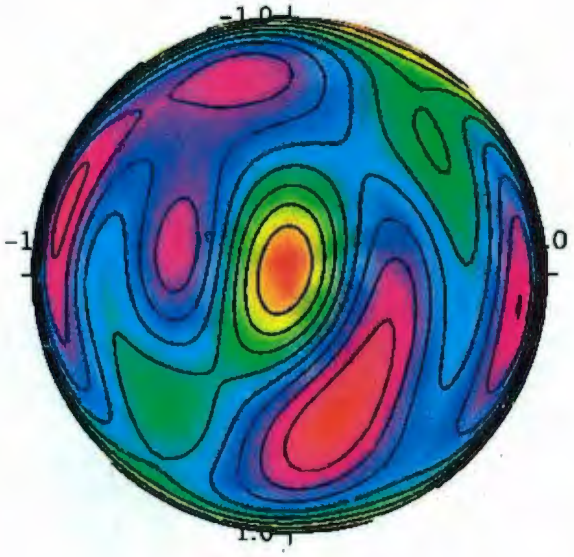

Figure 3.9: The plot of the distance function $d(\bar{X}^T C \bar{X}, \mathcal{L}^{mono})$ for C in Equation 3.32 viewed from the z-axis, where it is close to a minimum extremum. No symmetry can be observed from this point of view.

exact locations of the three minima of the function which are shown in Figure 3.8 as:

$$\begin{aligned}
\mathbf{v_3} &= \left(\sin\frac{4.92\pi}{180}\cos\frac{192.32\pi}{180}, \sin\frac{4.92\pi}{180}\sin\frac{192.32\pi}{180}, \cos\frac{4.92\pi}{180}\right), \\
\mathbf{v_2} &= \left(\sin\frac{87.58\pi}{180}\cos\frac{56.35\pi}{180}, \sin\frac{87.58\pi}{180}\sin\frac{56.35\pi}{180}, \cos\frac{87.58\pi}{180}\right), \\
\mathbf{v_1} &= \left(\sin\frac{87.83\pi}{180}\cos\frac{-10.07\pi}{180}, \sin\frac{87.83\pi}{180}\sin\frac{-10.07\pi}{180}, \cos\frac{87.83\pi}{180}\right),
\end{aligned}$$

where $\mathbf{v_3}, \mathbf{v_2}$ and $\mathbf{v_1}$ are the directions of the minima that are close to $\mathbf{e_3}$-, $\mathbf{e_2}$- and $\mathbf{e_1}$-axis, respectively. Note that the angle between $\mathbf{v_3}$ and $\mathbf{v_1}$ is 92.38°, $\mathbf{v_3}$ and $\mathbf{v_2}$ is 91.12°, $\mathbf{v_2}$ and $\mathbf{v_1}$ is 66.37°. The values of the monoclinic distance function in those directions are

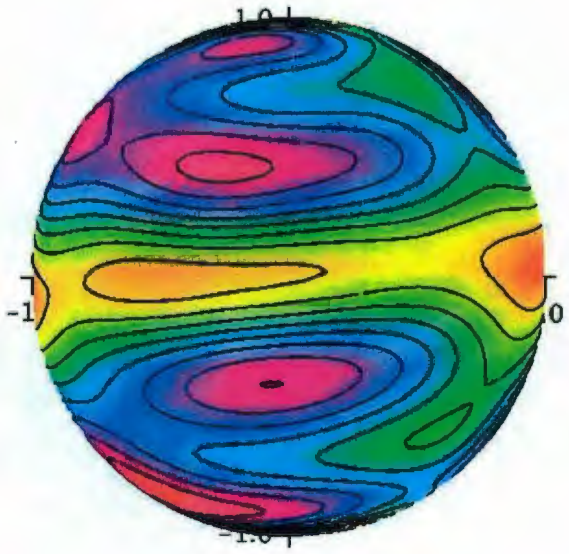

Figure 3.10: The plot of the distance function $d(\bar{X}^T C \bar{X}, \mathcal{L}^{mono})$ for C in Equation 3.32 viewed from the y-axis, where it is close to a minimum extremum. No symmetry can be observed but some correlations among the colors and among the shapes of the contours can be seen with respect to the equatorial plane.

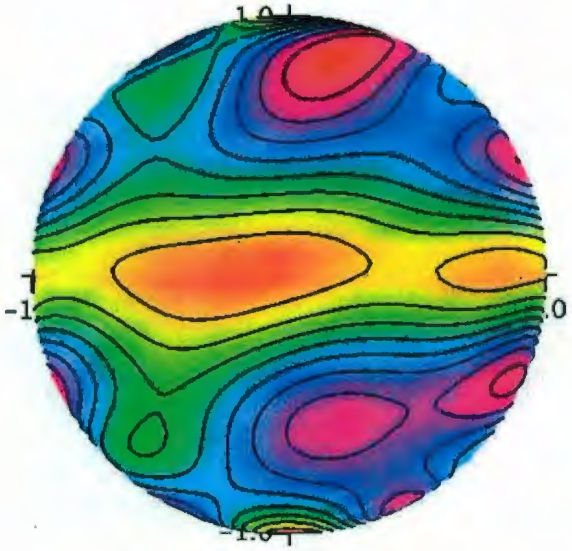

Figure 3.11: The plot of the distance function $d(\bar{X}^T C \bar{X}, \mathcal{L}^{mono})$ for C in Equation 3.32 viewed from the x-axis, where it is close to a minimum extrema. It is similar to y-axis view in terms of being symmetrical with respect to the equatorial plane. However, the extremum is closer to the x-axis when compared with the y-axis.

$$
\begin{aligned}
d(\bar{X}_3^T C \bar{X}_3, \mathcal{L}^{mono}) &= 0.281, \text{ where } X_3 \in SO(3) \text{ and } X_3(\mathbf{e_3}) = \mathbf{v_3} \\
d(\bar{X}_2^T C \bar{X}_2, \mathcal{L}^{mono}) &= 0.453, \text{ where } X_2 \in SO(3) \text{ and } X_2(\mathbf{e_3}) = \mathbf{v_2} \\
d(\bar{X}_1^T C \bar{X}_1, \mathcal{L}^{mono}) &= 0.353, \text{ where } X_1 \in SO(3) \text{ and } X_1(\mathbf{e_3}) = \mathbf{v_1}.
\end{aligned}
$$

In order to find the orientation of the coordinate system of the closest orthotropic elasticity tensor, we can use Theorem 7. The theorem implies that the orientation of the closest orthotropic tensor is determined by the orientation of the three mutually perpendicular directions which gives the minimum value for the sum of their monoclinic distance functions. Thus, one should search for the minimum around $\mathbf{v_3}, \mathbf{v_2}$ and $\mathbf{v_1}$ directions because those are the three minima of the function. To solve this optimization problem, we are restricting the search of coordinate systems in the 20° neighbourhood of $\mathbf{v_3}, \mathbf{v_2}$ and $\mathbf{v_1}$. Note that specifying two axes determines the other axis of the coordinate system. Figure 3.8 suggests that the minimum can be achieved whenever one of the axis of the coordinate system is aligned with $\mathbf{v_3}$ since the remaining two directions will be in the equatorial plane region whose distance to monoclinic is close to zero. However, the choice of x-axis should be made after finding the values along the equatorial plane. The first directions to be searched are along $\mathbf{v_1}$ and $\mathbf{v_2}$ vectors. However, if there are not many extrema along the equatorial plane then one can make the search all over the plane. In this particular example, we show all the cases for the restriction of the search where x-axis will be in the neighbourhood of $\mathbf{v_1}$ vector, $\mathbf{v_2}$ vector and also in all directions in the equatorial plane.

The orthogonal transformation that maps $\mathbf{e_1}$ and $\mathbf{e_3}$ to the 20° neighbourhood of $\mathbf{v_1}$ and $\mathbf{v_3}$, respectively, is given by

$$
A = \begin{bmatrix}
\cos\psi\cos\theta - \sin\psi\cos\phi\sin\theta & -\cos\psi\sin\theta - \sin\psi\cos\phi\cos\theta & \sin\psi\sin\phi \\
\sin\psi\cos\theta + \cos\psi\cos\phi\sin\theta & -\sin\psi\sin\theta + \cos\psi\cos\phi\cos\theta & -\cos\psi\sin\phi \\
\sin\phi\sin\theta & \sin\phi\cos\theta & \cos\phi.
\end{bmatrix} \tag{3.33}
$$

where

$$\begin{aligned}\phi &\in \left[\frac{\pi}{180}(4.9235-20), \frac{\pi}{180}(4.9235+20)\right],\\ \psi &\in \left[\frac{\pi}{180}(192.318-20+90), \frac{\pi}{180}(192.318+20+90)\right],\\ \theta &\in \left[\frac{\pi}{180}(68.07-20), \frac{\pi}{180}(68.07+20)\right].\end{aligned}$$

Recall that the relation between the Euler angle ψ of a rotation matrix and the vector that the matrix maps $\mathbf{e_3}$ to new z-axis is given in Equation 2.29. Thus, we present ψ in the form of $+90°$ to make its geometrical location clear. The minimum distance of C, in the above neighbourhood of the Euler angles, to the orthotropic symmetry is found as

$$\min_{X\in SO(3)}(d(\bar{X}^T C\bar{X}, \mathcal{L}^{ortho})) = 0.600933, \tag{3.34}$$

where the minimum distance is achieved for the transformation B. Euler angles of B are $\phi = 3.59°, \psi = 202.94° + 90°$ and $\theta = 48.07°$.

Similarly, the orthogonal transformation that maps $\mathbf{e_2}$ and $\mathbf{e_3}$ to the 20° neighbourhood of $\mathbf{v_2}$ and $\mathbf{v_3}$, respectively, is Equation 3.33 but the restrictions are changed as

$$\begin{aligned}\phi &\in \left[\frac{\pi}{180}(4.9235-20), \frac{\pi}{180}(4.9235+20)\right],\\ \psi &\in \left[\frac{\pi}{180}(192.318-20+90), \frac{\pi}{180}(192.318+20+90)\right],\\ \theta &\in \left[\frac{\pi}{180}(134.07-20), \frac{\pi}{180}(134.07+20)\right].\end{aligned}$$

Note that the only parameter that has changed is θ since $\mathbf{v_3}$ remains the same but the search is now restricted near the $\mathbf{v_2}$ direction instead of $\mathbf{v_1}$. The minimum distance of C, in the 20° neighbourhood of $\mathbf{v_2}$ and $\mathbf{v_3}$, to the orthotropic symmetry is found as

$$\min_{X\in SO(3)}(d(\bar{A}^T C\bar{A}, \mathcal{L}^{ortho})) = 0.600920, \tag{3.35}$$

where the minimum distance is achieved for the transformation A. Euler angles of A are $\phi = 3.57°, \psi = 203.54° + 90°$ and $\theta = 137.23°$.

Lastly, we restrict the search for the minimum along the equatorial plane and $\mathbf{v_3}$. Then the restrictions become

$$\begin{aligned}
\phi &\in \left[\frac{\pi}{180}(4.9235-20), \frac{\pi}{180}(4.9235+20)\right], \\
\psi &\in \left[\frac{\pi}{180}(192.318-20+90), \frac{\pi}{180}(192.318+20+90)\right], \\
\theta &\in [0, 2\pi].
\end{aligned}$$

Note that θ ranges from $0..2\pi$ since it covers the equatorial plane. Since there are not many extrema along the plane, Maple gives the minimum as

$$\min_{X \in SO(3)} (d(\bar{A}^T C \bar{A}, \mathcal{L}^{ortho})) = 0.600920, \tag{3.36}$$

where the minimum distance is achieved for the transformation A. Euler angles of A are $\phi = 3.57°, \psi = 203.54° + 90°$ and $\theta = 137.23°$.

As expected the minimum is achieved near one of those vectors, which is $\mathbf{v_2}$ in this example. Hence, the orientation of the coordinate system of the closest orthotropic elasticity tensor to C is

$$\begin{aligned}
\mathbf{e_3'} &= \left(\sin\frac{3.57\pi}{180}\cos\frac{203.54\pi}{180}, \sin\frac{3.57\pi}{180}\sin\frac{203.54\pi}{180}, \cos\frac{3.57\pi}{180}\right), \\
\mathbf{e_2'} &= \left(\sin\frac{92.62\pi}{180}\cos\frac{160.71\pi}{180}, \sin\frac{92.62\pi}{180}\sin\frac{160.71\pi}{180}, \cos\frac{92.62\pi}{180}\right), \\
\mathbf{e_1'} &= \left(\sin\frac{87.57\pi}{180}\cos\frac{70.85\pi}{180}, \sin\frac{87.57\pi}{180}\sin\frac{70.85\pi}{180}, \cos\frac{87.57\pi}{180}\right).
\end{aligned}$$

Thus, z-axis of the closest orthotropic elasticity tensor has only changed 3.57° from its original orientation. And the x-axis is close to the extremum which is near the $\mathbf{e_2}$-axis that can be seen from Figure 3.10. Note that the extremum near $\mathbf{e_2}$-axis is located 56.35° from $\mathbf{e_1}$-axis, whereas the orientation of the x-axis of the closest orthotropic tensor is 70.85° from $\mathbf{e_1}$-axis.

To find the closest orthotropic tensor in its natural coordinate system, first one rotates the elasticity tensor by $\bar{A}$ and get $\bar{A}^T C \bar{A}$, then finds $(\bar{A}^T C \bar{A})^{ortho}$ by using Equation 3.16. We obtain

$$(\bar{A}^T C \bar{A})^{ortho} = \begin{bmatrix} 8.38 & 3.36 & 2.49 & 0 & 0 & 0 \\ 3.36 & 7.77 & 2.43 & 0 & 0 & 0 \\ 2.49 & 2.43 & 7.08 & 0 & 0 & 0 \\ 0 & 0 & 0 & 4.16 & 0 & 0 \\ 0 & 0 & 0 & 0 & 3.30 & 0 \\ 0 & 0 & 0 & 0 & 0 & 4.66 \end{bmatrix}. \tag{3.37}$$

Note that although the orientation of $(\bar{A}^T C \bar{A})^{ortho}$ is tilted with respect to the orientation of C, its $z-, y-$ and x-axis is considered to be $\{\mathbf{e_1}, \mathbf{e_2}, \mathbf{e_3}\}$. In this way, we can express C^{ortho} in its natural coordinate system. However, to express $(\bar{A}^T C \bar{A})^{ortho}$ in the coordinate system where C is expressed in, then it should be rotated back to its original coordinate system, namely one gets $\bar{A}(\bar{A}^T C \bar{A})^{ortho}\bar{A}^T$.

3.4 Determining the Closest Tetragonal Elasticity Tensor

In this section, we consider the problem of closeness to the tetragonal symmetry class for a given elasticity tensor. The approach presented in this section is very similar to finding the closest orthotropic elasticity tensor which is presented in the previous section. However, we will not introduce a theorem which relates the tetragonal-distance function to the sum of monoclinic-distance functions for some directions as we did in Theorem 7. The equality between those distance functions does not hold for tetragonal symmetry because the symmetry group of tetragonal does not only consist of mirror planes but also it contains a four-fold rotation. Recall that monoclinic-distance function can be used for determining the normal directions of mirror planes of a medium. Nevertheless, the location of extrema of the tetragonal-distance function and the sum of monoclinic-distance functions for some particular

directions give values that are either equal or close to each other. These particular directions are aligned with the normals of the mirror planes that exist in a tetragonal medium. More precisely, there are four mirror planes which are lies in a plane that are 45° apart and another mirror plane along the normal of that plane. It seems that although the functions are different, the roots of their first-partial derivatives have some relationship since their extrema are close. This result may be expected since existence of mirror planes, whose normals are 45° apart lying in a plane, implies a four-fold rotation around the normal of that plane.

Before introducing an example of finding the closest-tetragonal elasticity tensor, we will formulate the tetragonal-distance function. In order to do that, firstly, we determine the projection of any elasticity tensor onto the space of tetragonal-elasticity tensors, namely onto $\mathcal{L}^{tetra}$. The projection function, which is defined in Equation 2.4, is

$$\begin{aligned} C^{tetra} &= \frac{1}{8}(C + \bar{M}_{\mathbf{e_1}}^T C \bar{M}_{\mathbf{e_1}} + \bar{M}_{\mathbf{e_2}}^T C \bar{M}_{\mathbf{e_2}} + \bar{M}_{\mathbf{e_3}}^T C \bar{M}_{\mathbf{e_3}} \\ &\quad + \bar{M}_{(1,1,0)}^T C \bar{M} v_{(1,1,0)} + \bar{M}_{(1,-1,0)}^T C \bar{M}_{(1,-1,0)} \\ &\quad + \bar{R}_{\frac{\pi}{2}}^T C \bar{R}_{\frac{\pi}{2}} + \bar{R}_{-\frac{\pi}{2}}^T C \bar{R}_{-\frac{\pi}{2}}), \end{aligned} \tag{3.38}$$

since

$$G^{Tetra} = \{\pm I, \pm M_{\mathbf{e_1}}, \pm M_{\mathbf{e_2}}, \pm M_{\mathbf{e_3}}, \pm M_{(1,1,0)}, \pm M_{(1,-1,0)}, \pm R_{\frac{\pi}{2}}, \pm R_{-\frac{\pi}{2}}\},$$

where $R_{\frac{\pi}{2}}, R_{-\frac{\pi}{2}}$ are clockwise and counter-clockwise rotations around $\mathbf{e_3}$-axis by $\frac{\pi}{2}$ radians, respectively. Note that we only consider eight elements of G^{Tetra} to find C^{tetra}. This is because of C being an even-rank tensor. More precisely, when an orthogonal transformation acts on an even-rank tensor, then it has the same effect as the negative of that orthogonal transformation has. Formally stating:

$$g^T C g = (-g)^T C (-g), \text{ for any } g \in O(3)$$

The form of C^{tetra} can be found by using Equation 3.38 as

$$C^{tetra} = \begin{bmatrix} \frac{1}{2}(C_{11}+C_{22}) & C_{12} & \frac{1}{2}(C_{13}+C_{23}) & 0 & 0 & 0 \\ C_{12} & \frac{1}{2}(C_{11}+C_{22}) & \frac{1}{2}(C_{13}+C_{23}) & 0 & 0 & 0 \\ C_{13} & C_{23} & C_{33} & 0 & 0 & 0 \\ 0 & 0 & 0 & \frac{1}{2}(C_{44}+C_{55}) & 0 & 0 \\ 0 & 0 & 0 & 0 & \frac{1}{2}(C_{44}+C_{55}) & 0 \\ 0 & 0 & 0 & 0 & 0 & C_{66} \end{bmatrix}. \tag{3.39}$$

In order to find the distance of a given C to the space of tetragonal-elasticity tensors represented in their natural coordinate systems, one applies Equation 2.13 to get

$$d(C, \mathcal{L}^{tetra}) := ||C||^2 - ||C^{tetra}||^2, \tag{3.40}$$

If one wants to find the orientation of the closest tetragonal tensor among all coordinate systems then the distance function, which is defined in Definition 4, should be used. Applying the definition for the tetragonal symmetry we get

$$d(\bar{X}^T C \bar{X}, \mathcal{L}^{tetra}) = ||C||^2 - ||(\bar{X}^T C \bar{X})^{tetra}||^2, \text{ for all } X \in SO(3). \tag{3.41}$$

Note that the projected tensor, namely $(\bar{X}^T C \bar{X})^{tetra}$, depends on the orientations of the coordinate axes. More precisely, as the coordinate system changes so does the tensor $(\bar{X}^T C \bar{X})^{tetra}$, which is also the case in orthotropic symmetry.

Consider the following elasticity tensor

$$C = \begin{bmatrix} 17 & 1 & -16 & 0 & 0 & 2\sqrt{2} \\ 1 & 17 & 6 & 0 & 0 & -2\sqrt{2} \\ -16 & 6 & 31 & 0 & 0 & 3\sqrt{2} \\ 0 & 0 & 0 & 10 & 0 & 0 \\ 0 & 0 & 0 & 0 & 10 & 0 \\ 2\sqrt{2} & -2\sqrt{2} & 3\sqrt{2} & 0 & 0 & 16 \end{bmatrix}. \tag{3.42}$$

Elasticity tensor C is chosen in such a way that it allows more symmetric wavefronts than its symmetry class. The form of C implies that it has a monoclinic symmetry class whereas its wavefronts have a four-fold rotational symmetry around $\mathbf{e_3}$-axis. The parameters of elasticity tensor in Equation 3.42 satisfy the following relations:

$$\begin{aligned} C_{11} &= C_{22} \\ C_{13} &= -C_{23} - C_{44} \\ C_{26} &= -C_{16} \\ C_{45} &= 0. \end{aligned} \tag{3.43}$$

The above relationships must be satisfied for a monoclinic elasticity tensor that allows the passage of more symmetric wavefronts as is stated in [7]. Then, it is proved in [7] that the symmetries of the wavefronts are $R_{\frac{\pi}{2}}$ and $M_{\mathbf{e_3}}$, where the latter is the element of the monoclinic-symmetry group. The higher symmetry of wavefronts can be viewed as an example of Curie's Principle which states that results are at least as symmetric as the causes. Below, we use the method developed in this thesis, to examine the case for which the material symmetry is lower than the wavefront symmetry.

The plot of monoclinic-distance function of C is shown in Figures 3.12, 3.13, 3.14, 3.15.

It can be shown that C is monoclinic since the monoclinic-distance function along $\mathbf{e_3}$ vanishes. We formally write this as

$$d(C, \mathcal{L}^{mono}) = 0.$$

Moreover, the medium is not more symmetric than monoclinic since the distance function along the other two extrema near $\mathbf{e_1}$-axis and $\mathbf{e_2}$-axis does not vanish. Searching for the minimum around the 20° neighbourhood of $\mathbf{e_1}$-axis gives

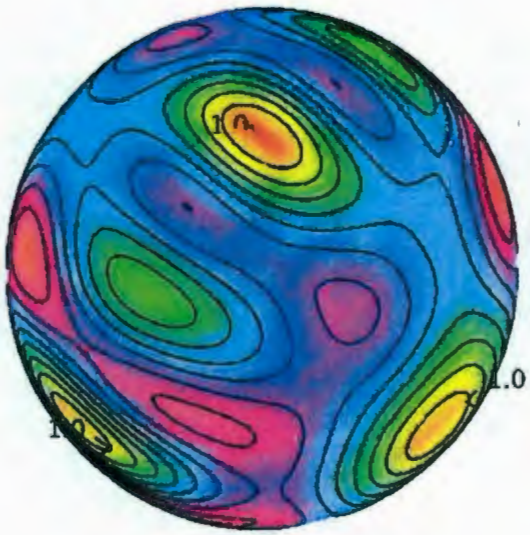

Figure 3.12: The plot of the distance function $d(\bar{X}^T C \bar{X}, \mathcal{L}^{mono})$ for C expressed in Equation 3.42. This view suggests that there is a direction near y-axis that can be close to being a four-fold rotation axis. This is also supported by the existence of 45° apart minima which lie in the plane almost perpendicular to y-axis.

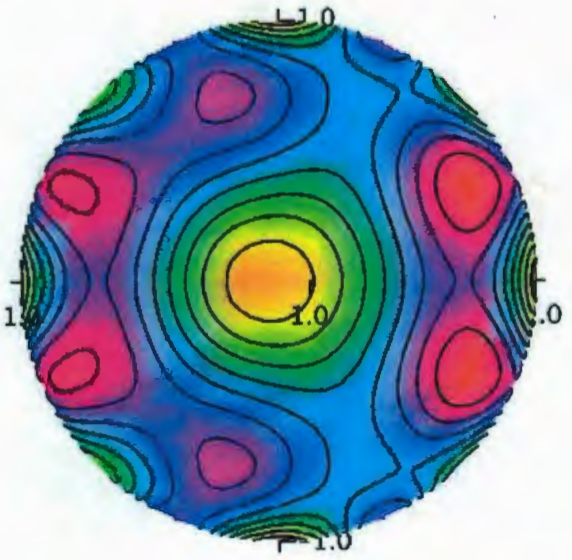

Figure 3.13: The plot of the distance function $d(\bar{X}^T C \bar{X}, \mathcal{L}^{mono})$ for C expressed in Equation 3.42 viewed from y-axis, where it is close to a minimum extremum. This view seems close to having a four-fold rotational symmetry. Thus, the closest tetragonal tensor should be searched around this direction.

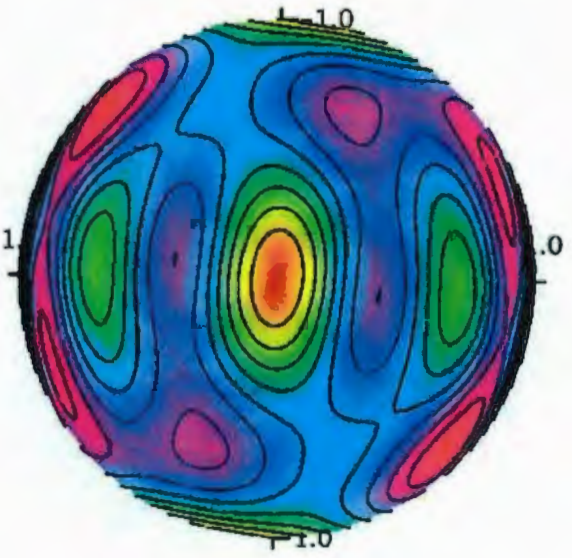

Figure 3.14: The plot of the distance function $d(\bar{X}^T C \bar{X}, \mathcal{L}^{mono})$ for C expressed in Equation 3.42 viewed from a direction perpendicular to the rotation axis of the closest tetragonal tensor. The angles between minima are around 45° apart which is expected in tetragonal symmetry.

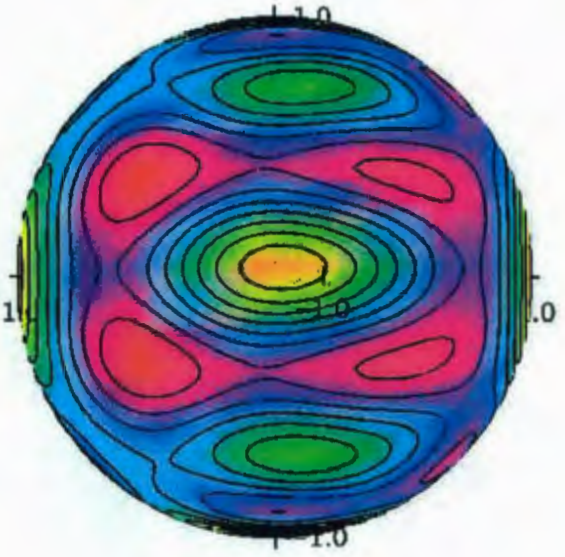

Figure 3.15: The plot of the distance function $d(\bar{X}^T C \bar{X}, \mathcal{L}^{mono})$ for C expressed in Equation 3.42 viewed from a direction perpendicular to the rotation axis of the closest tetragonal tensor. These minima are also oriented 45° apart.

$$\min_{X \in SO(3)} (d(\bar{X}^T C \bar{X}, \mathcal{L}^{mono})) = 22.07,$$

where the restriction for Euler angles of $\bar{X}$ are

$$\begin{aligned} \phi &\in \left[\frac{\pi}{180}(90-20), \frac{\pi}{180}(90+20)\right], \\ \psi &\in \left[\frac{\pi}{180}(0-20+90), \frac{\pi}{180}(0+20+90)\right]. \end{aligned}$$

Then, Euler angles that the minimum value is achieved for $d(\bar{X}^T C \bar{X}, \mathcal{L}^{mono})$ are $\phi = 90.00°, \psi = -9.33° + 90°$. Hence, the minimum distance to monoclinic symmetry is achieved along the vector

$$\mathbf{v_1} = \left(\cos\frac{-9.33\pi}{180}, \sin\frac{-9.33\pi}{180}, 0\right). \tag{3.44}$$

The minimum around $\mathbf{e_2}$-axis is

$$\min_{X \in SO(3)} (d(\bar{A}^T C \bar{A}, \mathcal{L}^{mono})) = 22.07,$$

where the restriction for Euler angles of $\bar{X}$ are

$$\begin{aligned} \phi &\in \left[\frac{\pi}{180}(90-20), \frac{\pi}{180}(90+20)\right], \\ \psi &\in \left[\frac{\pi}{180}(90-20+90), \frac{\pi}{180}(90+20+90)\right]. \end{aligned}$$

Then, Euler angles that give the minimum value for $d(\bar{X}^T C \bar{X}, \mathcal{L}^{mono})$ are $\phi = 90.00°, \psi = 80.67° + 90°$. Hence, the minimum distance to monoclinic symmetry is achieved along the vector

$$\mathbf{v_2} = \left(\cos\frac{80.67\pi}{180}, \sin\frac{80.67\pi}{180}, 0\right) \tag{3.45}$$

Now, we find the orientation of other local extrema that are between $\mathbf{e_1}$- and $\mathbf{e_3}$-axis and appear as a green region in the figures. Thus, the restrictions for Euler angles around one of those regions are

$$\begin{aligned} \phi &\in \left[\frac{\pi}{180}(45-20), \frac{\pi}{180}(45+20)\right], \\ \psi &\in \left[\frac{\pi}{180}(-10-20+90), \frac{\pi}{180}(-10+20+90)\right]. \end{aligned}$$

Then the minimum for $d(\bar{X}^T C \bar{X}, \mathcal{L}^{mono})$ is

$$\min_{X \in SO(3)} (d(\bar{X}^T C \bar{X}, \mathcal{L}^{mono})) = 172.56,$$

where it is attained for Euler angles $\phi = 44.82°, \psi = -3.46° + 90°$. Hence, the minimum distance to monoclinic symmetry is achieved along the vector

$$\mathbf{v_3} = \left(\cos\frac{-3.46\pi}{180}\sin\frac{44.82\pi}{180}, \sin\frac{-3.46\pi}{180}\sin\frac{44.82\pi}{180}, \cos\frac{44.82\pi}{180}\right). \tag{3.46}$$

For the other green region the minimum for $d(\bar{X}^T C \bar{X}, \mathcal{L}^{mono})$ is

$$\min_{X \in SO(3)} (d(\bar{X}^T C \bar{X}, \mathcal{L}^{mono})) = 172.56,$$

which is achieved along the vector

$$\mathbf{v_4} = \left(\cos\frac{176.54\pi}{180} \sin\frac{44.82\pi}{180}, \sin\frac{176.54\pi}{180} \sin\frac{44.82\pi}{180}, \cos\frac{44.82\pi}{180} \right). \tag{3.47}$$

Hence, we see that the directions of four extrema, namely $\mathbf{e_3}, \mathbf{v_1}, \mathbf{v_3}, \mathbf{v_4}$ that are almost perpendicular to $\mathbf{v_2}$, but they do not lie in the same plane. This may also be observed from Figure 3.15.

The plot of $d(\bar{A}^T C \bar{A}, \mathcal{L}^{mono})$ suggests that the coordinate system of the closest tetragonal elasticity tensor to C may be around $\{-\mathbf{v_1}, \mathbf{e_3}, \mathbf{v_2}\}$ or $\{\mathbf{v_4}, \mathbf{v_3}, \mathbf{v_2}\}$, where in either case $\mathbf{v_2}$ should be the z-axis of C^{tetra}. Note that the minus sign is put in front of $\mathbf{v_1}$ to make the coordinate system right-handed. Thus, we search for the minimum around those coordinate systems. For doing a search around 20° neighbourhood of the coordinate system $\{-\mathbf{v_1}, \mathbf{e_3}, \mathbf{v_2}\}$, the restrictions for Euler angles are

$$\begin{aligned}
\phi &\in \left[\frac{\pi}{180}(90-20), \frac{\pi}{180}(90+20)\right], \\
\psi &\in \left[\frac{\pi}{180}(80-20+90), \frac{\pi}{180}(80+20+90)\right], \\
\theta &\in \left[\frac{\pi}{180}(0-20), \frac{\pi}{180}(0+20)\right].
\end{aligned}$$

Then, the minimum for $d(\bar{X}^T C \bar{X}, \mathcal{L}^{tetra})$ can be found as

$$\min_{X \in SO(3)} (d(\bar{X}^T C \bar{X}, \mathcal{L}^{tetra})) = 187.70.$$

This minimum is achieved for Euler angles $\phi = 90°, \psi = 173.11°$ and $\theta = 0°$. Hence, the coordinate axes of the closest tetragonal tensor around this neigbourhood are

$$\begin{aligned}
x-axis &= \left(\cos\frac{173.11\pi}{180}, \sin\frac{173.11\pi}{180}, 0\right), \\
y-axis &= (0,0,1), \\
z-axis &= \left(\cos\frac{83.11\pi}{180}, \sin\frac{83.11\pi}{180}, 0\right).
\end{aligned} \tag{3.48}$$

Note that the z-axis of the closest tetragonal elasticity tensor to C is not aligned with $\mathbf{v_2}$ but is as close as 2°.

The search around the coordinate system $\{\mathbf{v_4}, \mathbf{v_3}, \mathbf{v_2}\}$ gives the minimum for $d(C, \mathcal{L}^{tetra})$ as

$$\min_{X \in SO(3)} (d(\bar{X}^T C \bar{X}, \mathcal{L}^{tetra})) = 187.70.$$

The coordinate axes of the closest tetragonal tensor in the neighbourhood of $\{\mathbf{v_4}, \mathbf{v_3}, \mathbf{v_2}\}$ are

$$\begin{aligned} x-axis &= \left(\cos\frac{173.11\pi}{180}\sin\frac{45\pi}{180}, \sin\frac{173.11\pi}{180}\sin\frac{45\pi}{180}, \cos\frac{45\pi}{180}\right), \\ y-axis &= \left(\cos\frac{-6.89\pi}{180}\sin\frac{45\pi}{180}, \sin\frac{-6.89\pi}{180}\sin\frac{45\pi}{180}, \cos\frac{45\pi}{180}\right), \\ z-axis &= \left(\cos\frac{83.11\pi}{180}, \sin\frac{83.11\pi}{180}, 0\right). \end{aligned} \tag{3.49}$$

Note that the minimum values for the search around the two coordinate systems are equal. This is because the coordinate systems, expressed in Equations 3.48 and 3.49, of the closest tetragonal tensor are 45° apart.

It can be shown that the value of the tetragonal-distance function of C is equal to the value of the function of the tensor rotated 45° around its z-axis. More precisely,

$$d(C, \mathcal{L}^{tetra}) = d(\bar{R}_{\frac{\pi}{4}}^T C \bar{R}_{\frac{\pi}{4}}, \mathcal{L}^{tetra}),$$

where $R_{\frac{\pi}{4}}$ is a 45° rotation around z-axis.

Now, we compare the distance function $d(C, \mathcal{L}^{tetra})$ with the sum of monoclinic-distance functions. In order to do that we repeat the same searches for the minimum of the sum of monoclinic-distance functions that we did for $d(C, \mathcal{L}^{tetra})$. The sum of monoclinic-distance functions is denoted by Δ in the following equation:

$$\begin{aligned} \Delta &= d(C, \mathcal{L}^{mono}) + d(\bar{R}_{\frac{\pi}{2},\mathbf{e_2}}^T C \bar{R}_{\frac{\pi}{2},\mathbf{e_2}}, \mathcal{L}^{mono}) + d(\bar{R}_{\frac{\pi}{2},\mathbf{e_1}}^T C \bar{R}_{\frac{\pi}{2},\mathbf{e_1}}, \mathcal{L}^{mono}) \\ &\quad + d(\bar{R}_{\frac{\pi}{2},(\mathbf{1,1,0})}^T C \bar{R}_{\frac{\pi}{2},(\mathbf{1,1,0})}, \mathcal{L}^{mono}) + d(\bar{R}_{\frac{\pi}{2},(\mathbf{-1,1,0})}^T C \bar{R}_{\frac{\pi}{2},(\mathbf{-1,1,0})}, \mathcal{L}^{mono}), \end{aligned}$$

where $90_{(1,1,0)}$ and $90_{(-1,1,0)}$ are 90° rotations that transform $\mathbf{e_3}$ to $(1,1,0)$ and $\mathbf{e_3}$ to $(-1,1,0)$, respectively.

Making a search for the minimum of Δ around the coordinate system $\{-\mathbf{v_1}, \mathbf{e_3}, \mathbf{v_2}\}$ gives the closest coordinate system as

$$\begin{aligned} x-axis &= \left(\cos\frac{172.21\pi}{180}, \sin\frac{172.21\pi}{180}, 0\right), \\ y-axis &= (0,0,1), \\ z-axis &= \left(\cos\frac{82.21\pi}{180}, \sin\frac{82.21\pi}{180}, 0\right). \end{aligned}$$

The value of Δ function for this coordinate system is 399.65.

Similarly, the search around $\{\mathbf{v_4}, \mathbf{v_3}, \mathbf{v_2}\}$ gives the coordinate system for the minimum as

$$\begin{aligned} x-axis &= \left(\cos\frac{172.21\pi}{180}\sin\frac{45\pi}{180}, \sin\frac{172.21\pi}{180}\sin\frac{45\pi}{180}, \cos\frac{45\pi}{180}\right), \\ y-axis &= \left(\cos\frac{-7.79\pi}{180}\sin\frac{45\pi}{180}, \sin\frac{-7.79\pi}{180}\sin\frac{45\pi}{180}, \cos\frac{45\pi}{180}\right), \\ z-axis &= \left(\cos\frac{82.21\pi}{180}, \sin\frac{82.21\pi}{180}, 0\right). \end{aligned}$$

The value of the minimum of Δ in this coordinate systems is 399.65, too. Note that the difference between the closest coordinate systems found by minimizing the functions $d(C, \mathcal{L}^{tetra})$ and Δ is around 1°.

Now, we search for the closest tetragonal tensor around a different orientation, namely around the coordinate systems whose z-axis is $\mathbf{e_3}$. Then, the minimum of $d(C, \mathcal{L}^{tetra})$ is found in the coordinate system

$$\begin{aligned} x-axis &= \left(\cos\frac{-22.49\pi}{180}, \sin\frac{-22.49\pi}{180}, 0\right) \\ y-axis &= \left(\cos\frac{67.49\pi}{180}, \sin\frac{67.49\pi}{180}, 0\right) \\ z-axis &= (0,0,1). \end{aligned} \tag{3.50}$$

The value of the minimum is 520.

We obtain the minimum of Δ function also in the same coordinate system that is expressed in Equation 3.50. Recall that it was 1° close in the previous example. These two examples may imply that there can be a relation among the roots of the first-partial derivatives of Δ and $d(C, \mathcal{L}^{tetra})$ since their extrema are close enough.

The plot of the monoclinic-distance function has already suggested that the coordinate system of the closest tetragonal elasticity tensor can be achieved around the coordinate system $\{-\mathbf{v_1}, \mathbf{e_3}, \mathbf{v_2}\}$. Thus, it is expected that the value of $d(C, \mathcal{L}^{tetra})$ for the coordinate system expressed in Equation 3.48, which is 187.70, is smaller than the value for the coordinate system expressed in Equation 3.50, which is 520.

To find the closest elasticity tensor to C, one should rotate the coordinate system to where the absolute minimum of the tetragonal-distance function is achieved. This corresponds to the coordinate system expressed in Equation 3.48. Then, we find the rotated C as

$$\bar{A}^T C \bar{A} = \begin{bmatrix} 16.07 & -16.39 & 1.92 & 0 & -2.50 & 0 \\ -16.39 & 31.00 & 6.39 & 0 & -0.42 & 0 \\ 1.92 & 6.39 & 16.07 & 0 & 2.50 & 0 \\ 0 & 0 & 0 & 10 & 0 & 0 \\ -2.50 & -0.42 & 2.50 & 0 & 17.84 & 0 \\ 0 & 0 & 0 & 0 & 0 & 10 \end{bmatrix},$$

where $A \in SO(3)$ that transforms the coordinate system to the one that is expressed in Equation 3.48. Now, the closest tetragonal elasticity tensor can be evaluated by applying Formula 3.39. We obtain the closest tetragonal tensor as

$$(\bar{A}^T C \bar{A})^{tetra} = \begin{bmatrix} \frac{1}{2}(16.07+31) & -16.39 & \frac{1}{2}(1.92+6.39) & 0 & 0 & 0 \\ -16.39 & \frac{1}{2}(16.07+31) & \frac{1}{2}(1.92+6.39) & 0 & 0 & 0 \\ \frac{1}{2}(1.92+6.39) & \frac{1}{2}(1.92+6.39) & 16.07 & 0 & 0 & 0 \\ 0 & 0 & 0 & \frac{1}{2}(10+17.84) & 0 & 0 \\ 0 & 0 & 0 & 0 & \frac{1}{2}(10+17.84) & 0 \\ 0 & 0 & 0 & 0 & 0 & 10 \end{bmatrix}.$$

Even though at the present time, the available criterion is provided by expressions 3.43, the presented method appear to offer another criterion to distinguish between a generic form of a monoclinic tensor and a particular form that allows for propagation of tetragonal wavefronts. Further investigations of this topic are a subject of future work.

In summary, the plot of the monoclinic-distance function can help to find the orientation of the closest tetragonal tensor. This is because of the relation between tetragonal-distance function and the sum of monoclinic distance functions along particular directions. Although we could not prove how close the extrema of the functions are, we see in the example that they are either equal or 1° close to each other. Hence, by observing the plot of monoclinic-distance function of a tensor, one can decide where to search for the closest tetragonal tensor.

3.5 Determining the Closest Trigonal and Cubic Elasticity Tensors

In this section, we consider the problem of closeness to the trigonal symmetry class for a given elasticity tensor. The approach presented in this section is very similar to finding the closest tetragonal elasticity tensor which is presented in the previous section. We will not introduce a theorem which relates the trigonal-distance function to the sum of monoclinic-distance functions for some directions as we did in Theorem 7. The equality between those distance functions does not hold for trigonal symmetry because the symmetry group of trigonal does not only consist of mirror planes but it also contains a three-fold rotation. Nevertheless, the location of extrema of the trigonal-distance function and the sum of monoclinic-distance functions, for directions which are 60° apart and lie in a plane, give either equal or close values to each other. Thus, it seems that although the functions are different, the roots of their first-

partial derivatives have some relationship since extrema are close. This result may be expected since existence of mirror planes whose normals are 60° apart and lie in a plane implies a three-fold rotation around the normal of that plane.

Now, we will formulate the trigonal-distance function. In order to do that, firstly, we determine the projection of any elasticity tensor onto the space of trigonal-elasticity tensors, namely onto $\mathcal{L}^{trigo}$. The projection function, which is defined in Equation 2.4, takes the form of the following equation when it is applied for trigonal symmetry:

$$\begin{aligned} C^{trigo} &= \frac{1}{6}(C + \bar{M}_{\mathbf{e_1}}^T C \bar{M}_{\mathbf{e_1}} + \bar{M}_{(\cos\frac{\pi}{6},\sin\frac{\pi}{6},0)}^T C \bar{M}_{(\cos\frac{\pi}{6},\sin\frac{\pi}{6},0)} \\ &\quad + \bar{M}_{(\cos\frac{5\pi}{6},\sin\frac{\pi}{6},0)}^T C \bar{M}_{(\cos\frac{5\pi}{6},\sin\frac{\pi}{6},0)} + \bar{R}_{\frac{\pi}{3}}^T C \bar{R}_{\frac{\pi}{3}} + \bar{R}_{-\frac{\pi}{3}}^T C \bar{R}_{-\frac{\pi}{3}}), \end{aligned} \quad (3.51)$$

since

$$G^{Trigo} = \{\pm I, \pm M_{\mathbf{e_1}}, \pm M_{(\cos\frac{\pi}{6},\sin\frac{\pi}{6},0)}, \pm M_{(\cos\frac{5\pi}{6},\sin\frac{\pi}{6},0)}, \pm R_{\frac{\pi}{3}}, \pm R_{-\frac{\pi}{3}}\}.$$

$R_{\frac{\pi}{3}}, R_{-\frac{\pi}{3}}$ are clockwise and counter-clockwise rotations around $\mathbf{e_3}$-axis, respectively and $M_{(\cos\frac{\pi}{6},\sin\frac{\pi}{6},0)}$, $M_{(\cos\frac{5\pi}{6},\sin\frac{5\pi}{6},0)}$ are mirror planes whose normals are shown in their subscripts.

In order to find the distance of a given C to the space of trigonal-elasticity tensors represented in its natural coordinate systems, one applies Equation 2.13 to get

$$d(C, \mathcal{L}^{trigo}) := ||C||^2 - ||C^{trigo}||^2. \quad (3.52)$$

If one wants to find the orientation of the closest trigonal tensor among all coordinate systems, then the distance function should be used which is defined in Definition 4. Applying the definition for the trigonal symmetry we get

$$d(\bar{X}^T C \bar{X}, \mathcal{L}^{trigo}) = ||C||^2 - ||(\bar{X}^T C \bar{X})^{trigo}||^2, \text{ for all } \bar{X} \in SO(3). \quad (3.53)$$

Note that the projected tensor, namely $(\bar{X}^T C \bar{X})^{trigo}$, depends on the orientations of the coordinate axes. More precisely, as the coordinate system changes so does the tensor $(\bar{X}^T C \bar{X})^{trigo}$.

In this section, we are not going to consider a detailed example as was done for the tetragonal symmetry in the previous section. Instead, we introduce an elasticity tensor and its plot of monoclinic-distance function. Then, we briefly state if it is close to the trigonal symmetry and which orientation is proper to choose to find the closest trigonal elasticity tensor.

Consider the following elasticity tensor:

$$C = \begin{bmatrix} 14.46 & 1.70 & 4.30 & -1.97 & -3.29 & -4.20 \\ 1.70 & 17.37 & -1.75 & -1.16 & -3.52 & 8.48 \\ 4.30 & -1.75 & 6.64 & 1.58 & -0.80 & -4.28 \\ -1.97 & -1.16 & 1.58 & 3.30 & -5.99 & 0.37 \\ -3.29 & -3.52 & -0.80 & -5.99 & 22.82 & -0.45 \\ -4.20 & 8.48 & -4.28 & 0.37 & -0.45 & 13.38 \end{bmatrix}. \tag{3.54}$$

The plot of monoclinic-distance function of C is shown in Figures 3.16, 3.17, 3.18. In Figure 3.17, one can observe an almost three-fold symmetry of the plot. Figure 3.18 shows some extrema which are approximately 60° apart and lie in a plane perpendicular to the rotation axis. These extrema imply that these directions are close to being a normal of a mirror plane which is expected in a trigonal symmetry. Thus, the closest trigonal elasticity tensor should be searched around the coordinate system whose z-axis is along the three-fold rotation axis. Then, x-axis can be chosen in the plane perpendicular to z-axis and along any of the directions in which an extrema takes place. This is because the trigonal-distance function takes the same value in every 60°.

In the plot of monoclinic-distance function of C, there are many extrema which can be seen in the figures. After observing the plot, one can see that there are several such triangular features. Then, one should make a search around all of these triangular features to find the orientation of the closest trigonal tensor. Two of those triangular features can be observed in Figure 3.19. Another triangle can be seen in

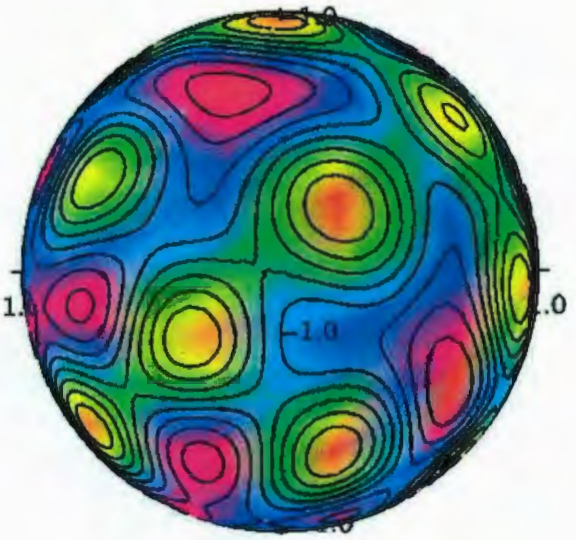

Figure 3.16: The plot of monoclinic-distance function of C expressed in Equation 3.54. This is a general view that shows the coordinate axes. There are many extrema in the plot suggesting that it may belong to a high symmetry class.

Figure 3.20. In total, there are four triangular features in one of the hemispheres. Four of them can be observed in Figure 3.21.

Now, we state the orientations and the value of the distances of C to the trigonal symmetry class around these triangular features. Then, we can decide which of these orientations give the absolute minimum value to the trigonal class. Making a search around the triangular feature shown in Figure 3.17 gives the minimum for the trigonal-distance function as

$$\min_{X \in SO(3)} d(\bar{X}^T C \bar{X}, \mathcal{L}^{Trigo}) = 90.89,$$

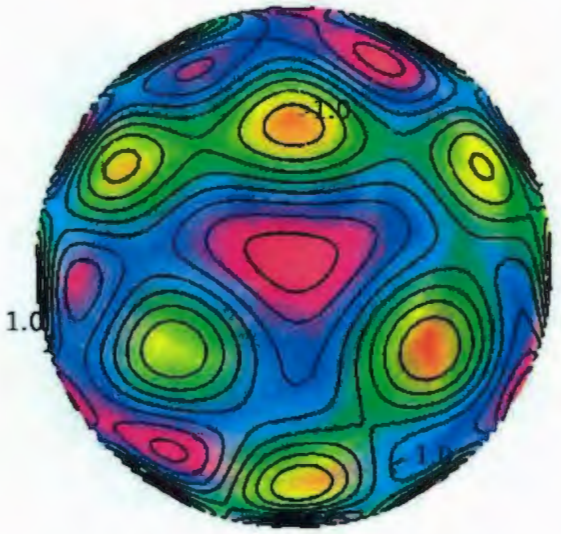

Figure 3.17: Observe the almost three-fold symmetry in the figure. Note that in trigonal symmetry three-fold rotation axis is not a normal of a mirror plane. Thus, along the rotation axis, which is in the middle of the triangular feature, there is no local minimum close to zero.

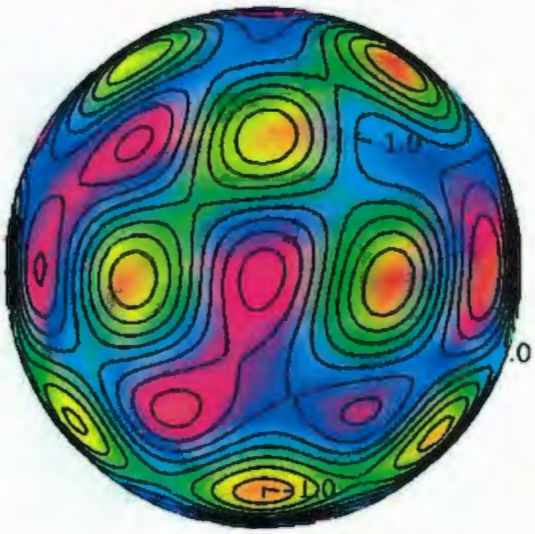

Figure 3.18: This view of the plot is perpendicular to the rotation axis of the triangular feature shown in Figure 3.17. We see two extrema, which are around 60° apart, in the centeral region of the plot. This is also expected in trigonal symmetry and thus in a medium close to the trigonal symmetry class.

where the minimum is achieved for the Euler angles:

$$\begin{aligned}\phi &= 35.36\frac{\pi}{180},\\ \psi &= 159.15\frac{\pi}{180},\\ \theta &= 179.6\frac{\pi}{180}.\end{aligned}$$

For the searches around the two triangular features shown in Figure 3.19, the one in the left-hand side of the figure gives the minimum as

$$\min_{X\in SO(3)} d(\bar{X}^T C\bar{X}, \mathcal{L}^{Trigo}) = 136.72,$$

where the minimum is achieved for the Euler angles:

$$\begin{aligned}\phi &= 88.51\frac{\pi}{180},\\ \psi &= 34.27\frac{\pi}{180},\\ \theta &= 89.57\frac{\pi}{180}.\end{aligned}$$

For the one that is in the right-hand side of Figure 3.19, we get

$$\min_{X\in SO(3)} d(\bar{X}^T C\bar{X}, \mathcal{L}^{Trigo}) = 95.20,$$

where the minimum is achieved for the Euler angles:

$$\begin{aligned}\phi &= 89.80\frac{\pi}{180},\\ \psi &= -75.77\frac{\pi}{180},\\ \theta &= 151.60\frac{\pi}{180}.\end{aligned}$$

The minimum of the trigonal-distance function around the triangular feature shown in Figure 3.20 is

$$\min_{X\in SO(3)} d(\bar{X}^T C\bar{X}, \mathcal{L}^{Trigo}) = 118.72,$$

where the minimum is achieved for the Euler angles:

$$\begin{aligned} \phi &= 33.67\frac{\pi}{180}, \\ \psi &= -21.34\frac{\pi}{180}, \\ \theta &= 181.04\frac{\pi}{180}. \end{aligned}$$

Thus, the absolute minimum is achieved around the triangular feature shown in Figure 3.17. To find the closest trigonal elasticity tensor, first, one should rotate the tensor to this coordinate system then, take the projection of it onto the space of trigonal elasticity tensors.

In addition to these observations, Figure 3.21 shows an almost four-fold symmetry axis. The plane perpendicular to this axis is shown in Figure 3.22. All of these figures suggest that C is close to a higher symmetry class than trigonal, namely cubic symmetry. In cubic symmetry, one expects to see three four-fold axes, which are aligned with the coordinate-axes and four three-fold axes which are aligned with the diagonals of a cube. Since C is generally anisotropic, none of the extrema is zero. Thus, they are neither rotation axes nor normals of a mirror plane but close to them.

Without loss of generalization, one can choose any of the combinations of the three four-fold rotation axes to make a search for the orientation of the closest cubic tensor. This is because all of these searches will give the same number.

Figure 3.19: Two triangular features can be observed from this view of the monoclinic plot. Thus, in order to determine the orientation of the closest trigonal tensor, one should make a search around both of these triangles.

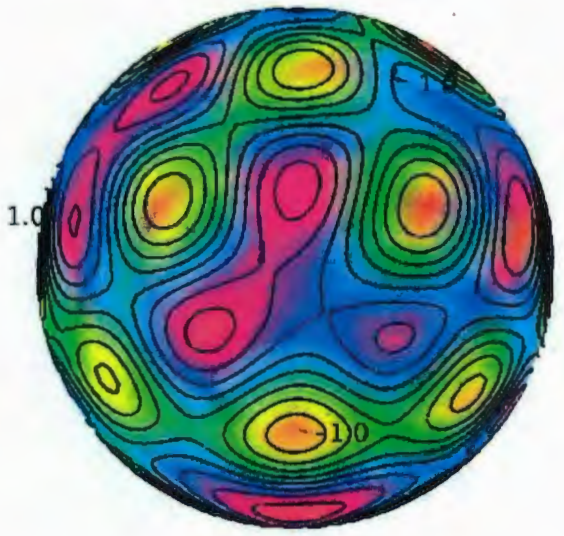

Figure 3.20: Another triangular feature can be observed from this view of the monoclinic plot. The three-fold rotation axis is in the center of the triangle.

Figure 3.21: Almost a four-fold symmetry is observed from this view. There are three orientations where an almost four-fold symmetry axis exists which implies that the elasticity tensor is close to the cubic symmetry. From this point of view, one can also observe four triangular features which are associated with violet and red colours lying in each side of the four-fold symmetry axis.

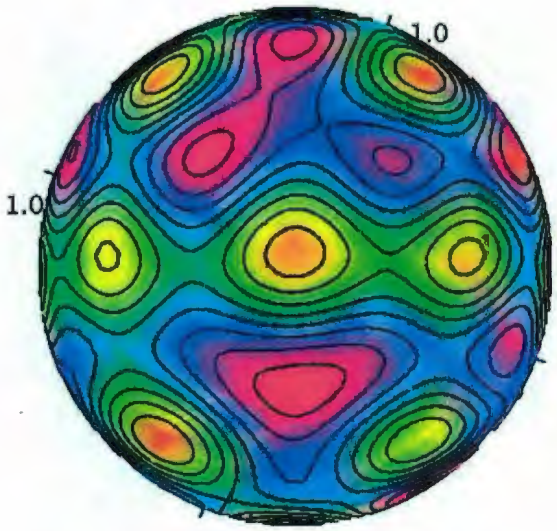

Figure 3.22: This view is perpendicular to the four-fold rotation axis shown in the previous figures. As expected, we see extrema where they almost lie in a plane and 45° apart.

Chapter 4

Oriented Cracks in a Layered Medium

In this chapter, we investigate the properties of the combination of two oriented features in a medium. In a rock, two oriented features can be a foliation and parallel cracks. In a subsurface, this may correspond to sedimentary rocks with bedding and cracks oriented in a particular direction. All of these features are planar structures. Thus, the medium has an effective TI symmetry when either of these features exists alone in a subsurface [26]. However, the combination of them reduces the symmetry of the medium in which they are present together. In this chapter, we combine two TI media. We consider the closest symmetry class of the combined medium. Then, we determine how the closest symmetry class of the medium changes as the angle between the oriented features varies.

The planar structures, like cracks, layering, foliation, are assumed individually to cause a TI symmetry in the medium. However, there is generally a small deviation from perfect TI symmetry. This deviation may have several reasons. First of all, there is no Hookean solid which behaves perfectly elastic as is assumed in the theory. Thus, one should expect to obtain an elasticity tensor of a real material which does not

belong to any symmetry class but is close to it. Another reason for such a deviation from TI symmetry may be due to these structures not being perfectly planar. In practice, there is always a distribution of orientations for the stress-aligned cracks leading to greater or smaller perturbations of the TI anisotropy [16]. Since the media that are to be combined are not perfectly TI but close to it, this will make a deviation in the symmetry class of the resultant medium. The method that we have presented in the previous chapter enables one to take this effect into account.

4.1 Combination of Two Planar Structures

In this section, we illustrate some examples of combining two TI media with different orientations of rotation axes. Then, we consider the closest symmetry class of the resulting medium. Before illustrating the examples, let us prove to which symmetry class the resulting medium belongs if the angle between the planes are 0°, 90° and any value between them.

If the rotation axes of TI tensors, C_1 and C_2, are aligned along any vector, say $\mathbf{v}$, then $C_1 + C_2$ is a TI tensor with rotation axis along $\mathbf{v}$ since

$$\begin{aligned} \bar{R}^T_{\theta,\mathbf{v}}(C_1 + C_2)\bar{R}_{\theta,\mathbf{v}} &= \bar{R}^T_{\theta,\mathbf{v}}C_1\bar{R}_{\theta,\mathbf{v}} + \bar{R}^T_{\theta,\mathbf{v}}C_2\bar{R}_{\theta,\mathbf{v}} \\ &= C_1 + C_2, \end{aligned}$$

where $R_{\theta,\mathbf{v}} \in SO(3)$ is a rotation matrix around vector $\mathbf{v}$ by any angle θ.

For the TI tensors whose rotation axes are 90° apart, we will show that the resulting medium is orthotropic. Assume that the rotation axes of two TI tensors, C_1 and C_2, are along the vectors $\mathbf{v_1}$ and $\mathbf{v_2}$ where they are perpendicular to one another. Then, we show that $C_1 + C_2$ has three mirror planes whose normals are along $\mathbf{v_1}$, $\mathbf{v_2}$

and $\mathbf{v_3}$, where $\mathbf{v_3}$ is perpendicular to $\mathbf{v_1}$ and $\mathbf{v_2}$. Consider the following equations:

$$\begin{aligned} \bar{M}_{\mathbf{v_1}}^T(C_1 + C_2)\bar{M}_{\mathbf{v_1}} &= \bar{M}_{\mathbf{v_1}}^T C_1 \bar{M}_{\mathbf{v_1}} + \bar{M}_{\mathbf{v_1}}^T C_2 \bar{M}_{\mathbf{v_1}} \\ &= C_1 + C_2, \text{ since } \bar{M}_{\mathbf{v_1}} \text{ is a symmetry element of } C_1 \text{ and } C_2. \end{aligned}$$

That is because a TI tensor has infinitely many mirror planes whose normals are perpendicular to its rotation axis and another mirror plane along its rotation axis. Similar equalities hold for $M_{\mathbf{v_2}}$ and $M_{\mathbf{v_3}}$.

For the last case, we consider two TI media whose rotation axes are neither parallel nor perpendicular to one another. Then, the resulting medium is monoclinic with mirror plane along the vector that is perpendicular to both rotation axes. That is because the two TI media have a mirror plane along that direction. Formally,

$$\begin{aligned} \bar{M}_{\mathbf{v}}^T(C_1 + C_2)\bar{M}_{\mathbf{v}} &= \bar{M}_{\mathbf{v}}^T C_1 \bar{M}_{\mathbf{v}} + \bar{M}_{\mathbf{v}}^T C_2 \bar{M}_{\mathbf{v}} \\ &= C_1 + C_2 \text{ since } \bar{M}_{\mathbf{v}} \text{ is a symmetry element of } C_1 \text{ and } C_2. \end{aligned}$$

Now, consider a TI elasticity tensor which is expressed in its natural coordinate system:

$$C_1 = \begin{bmatrix} 56.27 & 21.20 & 12.54 & 0 & 0 & 0 \\ 21.20 & 56.27 & 12.54 & 0 & 0 & 0 \\ 12.54 & 12.54 & 24.16 & 0 & 0 & 0 \\ 0 & 0 & 0 & 12.72 & 0 & 0 \\ 0 & 0 & 0 & 0 & 12.72 & 0 \\ 0 & 0 & 0 & 0 & 0 & 35.07 \end{bmatrix}. \tag{4.1}$$

Let us assume that this tensor represents a layered medium. Also consider the elas-

ticity tensor of a cracked medium:

$$C_2 = \begin{bmatrix} 83.47 & 25.48 & 17.17 & 0 & 0 & 0 \\ 25.48 & 83.47 & 17.17 & 0 & 0 & 0 \\ 17.17 & 17.17 & 51.54 & 0 & 0 & 0 \\ 0 & 0 & 0 & 46.48 & 0 & 0 \\ 0 & 0 & 0 & 0 & 46.48 & 0 \\ 0 & 0 & 0 & 0 & 0 & 58.32 \end{bmatrix}. \tag{4.2}$$

This is an effective elastic tensor for wave propagation through parallel cracks (normal to z-axis) in an isotropic solid with density $\rho = 2.6g/cm^3$ and velocities $\alpha = 5.8$ km/s and $\beta = 3.349$ km/s. The elastic constants are derived from the theoretical formulations of Hudson [29, 30] interpreted by Crampin [16].

Before adding these tensors, we make a further simplification. We assume that these two tensors have equal norms. Otherwise, the tensor with the greater norm can dominate the result and the combined medium becomes closer to that tensor. Evaluating the norms of the tensors, we get

$$||C_1|| = 100, \tag{4.3}$$

$$||C_2|| = 163.69. \tag{4.4}$$

In order to make the norms of C_2 and C_1 equivalent, we multiply the tensor C_2 by $\frac{100}{163.69}$ and get

$$C_2' = \begin{bmatrix} 51.00 & 15.56 & 10.49 & 0 & 0 & 0 \\ 15.56 & 51.00 & 10.49 & 0 & 0 & 0 \\ 10.49 & 10.49 & 31.48 & 0 & 0 & 0 \\ 0 & 0 & 0 & 28.39 & 0 & 0 \\ 0 & 0 & 0 & 0 & 28.39 & 0 \\ 0 & 0 & 0 & 0 & 0 & 35.63 \end{bmatrix}, \tag{4.5}$$

where $||C_2'|| = 100$. It is known that if two TI tensors whose rotation axes are along the z-axis are added then the result is a TI tensor with a rotation axis aligned in the same direction. This is because $\mathcal{L}^{TI}$ is a linear space. Instead, we change the orientation of cracks by rotating the elasticity tensor C_2'.

In our first example, we consider cracks oriented 75° to the rotation axis of the C_1, namely to the z-axis. Rotating C_2' by an orthogonal transformation matrix $A \in SO(3)$, whose Euler angles are $\phi = 75°$ and $\psi = 78° + 90°$, we get $C_2^{75°} = \bar{A}^T C_2' \bar{A}$ as

$$C_2^{75°} = \begin{bmatrix} 50.03 & 11.00 & 15.03 & -1.68 & -0.89 & -3.19 \\ 11.00 & 33.13 & 10.98 & -2.73 & -0.05 & -2.12 \\ 15.03 & 10.98 & 49.39 & -4.08 & -0.87 & -1.27 \\ -1.68 & -2.73 & -4.08 & 29.25 & -1.25 & 0.08 \\ -0.89 & -0.05 & -0.87 & -1.25 & 34.87 & -1.67 \\ -3.19 & -2.12 & -1.27 & 0.08 & -1.67 & 29.21 \end{bmatrix}. \tag{4.6}$$

The plot of the monoclinic-distance function of $C_2^{75°}$ can be seen in Figure 4.1. Adding $C_2^{75°}$ and C_1, one gets the elasticity tensor of the combined medium as

$$C^{75°} = \begin{bmatrix} 106.30 & 32.20 & 27.58 & -1.68 & -0.89 & -3.19 \\ 32.20 & 89.41 & 23.52 & -2.73 & -0.05 & -2.12 \\ 27.58 & 23.52 & 73.56 & -4.08 & -0.87 & -1.27 \\ -1.68 & -2.73 & -4.08 & 41.97 & -1.25 & 0.08 \\ -0.89 & -0.05 & -0.87 & -1.25 & 47.60 & -1.67 \\ -3.19 & -2.12 & -1.27 & 0.08 & -1.67 & 64.29 \end{bmatrix}. \tag{4.7}$$

Now, let us observe the plot of the monoclinic-distance function of $C^{75°}$ to consider which symmetry class the combined medium is closest to. See Figure 4.2 for the plot. Recall that in orthotropic symmetry one expects to have three mutually perpendicular directions where the monoclinic-distance function vanishes. Similarly, one can observe from Figure 4.2 that there are three local minima which are close to zero and almost

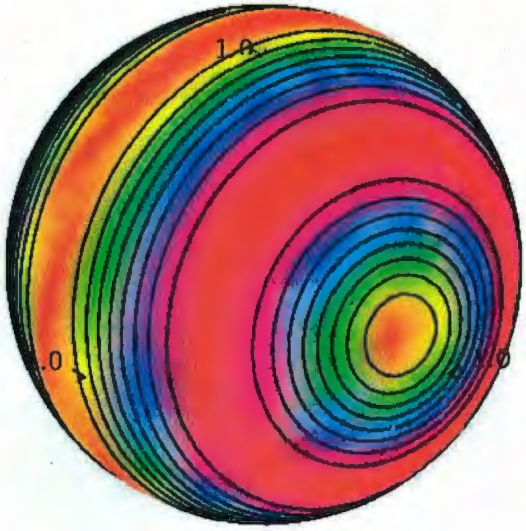

Figure 4.1: The plot of the monoclinic-distance function of $C_2^{75^\circ}$. The rotation axis is 75° away from the z-axis and its projection onto the $xy-$plane is 78° away from the x-axis which can be inferred from the choice of the Euler angles.

perpendicular to each other. By using the methods that are introduced in Chapter 3 one can find the orientation of the closest orthotropic tensor and then the tensor itself. Then, it turns out that the orientation of the closest orthotropic tensor is

$$\begin{aligned} x-axis &= \left(\cos\frac{-12\pi}{180}, \sin\frac{-12\pi}{180}, 0\right), \\ y-axis &= \left(\cos\frac{78\pi}{180}\sin\frac{3.36\pi}{180}, \sin\frac{78\pi}{180}\sin\frac{3.36\pi}{180}, \cos\frac{3.36\pi}{180}\right), \\ z-axis &= \left(\cos\frac{78\pi}{180}\sin\frac{93.36\pi}{180}, \sin\frac{78\pi}{180}\sin\frac{93.36\pi}{180}, \cos\frac{93.36\pi}{180}\right). \end{aligned} \tag{4.8}$$

The value of the absolute minimum of the orthotropic-distance function, that is obtained in this coordinate system, is 53.23. Similarly, the minimum distance of C^{75° to TI symmetry can be found as 250.06 for the coordinate system whose z-axis is $\left(\cos\frac{78\pi}{180}\sin\frac{5.07\pi}{180}, \sin\frac{78\pi}{180}\sin\frac{5.07\pi}{180}, \cos\frac{5.07\pi}{180}\right)$.

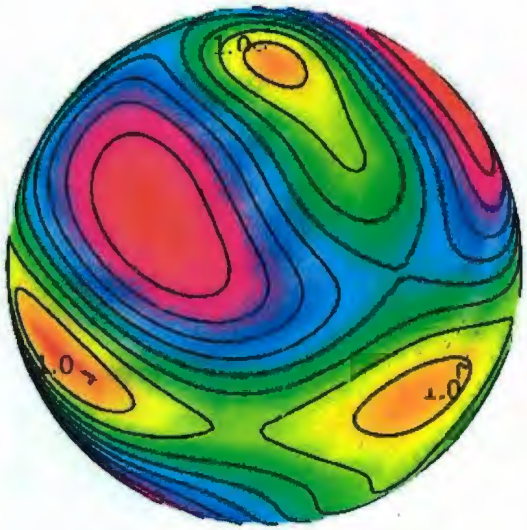

Figure 4.2: The plot of the monoclinic-distance function of the combined medium of two planar structures 75° apart. The plot suggests that it is close to orthotropic symmetry since there exist three local minima which are almost perpendicular to each other.

Since the sum of two TI medium, whose rotation axes are perpendicular, results in an orthotropic medium, it might be expected that the resultant tensor is close to the orthotropic symmetry because 75° angle is close to being perpendicular. Calculating the value of the monoclinic-distance function for $C^{75°}$ for the three local minima shown in the plot, we see that it vanishes along one of the the minimum directions which is close to the x-axis as shown in Figure 4.2 . More precisely, the function vanishes along the vector $\left(\cos\frac{-12\pi}{180}, \sin\frac{-12\pi}{180}, 0\right)$. Thus, $C^{75°}$ belongs to the monoclinic symmetry class where the normal of the mirror plane is along the vanishing direction of the distance function. Note that the direction of the normal of the mirror plane is perpendicular to both of the rotation axes of the two TI tensors, namely to the normal of cracks and layers.

Now, we change the direction of the crack orientation with respect to the layering. Thus, we rotate C_2' by an orthogonal transformation matrix $A \in SO(3)$,whose Euler angles are $\phi = 61°$ and $\psi = 78° + 90°$. Note that we have only changed the angle between the z-axis and the normal of cracks when compared to the previous example. We formally state this as

$$C_2^{61°} = \bar{A}^T C_2' \bar{A}.$$

Then, we added the rotated crack tensor to the vertical TI, namely C_1, which is expressed in Equation 4.1 and we get

$$\begin{aligned} C^{61°} &= C_1 + C_2^{61°} \\ &= \begin{bmatrix} 106.48 & 33 & 26.78 & -2.88 & -1.51 & -2.61 \\ 33 & 92.07 & 24.01 & -5.08 & -0.17 & -1.91 \\ 26.78 & 24.01 & 69.72 & -6.45 & -1.37 & -0.87 \\ -2.88 & -5.08 & -6.45 & 42.97 & -0.78 & 0.00 \\ -1.51 & -0.17 & -1.37 & -0.78 & 46.48 & -2.86 \\ -2.61 & -1.91 & -0.87 & 0.00 & -2.86 & 65.38 \end{bmatrix}. \end{aligned} \tag{4.9}$$

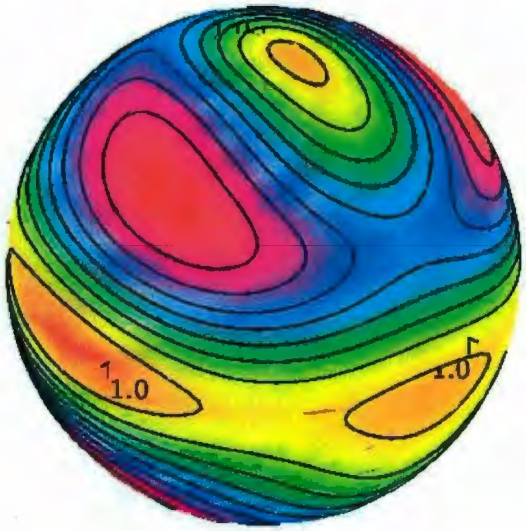

Figure 4.3: The plot of the monoclinic-distance function of the combined medium of two planar structures 61° apart. The plot suggests that it is close to orthotropic symmetry since there exist three local minima which are almost perpendicular to each other.

Observe the plot of the monoclinic-distance function of C^{61° in Figure 4.3.

Similar to the plot of C^{75°, we observe three local minima which are almost perpendicular to each other. The vanishing direction of the distance function is along the same direction as it was in the previous example, namely along the vector $\left(\cos\frac{-12\pi}{180}, \sin\frac{-12\pi}{180}, 0\right)$. Thus, the normal of the mirror plane of C^{61° has not changed when compared with C^{75°. However, locations of the other two minima has shifted away from the z- and y-axis. The main difference when compared with the plot of C^{75° is that an equatorial plane has started to form as the angle between the two TI media gets smaller. This may suggest that it is getting closer to TI symmetry. We find the orientation of the closest orthotropic tensor as

$$
\begin{aligned}
x-axis &= \left(\cos\frac{78\pi}{180}\sin\frac{100.97\pi}{180}, \sin\frac{78\pi}{180}\sin\frac{100.97\pi}{180}, \cos\frac{100.97\pi}{180}\right), \\
y-axis &= \left(\cos\frac{78\pi}{180}\sin\frac{10.97\pi}{180}, \sin\frac{78\pi}{180}\sin\frac{10.97\pi}{180}, \cos\frac{10.97\pi}{180}\right), \\
z-axis &= \left(\cos\frac{-12\pi}{180}, \sin\frac{-12\pi}{180}, 0\right). \qquad (4.10)
\end{aligned}
$$

The value of the absolute minimum of the orthotropic-distance function, which is obtained in this coordinate system, is 92.27. Similarly, the minimum distance of C^{61° to TI symmetry can be found as 203.6 for the coordinate system whose z-axis is $\left(\cos\frac{78\pi}{180}\sin\frac{10.83\pi}{180}, \sin\frac{78\pi}{180}\sin\frac{10.83\pi}{180}, \cos\frac{10.83\pi}{180}\right)$. Thus, we see that as the angle between the two TI media gets smaller, the distance of the combined medium to TI becomes smaller and its distance to orthotropic becomes greater.

Now, we investigate another example where the crack orientation with respect to the layering is 40°. In order to obtain such an angular relation, we rotate C_2' by an orthogonal transformation matrix $A \in SO(3)$,whose Euler angles are $\phi = 40^\circ$ and $\psi = 78^\circ + 90^\circ$. More precisely,

$$C_2^{40^\circ} = \bar{A}^T C_2' \bar{A}.$$

Adding the rotated cracks to the layering, we obtain an elasticity tensor whose plot is shown in Figure 4.4.

The plot suggests that the combined medium is close to TI-symmetry. Calculating the absolute minimum of the TI-distance function, we get 77.96. Comparing this number with the previous examples, where the crack orientation is greater with respect to the layering, we see that the combined medium is getting closer to the TI-symmetry as the angle between the two orientations decreases. The value of the orthotropic-distance function is found to be 47.96 whereas it was 92.27 in the previous example. It seems that the combined medium's symmetry is getting closer to orthotropic symmetry as well. However, recall that a TI elasticity tensor is also

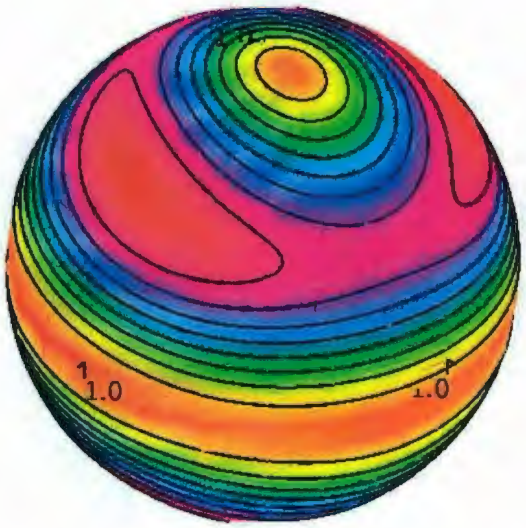

Figure 4.4: The plot of the monoclinic-distance function of the combined medium of two planar structures 40° apart. The plot suggests that it is close to TI symmetry since there exist an equatorial plane where the value of the monoclinic-distance function along any direction in that plane is almost zero.

an orthotropic tensor. Thus, it should be expected to have smaller values for the orthotropic-distance function as the angle between the orientations decreases. Even though the absolute minimum of the orthotropic-distance function is smaller than the TI-distance function, one should consider the TI-symmetry class as the approximation of this medium. It is normal to have smaller values for orthotropic than TI because of the same reason stated above, namely orthotropic symmetry is a superset of TI symmetry class. This phenomenon shows one of the main advantages of the plotting of the distance functions. In other words, numbers can be misleading because of the subgroup relations among the symmetry classes. However, the plot shows which symmetry class should be chosen to approximate a medium.

Finally, we consider the elasticity tensor which is obtained by combining layering and cracks that are 10° away from each other. Observe Figure 4.5 for the plot of the monoclinic-distance function of such an elasticity tensor.

The absolute minimum of the TI-distance function is achieved in the coordinate system whose z-axis is $\left(\cos\frac{78\pi}{180}\sin\frac{2.9\pi}{180}, \sin\frac{78\pi}{180}\sin\frac{2.9\pi}{180}, \cos\frac{2.9\pi}{180}\right)$. The value of the function is 3.37. Thus, it is also obvious from these values that this medium is very close to TI-symmetry class. The value of the orthotropic-distance function is 3.2. As we have mentioned in the last example, it is natural to have a number for the orthotropic-distance function smaller than TI-distance function. However, TI-symmetry class should be chosen to approximate this combined medium. Thus, we see that if the orientations of the two TI media are close to each other then, the symmetry of the combined medium is almost TI.

Up to now, we considered two TI-elasticity tensors that represent different structures. We have only changed the angle between these planar features. However, if we consider different TI-elasticity tensors than C_1 and C_2, it is possible to obtain different results for the closest symmetry class of the combined medium. In other words, the plot of the monoclinic-distance function may have different features. Now,

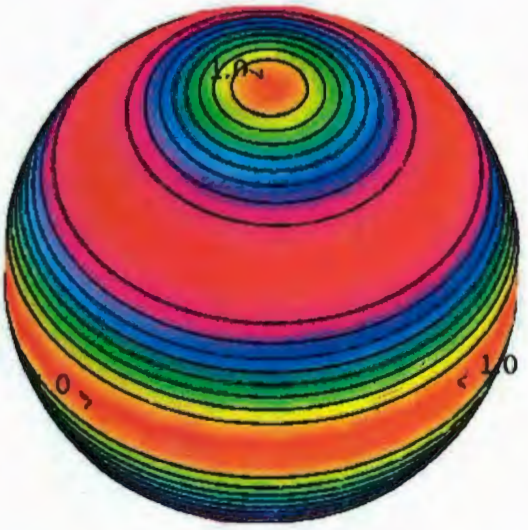

Figure 4.5: The plot of the monoclinic-distance function of the combined medium of two planar structures which are 10° apart. It is very close to TI symmetry since there exists an equatorial plane where the value of the monoclinic-distance function along any direction in that plane is almost zero. Also observe the minimum that is perpendicular to the equatorial plane. It is very close to being an infinite-fold rotation axis.

we change tensors and investigate the plot of the monoclinic-distance function of the combined medium.

Consider the two elasticity tensors in the following equations:

$$C_3 = \begin{bmatrix} 28.81 & 10.17 & 22.03 & 0 & 0 & 0 \\ 10.17 & 28.81 & 22.03 & 0 & 0 & 0 \\ 22.03 & 22.03 & 40.68 & 0 & 0 & 0 \\ 0 & 0 & 0 & 45.76 & 0 & 0 \\ 0 & 0 & 0 & 0 & 45.76 & 0 \\ 0 & 0 & 0 & 0 & 0 & 18.64 \end{bmatrix} \tag{4.11}$$

and

$$C_4 = \begin{bmatrix} 56.19 & 17.07 & 7.82 & 0 & 0 & 0 \\ 17.07 & 56.19 & 7.82 & 0 & 0 & 0 \\ 7.82 & 7.82 & 3.55 & 0 & 0 & 0 \\ 0 & 0 & 0 & 25.61 & 0 & 0 \\ 0 & 0 & 0 & 0 & 25.61 & 0 \\ 0 & 0 & 0 & 0 & 0 & 39.12 \end{bmatrix}. \tag{4.12}$$

Both of these tensors belong to TI-symmetry class and are expressed in their natural coordinate systems. Furthermore, we choose C_3 and C_4 in such a way that their norms are equivalent.

Now, we investigate the combination of these two tensors for different orientations of C_3. More precisely, we consider the monoclinic-distance plots of the elasticity tensors

$$\bar{A}_i^T C_3 \bar{A}_i + C_4 \text{ for } A_i \in SO(3),$$

where $i \in \{1,2,3\}$. Each $\bar{A}_i$ for $i \in \{1,2,3\}$ transforms the rotation axis of C_1 to a direction that is 10°, 41° and 75° away from $\mathbf{e_3}$, respectively. Consider Figures 4.6,

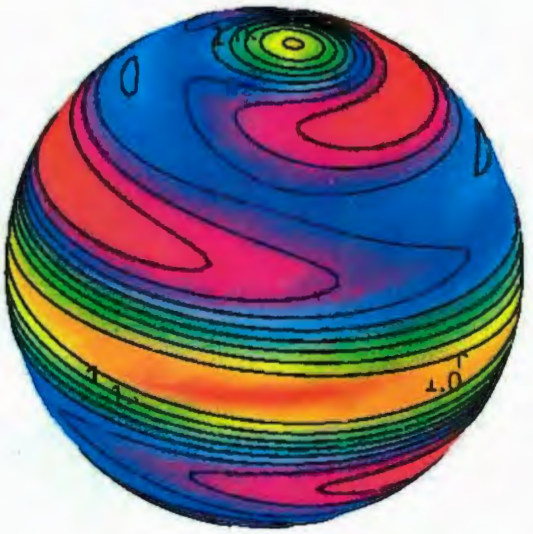

Figure 4.6: The plot of the monoclinic-distance function of the combined medium of two planar structures which are 10° apart. It is very close to TI symmetry since there exist an equatorial plane.

4.7, 4.8 for the plot of the monoclinic-distance functions of the combined elasticity tensors for different orientations.

Figure 4.7 shows that the combination of the two TI media whose orientations are around 45° apart may not be close to a higher symmetry class. This lack of closeness may depend on the parameters of the TI elasticity tensors. However, it is generally the case that if the two orientations are almost perpendicular to each other then the symmetry of the combined medium is close to orthotropic. Similarly, if the orientations of the TI media are close then the resultant medium can generally be approximated as a TI medium.

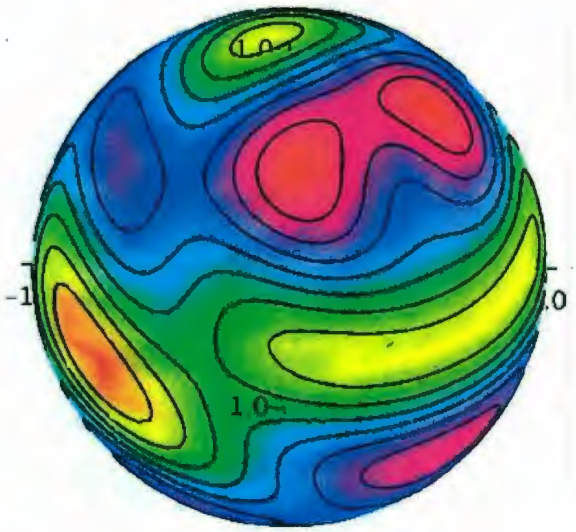

Figure 4.7: The plot of the monoclinic-distance function of the combined medium of two planar structures which are 41° apart. The orientation of the normal of the mirror plane can be observed from the orange region in the figure. This monoclinic tensor does not seem to be close to a higher symmetry class.

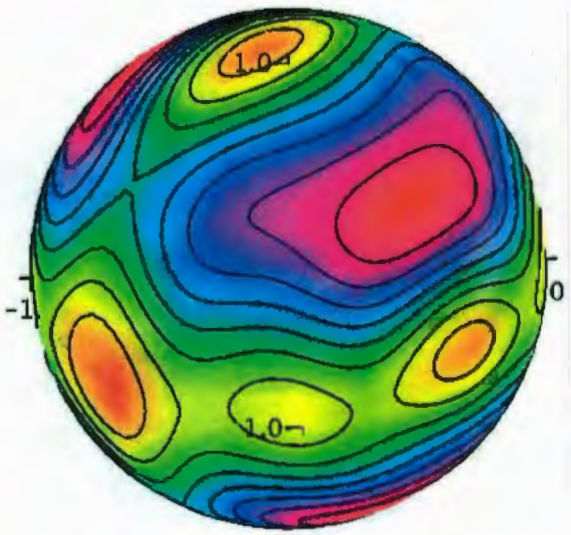

Figure 4.8: The plot of the monoclinic-distance function of the combined medium of two planar structures which are 75° apart. The plot suggests that the corresponding elasticity tensor is close to the orthotropic symmetry class. This is because of the fact that there are three minima that are almost perpendicular to each other.

4.2 Velocity Variations in the Symmetry Plane of a Combined Medium

In the previous section, we showed that the combination of two TI media is at least monoclinic. In this section, we investigate the velocities of S-waves propagating in the mirror plane of the monoclinic medium. The velocity variations are well known in a cracked isotropic medium. If parallel-oriented cracks are formed in an isotropic medium, then it becomes TI. It is generally assumed that the velocity of the S-wave propagating and polarizing parallel to the cracks is faster than the other S-wave polarizing perpendicular to the cracks [16]. Moreover, the fastest velocity for the S-waves is achieved for the wave propagating and polarizing parallel to the cracks in a cracked isotropic medium [16]. However, in this section, we will show that this may not be the case for a medium which has more than one planar structure, e. g. cracks in a layered medium. Consider the elasticity tensor, which is expressed in Equation 4.9 and whose plot of the monoclinic-distance function is shown in Figure 4.3. Recall that this tensor is a combination of two TI media one of which represents parallel oriented cracks while the other one represents layering. The angle between the rotation axis of these two structures is 61°. We showed in the last section that the normal of the mirror plane of the combined medium is perpendicular to the both of the rotation axes of TI media. In other words, the mirror plane contains the rotation axes.

We evaluate the velocities of the waves propagating in the mirror plane of the monoclinic elasticity tensor. To do that, first, we find the Christoffel matrix for every two degrees along the direction lying in the mirror plane. Then, eigenvalues of Christoffel matrices give the velocities of the P-wave and S-waves propagating along each of the directions which are two degrees apart. The code that evaluates all these matrices and eigenvalues is presented in the Appendix. According to these

calculations we obtained the minima and maxima velocities of the S-waves as follows:

$$Min(SV) = 28.50 \text{ at } 24°, \tag{4.13}$$

$$Max(SV) = 32.62 \text{ at } -66° \tag{4.14}$$

and

$$Min(SH) = 26.68 \text{ at } 74° \text{ and } -12°, \tag{4.15}$$

$$Max(SH) = 27.93 \text{ at } 32° \text{ and } -60°. \tag{4.16}$$

For P-wave we get

$$Min(P) = 74.88 \text{ at } 42°, \tag{4.17}$$

$$Max(P) = 91.56 \text{ at } -40°. \tag{4.18}$$

Note that the z-axis is at 0° and the normals to the cracks is at 61°. Thus, cracks are parallel to $-29°$. It seems that the maximum velocity direction of SV-waves is not aligned with the crack orientation. This suggests that whenever there are more planar structures in the medium the maximum velocity direction of the SV-wave, which is polarizing parallel to the cracks, may not aligned with the crack orientation. This feature prevents us from decomposing a given elasticity tensor into its components, namely into two TI media. More precisely, given a monoclinic elasticity tensor we cannot find two TI media whose sum is the monoclinic medium by using the method of maximum velocity directions.

Chapter 5

Conclusion and Future Work

5.1 Conclusion

The research presented in this dissertation solves two main problems. The first is identifying the symmetry class of a medium when it belongs to a particular symmetry class. Second, if the medium is generally anisotropic, then we develop a method to determine which symmetry class it is closest to. Moreover, we find the closest elasticity tensor that belongs to that symmetry class. The latter problem is more applicable since the elasticity tensor of a medium, which is obtained by inverting geophysical data, turns out to be generally anisotropic. Thus, instead of considering the problem to which symmetry class does the medium belong, the problem of determining the closest symmetry class for the medium becomes more important.

In Chapter 1, we begin by presenting the basic tensor properties and notations that are used throughout the text. Then, we introduce the eight symmetry classes of elasticity tensors. We present the form of the elasticity matrix for each symmetry class and the corresponding symmetry group whenever they are expressed in their natural coordinate systems.

In Section 2.1, we formulate the projection of a fourth-rank tensor onto the linear

space of elasticity tensors belonging to a particular symmetry class. This projection, which was first introduced by Gazis et al. [23], gives the closest symmetric elasticity tensor to a given generally anisotropic tensor. However, in this formulation the closest tensor is found in a particular coordinate system. In this section, we define the distance function in order to find the closest tensor among all coordinate systems. This function is highly nonlinear so that it is not possible to find its absolute minimum for all orientations of coordinate systems by using computer programmes. However, for TI and monoclinic symmetries, specification of the z-axis of the coordinate system gives a unique value for the distance function. In other words, the other axes, namely x- and y-axes, do not change the value of the function as is proved in Theorem 1 and Corollary 4. This property of the distance function for monoclinic and TI symmetries enables us to plot their distance functions.

By analyzing the plot of the monoclinic-distance function, we present a new method for recognizing the symmetries of an elasticity tensor. This method, when compared with the existing methods, is more efficient and direct for identifying the symmetry class of a tensor. In other methods, one needs to check some algebraical conditions on the invariants of a tensor, namely its eigenvalues and eigenvectors. However, our method enables one to see the symmetry by examining the plot.

The given elasticity tensor may be obtained by inverting the velocity and polarization of waves propagating in arbitrary directions through the medium. In other words, these directions are not necessarily aligned with the symmetry directions of the medium. This makes it more difficult to detect which symmetry class the elasticity tensor belongs to, since it is not defined in its natural coordinate system.

Based on the observations made in the plot of the monoclinic-distance function, one can prove the symmetry of a tensor belonging to any symmetry class. This is because the monoclinic symmetry, which contains only one mirror plane, is a subclass of all other symmetry classes. Theorem 6 states that the monoclinic-distance function

vanishes along the normal of a mirror plane. Then, by plotting the monoclinic-distance function of a tensor, we determine the orientations of any mirror planes that exist in the medium. Since the locations of the mirror planes are known for all symmetry classes, in order to determine the symmetry of a medium it remains only to detect the orientations of the directions where the monoclinic-distance function vanishes. Theorem 5 states that if the elasticity tensor has a symmetry, so does the plot of its monoclinic-distance function. More precisely, the symmetry elements of a tensor are also symmetries of the plot. This property of the plot gives an efficient way to detect any symmetry that a medium may have. In the rest of Chapter 2, we present an example from each symmetry class showing how to determine the symmetry of a medium by considering its plot. Also, we find the rotation matrix that transforms the elasticity tensor into its natural coordinate system.

In Chapter 3, given an elasticity tensor we solve the problem of determining the closest elasticity tensor belonging to a particular symmetry class. Since a Hookean solid is an idealization, the elasticity tensor, which is obtained by inverting the geophysical data, is found to be generally anisotropic. This is also the case when there are several planar structures in a region that exist together and thus combining them reduces the symmetry of the medium. Furthermore, those structures do not remain planar, but they get slightly curved as they extend to the deeper parts of subsurface. Hence, all of these effects and the errors in the measurements make the medium's symmetry generally anisotropic. Thus, the question of which symmetry class an elasticity tensor belongs to can be modified to which symmetry class it is closest to. By observing the plot of the monoclinic-distance function of a tensor, we also propose an answer to the closeness problem.

In the rest of Chapter 3, we consider examples of how the plot of the distance function of a tensor can be used to solve the problem of which symmetry class the tensor is closest to. The plot of monoclinic-distance function is a new and powerful

method in the sense that it gives information on the closeness to any higher symmetry than monoclinic. Since it is based on visualization, it is efficient and can easily guide the search for the absolute minimum of the distance function.

For elasticity tensors close to TI symmetry, one expects to see an equatorial plane in the plot of the monoclinic-distance function of the tensor. This is because in TI symmetry there are infinitely many mirror planes all of whose normals are perpendicular to the rotation axis. For the directions lying in the equatorial plane the values of the distance function are almost zero. Moreover, since it is possible to plot the TI-distance function, we can easily determine the location of the rotation axis of the closest TI tensor simply by observing the plot. After determining the orientation of the rotation axis of the closest TI, what remains is rotating the tensor in such a way that the rotation axis becomes z-axis of the tensor. Then, we project the tensor onto the linear space of TI elasticity tensors in this coordinate system.

For elasticity tensors close to orthotropic symmetry, one expects to see in the plot three mutually almost perpendicular directions whose values of monoclinic-distance functions are close to zero. It is proved in Theorem 7 that in order to determine the distance of a tensor to orthotropic symmetry class for any orientation of a coordinate system, one can sum three monoclinic-distance functions directed along the axes of the coordinate system and divide the sum by two. This theorem enables us to find the orientation of the closest-orthotropic tensor for a given anisotropic elasticity tensor from its monoclinic-distance function plot. Hence, one should make a search for the closest coordinate system around the neighbourhood of three almost mutually perpendicular extrema directions if such three extrema exist. Non-existence of such extrema implies that the tensor under consideration may not be close to orthotropic symmetry.

In Section 3.4, we introduce a generally anisotropic elasticity tensor whose monoclinic plot suggests that it may be close to the tetragonal symmetry. Unlike or-

thotropic symmetry, we are not stating a theorem that relates the tetragonal-distance function to the sum of monoclinic-distance functions along some particular directions. This is because tetragonal symmetry does not only consist of mirror planes but it also contains a four-fold rotation. Note that monoclinic-distance function determines only the location of mirror plane but not rotation axis. Thus, there is no linear relation between those two functions. However, the existence of such mirror planes implies the existence of a four-fold rotational symmetry. In fact, multiplication of two mirror planes that are 45° apart results in a four-fold rotation. Thus, there may be a nonlinear relation among those functions. In the example introduced in this section, we see that the restricted searches for the tetragonal- and the sum of monoclinic-distance functions give either the same orientation or as close as 1°. This suggests that the roots of their first-partial derivatives are close to each other and so are their extrema orientations.

The last example of Chapter 3 is about finding the orientation of the closest trigonal medium. We see that there are four triangular features that exist in the monoclinic plot of the given tensor. Thus, one should search for the absolute minimum around four triangular features to find the closest orientation. The existence of many extrema in the monoclinic plot indicates that one should look for the closeness to higher symmetries. Then, we find three orientations which are almost mutually perpendicular and close to being a four-fold rotation axis. This implies that the given tensor may be close to the cubic symmetry where three- and four-fold rotations are aligned with the diagonals and the coordinate axes of the cube, respectively.

We conclude that the plot of the monoclinic-distance function does not only identify the symmetry of a medium but it also determines which symmetry class the medium is closest to and its orientation. Then, one can calculate the closest symmetric elasticity tensor in that coordinate system.

In Chapter 4, we apply the methods that we have introduced on finding the

closest symmetry class to media which have several structures. More precisely, we combine two TI-media, which may correspond to bedding and cracks in a subsurface. Herein, combining refers to adding their elasticity tensors as done by Hudson [29]. We showed that adding two TI media results in a monoclinic medium if their rotation axes are neither parallel nor perpendicular. Thus, we investigate to which higher symmetry class the combined medium is closest. The main result is that if the angle between the orientations of the two TI media is small (< 20) then the resultant medium is close to TI symmetry. Similarly, if the angle between them is close to being perpendicular (> 70), then the combined medium can be approximated as an orthotropic medium. Lastly, if the angle is around 45° then the medium may or may not be close to any higher symmetry class. Since the combination is always monoclinic we can easily determine the orientation of the normal of the mirror plane from the plot of monoclinic-distance function. We find that the direction of the normal is perpendicular to both rotation axes of TI media. In other words, the rotation axes of TI media lie in the mirror plane of the resultant monoclinic medium.

In the last section of Chapter 4, we find the maximum and minimum velocity directions lying in the mirror plane of the combined medium. Our intention is to find the crack orientation by locating the maximum velocity direction of the SV wave propagating and polarizing parallel to the cracks. Note that in a cracked isotropic medium, the maximum velocity of the SV wave is aligned with crack orientation [16]. However, we show that it is not the case for a medium with more than one orientation, e.g. a layered medium with cracks. More precisely, if a tensor is obtained by adding two TI media in different orientations then, in general, the maximum velocity directions are not aligned with the orientation of any of the TI media.

5.2 Applications and Future Work

There may be several practical significant results of this thesis. The method of plotting the distance function can find various applications in different branches of science where the elasticity tensor of a medium is considered. For example, there are some experiments that are made to calculate the elasticity tensor of rocks in the laboratories. Furthermore, the tensor of a subsurface is also calculated by inverting velocity and polarization data of seismic waves in situ. These inversions are generally made to determine the structures in the medium or to come up with the number of parameters for modelling the medium. Furthermore, there is no a priori symmetry that is assumed for the medium before the experiment takes place. Thus, the inverted tensor has generally anisotropic symmetry. The closest symmetry class to the medium determines how many parameters to use for representing it in modelling. As we have pointed out in the last chapter, it may also show the number of structures that exist in the medium. Thus, finding the closest symmetry class is necessary for representing the medium with fewer parameters, or equivalently, with simpler structures. The plotting method is easy to implement compared to algebraical methods in the literature. Thus, in the future it can be used in any applications in which the elasticity tensor is the issue.

As a future work, we hope to apply these methods to a specific region where in-situ anisotropy is estimated by using seismic techniques. We would like to consider the causes of anisotropy by decomposing the elasticity tensor of a subsurface. It can be introduced as a forward problem by starting with initial guesses obtained from the geology of the region. More precisely, the number of the planar structures and their orientations can be derived from the previous work in the region. Then, this knowledge can be used as an initial guess for the forward problem. Combining the media and comparing the result with the measured elasticity tensor of the subsurface, one can understand the causes of anisotropy. Plotting the distance functions of the

elasticity tensors can show how close the results are and how to change the orientations to get closer values.

Recall that one result described in the last chapter is that the combination of two TI media, where their rotation axes are around 45° apart, may or may not be close to a higher symmetry class. We hope to characterize the situations when it is close to a higher symmetry class. We believe that whenever two TI tensors that are to be combined are close to each other, then the resulting tensor is close to a higher symmetry class.

Another area of future work is proving the relation between the sum of the monoclinic-distance functions for some particular directions and the trigonal-, tetragonal-, cubic-distance functions. Since the minimum of those functions is achieved either in the same or very close coordinate systems, there can be a relation between the roots of their first-partial derivatives. First, we hope to investigate how close their partial derivatives are. We believe that since the existence of the mirror planes in tetragonal and trigonal media implies their rotational symmetries, not only are the roots of these derivatives close but so are the derivatives themselves.

Another application of the plotting method for finding the closest symmetry class can be in mineralogy or physics. To study the effect of phase transition on elastic parameters of a mineral, its elasticity tensor is found before and after the transition. However, most of these applications assume a priori symmetry of the mineral before calculating its tensor by ultrasonic measurements. This a priori assumption is obtained by making an x-ray or neutron experiment on the mineral to determine its symmetry class. Now, one can calculate the tensor without any a priori assumption of its symmetry class, and measure the velocities and polarizations of the waves in any direction. Then, by using the plotting method that we have introduced in the thesis, its closest symmetry class and orientation can be obtained.

Appendix

A.1 Deformation

Let us suppose that a body having a particular configuration at some reference time t_0 has another configuration at time t. See Figure 1. A material point P undergoes a displacement $\mathbf{u}$, thus has the position

$$\mathbf{x} = \bar{\mathbf{X}} + \mathbf{u}(\bar{\mathbf{X}}, t).$$

At this point, we would like to mention what $\mathbf{x}$ and $\bar{\mathbf{X}}$ are. Refer to Figure (1) for their geometrical meanings. In continuum mechanics, one can describe the change of tensor quantities (temperature, velocity, stress) either by a material description or a spatial description. If we describe a tensor, say $\mathbf{T}$, by a function of $\bar{\mathbf{X}}$

$$\mathbf{T} = \mathbf{T}(\bar{X}_1, \bar{X}_2, \bar{X}_3)$$

then this representation is called the **material description** because $(\bar{X}_1, \bar{X}_2, \bar{X}_3)$ identifies the different particles of the body. To make the distinction between the material and the spatial description more clear, consider two vectors, $(\bar{X}_1, \bar{X}_2, \bar{X}_3)$ and $(\bar{X}_1', \bar{X}_2', \bar{X}_3')$ which are representing different particles of the body. We cannot infer about the positions of the particles at a particular time by using the material description. However, by using a spatial description of a tensor, one expresses the value of a tensor with respect to a position in the body. Spatial description corresponds to

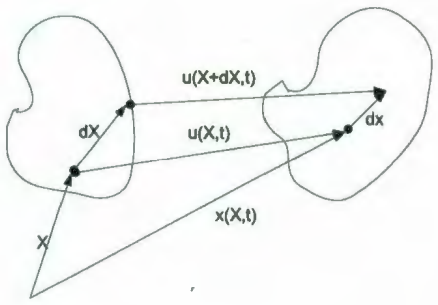

Figure 1: Geometry of a displacement that is associated with a deformation in a continuum

expressing a tensor by a function of $\mathbf{x}$:

$$\mathbf{T} = \mathbf{T}(x_1, x_2, x_3),$$

where $\mathbf{x} = (x_1, x_2, x_3)$ is the function of a position in the body. More precisely, the relation between $\mathbf{x}$ and $\bar{\mathbf{X}}$ can be given as

$$\mathbf{x} = \mathbf{x}(\bar{\mathbf{X}}, t) \text{ with } \bar{\mathbf{X}} = \mathbf{x}(\bar{\mathbf{X}}, t_0), \tag{A.1}$$

where t_o is considered to be the initial time. Thus, Equation A.1, which describes $\mathbf{x}$, gives the path line or trajectory of the particle $\bar{\mathbf{X}}$ as time t changes. Hence, the changes of tensor quantities can be considered either with respect to the particles in the body or with respect to the positions in the body, which are called **material** and **spatial descriptions** of a tensor, respectively. The transformation between these two variables are expressed by Equation A.1.

Now, we define the strain tensor to measure the amount of a deformation. To this end, we will derive the formulation of the displacement tensor by refering to

the geometry represented in Figure 1. As shown in Figure 1, displacement function, u, maps one point to another point where points are referring to the positions of a particle before and after the deformation. However, the displacement tensor, which is derived from the displacement function u, maps a given vector $d\bar{\mathbf{X}}$ to the vector $d\mathbf{x}$ where it is displaced to after the deformation.

Referring to the figure, a neighboring point $\mathbf{Q}$ at $\bar{\mathbf{X}} + d\bar{\mathbf{X}}$ arrives at $\mathbf{x} + d\mathbf{x} = \bar{\mathbf{X}} + d\bar{\mathbf{X}} + \mathbf{u}(\bar{\mathbf{X}} + d\bar{\mathbf{X}}, t)$. So we get

$$d\mathbf{x} = d\bar{\mathbf{X}} + \mathbf{u}(\bar{\mathbf{X}} + d\bar{\mathbf{X}}, t) - \mathbf{u}(\bar{\mathbf{X}}, t).$$

By using the definition of **gradient** of $\mathbf{u}$, denoted by $\nabla\mathbf{u}$, we may write this equation as

$$d\mathbf{x} = d\bar{\mathbf{X}} + \nabla\mathbf{u}(d\bar{\mathbf{X}}), \tag{A.2}$$

where $\nabla\mathbf{u}$ is known as the **displacement gradient**. Whatever deformation there is, it is included in the displacement gradient $\nabla\mathbf{u}$. Thus, we define the strain tensor which is embodied in the displacement tensor.

Note that the **gradient** of a vector-valued function $\mathbf{u}$ is defined to be the second-rank tensor which, when operating on $d\bar{\mathbf{X}}$, gives the difference of $\mathbf{u}$ at $\bar{\mathbf{X}} + d\bar{\mathbf{X}}$ and $\bar{\mathbf{X}}$. That is,

$$d\mathbf{u} = \mathbf{u}(\bar{\mathbf{X}} + d\bar{\mathbf{X}}) - \mathbf{u}(\bar{\mathbf{X}}) := \nabla\mathbf{u}(d\bar{\mathbf{X}}).$$

The components of $\nabla\mathbf{u}$ by using Cartesian coordinates is

$$(\nabla\mathbf{u})_{ij} = \frac{\partial u_i}{\partial \bar{X}_j},$$

in matrix notation,

$$(\nabla\mathbf{u}) = \begin{bmatrix} \frac{\partial u_1}{\partial \bar{X}_1} & \frac{\partial u_1}{\partial \bar{X}_2} & \frac{\partial u_1}{\partial \bar{X}_3} \\ \frac{\partial u_2}{\partial \bar{X}_1} & \frac{\partial u_2}{\partial \bar{X}_2} & \frac{\partial u_2}{\partial \bar{X}_3} \\ \frac{\partial u_3}{\partial \bar{X}_1} & \frac{\partial u_3}{\partial \bar{X}_2} & \frac{\partial u_3}{\partial \bar{X}_3} \end{bmatrix}.$$

Observe from Figure 1 that if the displacement were a rigid rotation then $\nabla \mathbf{u} \neq 0$ but there is no deformation in the material. In general, the displacement gradient, $\nabla \mathbf{u}$, contains a rigid rotation in its formulation. Thus, every displacement can be regarded as a combination of a deformation and a rotation. This can be seen when we decompose the second-rank tensor, $\nabla \mathbf{u}$, into the sum of its symmetric and skew-symmetric part, which can be done for all second-rank tensors. Obviously, a rigid rotation is not a form of deformation, so we should separate rigid rotations from $\nabla \mathbf{u}$. In fact,

$$\nabla \mathbf{u}_{ij} = \frac{\partial u_i}{\partial \bar{X}_j} = \frac{1}{2}\left(\frac{\partial u_i}{\partial \bar{X}_j} + \frac{\partial u_j}{\partial \bar{X}_i}\right) + \frac{1}{2}\left(\frac{\partial u_i}{\partial \bar{X}_j} - \frac{\partial u_j}{\partial \bar{X}_i}\right) \tag{A.3}$$

$$= \epsilon_{ij} + \omega_{ij}, \tag{A.4}$$

where the symmetric part ϵ_{ij} of the displacement gradient is called **strain tensor** and skew-symmetric part ω_{ij} describes a rigid rotation [44]. Thus, the strain tensor, denoted by ϵ_{ij}, is formulated as

$$\epsilon_{ij} = \frac{1}{2}\left(\frac{\partial u_i}{\partial \bar{X}_j} + \frac{\partial u_j}{\partial \bar{X}_i}\right).$$

Now, let us consider the physical meaning of the strain tensor. More precisely, we show how it gives the measure of deformation. To do so, we derive the tensor from the geometrical consideration of the particles in a body. In order to measure deformation, one has to consider two vectors and their angular relations after deformation. This is mainly because considering one vector may not reveal whether the displacement is a rigid rotation or not, as we have already pointed out. Thus, the amount of strain can be measured by the change in the angle between two vectors or the change in length when the two vectors are equal to each other.

Hence, the measure of deformation can be calculated by taking the dot product of $d\mathbf{x}^1$ and $d\mathbf{x}^2$, where they correspond to difference between two neighboring points

after deformation. Through the displacement $\mathbf{u}$, $d\bar{\mathbf{X}}^1$ becomes $d\mathbf{x}^1$ and $d\bar{\mathbf{X}}^2$ becomes $d\mathbf{x}^2$ by Equation A.2. So we get

$$d\mathbf{x}^1 = d\bar{\mathbf{X}}^1 + \nabla\mathbf{u}(d\bar{\mathbf{X}}^1) \tag{A.5}$$

$$d\mathbf{x}^2 = d\bar{\mathbf{X}}^2 + \nabla\mathbf{u}(d\bar{\mathbf{X}}^2). \tag{A.6}$$

Taking the dot product of $d\mathbf{x}^1$ and $d\mathbf{x}^2$, we get

$$d\mathbf{x}^1 \cdot d\mathbf{x}^2 = d\bar{\mathbf{X}}^1 \cdot d\bar{\mathbf{X}}^2 + d\bar{\mathbf{X}}^1 \cdot \nabla\mathbf{u}(d\bar{\mathbf{X}}^2) + d\bar{\mathbf{X}}^2 \cdot \nabla\mathbf{u}(d\bar{\mathbf{X}}^1) + \nabla\mathbf{u}(d\bar{\mathbf{X}}^1) \cdot \nabla\mathbf{u}(d\bar{\mathbf{X}}^2). \tag{A.7}$$

By using a property of the transpose operation, we get the following equalities

$$\begin{aligned} d\bar{\mathbf{X}}^2 \cdot \nabla\mathbf{u}(d\bar{\mathbf{X}}^1) &= d\bar{\mathbf{X}}^1 \cdot \nabla\mathbf{u}^T(d\bar{\mathbf{X}}^2), \\ \nabla\mathbf{u}(d\bar{\mathbf{X}}^1) \cdot \nabla\mathbf{u}(d\bar{\mathbf{X}}^2) &= d\bar{\mathbf{X}}^1 \cdot \nabla\mathbf{u}^T(\nabla\mathbf{u}(d\bar{\mathbf{X}}^2)). \end{aligned}$$

Thus, Equation A.7 becomes

$$d\mathbf{x}^1 \cdot d\mathbf{x}^2 = d\bar{\mathbf{X}}^1 \cdot d\bar{\mathbf{X}}^2 + d\bar{\mathbf{X}}^1 \cdot (\nabla\mathbf{u} + \nabla\mathbf{u}^T + (\nabla\mathbf{u}^T)(\nabla\mathbf{u}))(d\bar{\mathbf{X}}^2). \tag{A.8}$$

Let us denote the tensor appearing in the formula above by ϵ^*. More precisely,

$$\epsilon^* = (\nabla\mathbf{u} + \nabla\mathbf{u}^T + (\nabla\mathbf{u}^T)(\nabla\mathbf{u})).$$

Then we can rewrite Equation A.8 as

$$d\mathbf{x}^1 \cdot d\mathbf{x}^2 = d\bar{\mathbf{X}}^1 \cdot d\bar{\mathbf{X}}^2 + 2d\bar{\mathbf{X}}^1 \cdot \epsilon^*(d\bar{\mathbf{X}}^2). \tag{A.9}$$

Observe from equation A.9 that if $\epsilon^* = 0$, then lengths and angle between measurement axes remain unchanged. In other words, the second-order tensor ϵ^* characterizes the deformation in the neighborhood of the particle P. The components of ϵ^* with respect to Cartesian coordinates are given by

$$\epsilon^*_{ij} = \frac{1}{2}\left(\frac{\partial u_i}{\partial \bar{X}_j} + \frac{\partial u_j}{\partial \bar{X}_i} + \frac{\partial u_k}{\partial \bar{X}_i}\frac{\partial u_k}{\partial \bar{X}_j}\right),$$

where summation over k is implied.

The magnitudes of the components of the displacement gradient are much smaller than unity, so the product terms appearing in ϵ^* can be neglected. Then, for small deformations, we have

$$d\mathbf{x}^1 \cdot d\mathbf{x}^2 = d\bar{\mathbf{X}}^1 \cdot d\bar{\mathbf{X}}^2 + 2d\bar{\mathbf{X}}^1 \cdot \epsilon(d\bar{\mathbf{X}}^2), \tag{A.10}$$

where

$$\epsilon = \frac{1}{2}((\nabla \mathbf{u} + \nabla \mathbf{u}^T)).$$

Remark that ϵ is the symmetric part of $\nabla \mathbf{u}$ which is expressed in Equation A.3. Thus, whenever $\nabla \mathbf{u}$ is skew-symmetric, $\epsilon = 0$. It means that displacement characterizes a rigid body rotation in the neighborhood of the particle P. The Cartesian coordinates of ϵ, which are represented in orthogonal-coordinate system $\{e_1, e_2, e_3\}$, are given by

$$\epsilon_{ij} = \frac{1}{2}(\frac{\partial u_i}{\partial \bar{X}_j} + \frac{\partial u_j}{\partial \bar{X}_i}) \text{ for any } i, j \in \{1, 2, 3\}.$$

In matrix notation,

$$\epsilon = \begin{bmatrix} \frac{\partial u_1}{\partial \bar{X}_1} & \frac{1}{2}(\frac{\partial u_1}{\partial \bar{X}_2} + \frac{\partial u_2}{\partial \bar{X}_1}) & \frac{1}{2}(\frac{\partial u_1}{\partial \bar{X}_3} + \frac{\partial u_3}{\partial \bar{X}_1}) \\ \frac{1}{2}(\frac{\partial u_1}{\partial \bar{X}_2} + \frac{\partial u_2}{\partial \bar{X}_1}) & \frac{\partial u_2}{\partial \bar{X}_2} & \frac{1}{2}(\frac{\partial u_2}{\partial \bar{X}_3} + \frac{\partial u_3}{\partial \bar{X}_2}) \\ \frac{1}{2}(\frac{\partial u_1}{\partial \bar{X}_3} + \frac{\partial u_3}{\partial \bar{X}_1}) & \frac{1}{2}(\frac{\partial u_2}{\partial \bar{X}_3} + \frac{\partial u_3}{\partial \bar{X}_2}) & \frac{\partial u_3}{\partial \bar{X}_3} \end{bmatrix}. \tag{A.11}$$

Let us interpret the physical meanings of diagonal elements of the matrix ϵ. Consider a material particle $d\bar{\mathbf{X}}^1 = d\bar{\mathbf{X}}^2 = (dS)\mathbf{e_1}$, where $\mathbf{e_1}$ is a unit vector in the direction of the x-axis that the strain tensor is expressed in. Let $ds = |d\mathbf{x}|$, where it represents the deformed length of $d\bar{\mathbf{X}}^1$. Then Equation A.10 gives

$$\begin{aligned} (ds)^2 - (dS)^2 &= 2(dS)^2 \mathbf{e_1} \cdot \epsilon(\mathbf{e_1}) \\ &= 2(dS)^2 \epsilon_{11}, \end{aligned} \tag{A.12}$$

Figure 2: Uniaxial deformation.

where $\epsilon_{11} = \mathbf{e_1} \cdot \epsilon(\mathbf{e_1})$. Now, for small deformations we can assume that

$$(ds)^2 - (dS)^2 = (ds + dS)(ds - dS) \simeq 2dS(ds - dS).$$

Thus,

$$\frac{ds - dS}{dS} = \epsilon_{11}.$$

In other words, the first diagonal element of the strain tensor, namely ϵ_{11}, represents the change of length per unit length, known as **unit elongation**, or **normal strain**. Refer to Figure 2 for its geometrical meaning. Similarly, $\epsilon_{22}, \epsilon_{33}$ give unit elongation in the x_2- and x_3- directions, respectively.

To interpret the off-diagonal elements of the strain matrix, we should consider two basis vectors which are perpendicular to each other since the components of the tensor are defined according to the equation $\epsilon_{ij} = \mathbf{e_i} \cdot \epsilon(\mathbf{e_j})$. Let $d\bar{\mathbf{X}}^{\mathbf{1}} = (dS_1)\mathbf{e_1}$ and $d\bar{\mathbf{X}}^{\mathbf{2}} = (dS_2)\mathbf{e_2}$, where $\mathbf{e_1}$ and $\mathbf{e_2}$ are unit vectors in the direction of x-axis and y-axis, respectively. Then Equation A.10 gives

$$(ds_1)(ds_2)\cos\theta = 2(dS_1)(dS_2)\mathbf{e_1} \cdot \epsilon(\mathbf{e_2}), \tag{A.13}$$

where θ is the angle between $d\mathbf{x}^{\mathbf{1}}$ and $d\mathbf{x}^{\mathbf{2}}$. If we define $\theta = \frac{\Pi}{2} - \gamma$, then γ will measure the small decrease in the angle between $d\bar{\mathbf{X}}^{\mathbf{1}}$ and $d\bar{\mathbf{X}}^{\mathbf{2}}$, which is known as shear strain. Refer to Figure 3. Since

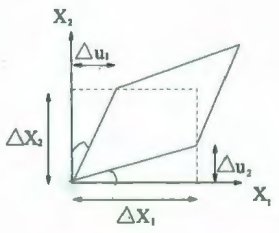

Figure 3: Shear strain.

$$\cos(\frac{\Pi}{2} - \gamma) = \sin\gamma$$

and for small strain $\sin\gamma = \gamma$, $\frac{ds_1}{dS_1} = \frac{ds_2}{dS_2} = 1$, then Equation A.13 becomes

$$\gamma = 2\mathbf{e_1} \cdot \epsilon(\mathbf{e_2}) = 2\epsilon_{12}.$$

Thus, $2\epsilon_{12}$ gives the decrease in the angle between two axes, namely x-axis and y-axis after the deformation. Similarly, $2\epsilon_{13}$ gives the decrease in the angle between x-axis and z-axis.

A.2 Stress

In the previous section, we considered a kinematical description of the motion of a continuum without any consideration of the forces that causes the motion and deformation. In this section, we formally define the forces in the interior of a body. In classical continuum theory, the internal forces are introduced through the concept of body forces and surface forces. Body forces are those that act throughout a volume by a long-range interaction with matter (e.g. gravity, magnetic, electrostatic forces). Surface forces act on a surface separating parts of the body. It will be assumed that a stress vector is adequate to describe the surface force at a point of a surface. This assumption is one of the basic axioms of classical continuum mechanics, and is known

as **Cauchy's stress principle**. We shall prove that the stress tensor is sufficient to evaluate the stress vector for any direction that represents normal of a surface at a point. In other words, stress tensor will be defined as a second-rank tensor which relates the normal of a surface to a stress vector.

Let S denote a surface passing through the point P. Let $\triangle\mathbf{F}$ be the resultant force acting on a small area $\triangle S$ containing the point P on the surface S. Then the stress vector at P is defined as

$$\mathbf{t_n} := \lim_{\triangle S \to 0} \frac{\triangle \mathbf{F}}{\triangle S}, \tag{A.14}$$

where n denotes the normal vector of $\triangle S$. If the normal of the tangent plane is $-n$, then by Newton's law of action and reaction, t_{-n} will be the stress vector acting on the same plane at the same point but in the opposite direction of $\mathbf{t_n}$. That is,

$$\mathbf{t_{-n}} = -\mathbf{t_n}.$$

We now state Cauchy's stress principle: The value of a stress vector at any point is unique up to its normal with specified orientation. In other words, the limit in Equation A.14 exists, hence it is unique, for any small area $\triangle S$ containing the point P.

Consider an element of a continuum in the form of a tetrahedron with the point P as one of its vertices. See Figure 4.

The size of the tetrahedron will ultimately be made to approach zero by taking the limit so that the inclined plane will pass through the point P. We wish to determine the stress vector acting on the oblique face whose normal is n. Assuming that the tetrahedron is subjected to both surface and body forces, using Newton's second law we write

$$\triangle\mathbf{F} + \triangle\mathbf{F_{e_1}} + \triangle\mathbf{F_{e_2}} + \triangle\mathbf{F_{e_3}} + \mathbf{f}\triangle V = \rho\triangle V\frac{d\mathbf{v}}{dt}, \tag{A.15}$$

where $\triangle\mathbf{F}$ is the surface force acting on the oblique face, $\triangle\mathbf{F}_{e_i}$ is the surface force acting on the orthogonal face normal to x_i-axis and $\mathbf{f}$ refers to the body force acting

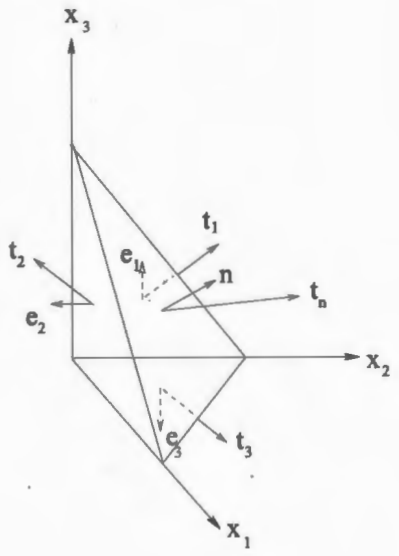

Figure 4: Cauchy's Tetrahedron that is used to find the stress vector in an oblique surface.

on the tetrahedron with volume $\triangle V$, mass density ρ and velocity $\mathbf{v}$. Thus, the left-hand side of Equation A.15 gives the sum of forces, while the right-hand side is the product of mass and average acceleration of the particle. Since we have not taken the limit of the tetrahedron yet, we can write the stress vector defined in Equation A.14 without considering the limit as

$$\triangle \mathbf{F} = \mathbf{t_n} \triangle S. \tag{A.16}$$

Substituting the above equation into Equation A.15, we get

$$\mathbf{t_n} \triangle S - \mathbf{t_{e_1}} \triangle S_1 - \mathbf{t_{e_2}} \triangle S_2 - \mathbf{t_{e_3}} \triangle S_3 + \mathbf{f} \triangle V = \rho \triangle V \frac{d\mathbf{v}}{dt}, \tag{A.17}$$

where $\triangle S$ is the area of the oblique face and $\triangle S_i$ is the area of an orthogonal face normal to the x_i-axis. Note that the orthogonal faces have unit-outward normals parallel and opposite in sign to the unit vectors of the coordinate axes $\mathbf{e_i}$. Hence, in the view of Newton's law of action and reaction, we put the negative signs in Equation A.17.

To make more simplification in Equation A.17, we introduce a relation between the surface areas of the tetrahedron, namely $\triangle S$ and $\triangle S_i$. The area of the oblique face is related to the orthogonal faces by the following equation

$$\triangle S_i = n_i \triangle S,$$

where n_i are the components of the unit vector n which is normal to the oblique face. And the relation between the $\triangle V$ and $\triangle S$ can be stated as

$$\triangle V = \frac{h}{3} \triangle S,$$

where h is the height and the oblique face, $\triangle S$, is the base of the tetrahedron.

Substituting the above relations to Equation A.17, we obtain

$$\mathbf{t_n} \triangle S - \mathbf{t_{e_1}} n_1 \triangle S - \mathbf{t_{e_2}} n_2 \triangle S - \mathbf{t_{e_3}} n_3 \triangle S + \frac{\mathbf{f} h}{3} \triangle S = \frac{\rho}{3} \triangle S \frac{d\mathbf{v}}{dt}. \tag{A.18}$$

Dividing both sides of the above equation by $\triangle S$

$$\mathbf{t_n} - \mathbf{t_{e_1}} n_1 - \mathbf{t_{e_2}} n_2 - \mathbf{t_{e_3}} n_3 + \frac{\mathbf{f}h}{3} = \frac{\rho}{3}\frac{d\mathbf{v}}{dt}. \tag{A.19}$$

For describing the state of stress at a point within the continuum, we let $h \to 0$, in other words, the finite-size of the tetrahedron reduces to infinitesimal tetrahedron at point P. Thus, after taking the limit the equation A.19 simplifies to

$$\mathbf{t_n} = \mathbf{t_{e_1}} n_1 + \mathbf{t_{e_2}} n_2 + \mathbf{t_{e_3}} n_3. \tag{A.20}$$

The above equation can be explicitly written in matrix notation as

$$\begin{aligned}
\begin{bmatrix} t_n^1 \\ t_n^2 \\ t_n^3 \end{bmatrix} &= \begin{bmatrix} t_{e_1}^1 \\ t_{e_1}^2 \\ t_{e_1}^3 \end{bmatrix} n_1 + \begin{bmatrix} t_{e_2}^1 \\ t_{e_2}^2 \\ t_{e_2}^3 \end{bmatrix} n_2 + \begin{bmatrix} t_{e_3}^1 \\ t_{e_3}^2 \\ t_{e_3}^3 \end{bmatrix} n_3 \\
&= \begin{bmatrix} t_{e_1}^1 & t_{e_2}^1 & t_{e_3}^1 \\ t_{e_1}^2 & t_{e_2}^2 & t_{e_3}^2 \\ t_{e_1}^3 & t_{e_2}^3 & t_{e_3}^3 \end{bmatrix} \begin{bmatrix} n_1 \\ n_2 \\ n_3 \end{bmatrix} && \text{(A.21)} \\
&= \sigma\mathbf{n} && \text{(A.22)}
\end{aligned}$$

where σ denotes the stress tensor which is explicitly given in the above expression.

From now on, we will denote the 3×3 matrix in the equation above by σ and denote its entities by σ_{ij}, more precisely we define σ by the following equation

$$\begin{bmatrix} \sigma_{11} & \sigma_{12} & \sigma_{13} \\ \sigma_{21} & \sigma_{22} & \sigma_{23} \\ \sigma_{31} & \sigma_{32} & \sigma_{33} \end{bmatrix} := \begin{bmatrix} t_{e_1}^1 & t_{e_2}^1 & t_{e_3}^1 \\ t_{e_1}^2 & t_{e_2}^2 & t_{e_3}^2 \\ t_{e_1}^3 & t_{e_2}^3 & t_{e_3}^3 \end{bmatrix} \tag{A.23}$$

Then, Equation A.21 can be expressed in matrix notation as

$$\mathbf{t_n} = \sigma\mathbf{n}, \tag{A.24}$$

where $\mathbf{n}$ denotes the normal of the oblique surface of the tetrahedron that $\mathbf{t_n}$ is acting on. Hence, we see that the transformation relating the normal of a surface at a

point to the stress vector, namely σ, is linear. Thus, σ is a second-rank tensor. It is clear that if the stress tensor is known, then the stress vector on any inclined plane is uniquely determined from Equation A.24. In other words, the state of stress at a point is completely characterized by the stress tensor σ. Moreover, any σ expressed in a particular coordinate system is a representative of all σ's expressed in any coordinate system since any of them can be obtained by transforming the coordinate system by an orthogonal transformation.

A.3 Stress-Strain Relation: Elasticity Tensor

In the previous sections, we have derived formulations of two physical quantities, namely stress and strain tensors, which are both independent of the material's intrinsic properties. These formulations are valid for any continuum irrespective of its constitution. In other words, they do not explicitly account for distinctive properties of a particular material. However, in this section we will consider a characteristic property of a material which describes the elastic behaviour or response of it when it is subjected to the stress. These equations are based on experimental observations of materials. It is assumed to be valid only for small deformations occurring in the material. Thus, an elastic continuum is defined by the consitutive equations which state that forces are linearly related to small deformations. At any point of a three-dimensional continuum, Hooke's law, which linearly relates each stress-tensor component, σ_{ij}, to all strain-tensor component, ϵ_{ij}, can be written as

$$\sigma_{ij} = \sum_{k=1}^{3}\sum_{l=1}^{3} c_{ijkl}\epsilon_{kl}, \text{ for any } i,j \in \{1,2,3\}, \tag{A.25}$$

where c_{ijkl} are the components of a tensor which is known as the elasticity tensor. We rewrite the above expression by using the summation convention as

$$\sigma_{ij} = c_{ijkl}\epsilon_{kl}, \text{ for any } i,j \in \{1,2,3\}. \tag{A.26}$$

Every elastic medium, which is also called a Hookean solid, has an unique elasticity tensor which completely defines its elastic behaviour.

The elasticity tensor is a fourth-rank tensor since it relates two second-rank tensors, namely stress and strain. The rank of a tensor indicates the number of directions involved for defining the corresponding physical quantity. For example, temperature is a zero-rank tensor since it is represented by a scalar value, hence no direction is associated with temperature. Force, which is represented by a vector, is a one-rank tensor. Stress and strain tensors, that we have defined in the last sections, are second-rank tensors because two directions are needed for defining those quantities. In other words, they relate two vectors. Stress tensor expresses a relation between the normal of a surface and the stress-vector applied to that surface. Strain tensor relates two directions in three-dimensional space which gives the value of the change of angle between them after a deformation takes place. If the given two directions are the same, then the corresponding value of the strain tensor is a measure of the relative change of its length, as it is shown in A.1. Thus elasticity tensor is a fourth-rank tensor where two of the four directions associated with the stress tensor and the remaining two are due to the strain tensor.

A.3.1 Strain-Energy Function

For the complete specification of any state of the body, one should know the configuration and the temperature of every part of the body. Unless the body is in equilibrium under the action of external forces such as body forces and surface tractions, it will move from one configuration to another configuration. As this happens, the external forces, in general, do some work.

In mechanics, the total energy of any portion of the body is the sum of its kinetic energy and its intrinsic energy. Then the total energy of the whole body can be evaluated by adding the total energies of the parts into which it is divided. This

property of the energy function makes it an exact differential, meaning that the integral (or sum) of the differential is independent of the path taken in the space of the parameters of the energy function. This is mathematically stated as

$$\int_i^f dU = U(f) - U(i),$$

where U denotes the energy state of the medium.

The First Law of Thermodynamics states that the increase in the internal energy of a system is equal to the amount of energy added by heating the system minus the amount lost as a result of the work done by the system on its surroundings. This can be expressed by the formula

$$dU = \delta Q - \delta W, \tag{A.27}$$

where δQ is the infinitesimal amount of heat added to the system and δW is the infinitesimal amount of work done by the system. The infinitesimal heat and work are denoted by δ rather than d because, in mathematical terms, they are not exact differentials.

As seismic waves pass through the material, we can expect that motion takes place too quickly to lose or gain any significant quantity of heat. Thus, we can assume that $\delta Q = 0$ in Equation A.27. Hence the differential of the work function becomes exact since it is equal to the energy of the system. It can be proved that if the work done in the system is independent of the displacement-path then stress must be a derivative of some function which is called potential function. This is mathematically stated as: There exists a function W that gives the value of the potential energy of the body and it has properties expressed by the equations

$$\frac{\partial W}{\partial \epsilon_{ij}} = \sigma_{ij}, \tag{A.28}$$

where ϵ_{ij} and σ_{ij} are components of the strain and stress tensors, respectively and $i, j \in \{1, 2, 3\}$. The function W, which has the properties expressed by Equations

A.28, is called the strain-energy function. The existence of such a function implies that the work done by the stress is independent of the path of the strain. So in order to evaluate the work done to the body by the stress, it is enough to consider the final and the initial configuration of the body.

Another assumption that is used in the theory of seismic wave-propagation is that as the wave passes through the material, any portion of the body executes small vibrations. Since the body is slightly strained, we can assume that stress components are linear functions of strain components, in other words Hooke's Law holds. Also, as we stated in the above paragraphs, since no heat is gained or lost during the passage of a seismic wave, components of the stress tensor are partial differential coefficients of the function W of strain components which can be expressed by Equations A.28. Now, substituting Hooke's law, expressed in Equation A.26 for σ_{ij} in Equation A.28 we get

$$\frac{\partial W}{\partial \epsilon_{ij}} = c_{ijkl}\epsilon_{kl}, i, j \in \{1, 2, 3\}. \tag{A.29}$$

Then, integrating with respect to ϵ_{ij}, we find that the strain energy function is a homogeneous quadratic function of strain components and it is in the form

$$\begin{aligned} 2W = C_{1111}\varepsilon_{11}^2 &+2C_{1122}\varepsilon_{11}\varepsilon_{22} &+2C_{1133}\varepsilon_{11}\varepsilon_{33} &+2C_{1123}\varepsilon_{11}\varepsilon_{23} &+2C_{1113}\varepsilon_{11}\varepsilon_{13} &+2C_{1112}\varepsilon_{11}\varepsilon_{12} \\ &+C_{2222}\varepsilon_{22}^2 &+2C_{2233}\varepsilon_{22}\varepsilon_{33} &+2C_{2223}\varepsilon_{22}\varepsilon_{23} &+2C_{2213}\varepsilon_{22}\varepsilon_{13} &+2C_{2212}\varepsilon_{22}\varepsilon_{12} \\ &&+C_{3333}\varepsilon_{33}^2 &+2C_{3323}\varepsilon_{33}\varepsilon_{23} &+2C_{3313}\varepsilon_{33}\varepsilon_{13} &+2C_{3312}\varepsilon_{33}\varepsilon_{12} \\ &&&+C_{2323}\varepsilon_{23}^2 &+2C_{2313}\varepsilon_{23}\varepsilon_{13} &+2C_{2312}\varepsilon_{23}\varepsilon_{12} \\ &&&&+C_{1313}\varepsilon_{13}^2 &+2C_{1312}\varepsilon_{13}\varepsilon_{12} \\ &&&&&+C_{1212}\varepsilon_{12}^2, \end{aligned} \tag{A.30}$$

or, we can show it in tensor notation and using Einstein's summation convention as

$$2W = c_{ijkl}\epsilon_{ij}\epsilon_{kl}.$$

For an elastic medium, we assume that all the expended energy is stored in the strained medium as a potential energy. In other words, we are dealing with a conser-

vative system. A conservative system means that the total energy of the medium is preserved during the physical phenomena that take place. An equivalent statement is that no heat is lost or gained in the system.

It is necessary to expend energy in order to deform a material. In other words, if energy is not expended, the material remains stable in its undeformed state. This constraint on the strain-energy function is called the stability condition. In general, energy is a positive quantity. Thus, the strain-energy function must be a positive quantity that vanishes only in the undeformed state. Mathematically, the stability conditions are equivalent to the positive-definiteness of the elasticity tensor. A fourth-rank tensor is positive-definite if

$$c_{ijkl}\epsilon_{ij}\epsilon_{kl} \geq 0, \text{ for every } \epsilon.$$

Then the corresponding fourth-rank tensor may correspond to the elasticity tensor of a real material since it means that one needs energy to deform the material, where deformation is represented by ϵ.

A.3.2 Intrinsic Symmetries of Elasticity Tensor

In this section, we will consider the symmetries of the elasticity tensor. Since the elasticity tensor, c_{ijkl} where $i, j, k, l \in \{1, 2, 3\}$, has four subscripts, it has $3^4 = 81$ components. However, due to the symmetries of stress and strain tensor, the number of independent components decreases to thirty-six as will be shown below. The number of independent parameters is important in applications because in modelling, one wants to know how many parameters is enough to represent the medium under consideration.

It can be shown that in view of balance of angular momentum the stress tensor is symmetric, namely, $\sigma_{ij} = \sigma_{ji}$. Also, the strain tensor, which is expressed in Equation A.11, is symmetric by definition, $\epsilon_{ij} = \epsilon_{ji}$. Considering the symmetry of the stress

tensor, one can write stress-strain Equation A.26 as

$$c_{ijkl}\epsilon_{kl} = \sigma_{ij} = \sigma_{ji} = c_{jikl}\epsilon_{kl}, \quad i,j \in \{1,2,3\}. \tag{A.31}$$

Subtracting the first double-summation term from the second one, we get

$$c_{ijkl}\epsilon_{kl} - c_{jikl}\epsilon_{kl} = (c_{ijkl} - c_{jikl})\epsilon_{kl} = 0, \tag{A.32}$$

where $i,j \in \{1,2,3\}$. Thus, for this equation to be satisfied for all strain tensor components, we require

$$c_{ijkl} = c_{jikl}, \text{ for all } i,j,k,l \in \{1,2,3\}. \tag{A.33}$$

Hence, due to the symmetry of the stress tensor, the elasticity tensor is invariant under permutations in the first pair of subscripts. Note that the order of k and l has no effect on stress-strain Equation A.26 since they are summation indices. Thus, the following equation holds

$$c_{ijkl}\epsilon_{kl} = c_{ijlk}\epsilon_{lk}, \quad i,j \in \{1,2,3\}.$$

Considering the symmetry of strain tensor, we can interchange the indices of strain tensor and the above equation becomes

$$c_{ijkl}\epsilon_{kl} = c_{ijlk}\epsilon_{kl}, \quad i,j \in \{1,2,3\},$$

which can be also stated as

$$c_{ijkl}\epsilon_{kl} - c_{ijlk}\epsilon_{kl} = (c_{ijkl} - c_{ijlk})\epsilon_{kl} = 0,$$

where $i,j \in \{1,2,3\}$. For this equation to be satisfied for all strain tensor components, we require

$$c_{ijkl} = c_{ijlk}, \text{ for all } i,j,k,l \in \{1,2,3\}. \tag{A.34}$$

Hence, due to the symmetry of the strain tensor, the elasticity tensor is invariant under permutations in the second pair of subscripts.

In view of Equalities A.34 and A.33, the number of components of the elasticity tensor is thirty-six.

Furthermore, by considering the existence of the strain-energy function, it can be found that the elasticity tensor is invariant under permutations of subscripts ij and kl which reduces the number of parameters of the tensor to twenty-one. This can be derived in the following manner. Let us remember Equation A.29

$$\frac{\partial W}{\partial \epsilon_{ij}} = c_{ijkl}\epsilon_{kl}, \quad i,j \in \{1,2,3\}. \tag{A.35}$$

Differentiating both sides of these equations with respect to ϵ_{kl}, we obtain

$$\frac{\partial^2 W(\epsilon)}{\partial \epsilon_{kl}\partial \epsilon_{ij}} = c_{ijkl}, \quad i,j,k,l \in \{1,2,3\}. \tag{A.36}$$

Now, let us invoke the equality of mixed partial derivatives, which states that, if W has a continuous derivative then the order of differentiation is interchangeable. Since W is a quadratic polynomial as expressed in Equation A.30, it has a continuous derivative. Then, Equation A.36 implies that

$$c_{ijkl} = c_{klij}. \tag{A.37}$$

Hence, we conclude that the elasticity tensor is invariant under permutations of pairs of subscripts ij and kl.

A.3.3 Matrix Representation of Elasticity Tensor

Due to the symmetries of stress and strain tensors, the constitutive equations, which are expressed in Equations A.26, can be conveniently written in a matrix form, containing six independent equations. This form allows us to express elasticity tensor as an elasticity matrix. The thirty-six independent components of the elasticity tensor can be written as entities of a 6×6 elasticity matrix, denoted by C_{mn} and it

relates each independent stress-tensor components to the six independent strain components. To construct this matrix, in view of symmetries A.33 and A.34, it is enough to consider the pairs of (i,j) and (k,l) for $i \leq j$ and $k \leq l$, respectively.

Consider such pairs (i,j), where $i,j \in \{1,2,3\}$. Let us arrange them in the order given by

$$(1,1),(2,2),(3,3),(2,3),(1,3),(1,2).$$

Now, we can replace each pair by a single number m that gives the position of the pair in the above list, thus $m \in \{1,...,6\}$. In other words, we make the following replacement $(i,j) \rightarrow m$:

$$(1,1) \rightarrow 1, (2,2) \rightarrow 2, (3,3) \rightarrow 3$$
$$(2,3) \rightarrow 4, (1,3) \rightarrow 5, (1,2) \rightarrow 6.$$

We can formally write this replacement map as

$$\begin{aligned} m &= i \text{ if } i = j \\ m &= 9 - (i+j) \text{ if } i \neq j, \end{aligned}$$

where $i,j \in \{1,2,3\}$. Considering the analogous pairs (k,l), where $k,l \in \{1,2,3\}$, one can have the identical replacements. Consequently, we can replace c_{ijkl}, where $i,j,k,l \in \{1,2,3\}$ by C_{mn}, where $m,n \in \{1,...,6\}$ to obtain the elasticity matrix given by

$$C = \begin{bmatrix} C_{11} & C_{12} & C_{13} & C_{14} & C_{15} & C_{16} \\ C_{21} & C_{22} & C_{23} & C_{24} & C_{25} & C_{26} \\ C_{31} & C_{32} & C_{33} & C_{34} & C_{35} & C_{36} \\ C_{41} & C_{42} & C_{43} & C_{44} & C_{45} & C_{46} \\ C_{51} & C_{52} & C_{53} & C_{54} & C_{55} & C_{56} \\ C_{61} & C_{62} & C_{63} & C_{64} & C_{65} & C_{66} \end{bmatrix}. \tag{A.38}$$

Furthermore, by using the symmetry of elasticity tensor due to the existence of strain-energy function, we see that $c_{ijkl} = c_{klij}$ which implies that $C_{mn} = C_{nm}$ since switching

ij with kl is equivalent to switching m with n. Hence, the above elasticity matrix A.38 turns out to be a symmetric 6×6 matrix which can be expressed by

$$C = \begin{bmatrix} C_{11} & C_{12} & C_{13} & C_{14} & C_{15} & C_{16} \\ C_{12} & C_{22} & C_{23} & C_{24} & C_{25} & C_{26} \\ C_{13} & C_{23} & C_{33} & C_{34} & C_{35} & C_{36} \\ C_{14} & C_{24} & C_{34} & C_{44} & C_{45} & C_{46} \\ C_{15} & C_{25} & C_{35} & C_{45} & C_{55} & C_{56} \\ C_{16} & C_{26} & C_{36} & C_{46} & C_{56} & C_{66} \end{bmatrix}. \tag{A.39}$$

Hence, stress-strain Equation A.26 for a general elastic continuum that obeys Hooke's law can be written in matrix form as

$$\begin{bmatrix} \sigma_{11} \\ \sigma_{22} \\ \sigma_{33} \\ \sigma_{23} \\ \sigma_{13} \\ \sigma_{12} \end{bmatrix} = \begin{bmatrix} C_{11} & C_{12} & C_{13} & C_{14} & C_{15} & C_{16} \\ C_{12} & C_{22} & C_{23} & C_{24} & C_{25} & C_{26} \\ C_{13} & C_{23} & C_{33} & C_{34} & C_{35} & C_{36} \\ C_{14} & C_{24} & C_{34} & C_{44} & C_{45} & C_{46} \\ C_{15} & C_{25} & C_{35} & C_{45} & C_{55} & C_{56} \\ C_{16} & C_{26} & C_{36} & C_{46} & C_{56} & C_{66} \end{bmatrix} \begin{bmatrix} \epsilon_{11} \\ \epsilon_{22} \\ \epsilon_{33} \\ 2\epsilon_{23} \\ 2\epsilon_{13} \\ 2\epsilon_{12} \end{bmatrix}, \tag{A.40}$$

where the stress and the strain tensor components are mapped to the corresponding matrix entries in the following way

$$\begin{bmatrix} \sigma_{11} & \sigma_{12} & \sigma_{13} \\ \sigma_{12} & \sigma_{22} & \sigma_{23} \\ \sigma_{13} & \sigma_{23} & \sigma_{33} \end{bmatrix} \rightarrow \begin{bmatrix} \sigma_{11} \\ \sigma_{22} \\ \sigma_{33} \\ \sigma_{23} \\ \sigma_{13} \\ \sigma_{12} \end{bmatrix}, \begin{bmatrix} \epsilon_{11} & \epsilon_{12} & \epsilon_{13} \\ \epsilon_{12} & \epsilon_{22} & \epsilon_{23} \\ \epsilon_{13} & \epsilon_{23} & \epsilon_{33} \end{bmatrix} \rightarrow \begin{bmatrix} \epsilon_{11} \\ \epsilon_{22} \\ \epsilon_{33} \\ 2\epsilon_{23} \\ 2\epsilon_{13} \\ 2\epsilon_{12} \end{bmatrix}. \tag{A.41}$$

The above representation of the tensors is called Voigt notation. Remark that since stress and strain tensors are symmetric, they have only six independent components.

This allows us to represent those second-rank tensors as a vector in six-dimensional (6D) space. However, the 6D-vector space for representing the stress tensor is not equivalent to the 6D-vector space of strains because of the factor 2 appearing in the last three rows of strain vector. Treating stress and strain differently prevents construction of an isomorphism between these two spaces and furthermore, the elasticity tensor cannot be regarded as a linear transformation on a 6D-vector space. Thus, many advantages of tensor algebra are lost. In particular, these vectors do not obey the transformation rule when they are represented by Voigt notation. The only condition for the new representation to be a tensor is that the representation mapping should preserve the norm. Note that the maps in A.41 do not preserve the norm, where norm is defined as the square root of the sum of the squares of the components of the corresponding entity. In order to make the representation mapping norm-preserving, we can change it as

$$\begin{bmatrix} \sigma_{11} & \sigma_{12} & \sigma_{13} \\ \sigma_{12} & \sigma_{22} & \sigma_{23} \\ \sigma_{13} & \sigma_{23} & \sigma_{33} \end{bmatrix} \rightarrow \begin{bmatrix} \sigma_{11} \\ \sigma_{22} \\ \sigma_{33} \\ \sqrt{2}\sigma_{23} \\ \sqrt{2}\sigma_{13} \\ \sqrt{2}\sigma_{12} \end{bmatrix}, \begin{bmatrix} \epsilon_{11} & \epsilon_{12} & \epsilon_{13} \\ \epsilon_{12} & \epsilon_{22} & \epsilon_{23} \\ \epsilon_{13} & \epsilon_{23} & \epsilon_{33} \end{bmatrix} \rightarrow \begin{bmatrix} \epsilon_{11} \\ \epsilon_{22} \\ \epsilon_{33} \\ \sqrt{2}\epsilon_{23} \\ \sqrt{2}\epsilon_{13} \\ \sqrt{2}\epsilon_{12} \end{bmatrix}. \tag{A.42}$$

Then, according to the new representation, the stress-strain equation can be written

as

$$\begin{bmatrix} \sigma_{11} \\ \sigma_{22} \\ \sigma_{33} \\ \sqrt{2}\sigma_{23} \\ \sqrt{2}\sigma_{13} \\ \sqrt{2}\sigma_{12} \end{bmatrix} = \begin{bmatrix} c_{1111} & c_{1122} & c_{1133} & \sqrt{2}c_{1123} & \sqrt{2}c_{1113} & \sqrt{2}c_{1112} \\ c_{2211} & c_{2222} & c_{2233} & \sqrt{2}c_{2223} & \sqrt{2}c_{2213} & \sqrt{2}c_{2212} \\ c_{3311} & c_{3322} & c_{3333} & \sqrt{2}c_{3323} & \sqrt{2}c_{3313} & \sqrt{2}c_{3312} \\ \sqrt{2}c_{1123} & \sqrt{2}c_{2223} & \sqrt{2}c_{3323} & 2c_{2323} & 2c_{2313} & 2c_{2312} \\ \sqrt{2}c_{1113} & \sqrt{2}c_{2213} & \sqrt{2}c_{3313} & 2c_{2313} & 2c_{1313} & 2c_{1312} \\ \sqrt{2}c_{1112} & \sqrt{2}c_{2212} & \sqrt{2}c_{3312} & 2c_{2312} & 2c_{1312} & 2c_{1212} \end{bmatrix} \begin{bmatrix} \varepsilon_{11} \\ \varepsilon_{22} \\ \varepsilon_{33} \\ \sqrt{2}\varepsilon_{23} \\ \sqrt{2}\varepsilon_{13} \\ \sqrt{2}\varepsilon_{12} \end{bmatrix} \tag{A.43}$$

The above representation of the tensors is called Kelvin notation. Note that the elasticity matrix in this representation has the same norm as the original tensor has. Thus, it becomes a second-rank tensor in 6D since it connects two 6D vectors, instead of a fourth-rank tensor in 3D. Also, in this representation, the vector spaces of strain and stress are isomorphic to each other and the second-rank tensors have the same norm as the vectors in 6D. The numerical values of the components of the 6D stress-, strain-vectors and elasticity matrix differ from the components of 3D second- and fourth-rank tensors whereas their norms are equivalent. This enables us to use tensor algebra for the matrix representations in 6D. Kelvin notation is also more convenient for investigating the eigensystem of the elasticity matrix. Investigating eigensystems enables us to gain insight into the invariants of the stress-strain equations.

We will use a further simplification in Kelvin notation. As a matter of fact, we will use the representation that we have introduced in Equation A.38 for the strain and stress vectors denoted by Kelvin notation in Equation A.43. By doing this

simplification, we get rid of $\sqrt{2}$'s in the equation. We apply the following mapping:

$$\begin{bmatrix} \sigma_{11} \\ \sigma_{22} \\ \sigma_{33} \\ \sqrt{2}\sigma_{23} \\ \sqrt{2}\sigma_{13} \\ \sqrt{2}\sigma_{12} \end{bmatrix} \rightarrow \begin{bmatrix} \sigma_1 \\ \sigma_2 \\ \sigma_3 \\ \sigma_4 \\ \sigma_5 \\ \sigma_6 \end{bmatrix}, \begin{bmatrix} \epsilon_{11} \\ \epsilon_{22} \\ \epsilon_{33} \\ \sqrt{2}\epsilon_{23} \\ \sqrt{2}\epsilon_{13} \\ \sqrt{2}\epsilon_{12} \end{bmatrix} \rightarrow \begin{bmatrix} \epsilon_1 \\ \epsilon_2 \\ \epsilon_3 \\ \epsilon_4 \\ \epsilon_5 \\ \epsilon_6 \end{bmatrix}. \tag{A.44}$$

Note that we have not changed the numerical values of any components of the vectors above but only renamed them so that it looks simpler. Thus, the norm of vectors above are equal to each other. Hence, we did not lose the tensorship of the vectors. We will use the same trick for the elasticity matrix appearing in Equation A.39:

$$\begin{bmatrix} c_{1111} & c_{1122} & c_{1133} & \sqrt{2}c_{1123} & \sqrt{2}c_{1113} & \sqrt{2}c_{1112} \\ c_{2211} & c_{2222} & c_{2233} & \sqrt{2}c_{2223} & \sqrt{2}c_{2213} & \sqrt{2}c_{2212} \\ c_{3311} & c_{3322} & c_{3333} & \sqrt{2}c_{3323} & \sqrt{2}c_{3313} & \sqrt{2}c_{3312} \\ \sqrt{2}c_{1123} & \sqrt{2}c_{2223} & \sqrt{2}c_{3323} & 2c_{2323} & 2c_{2313} & 2c_{2312} \\ \sqrt{2}c_{1113} & \sqrt{2}c_{2213} & \sqrt{2}c_{3313} & 2c_{2313} & 2c_{1313} & 2c_{1312} \\ \sqrt{2}c_{1112} & \sqrt{2}c_{2212} & \sqrt{2}c_{3312} & 2c_{2312} & 2c_{1312} & 2c_{1212} \end{bmatrix} \rightarrow \begin{bmatrix} C_{11} & C_{12} & C_{13} & C_{14} & C_{15} & C_{16} \\ C_{12} & C_{22} & C_{23} & C_{24} & C_{25} & C_{26} \\ C_{13} & C_{23} & C_{33} & C_{34} & C_{35} & C_{36} \\ C_{14} & C_{24} & C_{34} & C_{44} & C_{45} & C_{46} \\ C_{15} & C_{25} & C_{35} & C_{45} & C_{55} & C_{56} \\ C_{16} & C_{26} & C_{36} & C_{46} & C_{56} & C_{66} \end{bmatrix}$$

Note that the above notation is as the same as the Voigt notation introduced in Equation A.39. However, they are not equal component-wise. Since in the rest of this thesis, we are going to use the simplified Kelvin notation, whenever an elasticity-matrix appears it should be understood that it is presented in simplified Kelvin notation and not Voigt.

We can write down the stress-strain relation by using the simplified Kelvin nota-

tion as

$$\begin{bmatrix} \sigma_1 \\ \sigma_2 \\ \sigma_3 \\ \sigma_4 \\ \sigma_5 \\ \sigma_6 \end{bmatrix} = \begin{bmatrix} C_{11} & C_{12} & C_{13} & C_{14} & C_{15} & C_{16} \\ C_{12} & C_{22} & C_{23} & C_{24} & C_{25} & C_{26} \\ C_{13} & C_{23} & C_{33} & C_{34} & C_{35} & C_{36} \\ C_{14} & C_{24} & C_{34} & C_{44} & C_{45} & C_{46} \\ C_{15} & C_{25} & C_{35} & C_{45} & C_{55} & C_{56} \\ C_{16} & C_{26} & C_{36} & C_{46} & C_{56} & C_{66} \end{bmatrix} \begin{bmatrix} \epsilon_1 \\ \epsilon_2 \\ \epsilon_3 \\ \epsilon_4 \\ \epsilon_5 \\ \epsilon_6 \end{bmatrix}. \tag{A.45}$$

In the main part of the thesis, we use the above elasticity matrix, which is represented in Kelvin notation, to study the symmetry classes of the elasticity tensor.

A.3.4 Obtaining the Orthogonal Transformation for the Elasticity Matrix

In this section, we derive the formula for obtaining the orthogonal transformation in 6D from its corresponding 3D transformation. Recall that in the previous section we represent the elasticity tensor by a 6×6 matrix. Thus, it becomes a second-rank tensor in 6D instead of a fourth-rank tensor in 3D.

Therefore, we should also convert an orthogonal transformation in 3D to a transformation in 6D in order to express the elasticity matrix in a different coordinate system. To do so, one should consider where the basis elements of a 6D-vector space are transformed by the orthogonal transformation in 3D. The basis elements of 6D-

vector space, where strain and stress tensors are defined, are

$$\begin{aligned}
\sigma_1 &:= (1,0,0,0,0,0),\\
\sigma_2 &:= (0,1,0,0,0,0),\\
\sigma_3 &:= (0,0,1,0,0,0),\\
\sigma_4 &:= (0,0,0,1,0,0),\\
\sigma_5 &:= (0,0,0,0,1,0),\\
\sigma_6 &:= (0,0,0,0,0,1).
\end{aligned}$$

Then, these elements are transformed by an orthogonal transformation in 6D by the following formula

$$\sigma_i' = \bar{A}\sigma_i, \text{ for any } i \in \{1,...,6\}, \tag{A.46}$$

where $\bar{A}$ is any orthogonal transformation in 6D, namely $\bar{A} \in SO(6)$. To find the entries of $\bar{A}$, we find where each of the σ_i is transformed by it. Then, the transformed element, namely σ_i' will become the *ith* column of the $\bar{A} \in SO(6)$.

First, let us consider σ_1. σ_1 represents a second-rank tensor which is represented by the following matrix

$$\begin{bmatrix} 1 & 0 & 0 \\ 0 & 0 & 0 \\ 0 & 0 & 0 \end{bmatrix}.$$

Thus, it is transformed according to the transformation-law which is represented in matrix notation in Equation 1.19 as

$$\sigma_1' = A\sigma_1 A^T.$$

Then, we can compute σ_1' in terms of the components of the orthogonal transformation

$A \in SO(3)$ as

$$\sigma_1' = \begin{bmatrix} A_{11} & A_{21} & A_{31} \\ A_{12} & A_{22} & A_{32} \\ A_{13} & A_{23} & A_{33} \end{bmatrix} \begin{bmatrix} 1 & 0 & 0 \\ 0 & 0 & 0 \\ 0 & 0 & 0 \end{bmatrix} \begin{bmatrix} A_{11} & A_{12} & A_{13} \\ A_{21} & A_{22} & A_{23} \\ A_{31} & A_{32} & A_{33} \end{bmatrix} \tag{A.47}$$

$$= \begin{bmatrix} A_{11}A_{11} & A_{11}A_{21} & A_{11}A_{31} \\ A_{11}A_{21} & A_{21}A_{21} & A_{21}A_{31} \\ A_{11}A_{31} & A_{21}A_{32} & A_{31}A_{31} \end{bmatrix}. \tag{A.48}$$

Since we denote the second-rank tensors in 3D as a vector in 6D, the transformed tensor can be written as

$$\sigma_1' = \begin{bmatrix} A_{11}A_{11} \\ A_{21}A_{21} \\ A_{31}A_{31} \\ \sqrt{2}A_{21}A_{31} \\ \sqrt{2}A_{11}A_{31} \\ \sqrt{2}A_{11}A_{21} \end{bmatrix}. \tag{A.49}$$

Note that we use the norm-preserving representation-mapping defined in Equation A.42 to change the second-rank tensor from its matrix representation to the vector representation. Thus, the first column of the $\bar{A}$ is σ_1'. Similarly, one can calculate the second and the third coloumn by transforming the basis vectors σ_2, σ_3, respectively.

To find the fourth column of $\bar{A}$, we use $\sigma_4 = (0, 0, 0, 1, 0, 0)$ which is equivalent in matrix notation to

$$\sigma = \begin{bmatrix} 0 & 0 & 0 \\ 0 & 0 & \frac{1}{\sqrt{2}} \\ 0 & \frac{1}{\sqrt{2}} & 0 \end{bmatrix},$$

since we use the norm-preserving representation-mapping defined in Equation A.42.

Then, using Equation A.47 for the tensor above, the fourth column turns out to be

$$\sigma' = \begin{bmatrix} \sqrt{2}A_{12}A_{13} \\ \sqrt{2}A_{22}A_{23} \\ \sqrt{2}A_{32}A_{33} \\ A_{22}A_{33} + A_{23}A_{32} \\ A_{12}A_{33} + A_{13}A_{32} \\ A_{12}A_{23} + A_{13}A_{22} \end{bmatrix}. \tag{A.50}$$

Analogously, we compute the fifth and the sixth column of $\bar{A}$ by evaluating σ'_5, σ'_6, respectively.

Now putting together the six columns of $\bar{A}$, we obtain

$$\bar{A} = \begin{bmatrix} A_{11}A_{11} & A_{12}A_{12} & A_{13}A_{13} & \sqrt{2}A_{12}A_{13} & \sqrt{2}A_{11}A_{13} & \sqrt{2}A_{11}A_{12} \\ A_{21}A_{21} & A_{22}A_{22} & A_{23}A_{23} & \sqrt{2}A_{22}A_{23} & \sqrt{2}A_{21}A_{23} & \sqrt{2}A_{21}A_{22} \\ A_{31}A_{31} & A_{32}A_{32} & A_{33}A_{33} & \sqrt{2}A_{32}A_{33} & \sqrt{2}A_{31}A_{33} & \sqrt{2}A_{31}A_{32} \\ \sqrt{2}A_{21}A_{31} & \sqrt{2}A_{22}A_{32} & \sqrt{2}A_{23}A_{33} & A_{22}A_{33} + A_{23}A_{32} & A_{21}A_{33} + A_{23}A_{31} & A_{21}A_{32} + A_{22}A_{31} \\ \sqrt{2}A_{11}A_{31} & \sqrt{2}A_{12}A_{32} & \sqrt{2}A_{13}A_{33} & A_{12}A_{33} + A_{13}A_{32} & A_{11}A_{33} + A_{13}A_{31} & A_{11}A_{32} + A_{12}A_{31} \\ \sqrt{2}A_{11}A_{21} & \sqrt{2}A_{12}A_{22} & \sqrt{2}A_{13}A_{23} & A_{12}A_{23} + A_{13}A_{22} & A_{11}A_{23} + A_{13}A_{21} & A_{11}A_{22} + A_{12}A_{21} \end{bmatrix}.$$

By using the 6×6 rotation transformation matrix, namely $\bar{A}$ which is expressed above, we can find the transformed elasticity tensor. In Section 1.2, we have introduced the transformation law for a fourth-rank tensor in Equation 1.20. However, we are working with a 6×6-elasticity matrix, which is a second-rank tensor in 6D instead of a fourth-rank tensor in 3D. Thus, we use the transformation law, which is expressed in the matrix form in Equation 1.19, for the second-rank tensors. Namely, the transformed elasticity matrix is achieved by the following formula

$$C' = \bar{A}^T C \bar{A}, \tag{A.51}$$

where $\bar{A}$ is the 6×6 orthogonal transformation matrix, C' and C are the elasticity matrices represented in the transformed and original coordinates, respectively.

A.4 Maple Codes

In this appendix, we present the codes that are used throughout the thesis.

Plotting the Monoclinic- and TI-distance Functions

We introduce the packages that are going to be used in the code.

```
restart;
with(LinearAlgebra);
with(Optimization);
```

The rotation matrix that transforms $\mathbf{e_3}$ to the new z-axis.

```
AEuler := Matrix([[cos(psi), -sin(psi), 0], [sin(psi), cos(psi), 0], [0, 0, 1]]).
Matrix([[1, 0, 0], [0, cos(phi), -sin(phi)], [0, sin(phi), cos(phi)]]));
```

We do not take into account of the locations of x-axis and y-axis since for TI- and monoclinic-distance functions their orientation does not change the result.

```
Rot := IdentityMatrix(3);
A := Rot. AEuler;
```

Expressing $A \in SO(3)$ in 6D since it is going to act on the elasticity tensor.

```
Atilde := simplify(Matrix([[A[1, 1]^2, A[1, 2]^2, A[1, 3]^2, sqrt(2)*A[1, 2]*A[1, 3],
sqrt(2)*A[1, 1]*A[1, 3], sqrt(2)*A[1, 1]*A[1, 2]], [A[2, 1]^2, A[2, 2]^2, A[2, 3]^2,
sqrt(2)*A[2, 2]*A[2, 3], sqrt(2)*A[2, 1]*A[2, 3], sqrt(2)*A[2, 1]*A[2, 2]],
[A[3, 1]^2, A[3, 2]^2, A[3, 3]^2, sqrt(2)*A[3, 2]*A[3, 3], sqrt(2)*A[3, 1]
*A[3, 3], sqrt(2)*A[3, 1]*A[3, 2]], [sqrt(2)*A[2, 1]*A[3, 1], sqrt(2)*A[2, 2]*A[3, 2],
sqrt(2)*A[2, 3]*A[3, 3], A[2, 3]*A[3, 2]+A[2, 2]*A[3, 3], A[2, 3]*A[3, 1]+
A[2, 1]*A[3, 3], A[2, 2]*A[3, 1]+A[2, 1]*A[3, 2]], [sqrt(2)*A[1, 1]*A[3, 1],
sqrt(2)*A[1, 2]*A[3, 2], sqrt(2)*A[1, 3]*A[3, 3], A[1, 3]*A[3, 2]+A[1, 2]*A[3, 3],
A[1, 3]*A[3, 1]+A[1, 1]*A[3, 3], A[1, 2]*A[3, 1]+A[1, 1]*A[3, 2]],
[sqrt(2)*A[1, 1]*A[2, 1], sqrt(2)*A[1, 2]*A[2, 2], sqrt(2)*A[1, 3]*A[2, 3],
A[1, 3]*A[2, 2]+A[1, 2]*A[2, 3], A[1, 3]*A[2, 1]+A[1, 1]*A[2, 3], A[1, 2]*A[2, 1]+
A[1, 1]*A[2, 2]]])):
```

Introducing the elasticity matrix C in its general form.

```
C := Matrix(6, symbol = c, shape = symmetric);
```

This line is for changing the Voigt notation to Kelvin or vice versa. Herein, since we represent it in Kelvin notation, we do not change anything.

```
C[1 .. 3, 4 .. 6] := C[1 .. 3, 4 .. 6];
C[4 .. 6, 4 .. 6] := C[4 .. 6, 4 .. 6];
```

Introducing the parameters of elasticity matrix.

```
c := Matrix(6, 6, {(1, 1) = 42.03357978, (1, 2) = 32.49305220,
(1, 3) = 26.42291512, (1, 4) = 5.799531000, (1, 5) = 9.938160420,
(1, 6) = 21.33549018, (2, 1) = 32.49305219, (2, 2) = 36.72218489,
(2, 3) = 34.84774953, (2, 4) = -5.221667422, (2, 5) = -35.36967653,
(2, 6) = -23.60019509, (3, 1) = 26.42291511, (3, 2) = 34.84774954,
(3, 3) = 31.71680164, (3, 4) = 12.16688779, (3, 5) = 3.767088965,
(3, 6) = 10.24209672, (4, 1) = 5.799531000, (4, 2) = -5.221667442,
(4, 3) = 12.16688780, (4, 4) = 32.84181099, (4, 5) = 20.98631307,
(4, 6) = 2.36291613, (5, 1) = 9.938160440, (5, 2) = -35.36967653,
(5, 3) = 3.767088965, (5, 4) = 20.98631308, (5, 5) = -22.64105584,
(5, 6) = -9.709913499, (6, 1) = 21.33549018, (6, 2) = -23.60019510,
(6, 3) = 10.24209672, (6, 4) = 2.36291613, (6, 5) = -9.709913499,
(6, 6) = 11.32667859});
```

Expressing the elasticity matrix C in all coordinate systems by rotating it with a generic orthogonal transformation that is introduced in the above lines.

```
R := evalf((Transpose(Atilde).C.Atilde);
```

Evaluating the monoclinic-distance function, namely $d(Atilde^T C Atilde, \mathcal{L}^{mono})$

```
Dist := simplify(2*(R[1, 4]^2+R[1, 5]^2+R[2, 4]^2+R[2, 5]^2+R[3, 4]^2+
R[3, 5]^2+R[4, 6]^2+R[5, 6]^2));
```

Evaluating the TI-distance function, namely $d(Atilde^T C Atilde, \mathcal{L}^{TI})$

```
Delta := $simplify(R[1, 1]^2+R[2, 2]^2+R[3, 3]^2+R[4, 4]^2+R[5, 5]^2+R[6, 6]^2+
2*(R[1, 2]^2+R[1, 3]^2+R[2, 3]^2+R[1, 6]^2+R[2, 6]^2+R[3, 6]^2+R[4, 5]^2+
R[1, 4]^2+R[1, 5]^2+R[2, 4]^2+R[2, 5]^2+R[3, 4]^2+R[3, 5]^2+R[4, 6]^2+
R[5, 6]^2)-(3/8)*R[1, 1]^2-(3/2)*R[1, 2]^2-R[1, 3]^2-(3/8)*R[2, 2]^2-
2*R[1, 3]*R[2, 3]-R[2, 3]^2-R[3, 3]^2-(1/2)*R[4, 4]^2-R[4, 4]*R[5, 5]-
(1/2)*R[5, 5]^2-(1/2)*R[1, 2]*(R[2, 2]-2*R[6, 6])-(1/2)*R[2, 2]*R[6, 6]-
(1/2)*R[6, 6]^2-R[1, 1]*((1/2)*R[1, 2]+(3/4)*R[2, 2]+(1/2)*R[6, 6]));
```

Plotting the function Dist onto the surface of a sphere.

```
plot3d([sin(phi)*cos(psi-(1/2)*Pi), sin(phi)*sin(psi-(1/2)*Pi), cos(phi)],
phi = 0 .. Pi, psi = (1/2)*Pi .. 2*Pi+(1/2)*Pi, style = patchnogrid, color = Dist,
axes = normal);
```

Plotting the function Delta onto the surface of a sphere.

```
plot3d([sin(phi)*cos(psi-(1/2)*Pi), sin(phi)*sin(psi-(1/2)*Pi), cos(phi)],
phi = 0 .. Pi, psi = (1/2)*Pi .. 2*Pi+(1/2)*Pi, style = patchnogrid, color = Delta,
axes = normal);
```

Naming the 3D plot as S1.

```
S1 := %
```

Introducing the transformations that maps Euler angles onto the surface of the sphere

```
u :=  (phi, psi)→ sin(phi)*cos(psi-(1/2)*Pi):
v :=  (phi, psi)→ sin(phi)*sin(psi-(1/2)*Pi):
w :=  (phi, psi)→ cos(phi):
```

Plotting Packages

```
with(plots);
with(plottools);
```

Plotting the contours of the function Dist on a plane.

```
T1 := transform((phi, psi) →  [u(phi, psi), v(phi, psi), w(phi, psi)] ;

contourplot(Dist, phi = 0 .. Pi, psi = (1/2)*Pi .. 2*Pi+(1/2)*Pi, color = black,
grid = [100, 100]);
```

Naming the contour plot as A1.

```
A1 := %
```

Displaying the 3D plot with the contours

```
display(S1, T1(A1));
```

In order to find a local minima ,which may be observed from the plot, around some neighborhood, one should use the line:

```
Min_data := Minimize(Dist, phi = 30*(1/180)*Pi .. 50*(1/180)*Pi,
psi = (1/180)*(90-44)*Pi .. (1/180)*(90-24)*Pi);
```

Now, we present the code that evaluates the orthotropic-, tetragonal-, trigonal-distance functions around some neighborhood. Moreover, we present the sum of monoclinic-distance functions along some particular directions for orthotropic, tetragonal, trigonal symmetries. Thus, one can compare the results of these functions and determine how close they are.

Orthotropic-distance function

```
restart;
with(LinearAlgebra);
with(Optimization);
```

The rotation matrix that transforms $\mathbf{e}_3$ to the new z-axis.

```
AEuler := Matrix([[cos(psi), -sin(psi), 0], [sin(psi), cos(psi), 0], [0, 0, 1]]).
Matrix([[1, 0, 0], [0, cos(phi), -sin(phi)], [0, sin(phi), cos(phi)]]));
```

Since the orientations of x-axis and y-axis matter when calculating the distance of C to orthotropic symmetry in some coordinate system, we should multiply AEuler with another elementary transformation. This elementary transformation determines the orientations of x-axis and y-axis.

```
Rot := Matrix([[cos(theta), -sin(theta), 0], [sin(theta), cos(theta), 0], [0, 0, 1]]);
A := AEuler.Rot.;
```

Expressing $A \in SO(3)$ in 6D since it is going to act on the elasticity tensor.

```
Atilde := simplify(Matrix([[A[1, 1]^2, A[1, 2]^2, A[1, 3]^2, sqrt(2)*A[1, 2]*A[1, 3],
sqrt(2)*A[1, 1]*A[1, 3], sqrt(2)*A[1, 1]*A[1, 2]], [A[2, 1]^2, A[2, 2]^2, A[2, 3]^2,
sqrt(2)*A[2, 2]*A[2, 3], sqrt(2)*A[2, 1]*A[2, 3], sqrt(2)*A[2, 1]*A[2, 2]],
[A[3, 1]^2, A[3, 2]^2, A[3, 3]^2, sqrt(2)*A[3, 2]*A[3, 3], sqrt(2)*A[3, 1]
*A[3, 3], sqrt(2)*A[3, 1]*A[3, 2]], [sqrt(2)*A[2, 1]*A[3, 1], sqrt(2)*A[2, 2]*A[3, 2],
sqrt(2)*A[2, 3]*A[3, 3], A[2, 3]*A[3, 2]+A[2, 2]*A[3, 3], A[2, 3]*A[3, 1]+
A[2, 1]*A[3, 3], A[2, 2]*A[3, 1]+A[2, 1]*A[3, 2]], [sqrt(2)*A[1, 1]*A[3, 1],
sqrt(2)*A[1, 2]*A[3, 2], sqrt(2)*A[1, 3]*A[3, 3], A[1, 3]*A[3, 2]+A[1, 2]*A[3, 3],
A[1, 3]*A[3, 1]+A[1, 1]*A[3, 3], A[1, 2]*A[3, 1]+A[1, 1]*A[3, 2]],
[sqrt(2)*A[1, 1]*A[2, 1], sqrt(2)*A[1, 2]*A[2, 2], sqrt(2)*A[1, 3]*A[2, 3],
A[1, 3]*A[2, 2]+A[1, 2]*A[2, 3], A[1, 3]*A[2, 1]+A[1, 1]*A[2, 3], A[1, 2]*A[2, 1]+
A[1, 1]*A[2, 2]]])):
```

Introducing the elasticity matrix C in its general form.

```
C := Matrix(6, symbol = c, shape = symmetric);
```

This line is for changing the Voigt notation to Kelvin or vice versa. Herein, since we represent it in Kelvin notation, we do not change anything.

```
C[1 .. 3, 4 .. 6] := C[1 .. 3, 4 .. 6];
C[4 .. 6, 4 .. 6] := C[4 .. 6, 4 .. 6];
```

Introducing the parameters of elasticity matrix.

```
c := Matrix(6, 6, {(1, 1) = 42.03357978, (1, 2) = 32.49305220,
(1, 3) = 26.42291512, (1, 4) = 5.799531000, (1, 5) = 9.938160420,
(1, 6) = 21.33549018, (2, 1) = 32.49305219, (2, 2) = 36.72218489,
(2, 3) = 34.84774953, (2, 4) = -5.221667422, (2, 5) = -35.36967653,
(2, 6) = -23.60019509, (3, 1) = 26.42291511, (3, 2) = 34.84774954,
(3, 3) = 31.71680164, (3, 4) = 12.16688779, (3, 5) = 3.767088965,
(3, 6) = 10.24209672, (4, 1) = 5.799531000, (4, 2) = -5.221667442,
```

```
(4, 3) = 12.16688780, (4, 4) = 32.84181099, (4, 5) = 20.98631307,
(4, 6) = 2.36291613, (5, 1) = 9.938160440, (5, 2) = -35.36967653,
(5, 3) = 3.767088965, (5, 4) = 20.98631308, (5, 5) = -22.64105584,
(5, 6) = -9.709913499, (6, 1) = 21.33549018, (6, 2) = -23.60019510,
(6, 3) = 10.24209672, (6, 4) = 2.36291613, (6, 5) = -9.709913499,
(6, 6) = 11.32667859});
```

Expressing the elasticity matrix C in all coordinate systems by rotating it with a generic orthogonal transformation that is introduced in the above lines.

```
R := evalf((Transpose(Atilde).C.Atilde);
```

Evaluating the orthotropic-distance function, namely $d(Atilde^T C Atilde, \mathcal{L}^{ortho})$. Note that this function cannot be plotted because it is a 4-dimensional function.

```
Delta-ortho := evalf(2*(R[1, 4]^2+R[1, 5]^2+R[1, 6]^2+R[2, 4]^2+R[2, 5]^2+
R[2, 6]^2+R[3, 4]^2+R[3, 5]^2+R[3, 6]^2+R[4, 5]^2+R[4, 6]^2+R[5, 6]^2));
```

In order to find a local minima ,which may be observed from the plot of the monoclinic distance function, around some neighborhood, one should use the line:

```
Min_data := Minimize(Delta-ortho, phi = 30*(1/180)*Pi .. 50*(1/180)*Pi,
psi = (1/180)*(90-44)*Pi .. (1/180)*(90-24)*Pi);
```

Sum of monoclinic-distance functions along the normals of the mirror planes of orthotropic symmetry

```
restart;
with(LinearAlgebra);
with(Optimization);
```

The rotation matrix that transforms $\mathbf{e_3}$ to the new z-axis.

```
AEuler := Matrix([[cos(psi), -sin(psi), 0], [sin(psi), cos(psi), 0], [0, 0, 1]]).
Matrix([[1, 0, 0], [0, cos(phi), -sin(phi)], [0, sin(phi), cos(phi)]]));
```

Since the orientations of x-axis and y-axis matter when calculating the distance of C to orthotropic symmetry in some coordinate system, we should multiply AEuler with another elementary transformation. This elementary transformation determines the orientations of x-axis and y-axis.

```
Rot := Matrix([[cos(theta), -sin(theta), 0], [sin(theta), cos(theta), 0], [0, 0, 1]]);
A := AEuler.Rot.;
```

Expressing $A \in SO(3)$ in 6D since it is going to act on the elasticity tensor.

```
Atilde := simplify(Matrix([[A[1, 1]^2, A[1, 2]^2, A[1, 3]^2, sqrt(2)*A[1, 2]*A[1, 3],
sqrt(2)*A[1, 1]*A[1, 3], sqrt(2)*A[1, 1]*A[1, 2]], [A[2, 1]^2, A[2, 2]^2, A[2, 3]^2,
sqrt(2)*A[2, 2]*A[2, 3], sqrt(2)*A[2, 1]*A[2, 3], sqrt(2)*A[2, 1]*A[2, 2]],
[A[3, 1]^2, A[3, 2]^2, A[3, 3]^2, sqrt(2)*A[3, 2]*A[3, 3], sqrt(2)*A[3, 1]
*A[3, 3], sqrt(2)*A[3, 1]*A[3, 2]], [sqrt(2)*A[2, 1]*A[3, 1], sqrt(2)*A[2, 2]*A[3, 2],
sqrt(2)*A[2, 3]*A[3, 3], A[2, 3]*A[3, 2]+A[2, 2]*A[3, 3], A[2, 3]*A[3, 1]+
A[2, 1]*A[3, 3], A[2, 2]*A[3, 1]+A[2, 1]*A[3, 2]], [sqrt(2)*A[1, 1]*A[3, 1],
sqrt(2)*A[1, 2]*A[3, 2], sqrt(2)*A[1, 3]*A[3, 3], A[1, 3]*A[3, 2]+A[1, 2]*A[3, 3],
A[1, 3]*A[3, 1]+A[1, 1]*A[3, 3], A[1, 2]*A[3, 1]+A[1, 1]*A[3, 2]],
[sqrt(2)*A[1, 1]*A[2, 1], sqrt(2)*A[1, 2]*A[2, 2], sqrt(2)*A[1, 3]*A[2, 3],
A[1, 3]*A[2, 2]+A[1, 2]*A[2, 3], A[1, 3]*A[2, 1]+A[1, 1]*A[2, 3], A[1, 2]*A[2, 1]+
A[1, 1]*A[2, 2]]])):
```

Introducing the elasticity matrix C in its general form.

```
C := Matrix(6, symbol = c, shape = symmetric);
```

This line is for changing the Voigt notation to Kelvin or vice versa. Herein, since we represent it in Kelvin notation, we do not change anything.

```
C[1 .. 3, 4 .. 6] := C[1 .. 3, 4 .. 6];
C[4 .. 6, 4 .. 6] := C[4 .. 6, 4 .. 6];
```

Introducing the parameters of elasticity matrix.

```
c := Matrix(6, 6, {(1, 1) = 42.03357978, (1, 2) = 32.49305220,
(1, 3) = 26.42291512, (1, 4) = 5.799531000, (1, 5) = 9.938160420,
```

```
(1, 6) = 21.33549018, (2, 1) = 32.49305219, (2, 2) = 36.72218489,
(2, 3) = 34.84774953, (2, 4) = -5.221667422, (2, 5) = -35.36967653,
(2, 6) = -23.60019509, (3, 1) = 26.42291511, (3, 2) = 34.84774954,
(3, 3) = 31.71680164, (3, 4) = 12.16688779, (3, 5) = 3.767088965,
(3, 6) = 10.24209672, (4, 1) = 5.799531000, (4, 2) = -5.221667442,
(4, 3) = 12.16688780, (4, 4) = 32.84181099, (4, 5) = 20.98631307,
(4, 6) = 2.36291613, (5, 1) = 9.938160440, (5, 2) = -35.36967653,
(5, 3) = 3.767088965, (5, 4) = 20.98631308, (5, 5) = -22.64105584,
(5, 6) = -9.709913499, (6, 1) = 21.33549018, (6, 2) = -23.60019510,
(6, 3) = 10.24209672, (6, 4) = 2.36291613, (6, 5) = -9.709913499,
(6, 6) = 11.32667859});
```

Expressing the elasticity matrix C in all coordinate systems by rotating it with a generic orthogonal transformation that is introduced in the above lines.

```
R := evalf(Transpose(Atilde).C.Atilde);
```

This line evaluates the distance of C to monoclinic along the z-axis of the rotated C:

```
Dist := evalf(2*(R[1, 4]^2+R[1, 5]^2+R[2, 4]^2+R[2, 5]^2+R[3, 4]^2+R[3, 5]^2
+R[4, 6]^2+R[5, 6]^2)):
```

In order to rotate the z-axis of C to the x-axis, we introduce 90° rotation:

```
ninetyx := Matrix([[0, 0, 1], [0, 1, 0], [-1, 0, 0]]);
Ax := A.ninetyx;
```

Expressing the above orthogonal transformation in 6D so that it acts the elasticity tensor

```
Atildex := simplify(Matrix([[Ax[1, 1]^2, Ax[1, 2]^2, Ax[1, 3]^2, sqrt(2)*
Ax[1, 2]*Ax[1, 3], sqrt(2)*Ax[1, 1]*Ax[1, 3], sqrt(2)*Ax[1, 1]*Ax[1, 2]],
[Ax[2, 1]^2, Ax[2, 2]^2, Ax[2, 3]^2, sqrt(2)*Ax[2, 2]*Ax[2, 3], sqrt(2)*
Ax[2, 1]*Ax[2, 3], sqrt(2)*Ax[2, 1]*Ax[2, 2]], [Ax[3, 1]^2, Ax[3, 2]^2,
Ax[3, 3]^2, sqrt(2)*Ax[3, 2]*Ax[3, 3], sqrt(2)*Ax[3, 1]*Ax[3, 3], sqrt(2)*
Ax[3, 1]*Ax[3, 2]], [sqrt(2)*Ax[2, 1]*Ax[3, 1], sqrt(2)*Ax[2, 2]*Ax[3, 2],
```

```
sqrt(2)*Ax[2, 3]*Ax[3, 3], Ax[2, 3]*Ax[3, 2]+Ax[2, 2]*Ax[3, 3], Ax[2, 3]*
Ax[3, 1]+Ax[2, 1]*Ax[3, 3], Ax[2, 2]*Ax[3, 1]+Ax[2, 1]*Ax[3, 2]],
[sqrt(2)*Ax[1, 1]*Ax[3, 1], sqrt(2)*Ax[1, 2]*Ax[3, 2], sqrt(2)*Ax[1, 3]*Ax[3, 3],
Ax[1, 3]*Ax[3, 2]+Ax[1, 2]*Ax[3, 3], Ax[1, 3]*Ax[3, 1]+Ax[1, 1]*Ax[3, 3],
Ax[1, 2]*Ax[3, 1]+Ax[1, 1]*Ax[3, 2]], [sqrt(2)*Ax[1, 1]*Ax[2, 1],
sqrt(2)*Ax[1, 2]*Ax[2, 2], sqrt(2)*Ax[1, 3]*Ax[2, 3], Ax[1, 3]*Ax[2, 2]+
Ax[1, 2]*Ax[2, 3], Ax[1, 3]*Ax[2, 1]+Ax[1, 1]*Ax[2, 3], Ax[1, 2]*Ax[2, 1]+
Ax[1, 1]*Ax[2, 2]]])):
```

Atildex acts the elasticity matrix in order to express it in a coordinate system where its new z-axis is the x-axis.

```
Rx := evalf(Transpose(Atildex).C.Atildex);
```

This line evaluates the distance of C to monoclinic along the x-axis of the rotated C:

```
Distx := evalf(2*(Rx[1, 4]^2+Rx[1, 5]^2+Rx[2, 4]^2+Rx[2, 5]^2+
Rx[3, 4]^2+Rx[3, 5]^2+Rx[4, 6]^2+Rx[5, 6]^2)):
```

Now, we repeat the same procedure for y-axis:

```
ninetyy := Matrix([[1, 0, 0], [0, 0, 1], [0, -1, 0]]):
Ay := A.ninetyy;

Atildey := simplify(Matrix([[Ay[1, 1]^2, Ay[1, 2]^2, Ay[1, 3]^2,
sqrt(2)*Ay[1, 2]*Ay[1, 3], sqrt(2)*Ay[1, 1]*Ay[1, 3], sqrt(2)*Ay[1, 1]*
Ay[1, 2]], [Ay[2, 1]^2, Ay[2, 2]^2, Ay[2, 3]^2, sqrt(2)*Ay[2, 2]*Ay[2, 3],
sqrt(2)*Ay[2, 1]*Ay[2, 3], sqrt(2)*Ay[2, 1]*Ay[2, 2]], [Ay[3, 1]^2,
Ay[3, 2]^2, Ay[3, 3]^2, sqrt(2)*Ay[3, 2]*Ay[3, 3], sqrt(2)*Ay[3, 1]*Ay[3, 3],
sqrt(2)*Ay[3, 1]*Ay[3, 2]], [sqrt(2)*Ay[2, 1]*Ay[3, 1], sqrt(2)*Ay[2, 2]*
Ay[3, 2], sqrt(2)*Ay[2, 3]*Ay[3, 3], Ay[2, 3]*Ay[3, 2]+Ay[2, 2]*Ay[3, 3],
Ay[2, 3]*Ay[3, 1]+Ay[2, 1]*Ay[3, 3], Ay[2, 2]*Ay[3, 1]+Ay[2, 1]*Ay[3, 2]],
[sqrt(2)*Ay[1, 1]*Ay[3, 1], sqrt(2)*Ay[1, 2]*Ay[3, 2], sqrt(2)*Ay[1, 3]*
Ay[3, 3], Ay[1, 3]*Ay[3, 2]+Ay[1, 2]*Ay[3, 3], Ay[1, 3]*Ay[3, 1]+Ay[1, 1]*
Ay[3, 3], Ay[1, 2]*Ay[3, 1]+Ay[1, 1]*Ay[3, 2]], [sqrt(2)*Ay[1, 1]*Ay[2, 1],
```

```
sqrt(2)*Ay[1, 2]*Ay[2, 2], sqrt(2)*Ay[1, 3]*Ay[2, 3], Ay[1, 3]*Ay[2, 2]+
Ay[1, 2]*Ay[2, 3], Ay[1, 3]*Ay[2, 1]+Ay[1, 1]*Ay[2, 3], Ay[1, 2]*Ay[2, 1]
+Ay[1, 1]*Ay[2, 2]]]));

Ry := evalf(Transpose(Atildey).C.Atildey);
Disty := evalf(2*(Ry[1, 4]^2+Ry[1, 5]^2+Ry[2, 4]^2+Ry[2, 5]^2+Ry[3, 4]^2+
Ry[3, 5]^2+Ry[4, 6]^2+Ry[5, 6]^2));
```

Evaluating the sum of monoclinic-distance functions along the three perpendicular directions which are aligned with the coordinate axes:

```
Distall := Dist+Distx+Disty
```

For minimizing the Distall function around some restricted region

```
Mindata := Minimize(Distall, phi= 0. .. 10*(1/180)*Pi,
psi = (1/2)*Pi .. 2*Pi+(1/2)*Pi, theta = 0 .. 2*Pi)
```

Tetragonal-distance function

```
restart;
with(LinearAlgebra);
with(Optimization);
```

The rotation matrix that transforms $\mathbf{e_3}$ to the new z-axis.

```
AEuler := Matrix([[cos(psi), -sin(psi), 0], [sin(psi), cos(psi), 0], [0, 0, 1]]).
Matrix([[1, 0, 0], [0, cos(phi), -sin(phi)], [0, sin(phi), cos(phi)]]));
```

Since the orientations of x-axis and y-axis matter when calculating the distance of C to orthotropic symmetry in some coordinate system, we should multiply AEuler with another elementary transformation. This elementary transformation determines the orientations of x-axis and y-axis.

```
Rot := Matrix([[cos(theta), -sin(theta), 0], [sin(theta), cos(theta), 0], [0, 0, 1]]);
A := AEuler.Rot.;
```

Expressing $A \in SO(3)$ in 6D since it is going to act on the elasticity tensor.

```
Atilde := simplify(Matrix([[A[1, 1]^2, A[1, 2]^2, A[1, 3]^2, sqrt(2)*A[1, 2]*A[1, 3],
sqrt(2)*A[1, 1]*A[1, 3], sqrt(2)*A[1, 1]*A[1, 2]], [A[2, 1]^2, A[2, 2]^2, A[2, 3]^2,
sqrt(2)*A[2, 2]*A[2, 3], sqrt(2)*A[2, 1]*A[2, 3], sqrt(2)*A[2, 1]*A[2, 2]],
[A[3, 1]^2, A[3, 2]^2, A[3, 3]^2, sqrt(2)*A[3, 2]*A[3, 3], sqrt(2)*A[3, 1]
*A[3, 3], sqrt(2)*A[3, 1]*A[3, 2]], [sqrt(2)*A[2, 1]*A[3, 1], sqrt(2)*A[2, 2]*A[3, 2],
sqrt(2)*A[2, 3]*A[3, 3], A[2, 3]*A[3, 2]+A[2, 2]*A[3, 3], A[2, 3]*A[3, 1]+
A[2, 1]*A[3, 3], A[2, 2]*A[3, 1]+A[2, 1]*A[3, 2]], [sqrt(2)*A[1, 1]*A[3, 1],
sqrt(2)*A[1, 2]*A[3, 2], sqrt(2)*A[1, 3]*A[3, 3], A[1, 3]*A[3, 2]+A[1, 2]*A[3, 3],
A[1, 3]*A[3, 1]+A[1, 1]*A[3, 3], A[1, 2]*A[3, 1]+A[1, 1]*A[3, 2]],
[sqrt(2)*A[1, 1]*A[2, 1], sqrt(2)*A[1, 2]*A[2, 2], sqrt(2)*A[1, 3]*A[2, 3],
A[1, 3]*A[2, 2]+A[1, 2]*A[2, 3], A[1, 3]*A[2, 1]+A[1, 1]*A[2, 3], A[1, 2]*A[2, 1]+
A[1, 1]*A[2, 2]]])):
```

Introducing the elasticity matrix C in its general form.

```
C := Matrix(6, symbol = c, shape = symmetric);
```

This line is for changing the Voigt notation to Kelvin or vice versa. Herein, since we represent it in Kelvin notation, we do not change anything.

```
C[1 .. 3, 4 .. 6] := C[1 .. 3, 4 .. 6];
C[4 .. 6, 4 .. 6] := C[4 .. 6, 4 .. 6];
```

Introducing the parameters of elasticity matrix.

```
c := Matrix(6, 6, {(1, 1) = 42.03357978, (1, 2) = 32.49305220,
(1, 3) = 26.42291512, (1, 4) = 5.799531000, (1, 5) = 9.938160420,
(1, 6) = 21.33549018, (2, 1) = 32.49305219, (2, 2) = 36.72218489,
(2, 3) = 34.84774953, (2, 4) = -5.221667422, (2, 5) = -35.36967653,
(2, 6) = -23.60019509, (3, 1) = 26.42291511, (3, 2) = 34.84774954,
(3, 3) = 31.71680164, (3, 4) = 12.16688779, (3, 5) = 3.767088965,
(3, 6) = 10.24209672, (4, 1) = 5.799531000, (4, 2) = -5.221667442,
(4, 3) = 12.16688780, (4, 4) = 32.84181099, (4, 5) = 20.98631307,
(4, 6) = 2.36291613, (5, 1) = 9.938160440, (5, 2) = -35.36967653,
(5, 3) = 3.767088965, (5, 4) = 20.98631308, (5, 5) = -22.64105584,
(5, 6) = -9.709913499, (6, 1) = 21.33549018, (6, 2) = -23.60019510,
```

```
(6, 3) = 10.24209672, (6, 4) = 2.36291613, (6, 5) = -9.709913499,
(6, 6) = 11.32667859});
```

Expressing the elasticity matrix C in all coordinate systems by rotating it with a generic orthogonal transformation that is introduced in the above lines.

```
R := evalf((Transpose(Atilde).C.Atilde);
```

Introducing the symmetry group of tetragonal class for taking the projection of an elasticity tensor onto the tetragonal space

```
Me3 := Matrix([[1, 0, 0], [0, 1, 0], [0, 0, -1]]);
Me2 := Matrix([[1, 0, 0], [0, -1, 0], [0, 0, 1]]);
Me1 := Matrix([[-1, 0, 0], [0, 1, 0], [0, 0, 1]]);
Meff := Matrix([[0, -1, 0], [-1, 0, 0], [0, 0, 1]]);
Mehff := Matrix([[0, 1, 0], [1, 0, 0], [0, 0, 1]]);
Mcomb1 := Matrix([[0, -1, 0], [1, 0, 0], [0, 0, 1]]);
Mcomb2 := Matrix([[0, 1, 0], [-1, 0, 0], [0, 0, 1]]);
```

Expressing the above orthogonal transformations in 6D

```
Me3tilde := simplify(Matrix([[Me3[1, 1]^2, Me3[1, 2]^2, Me3[1, 3]^2,
sqrt(2)*Me3[1, 2]*Me3[1, 3], sqrt(2)*Me3[1, 1]*Me3[1, 3],
sqrt(2)*Me3[1, 1]*Me3[1, 2]], [Me3[2, 1]^2, Me3[2, 2]^2, Me3[2, 3]^2,
sqrt(2)*Me3[2, 2]*Me3[2, 3], sqrt(2)*Me3[2, 1]*Me3[2, 3], sqrt(2)*
Me3[2, 1]*Me3[2, 2]], [Me3[3, 1]^2, Me3[3, 2]^2, Me3[3, 3]^2, sqrt(2)*
Me3[3, 2]*Me3[3, 3], sqrt(2)*Me3[3, 1]*Me3[3, 3], sqrt(2)*Me3[3, 1]*
Me3[3, 2]], [sqrt(2)*Me3[2, 1]*Me3[3, 1], sqrt(2)*Me3[2, 2]*Me3[3, 2],
sqrt(2)*Me3[2, 3]*Me3[3, 3], Me3[2, 3]*Me3[3, 2]+Me3[2, 2]*Me3[3, 3],
Me3[2, 3]*Me3[3, 1]+Me3[2, 1]*Me3[3, 3], Me3[2, 2]*Me3[3, 1]+
Me3[2, 1]*Me3[3, 2]], [sqrt(2)*Me3[1, 1]*Me3[3, 1], sqrt(2)*Me3[1, 2]*
Me3[3, 2], sqrt(2)*Me3[1, 3]*Me3[3, 3], Me3[1, 3]*Me3[3, 2]+Me3[1, 2]*
Me3[3, 3], Me3[1, 3]*Me3[3, 1]+Me3[1, 1]*Me3[3, 3], Me3[1, 2]*
Me3[3, 1]+Me3[1, 1]*Me3[3, 2]], [sqrt(2)*Me3[1, 1]*Me3[2, 1], sqrt(2)
*Me3[1, 2]*Me3[2, 2], sqrt(2)*Me3[1, 3]*Me3[2, 3], Me3[1, 3]*Me3[2, 2]+
Me3[1, 2]*Me3[2, 3], Me3[1, 3]*Me3[2, 1]+Me3[1, 1]*Me3[2, 3],
Me3[1, 2]*Me3[2, 1]+Me3[1, 1]*Me3[2, 2]]]));
```

```
Me2tilde := simplify(Matrix([[Me2[1, 1]^2, Me2[1, 2]^2, Me2[1, 3]^2,
sqrt(2)*Me2[1, 2]*Me2[1, 3], sqrt(2)*Me2[1, 1]*Me2[1, 3],
sqrt(2)*Me2[1, 1]*Me2[1, 2]], [Me2[2, 1]^2, Me2[2, 2]^2, Me2[2, 3]^2,
sqrt(2)*Me2[2, 2]*Me2[2, 3], sqrt(2)*Me2[2, 1]*Me2[2, 3],
sqrt(2)*Me2[2, 1]*Me2[2, 2]], [Me2[3, 1]^2, Me2[3, 2]^2, Me2[3, 3]^2,
sqrt(2)*Me2[3, 2]*Me2[3, 3], sqrt(2)*Me2[3, 1]*Me2[3, 3],
sqrt(2)*Me2[3, 1]*Me2[3, 2]], [sqrt(2)*Me2[2, 1]*Me2[3, 1], sqrt(2)*
Me2[2, 2]*Me2[3, 2], sqrt(2)*Me2[2, 3]*Me2[3, 3], Me2[2, 3]*
Me2[3, 2]+Me2[2, 2]*Me2[3, 3], Me2[2, 3]*Me2[3, 1]+Me2[2, 1]*
Me2[3, 3], Me2[2, 2]*Me2[3, 1]+Me2[2, 1]*Me2[3, 2]], [sqrt(2)*
Me2[1, 1]*Me2[3, 1], sqrt(2)*Me2[1, 2]*Me2[3, 2], sqrt(2)*
Me2[1, 3]*Me2[3, 3], Me2[1, 3]*Me2[3, 2]+Me2[1, 2]*Me2[3, 3],
Me2[1, 3]*Me2[3, 1]+Me2[1, 1]*Me2[3, 3], Me2[1, 2]*Me2[3, 1]+
Me2[1, 1]*Me2[3, 2]], [sqrt(2)*Me2[1, 1]*Me2[2, 1], sqrt(2)*Me2[1, 2]*
Me2[2, 2], sqrt(2)*Me2[1, 3]*Me2[2, 3], Me2[1, 3]*Me2[2, 2]+
Me2[1, 2]*Me2[2, 3], Me2[1, 3]*Me2[2, 1]+Me2[1, 1]*Me2[2, 3],
Me2[1, 2]*Me2[2, 1]+Me2[1, 1]*Me2[2, 2]]]));

Me1tilde := simplify(Matrix([[Me1[1, 1]^2, Me1[1, 2]^2,
Me1[1, 3]^2, sqrt(2)*Me1[1, 2]*Me1[1, 3], sqrt(2)*Me1[1, 1]*
Me1[1, 3], sqrt(2)*Me1[1, 1]*Me1[1, 2]], [Me1[2, 1]^2, Me1[2, 2]^2,
Me1[2, 3]^2, sqrt(2)*Me1[2, 2]*Me1[2, 3], sqrt(2)*Me1[2, 1]*Me1[2, 3],
sqrt(2)*Me1[2, 1]*Me1[2, 2]], [Me1[3, 1]^2, Me1[3, 2]^2, Me1[3, 3]^2,
sqrt(2)*Me1[3, 2]*Me1[3, 3], sqrt(2)*Me1[3, 1]*Me1[3, 3], sqrt(2)*
Me1[3, 1]*Me1[3, 2]], [sqrt(2)*Me1[2, 1]*Me1[3, 1], sqrt(2)*
Me1[2, 2]*Me1[3, 2], sqrt(2)*Me1[2, 3]*Me1[3, 3], Me1[2, 3]*
Me1[3, 2]+Me1[2, 2]*Me1[3, 3], Me1[2, 3]*Me1[3, 1]+Me1[2, 1]*
Me1[3, 3], Me1[2, 2]*Me1[3, 1]+Me1[2, 1]*Me1[3, 2]], [sqrt(2)*
Me1[1, 1]*Me1[3, 1], sqrt(2)*Me1[1, 2]*Me1[3, 2], sqrt(2)*Me1[1, 3]*
Me1[3, 3], Me1[1, 3]*Me1[3, 2]+Me1[1, 2]*Me1[3, 3], Me1[1, 3]*
Me1[3, 1]+Me1[1, 1]*Me1[3, 3], Me1[1, 2]*Me1[3, 1]+Me1[1, 1]*
Me1[3, 2]], [sqrt(2)*Me1[1, 1]*Me1[2, 1], sqrt(2)*Me1[1, 2]*Me1[2, 2],
sqrt(2)*Me1[1, 3]*Me1[2, 3], Me1[1, 3]*Me1[2, 2]+Me1[1, 2]*
```

```
Me1[2, 3], Me1[1, 3]*Me1[2, 1]+Me1[1, 1]*Me1[2, 3], Me1[1, 2]*
Me1[2, 1]+Me1[1, 1]*Me1[2, 2]]]));

Mefftilde := simplify(Matrix([[Meff[1, 1]^2, Meff[1, 2]^2, Meff[1, 3]^2,
sqrt(2)*Meff[1, 2]*Meff[1, 3], sqrt(2)*Meff[1, 1]*Meff[1, 3], sqrt(2)*
Meff[1, 1]*Meff[1, 2]], [Meff[2, 1]^2, Meff[2, 2]^2, Meff[2, 3]^2, sqrt(2)*
Meff[2, 2]*Meff[2, 3], sqrt(2)*Meff[2, 1]*Meff[2, 3], sqrt(2)*
Meff[2, 1]*Meff[2, 2]], [Meff[3, 1]^2, Meff[3, 2]^2, Meff[3, 3]^2,
sqrt(2)*Meff[3, 2]*Meff[3, 3], sqrt(2)*Meff[3, 1]*Meff[3, 3], sqrt(2)*
Meff[3, 1]*Meff[3, 2]], [sqrt(2)*Meff[2, 1]*Meff[3, 1], sqrt(2)*
Meff[2, 2]*Meff[3, 2], sqrt(2)*Meff[2, 3]*Meff[3, 3], Meff[2, 3]*Meff[3, 2]+
Meff[2, 2]*Meff[3, 3], Meff[2, 3]*Meff[3, 1]+Meff[2, 1]*Meff[3, 3],
Meff[2, 2]*Meff[3, 1]+Meff[2, 1]*Meff[3, 2]], [sqrt(2)*Meff[1, 1]*Meff[3, 1],
sqrt(2)*Meff[1, 2]*Meff[3, 2], sqrt(2)*Meff[1, 3]*Meff[3, 3], Meff[1, 3]*
Meff[3, 2]+Meff[1, 2]*Meff[3, 3], Meff[1, 3]*Meff[3, 1]+Meff[1, 1]*
Meff[3, 3], Meff[1, 2]*Meff[3, 1]+Meff[1, 1]*Meff[3, 2]], [sqrt(2)*Meff[1, 1]*
Meff[2, 1], sqrt(2)*Meff[1, 2]*Meff[2, 2], sqrt(2)*Meff[1, 3]*Meff[2, 3],
Meff[1, 3]*Meff[2, 2]+Meff[1, 2]*Meff[2, 3], Meff[1, 3]*Meff[2, 1]+
Meff[1, 1]*Meff[2, 3], Meff[1, 2]*Meff[2, 1]+Meff[1, 1]*Meff[2, 2]]]));

Mehfftilde := simplify(Matrix([[Mehff[1, 1]^2, Mehff[1, 2]^2,
Mehff[1, 3]^2, sqrt(2)*Mehff[1, 2]*Mehff[1, 3], sqrt(2)*Mehff[1, 1]*
Mehff[1, 3], sqrt(2)*Mehff[1, 1]*Mehff[1, 2]], [Mehff[2, 1]^2, Mehff[2, 2]^2,
Mehff[2, 3]^2, sqrt(2)*Mehff[2, 2]*Mehff[2, 3], sqrt(2)*Mehff[2, 1]*Mehff[2, 3],
sqrt(2)*Mehff[2, 1]*Mehff[2, 2]], [Mehff[3, 1]^2, Mehff[3, 2]^2,
Mehff[3, 3]^2, sqrt(2)*Mehff[3, 2]*Mehff[3, 3], sqrt(2)*Mehff[3, 1]*
Mehff[3, 3], sqrt(2)*Mehff[3, 1]*Mehff[3, 2]], [sqrt(2)*Mehff[2, 1]*
Mehff[3, 1], sqrt(2)*Mehff[2, 2]*Mehff[3, 2], sqrt(2)*Mehff[2, 3]*Mehff[3, 3],
Mehff[2, 3]*Mehff[3, 2]+Mehff[2, 2]*Mehff[3, 3], Mehff[2, 3]*Mehff[3, 1]+
Mehff[2, 1]*Mehff[3, 3], Mehff[2, 2]*Mehff[3, 1]+Mehff[2, 1]*Mehff[3, 2]],
[sqrt(2)*Mehff[1, 1]*Mehff[3, 1], sqrt(2)*Mehff[1, 2]*Mehff[3, 2],
sqrt(2)*Mehff[1, 3]*Mehff[3, 3], Mehff[1, 3]*Mehff[3, 2]+Mehff[1, 2]*
Mehff[3, 3], Mehff[1, 3]*Mehff[3, 1]+Mehff[1, 1]*Mehff[3, 3], Mehff[1, 2]*
Mehff[3, 1]+Mehff[1, 1]*Mehff[3, 2]], [sqrt(2)*Mehff[1, 1]*Mehff[2, 1],
```

```
sqrt(2)*Mehff[1, 2]*Mehff[2, 2], sqrt(2)*Mehff[1, 3]*Mehff[2, 3],
Mehff[1, 3]*Mehff[2, 2]+Mehff[1, 2]*Mehff[2, 3], Mehff[1, 3]*Mehff[2, 1]+
Mehff[1, 1]*Mehff[2, 3], Mehff[1, 2]*Mehff[2, 1]+Mehff[1, 1]*Mehff[2, 2]]]));

Mcomb1tilde := simplify(Matrix([[Mcomb1[1, 1]^2, Mcomb1[1, 2]^2,
Mcomb1[1, 3]^2, sqrt(2)*Mcomb1[1, 2]*Mcomb1[1, 3], sqrt(2)*
Mcomb1[1, 1]*Mcomb1[1, 3], sqrt(2)*Mcomb1[1, 1]*Mcomb1[1, 2]],
[Mcomb1[2, 1]^2, Mcomb1[2, 2]^2, Mcomb1[2, 3]^2, sqrt(2)*
Mcomb1[2, 2]*Mcomb1[2, 3], sqrt(2)*Mcomb1[2, 1]*Mcomb1[2, 3],
sqrt(2)*Mcomb1[2, 1]*Mcomb1[2, 2]], [Mcomb1[3, 1]^2,
Mcomb1[3, 2]^2, Mcomb1[3, 3]^2, sqrt(2)*Mcomb1[3, 2]*Mcomb1[3, 3],
sqrt(2)*Mcomb1[3, 1]*Mcomb1[3, 3], sqrt(2)*Mcomb1[3, 1]*Mcomb1[3, 2]],
[sqrt(2)*Mcomb1[2, 1]*Mcomb1[3, 1], sqrt(2)*Mcomb1[2, 2]*Mcomb1[3, 2],
sqrt(2)*Mcomb1[2, 3]*Mcomb1[3, 3], Mcomb1[2, 3]*Mcomb1[3, 2]+
Mcomb1[2, 2]*Mcomb1[3, 3], Mcomb1[2, 3]*Mcomb1[3, 1]+Mcomb1[2, 1]*
Mcomb1[3, 3], Mcomb1[2, 2]*Mcomb1[3, 1]+Mcomb1[2, 1]*Mcomb1[3, 2]],
[sqrt(2)*Mcomb1[1, 1]*Mcomb1[3, 1], sqrt(2)*Mcomb1[1, 2]*Mcomb1[3, 2],
sqrt(2)*Mcomb1[1, 3]*Mcomb1[3, 3], Mcomb1[1, 3]*Mcomb1[3, 2]+
Mcomb1[1, 2]*Mcomb1[3, 3], Mcomb1[1, 3]*Mcomb1[3, 1]+Mcomb1[1, 1]*
Mcomb1[3, 3], Mcomb1[1, 2]*Mcomb1[3, 1]+Mcomb1[1, 1]*Mcomb1[3, 2]],
[sqrt(2)*Mcomb1[1, 1]*Mcomb1[2, 1], sqrt(2)*Mcomb1[1, 2]*Mcomb1[2, 2],
sqrt(2)*Mcomb1[1, 3]*Mcomb1[2, 3], Mcomb1[1, 3]*Mcomb1[2, 2]+
Mcomb1[1, 2]*Mcomb1[2, 3], Mcomb1[1, 3]*Mcomb1[2, 1]+Mcomb1[1, 1]
*Mcomb1[2, 3], Mcomb1[1, 2]*Mcomb1[2, 1]+Mcomb1[1, 1]*Mcomb1[2, 2]]]));

Mcomb2tilde := simplify(Matrix([[Mcomb2[1, 1]^2, Mcomb2[1, 2]^2,
Mcomb2[1, 3]^2, sqrt(2)*Mcomb2[1, 2]*Mcomb2[1, 3],
sqrt(2)*Mcomb2[1, 1]*Mcomb2[1, 3], sqrt(2)*Mcomb2[1, 1]*
Mcomb2[1, 2]], [Mcomb2[2, 1]^2, Mcomb2[2, 2]^2, Mcomb2[2, 3]^2,
sqrt(2)*Mcomb2[2, 2]*Mcomb2[2, 3], sqrt(2)*Mcomb2[2, 1]*
Mcomb2[2, 3], sqrt(2)*Mcomb2[2, 1]*Mcomb2[2, 2]], [Mcomb2[3, 1]^2,
Mcomb2[3, 2]^2, Mcomb2[3, 3]^2, sqrt(2)*Mcomb2[3, 2]*Mcomb2[3, 3],
sqrt(2)*Mcomb2[3, 1]*Mcomb2[3, 3], sqrt(2)*Mcomb2[3, 1]*Mcomb2[3, 2]],
[sqrt(2)*Mcomb2[2, 1]*Mcomb2[3, 1], sqrt(2)*Mcomb2[2, 2]*Mcomb2[3, 2],
```

```
sqrt(2)*Mcomb2[2, 3]*Mcomb2[3, 3], Mcomb2[2, 3]*Mcomb2[3, 2]+
Mcomb2[2, 2]*Mcomb2[3, 3], Mcomb2[2, 3]*Mcomb2[3, 1]+
Mcomb2[2, 1]*Mcomb2[3, 3], Mcomb2[2, 2]*Mcomb2[3, 1]+
Mcomb2[2, 1]*Mcomb2[3, 2]], [sqrt(2)*Mcomb2[1, 1]*Mcomb2[3, 1],
sqrt(2)*Mcomb2[1, 2]*Mcomb2[3, 2], sqrt(2)*Mcomb2[1, 3]*Mcomb2[3, 3],
Mcomb2[1, 3]*Mcomb2[3, 2]+Mcomb2[1, 2]*Mcomb2[3, 3],
Mcomb2[1, 3]*Mcomb2[3, 1]+Mcomb2[1, 1]*Mcomb2[3, 3],
Mcomb2[1, 2]*Mcomb2[3, 1]+Mcomb2[1, 1]*Mcomb2[3, 2]],
[sqrt(2)*Mcomb2[1, 1]*Mcomb2[2, 1], sqrt(2)*Mcomb2[1, 2]*
Mcomb2[2, 2], sqrt(2)*Mcomb2[1, 3]*Mcomb2[2, 3], Mcomb2[1, 3]*
Mcomb2[2, 2]+Mcomb2[1, 2]*Mcomb2[2, 3], Mcomb2[1, 3]*
Mcomb2[2, 1]+Mcomb2[1, 1]*Mcomb2[2, 3], Mcomb2[1, 2]*Mcomb2[2, 1]
+Mcomb2[1, 1]*Mcomb2[2, 2]]]));
```

Evaluating the closest tetragonal elasticity tensor in the rotated coordinate system:

```
Ctetrar := evalf(1/8*(R+Transpose(Me3tilde). R.Me3tilde+
Transpose(Me2tilde).R.Me2tilde)+Transpose(Me1tilde.R.Me1tilde)+
Transpose(Mefftilde.R.Mefftilde+Transpose(Mehfftilde.R.Mehfftilde)+
Transpose(Mcomb1tilde).R. Mcomb1tilde)+
Transpose(Mcomb2tilde).R. Mcomb2tilde)
```

Evaluating the norm of $Ctetrar$ and C to calculate distance to tetragonal.

```
Nctetrar := Norm(Ctetrar, Frobenius)^2;
Nc := Norm(C, Frobenius)^2
```

Evaluating the tetragonal-distance function, namely $d(Atilde^T C Atilde, \mathcal{L}^{tetra})$. Note that this function cannot be plotted because it is a 4-dimensional function.

```
Delta-tetra := evalf(Nc-Nctetrar):
```

In order to find a local minima ,which may be observed from the plot of the monoclinic distance function, around some neighborhood, one should use the line:

```
Mindata := Minimize(Delta-tetra, phi = 30*(1/180)*Pi .. 50*(1/180)*Pi,
psi = (1/180)*(90-44)*Pi .. (1/180)*(90-24)*Pi);
```

Sum of monoclinic-distance functions along the normals of the mirror planes of the tetragonal symmetry

```
restart;
with(LinearAlgebra);
with(Optimization);
```

The rotation matrix that transforms $\mathbf{e_3}$ to the new z-axis.

```
AEuler := Matrix([[cos(psi), -sin(psi), 0], [sin(psi), cos(psi), 0], [0, 0, 1]]).
Matrix([[1, 0, 0], [0, cos(phi), -sin(phi)], [0, sin(phi), cos(phi)]]));
```

Since the orientations of x-axis and y-axis matter when calculating the distance of C to orthotropic symmetry in some coordinate system, we should multiply AEuler with another elementary transformation. This elementary transformation determines the orientations of x-axis and y-axis.

```
Rot := Matrix([[cos(theta), -sin(theta), 0], [sin(theta), cos(theta), 0], [0, 0, 1]]);
A := AEuler.Rot.;
```

Expressing $A \in SO(3)$ in 6D since it is going to act on the elasticity tensor.

```
Atilde := simplify(Matrix([[A[1, 1]^2, A[1, 2]^2, A[1, 3]^2, sqrt(2)*A[1, 2]*A[1, 3],
sqrt(2)*A[1, 1]*A[1, 3], sqrt(2)*A[1, 1]*A[1, 2]], [A[2, 1]^2, A[2, 2]^2, A[2, 3]^2,
sqrt(2)*A[2, 2]*A[2, 3], sqrt(2)*A[2, 1]*A[2, 3], sqrt(2)*A[2, 1]*A[2, 2]],
[A[3, 1]^2, A[3, 2]^2, A[3, 3]^2, sqrt(2)*A[3, 2]*A[3, 3], sqrt(2)*A[3, 1]
*A[3, 3], sqrt(2)*A[3, 1]*A[3, 2]], [sqrt(2)*A[2, 1]*A[3, 1], sqrt(2)*A[2, 2]*A[3, 2],
sqrt(2)*A[2, 3]*A[3, 3], A[2, 3]*A[3, 2]+A[2, 2]*A[3, 3], A[2, 3]*A[3, 1]+
A[2, 1]*A[3, 3], A[2, 2]*A[3, 1]+A[2, 1]*A[3, 2]], [sqrt(2)*A[1, 1]*A[3, 1],
sqrt(2)*A[1, 2]*A[3, 2], sqrt(2)*A[1, 3]*A[3, 3], A[1, 3]*A[3, 2]+A[1, 2]*A[3, 3],
A[1, 3]*A[3, 1]+A[1, 1]*A[3, 3], A[1, 2]*A[3, 1]+A[1, 1]*A[3, 2]],
[sqrt(2)*A[1, 1]*A[2, 1], sqrt(2)*A[1, 2]*A[2, 2], sqrt(2)*A[1, 3]*A[2, 3],
A[1, 3]*A[2, 2]+A[1, 2]*A[2, 3], A[1, 3]*A[2, 1]+A[1, 1]*A[2, 3], A[1, 2]*A[2, 1]+
A[1, 1]*A[2, 2]]])):
```

Introducing the elasticity matrix C in its general form.

```
C := Matrix(6, symbol = c, shape = symmetric);
```

This line is for changing the Voigt notation to Kelvin or vice versa. Herein, since we represent it in Kelvin notation, we do not change anything.

```
C[1 .. 3, 4 .. 6] := C[1 .. 3, 4 .. 6];
C[4 .. 6, 4 .. 6] := C[4 .. 6, 4 .. 6];
```

Introducing the parameters of elasticity matrix.

```
c := Matrix(6, 6, {(1, 1) = 42.03357978, (1, 2) = 32.49305220,
(1, 3) = 26.42291512, (1, 4) = 5.799531000, (1, 5) = 9.938160420,
(1, 6) = 21.33549018, (2, 1) = 32.49305219, (2, 2) = 36.72218489,
(2, 3) = 34.84774953, (2, 4) = -5.221667422, (2, 5) = -35.36967653,
(2, 6) = -23.60019509, (3, 1) = 26.42291511, (3, 2) = 34.84774954,
(3, 3) = 31.71680164, (3, 4) = 12.16688779, (3, 5) = 3.767088965,
(3, 6) = 10.24209672, (4, 1) = 5.799531000, (4, 2) = -5.221667442,
(4, 3) = 12.16688780, (4, 4) = 32.84181099, (4, 5) = 20.98631307,
(4, 6) = 2.36291613, (5, 1) = 9.938160440, (5, 2) = -35.36967653,
(5, 3) = 3.767088965, (5, 4) = 20.98631308, (5, 5) = -22.64105584,
(5, 6) = -9.709913499, (6, 1) = 21.33549018, (6, 2) = -23.60019510,
(6, 3) = 10.24209672, (6, 4) = 2.36291613, (6, 5) = -9.709913499,
(6, 6) = 11.32667859});
```

Expressing the elasticity matrix C in all coordinate systems by rotating it with a generic orthogonal transformation that is introduced in the above lines.

```
R := evalf(Transpose(Atilde).C.Atilde);
```

This line evaluates the distance of C to monoclinic along the z-axis of the rotated $\dot{C}$:

```
Dist := evalf(2*(R[1, 4]^2+R[1, 5]^2+R[2, 4]^2+R[2, 5]^2+R[3, 4]^2+R[3, 5]^2
+R[4, 6]^2+R[5, 6]^2)):
```

In order to rotate the z-axis of C to the x-axis, we introduce 90° rotation:

```
ninetyx := Matrix([[0, 0, 1], [0, 1, 0], [-1, 0, 0]]);
Ax := A.ninetyx;
```

Expressing the above orthogonal transformation in 6D so that it acts the elasticity tensor

```
Atildex := simplify(Matrix([[Ax[1, 1]^2, Ax[1, 2]^2, Ax[1, 3]^2, sqrt(2)*
Ax[1, 2]*Ax[1, 3], sqrt(2)*Ax[1, 1]*Ax[1, 3], sqrt(2)*Ax[1, 1]*Ax[1, 2]],
[Ax[2, 1]^2, Ax[2, 2]^2, Ax[2, 3]^2, sqrt(2)*Ax[2, 2]*Ax[2, 3], sqrt(2)*
Ax[2, 1]*Ax[2, 3], sqrt(2)*Ax[2, 1]*Ax[2, 2]], [Ax[3, 1]^2, Ax[3, 2]^2,
Ax[3, 3]^2, sqrt(2)*Ax[3, 2]*Ax[3, 3], sqrt(2)*Ax[3, 1]*Ax[3, 3], sqrt(2)*
Ax[3, 1]*Ax[3, 2]], [sqrt(2)*Ax[2, 1]*Ax[3, 1], sqrt(2)*Ax[2, 2]*Ax[3, 2],
sqrt(2)*Ax[2, 3]*Ax[3, 3], Ax[2, 3]*Ax[3, 2]+Ax[2, 2]*Ax[3, 3], Ax[2, 3]*
Ax[3, 1]+Ax[2, 1]*Ax[3, 3], Ax[2, 2]*Ax[3, 1]+Ax[2, 1]*Ax[3, 2]],
[sqrt(2)*Ax[1, 1]*Ax[3, 1], sqrt(2)*Ax[1, 2]*Ax[3, 2], sqrt(2)*Ax[1, 3]*Ax[3, 3],
Ax[1, 3]*Ax[3, 2]+Ax[1, 2]*Ax[3, 3], Ax[1, 3]*Ax[3, 1]+Ax[1, 1]*Ax[3, 3],
Ax[1, 2]*Ax[3, 1]+Ax[1, 1]*Ax[3, 2]], [sqrt(2)*Ax[1, 1]*Ax[2, 1],
sqrt(2)*Ax[1, 2]*Ax[2, 2], sqrt(2)*Ax[1, 3]*Ax[2, 3], Ax[1, 3]*Ax[2, 2]+
Ax[1, 2]*Ax[2, 3], Ax[1, 3]*Ax[2, 1]+Ax[1, 1]*Ax[2, 3], Ax[1, 2]*Ax[2, 1]+
Ax[1, 1]*Ax[2, 2]]])):
```

Atildex acts the elasticity matrix in order to express it in a coordinate system where its new z-axis is the x-axis.

```
Rx := evalf(Transpose(Atildex).C.Atildex);
```

This line evaluates the distance of C to monoclinic along the x-axis of the rotated C:

```
Distx := evalf(2*(Rx[1, 4]^2+Rx[1, 5]^2+Rx[2, 4]^2+Rx[2, 5]^2+
Rx[3, 4]^2+Rx[3, 5]^2+Rx[4, 6]^2+Rx[5, 6]^2)):
```

Now, we repeat the same procedure for y-axis:

```
ninetyy := Matrix([[1, 0, 0], [0, 0, 1], [0, -1,.0]]):
Ay := A.ninetyy;

Atildey := simplify(Matrix([[Ay[1, 1]^2, Ay[1, 2]^2, Ay[1, 3]^2,
sqrt(2)*Ay[1, 2]*Ay[1, 3], sqrt(2)*Ay[1, 1]*Ay[1, 3], sqrt(2)*Ay[1, 1]*
Ay[1, 2]], [Ay[2, 1]^2, Ay[2, 2]^2, Ay[2, 3]^2, sqrt(2)*Ay[2, 2]*Ay[2, 3],
```

```
sqrt(2)*Ay[2, 1]*Ay[2, 3], sqrt(2)*Ay[2, 1]*Ay[2, 2]], [Ay[3, 1]^2,
Ay[3, 2]^2, Ay[3, 3]^2, sqrt(2)*Ay[3, 2]*Ay[3, 3], sqrt(2)*Ay[3, 1]*Ay[3, 3],
sqrt(2)*Ay[3, 1]*Ay[3, 2]], [sqrt(2)*Ay[2, 1]*Ay[3, 1], sqrt(2)*Ay[2, 2]*
Ay[3, 2], sqrt(2)*Ay[2, 3]*Ay[3, 3], Ay[2, 3]*Ay[3, 2]+Ay[2, 2]*Ay[3, 3],
Ay[2, 3]*Ay[3, 1]+Ay[2, 1]*Ay[3, 3], Ay[2, 2]*Ay[3, 1]+Ay[2, 1]*Ay[3, 2]],
[sqrt(2)*Ay[1, 1]*Ay[3, 1], sqrt(2)*Ay[1, 2]*Ay[3, 2], sqrt(2)*Ay[1, 3]*
Ay[3, 3], Ay[1, 3]*Ay[3, 2]+Ay[1, 2]*Ay[3, 3], Ay[1, 3]*Ay[3, 1]+Ay[1, 1]*
Ay[3, 3], Ay[1, 2]*Ay[3, 1]+Ay[1, 1]*Ay[3, 2]], [sqrt(2)*Ay[1, 1]*Ay[2, 1],
sqrt(2)*Ay[1, 2]*Ay[2, 2], sqrt(2)*Ay[1, 3]*Ay[2, 3], Ay[1, 3]*Ay[2, 2]+
Ay[1, 2]*Ay[2, 3], Ay[1, 3]*Ay[2, 1]+Ay[1, 1]*Ay[2, 3], Ay[1, 2]*Ay[2, 1]
+Ay[1, 1]*Ay[2, 2]]]));

Ry := evalf(Transpose(Atildey).C.Atildey);
Disty := evalf(2*(Ry[1, 4]^2+Ry[1, 5]^2+Ry[2, 4]^2+Ry[2, 5]^2+Ry[3, 4]^2+
Ry[3, 5]^2+Ry[4, 6]^2+Ry[5, 6]^2));
```

We repeat the same procedure for the directions which are the normals of a mirror plane of a tetragonal medium :

```
fourtyfive := Matrix([[1/2, -1/2, (1/2)*sqrt(2)], [-1/2, 1/2, (1/2)*sqrt(2)],
[-(1/2)*sqrt(2), -(1/2)*sqrt(2), 0]]);
Aff := A.fourtyfive;

Atildeff := simplify(Matrix([[Aff[1, 1]^2, Aff[1, 2]^2, Aff[1, 3]^2,
sqrt(2)*Aff[1, 2]*Aff[1, 3], sqrt(2)*Aff[1, 1]*Aff[1, 3], sqrt(2)*Aff[1, 1]*
Aff[1, 2]], [Aff[2, 1]^2, Aff[2, 2]^2, Aff[2, 3]^2, sqrt(2)*Aff[2, 2]*Aff[2, 3],
sqrt(2)*Aff[2, 1]*Aff[2, 3], sqrt(2)*Aff[2, 1]*Aff[2, 2]], [Aff[3, 1]^2, Aff[3, 2]^2,
Aff[3, 3]^2, sqrt(2)*Aff[3, 2]*Aff[3, 3], sqrt(2)*Aff[3, 1]*Aff[3, 3], sqrt(2)*
Aff[3, 1]*Aff[3, 2]], [sqrt(2)*Aff[2, 1]*Aff[3, 1], sqrt(2)*Aff[2, 2]*Aff[3, 2],
sqrt(2)*Aff[2, 3]*Aff[3, 3], Aff[2, 3]*Aff[3, 2]+Aff[2, 2]*Aff[3, 3], Aff[2, 3]*
Aff[3, 1]+Aff[2, 1]*Aff[3, 3], Aff[2, 2]*Aff[3, 1]+Aff[2, 1]*Aff[3, 2]], [sqrt(2)*
Aff[1, 1]*Aff[3, 1], sqrt(2)*Aff[1, 2]*Aff[3, 2], sqrt(2)*Aff[1, 3]*Aff[3, 3],
Aff[1, 3]*Aff[3, 2]+Aff[1, 2]*Aff[3, 3], Aff[1, 3]*Aff[3, 1]+Aff[1, 1]*Aff[3, 3],
Aff[1, 2]*Aff[3, 1]+Aff[1, 1]*Aff[3, 2]], [sqrt(2)*Aff[1, 1]*Aff[2, 1], sqrt(2)*
Aff[1, 2]*Aff[2, 2], sqrt(2)*Aff[1, 3]*Aff[2, 3], Aff[1, 3]*Aff[2, 2]+Aff[1, 2]*
```

```
Aff[2, 3], Aff[1, 3]*Aff[2, 1]+Aff[1, 1]*Aff[2, 3], Aff[1, 2]*Aff[2, 1]+Aff[1, 1]*
Aff[2, 2]]]));

Rff := evalf(Transpose(Atildeff.C.Atildeff));

Distff := evalf(2*(Rff[1, 4]^2+Rff[1, 5]^2+Rff[2, 4]^2+Rff[2, 5]^2+
Rff[3, 4]^2+Rff[3, 5]^2+Rff[4, 6]^2+Rff[5, 6]^2));

hundredfourtyfive := Matrix([[1/2, 1/2, -(1/2)*sqrt(2)], [1/2, 1/2, (1/2)*sqrt(2)],
[(1/2)*sqrt(2), -(1/2)*sqrt(2), 0]]);

Ahff := A.hundredfourtyfive;
[(1/2)*sqrt(2), -(1/2)*sqrt(2), 0]]);

Atildehff := simplify(Matrix([[Ahff[1, 1]^2, Ahff[1, 2]^2, Ahff[1, 3]^2,
sqrt(2)*Ahff[1, 2]*Ahff[1, 3], sqrt(2)*Ahff[1, 1]*Ahff[1, 3], sqrt(2)*
Ahff[1, 1]*Ahff[1, 2]], [Ahff[2, 1]^2, Ahff[2, 2]^2, Ahff[2, 3]^2, sqrt(2)*
Ahff[2, 2]*Ahff[2, 3], sqrt(2)*Ahff[2, 1]*Ahff[2, 3], sqrt(2)*Ahff[2, 1]*
Ahff[2, 2]], [Ahff[3, 1]^2, Ahff[3, 2]^2, Ahff[3, 3]^2, sqrt(2)*Ahff[3, 2]*
Ahff[3, 3], sqrt(2)*Ahff[3, 1]*Ahff[3, 3], sqrt(2)*Ahff[3, 1]*Ahff[3, 2]],
[sqrt(2)*Ahff[2, 1]*Ahff[3, 1], sqrt(2)*Ahff[2, 2]*Ahff[3, 2], sqrt(2)*
Ahff[2, 3]*Ahff[3, 3], Ahff[2, 3]*Ahff[3, 2]+Ahff[2, 2]*Ahff[3, 3], Ahff[2, 3]*
Ahff[3, 1]+Ahff[2, 1]*Ahff[3, 3], Ahff[2, 2]*Ahff[3, 1]+Ahff[2, 1]*Ahff[3, 2]],
[sqrt(2)*Ahff[1, 1]*Ahff[3, 1], sqrt(2)*Ahff[1, 2]*Ahff[3, 2], sqrt(2)*
Ahff[1, 3]*Ahff[3, 3], Ahff[1, 3]*Ahff[3, 2]+Ahff[1, 2]*Ahff[3, 3], Ahff[1, 3]*
Ahff[3, 1]+Ahff[1, 1]*Ahff[3, 3], Ahff[1, 2]*Ahff[3, 1]+Ahff[1, 1]*Ahff[3, 2]],
[sqrt(2)*Ahff[1, 1]*Ahff[2, 1], sqrt(2)*Ahff[1, 2]*Ahff[2, 2], sqrt(2)*Ahff[1, 3]*
Ahff[2, 3], Ahff[1, 3]*Ahff[2, 2]+Ahff[1, 2]*Ahff[2, 3], Ahff[1, 3]*Ahff[2, 1]+
Ahff[1, 1]*Ahff[2, 3], Ahff[1, 2]*Ahff[2, 1]+Ahff[1, 1]*Ahff[2, 2]]]));
[(1/2)*sqrt(2), -(1/2)*sqrt(2), 0]]);

Rhff := evalf(Transpose(Atildehff.C.Atildehff));

Disthff := evalf(2*(Rhff[1, 4]^2+Rhff[1, 5]^2+Rhff[2, 4]^2+Rhff[2, 5]^2
+Rhff[3, 4]^2+Rhff[3, 5]^2+Rhff[4, 6]^2+Rhff[5, 6]^2));
```

Evaluating the sum of monoclinic-distance functions along the normals of mirror planes of tetragonal symmetry:

```
Distall := Dist+Distx+Disty+Distff+Disthff
```

For minimizing the Distall function around some restricted region

```
Mindata := Minimize(Distall, phi= 0. .. 10*(1/180)*Pi,
psi = (1/2)*Pi .. 2*Pi+(1/2)*Pi, theta = 0 .. 2*Pi);
```

Trigonal-distance function

```
restart;
with(LinearAlgebra);
with(Optimization);
```

The rotation matrix that transforms $\mathbf{e_3}$ to the new z-axis.

```
AEuler := Matrix([[cos(psi), -sin(psi), 0], [sin(psi), cos(psi), 0], [0, 0, 1]]).
Matrix([[1, 0, 0], [0, cos(phi), -sin(phi)], [0, sin(phi), cos(phi)]]));
```

Since the orientations of x-axis and y-axis matter when calculating the distance of C to orthotropic symmetry in some coordinate system, we should multiply AEuler with another elementary transformation. This elementary transformation determines the orientations of x-axis and y-axis.

```
Rot := Matrix([[cos(theta), -sin(theta), 0], [sin(theta), cos(theta), 0], [0, 0, 1]]);
A := AEuler.Rot.;
```

Expressing $A \in SO(3)$ in 6D since it is going to act on the elasticity tensor.

```
Atilde := simplify(Matrix([[A[1, 1]^2, A[1, 2]^2, A[1, 3]^2, sqrt(2)*A[1, 2]*A[1, 3],
sqrt(2)*A[1, 1]*A[1, 3], sqrt(2)*A[1, 1]*A[1, 2]], [A[2, 1]^2, A[2, 2]^2, A[2, 3]^2,
sqrt(2)*A[2, 2]*A[2, 3], sqrt(2)*A[2, 1]*A[2, 3], sqrt(2)*A[2, 1]*A[2, 2]],
[A[3, 1]^2, A[3, 2]^2, A[3, 3]^2, sqrt(2)*A[3, 2]*A[3, 3], sqrt(2)*A[3, 1]
*A[3, 3], sqrt(2)*A[3, 1]*A[3, 2]], [sqrt(2)*A[2, 1]*A[3, 1], sqrt(2)*A[2, 2]*A[3, 2],
sqrt(2)*A[2, 3]*A[3, 3], A[2, 3]*A[3, 2]+A[2, 2]*A[3, 3], A[2, 3]*A[3, 1]+
A[2, 1]*A[3, 3], A[2, 2]*A[3, 1]+A[2, 1]*A[3, 2]], [sqrt(2)*A[1, 1]*A[3, 1],
```

```
sqrt(2)*A[1, 2]*A[3, 2], sqrt(2)*A[1, 3]*A[3, 3], A[1, 3]*A[3, 2]+A[1, 2]*A[3, 3],
A[1, 3]*A[3, 1]+A[1, 1]*A[3, 3], A[1, 2]*A[3, 1]+A[1, 1]*A[3, 2]],
[sqrt(2)*A[1, 1]*A[2, 1], sqrt(2)*A[1, 2]*A[2, 2], sqrt(2)*A[1, 3]*A[2, 3],
A[1, 3]*A[2, 2]+A[1, 2]*A[2, 3], A[1, 3]*A[2, 1]+A[1, 1]*A[2, 3], A[1, 2]*A[2, 1]+
A[1, 1]*A[2, 2]]]]):
```

Introducing the elasticity matrix C in its general form.

```
C := Matrix(6, symbol = c, shape = symmetric);
```

This line is for changing the Voigt notation to Kelvin or vice versa. Herein, since we represent it in Kelvin notation, we do not change anything.

```
C[1 .. 3, 4 .. 6] := C[1 .. 3, 4 .. 6];
C[4 .. 6, 4 .. 6] := C[4 .. 6, 4 .. 6];
```

Introducing the parameters of elasticity matrix.

```
c := Matrix(6, 6, {(1, 1) = 42.03357978, (1, 2) = 32.49305220,
(1, 3) = 26.42291512, (1, 4) = 5.799531000, (1, 5) = 9.938160420,
(1, 6) = 21.33549018, (2, 1) = 32.49305219, (2, 2) = 36.72218489,
(2, 3) = 34.84774953, (2, 4) = -5.221667422, (2, 5) = -35.36967653,
(2, 6) = -23.60019509, (3, 1) = 26.42291511, (3, 2) = 34.84774954,
(3, 3) = 31.71680164, (3, 4) = 12.16688779, (3, 5) = 3.767088965,
(3, 6) = 10.24209672, (4, 1) = 5.799531000, (4, 2) = -5.221667442,
(4, 3) = 12.16688780, (4, 4) = 32.84181099, (4, 5) = 20.98631307,
(4, 6) = 2.36291613, (5, 1) = 9.938160440, (5, 2) = -35.36967653,
(5, 3) = 3.767088965, (5, 4) = 20.98631308, (5, 5) = -22.64105584,
(5, 6) = -9.709913499, (6, 1) = 21.33549018, (6, 2) = -23.60019510,
(6, 3) = 10.24209672, (6, 4) = 2.36291613, (6, 5) = -9.709913499,
(6, 6) = 11.32667859});
```

Expressing the elasticity matrix C in all coordinate systems by rotating it with a generic orthogonal transformation that is introduced in the above lines.

```
R := evalf((Transpose(Atilde).C.Atilde);
```

Introducing the symmetry group of tetragonal class for taking the projection of an elasticity tensor onto the tetragonal space

```
Me1 := Matrix([[-1, 0, 0], [0, 1, 0], [0, 0, 1]]);
Mesixty := Matrix([[1/2, -(1/2)*sqrt(3), 0], [-(1/2)*sqrt(3), -1/2, 0], [0, 0, 1]]);
Mehtwenty := Matrix([[1/2, (1/2)*sqrt(3), 0], [(1/2)*sqrt(3), -1/2, 0], [0, 0, 1]]);
Mcomb1 := Mesixty. Me1;
Mcomb2 := Transpose(Mesixty.Me1);
```

Expressing the above orthogonal transformations in 6D

```
Me1tilde := simplify(Matrix([[Me1[1, 1]^2, Me1[1, 2]^2,
Me1[1, 3]^2, sqrt(2)*Me1[1, 2]*Me1[1, 3], sqrt(2)*Me1[1, 1]*
Me1[1, 3], sqrt(2)*Me1[1, 1]*Me1[1, 2]], [Me1[2, 1]^2, Me1[2, 2]^2,
Me1[2, 3]^2, sqrt(2)*Me1[2, 2]*Me1[2, 3], sqrt(2)*Me1[2, 1]*Me1[2, 3],
sqrt(2)*Me1[2, 1]*Me1[2, 2]], [Me1[3, 1]^2, Me1[3, 2]^2, Me1[3, 3]^2,
sqrt(2)*Me1[3, 2]*Me1[3, 3], sqrt(2)*Me1[3, 1]*Me1[3, 3], sqrt(2)*
Me1[3, 1]*Me1[3, 2]], [sqrt(2)*Me1[2, 1]*Me1[3, 1], sqrt(2)*
Me1[2, 2]*Me1[3, 2], sqrt(2)*Me1[2, 3]*Me1[3, 3], Me1[2, 3]*
Me1[3, 2]+Me1[2, 2]*Me1[3, 3], Me1[2, 3]*Me1[3, 1]+Me1[2, 1]*
Me1[3, 3], Me1[2, 2]*Me1[3, 1]+Me1[2, 1]*Me1[3, 2]], [sqrt(2)*
Me1[1, 1]*Me1[3, 1], sqrt(2)*Me1[1, 2]*Me1[3, 2], sqrt(2)*Me1[1, 3]*
Me1[3, 3], Me1[1, 3]*Me1[3, 2]+Me1[1, 2]*Me1[3, 3], Me1[1, 3]*
Me1[3, 1]+Me1[1, 1]*Me1[3, 3], Me1[1, 2]*Me1[3, 1]+Me1[1, 1]*
Me1[3, 2]], [sqrt(2)*Me1[1, 1]*Me1[2, 1], sqrt(2)*Me1[1, 2]*Me1[2, 2],
sqrt(2)*Me1[1, 3]*Me1[2, 3], Me1[1, 3]*Me1[2, 2]+Me1[1, 2]*
Me1[2, 3], Me1[1, 3]*Me1[2, 1]+Me1[1, 1]*Me1[2, 3], Me1[1, 2]*
Me1[2, 1]+Me1[1, 1]*Me1[2, 2]]]));

Mesixtytilde := simplify(Matrix([[Mesixty[1, 1]^2, Mesixty[1, 2]^2,
Mesixty[1, 3]^2, sqrt(2)*Mesixty[1, 2]*Mesixty[1, 3], sqrt(2)*
Mesixty[1, 1]*Mesixty[1, 3], sqrt(2)*Mesixty[1, 1]*Mesixty[1, 2]],
[Mesixty[2, 1]^2, Mesixty[2, 2]^2, Mesixty[2, 3]^2, sqrt(2)*
Mesixty[2, 2]*Mesixty[2, 3], sqrt(2)*Mesixty[2, 1]*Mesixty[2, 3],
sqrt(2)*Mesixty[2, 1]*Mesixty[2, 2]], [Mesixty[3, 1]^2, Mesixty[3, 2]^2,
```

```
Mesixty[3, 3]^2, sqrt(2)*Mesixty[3, 2]*Mesixty[3, 3], sqrt(2)*Mesixty[3, 1]*
Mesixty[3, 3], sqrt(2)*Mesixty[3, 1]*Mesixty[3, 2]], [sqrt(2)*Mesixty[2, 1]*
Mesixty[3, 1], sqrt(2)*Mesixty[2, 2]*Mesixty[3, 2], sqrt(2)*Mesixty[2, 3]*
Mesixty[3, 3], Mesixty[2, 3]*Mesixty[3, 2]+Mesixty[2, 2]*Mesixty[3, 3],
Mesixty[2, 3]*Mesixty[3, 1]+Mesixty[2, 1]*Mesixty[3, 3], Mesixty[2, 2]*
Mesixty[3, 1]+Mesixty[2, 1]*Mesixty[3, 2]], [sqrt(2)*Mesixty[1, 1]*
Mesixty[3, 1], sqrt(2)*Mesixty[1, 2]*Mesixty[3, 2], sqrt(2)*Mesixty[1, 3]*
Mesixty[3, 3], Mesixty[1, 3]*Mesixty[3, 2]+Mesixty[1, 2]*Mesixty[3, 3],
Mesixty[1, 3]*Mesixty[3, 1]+Mesixty[1, 1]*Mesixty[3, 3], Mesixty[1, 2]*
Mesixty[3, 1]+Mesixty[1, 1]*Mesixty[3, 2]], [sqrt(2)*Mesixty[1, 1]*
Mesixty[2, 1], sqrt(2)*Mesixty[1, 2]*Mesixty[2, 2], sqrt(2)*Mesixty[1, 3]*
Mesixty[2, 3], Mesixty[1, 3]*Mesixty[2, 2]+Mesixty[1, 2]*Mesixty[2, 3],
Mesixty[1, 3]*Mesixty[2, 1]+Mesixty[1, 1]*Mesixty[2, 3], Mesixty[1, 2]*
Mesixty[2, 1]+Mesixty[1, 1]*Mesixty[2, 2]]])):

Mehtwentytilde := simplify(Matrix([[Mehtwenty[1, 1]^2, Mehtwenty[1, 2]^2,
Mehtwenty[1, 3]^2, sqrt(2)*Mehtwenty[1, 2]*Mehtwenty[1, 3], sqrt(2)*
Mehtwenty[1, 1]*Mehtwenty[1, 3], sqrt(2)*Mehtwenty[1, 1]*Mehtwenty[1, 2]],
[Mehtwenty[2, 1]^2, Mehtwenty[2, 2]^2, Mehtwenty[2, 3]^2, sqrt(2)*
Mehtwenty[2, 2]*Mehtwenty[2, 3], sqrt(2)*Mehtwenty[2, 1]*Mehtwenty[2, 3],
sqrt(2)*Mehtwenty[2, 1]*Mehtwenty[2, 2]], [Mehtwenty[3, 1]^2,
Mehtwenty[3, 2]^2, Mehtwenty[3, 3]^2, sqrt(2)*Mehtwenty[3, 2]*
Mehtwenty[3, 3], sqrt(2)*Mehtwenty[3, 1]*Mehtwenty[3, 3], sqrt(2)*
Mehtwenty[3, 1]*Mehtwenty[3, 2]], [sqrt(2)*Mehtwenty[2, 1]*Mehtwenty[3, 1],
sqrt(2)*Mehtwenty[2, 2]*Mehtwenty[3, 2], sqrt(2)*Mehtwenty[2, 3]*
Mehtwenty[3, 3], Mehtwenty[2, 3]*Mehtwenty[3, 2]+Mehtwenty[2, 2]*
Mehtwenty[3, 3], Mehtwenty[2, 3]*Mehtwenty[3, 1]+Mehtwenty[2, 1]*
Mehtwenty[3, 3], Mehtwenty[2, 2]*Mehtwenty[3, 1]+Mehtwenty[2, 1]*
Mehtwenty[3, 2]], [sqrt(2)*Mehtwenty[1, 1]*Mehtwenty[3, 1], sqrt(2)*
Mehtwenty[1, 2]*Mehtwenty[3, 2], sqrt(2)*Mehtwenty[1, 3]*Mehtwenty[3, 3],
Mehtwenty[1, 3]*Mehtwenty[3, 2]+Mehtwenty[1, 2]*Mehtwenty[3, 3],
Mehtwenty[1, 3]*Mehtwenty[3, 1]+Mehtwenty[1, 1]*Mehtwenty[3, 3],
Mehtwenty[1, 2]*Mehtwenty[3, 1]+Mehtwenty[1, 1]*Mehtwenty[3, 2]],
```

```
[sqrt(2)*Mehtwenty[1, 1]*Mehtwenty[2, 1], sqrt(2)*Mehtwenty[1, 2]*
Mehtwenty[2, 2], sqrt(2)*Mehtwenty[1, 3]*Mehtwenty[2, 3], Mehtwenty[1, 3]*
Mehtwenty[2, 2]+Mehtwenty[1, 2]*Mehtwenty[2, 3], Mehtwenty[1, 3]*
Mehtwenty[2, 1]+Mehtwenty[1, 1]*Mehtwenty[2, 3], Mehtwenty[1, 2]*
Mehtwenty[2, 1]+Mehtwenty[1, 1]*Mehtwenty[2, 2]]])):

Mcomb1tilde := simplify(Matrix([[Mcomb1[1, 1]^2, Mcomb1[1, 2]^2,
Mcomb1[1, 3]^2, sqrt(2)*Mcomb1[1, 2]*Mcomb1[1, 3], sqrt(2)*
Mcomb1[1, 1]*Mcomb1[1, 3], sqrt(2)*Mcomb1[1, 1]*Mcomb1[1, 2]],
[Mcomb1[2, 1]^2, Mcomb1[2, 2]^2, Mcomb1[2, 3]^2, sqrt(2)*
Mcomb1[2, 2]*Mcomb1[2, 3], sqrt(2)*Mcomb1[2, 1]*Mcomb1[2, 3],
sqrt(2)*Mcomb1[2, 1]*Mcomb1[2, 2]], [Mcomb1[3, 1]^2,
Mcomb1[3, 2]^2, Mcomb1[3, 3]^2, sqrt(2)*Mcomb1[3, 2]*Mcomb1[3, 3],
sqrt(2)*Mcomb1[3, 1]*Mcomb1[3, 3], sqrt(2)*Mcomb1[3, 1]*Mcomb1[3, 2]],
[sqrt(2)*Mcomb1[2, 1]*Mcomb1[3, 1], sqrt(2)*Mcomb1[2, 2]*Mcomb1[3, 2],
sqrt(2)*Mcomb1[2, 3]*Mcomb1[3, 3], Mcomb1[2, 3]*Mcomb1[3, 2]+
Mcomb1[2, 2]*Mcomb1[3, 3], Mcomb1[2, 3]*Mcomb1[3, 1]+Mcomb1[2, 1]*
Mcomb1[3, 3], Mcomb1[2, 2]*Mcomb1[3, 1]+Mcomb1[2, 1]*Mcomb1[3, 2]],
[sqrt(2)*Mcomb1[1, 1]*Mcomb1[3, 1], sqrt(2)*Mcomb1[1, 2]*Mcomb1[3, 2],
sqrt(2)*Mcomb1[1, 3]*Mcomb1[3, 3], Mcomb1[1, 3]*Mcomb1[3, 2]+
Mcomb1[1, 2]*Mcomb1[3, 3], Mcomb1[1, 3]*Mcomb1[3, 1]+Mcomb1[1, 1]*
Mcomb1[3, 3], Mcomb1[1, 2]*Mcomb1[3, 1]+Mcomb1[1, 1]*Mcomb1[3, 2]],
[sqrt(2)*Mcomb1[1, 1]*Mcomb1[2, 1], sqrt(2)*Mcomb1[1, 2]*Mcomb1[2, 2],
sqrt(2)*Mcomb1[1, 3]*Mcomb1[2, 3], Mcomb1[1, 3]*Mcomb1[2, 2]+
Mcomb1[1, 2]*Mcomb1[2, 3], Mcomb1[1, 3]*Mcomb1[2, 1]+Mcomb1[1, 1]
*Mcomb1[2, 3], Mcomb1[1, 2]*Mcomb1[2, 1]+Mcomb1[1, 1]*Mcomb1[2, 2]]]));

Mcomb2tilde := simplify(Matrix([[Mcomb2[1, 1]^2, Mcomb2[1, 2]^2,
Mcomb2[1, 3]^2, sqrt(2)*Mcomb2[1, 2]*Mcomb2[1, 3],
sqrt(2)*Mcomb2[1, 1]*Mcomb2[1, 3], sqrt(2)*Mcomb2[1, 1]*
Mcomb2[1, 2]], [Mcomb2[2, 1]^2, Mcomb2[2, 2]^2, Mcomb2[2, 3]^2,
sqrt(2)*Mcomb2[2, 2]*Mcomb2[2, 3], sqrt(2)*Mcomb2[2, 1]*
Mcomb2[2, 3], sqrt(2)*Mcomb2[2, 1]*Mcomb2[2, 2]], [Mcomb2[3, 1]^2,
Mcomb2[3, 2]^2, Mcomb2[3, 3]^2, sqrt(2)*Mcomb2[3, 2]*Mcomb2[3, 3],
```

```
sqrt(2)*Mcomb2[3, 1]*Mcomb2[3, 3], sqrt(2)*Mcomb2[3, 1]*Mcomb2[3, 2]],
[sqrt(2)*Mcomb2[2, 1]*Mcomb2[3, 1], sqrt(2)*Mcomb2[2, 2]*Mcomb2[3, 2],
sqrt(2)*Mcomb2[2, 3]*Mcomb2[3, 3], Mcomb2[2, 3]*Mcomb2[3, 2]+
Mcomb2[2, 2]*Mcomb2[3, 3], Mcomb2[2, 3]*Mcomb2[3, 1]+
Mcomb2[2, 1]*Mcomb2[3, 3], Mcomb2[2, 2]*Mcomb2[3, 1]+
Mcomb2[2, 1]*Mcomb2[3, 2]], [sqrt(2)*Mcomb2[1, 1]*Mcomb2[3, 1],
sqrt(2)*Mcomb2[1, 2]*Mcomb2[3, 2], sqrt(2)*Mcomb2[1, 3]*Mcomb2[3, 3],
Mcomb2[1, 3]*Mcomb2[3, 2]+Mcomb2[1, 2]*Mcomb2[3, 3],
Mcomb2[1, 3]*Mcomb2[3, 1]+Mcomb2[1, 1]*Mcomb2[3, 3],
Mcomb2[1, 2]*Mcomb2[3, 1]+Mcomb2[1, 1]*Mcomb2[3, 2]],
[sqrt(2)*Mcomb2[1, 1]*Mcomb2[2, 1], sqrt(2)*Mcomb2[1, 2]*
Mcomb2[2, 2], sqrt(2)*Mcomb2[1, 3]*Mcomb2[2, 3], Mcomb2[1, 3]*
Mcomb2[2, 2]+Mcomb2[1, 2]*Mcomb2[2, 3], Mcomb2[1, 3]*
Mcomb2[2, 1]+Mcomb2[1, 1]*Mcomb2[2, 3], Mcomb2[1, 2]*Mcomb2[2, 1]
+Mcomb2[1, 1]*Mcomb2[2, 2]]]));
```

Evaluating the closest trigonal elasticity tensor in the rotated coordinate system:

```
Ctrigor := evalf(1/6*(R+Transpose(Me1tilde).R.Me1tilde)+
Transpose(Mesixtytilde.R.Mesixtytilde)+Transpose(Mehtwentytilde.R.Mehtwentytilde)+
Transpose(Mcomb1tilde.R.Mcomb1tilde)+Transpose(Mcomb2tilde.R.Mcomb2tilde)))
```

Evaluating the norm of $Ctetrar$ and C to calculate distance to triginal.

```
NCtrigor  := Norm(Ctrigor , Frobenius)^2;
Nc := Norm(C, Frobenius)^2;
```

Evaluating the trigonal-distance function, namely $d(Atilde^T C Atilde, \mathcal{L}^{trigo})$. Note that this function cannot be plotted because it is a 4-dimensional function.

```
Delta-trigo := evalf(Nc-NCtrigor ):
```

In order to find a local minima ,which may be observed from the plot of the monoclinic distance function, around some neighborhood, one should use the line:

```
Mindata := Minimize(Delta-trigo, phi = 30*(1/180)*Pi .. 50*(1/180)*Pi,
psi = (1/180)*(90-44)*Pi .. (1/180)*(90-24)*Pi);
```

Sum of monoclinic-distance functions along the normals of the mirror planes of the trigonal symmetry

```
restart;
with(LinearAlgebra);
with(Optimization);
```

The rotation matrix that transforms $\mathbf{e_3}$ to the new z-axis.

```
AEuler := Matrix([[cos(psi), -sin(psi), 0], [sin(psi), cos(psi), 0], [0, 0, 1]]).
Matrix([[1, 0, 0], [0, cos(phi), -sin(phi)], [0, sin(phi), cos(phi)]]));
```

Since the orientations of x-axis and y-axis matter when calculating the distance of C to orthotropic symmetry in some coordinate system, we should multiply AEuler with another elementary transformation. This elementary transformation determines the orientations of x-axis and y-axis.

```
Rot := Matrix([[cos(theta), -sin(theta), 0], [sin(theta), cos(theta), 0], [0, 0, 1]]);
A := AEuler.Rot.;
```

Expressing $A \in SO(3)$ in 6D since it is going to act on the elasticity tensor.

```
Atilde := simplify(Matrix([[A[1, 1]^2, A[1, 2]^2, A[1, 3]^2, sqrt(2)*A[1, 2]*A[1, 3],
sqrt(2)*A[1, 1]*A[1, 3], sqrt(2)*A[1, 1]*A[1, 2]], [A[2, 1]^2, A[2, 2]^2, A[2, 3]^2,
sqrt(2)*A[2, 2]*A[2, 3], sqrt(2)*A[2, 1]*A[2, 3], sqrt(2)*A[2, 1]*A[2, 2]],
[A[3, 1]^2, A[3, 2]^2, A[3, 3]^2, sqrt(2)*A[3, 2]*A[3, 3], sqrt(2)*A[3, 1]
*A[3, 3], sqrt(2)*A[3, 1]*A[3, 2]], [sqrt(2)*A[2, 1]*A[3, 1], sqrt(2)*A[2, 2]*A[3, 2],
sqrt(2)*A[2, 3]*A[3, 3], A[2, 3]*A[3, 2]+A[2, 2]*A[3, 3], A[2, 3]*A[3, 1]+
A[2, 1]*A[3, 3], A[2, 2]*A[3, 1]+A[2, 1]*A[3, 2]], [sqrt(2)*A[1, 1]*A[3, 1],
sqrt(2)*A[1, 2]*A[3, 2], sqrt(2)*A[1, 3]*A[3, 3], A[1, 3]*A[3, 2]+A[1, 2]*A[3, 3],
A[1, 3]*A[3, 1]+A[1, 1]*A[3, 3], A[1, 2]*A[3, 1]+A[1, 1]*A[3, 2]],
[sqrt(2)*A[1, 1]*A[2, 1], sqrt(2)*A[1, 2]*A[2, 2], sqrt(2)*A[1, 3]*A[2, 3],
A[1, 3]*A[2, 2]+A[1, 2]*A[2, 3], A[1, 3]*A[2, 1]+A[1, 1]*A[2, 3], A[1, 2]*A[2, 1]+
A[1, 1]*A[2, 2]]])):
```

Introducing the elasticity matrix C in its general form.

```
C := Matrix(6, symbol = c, shape = symmetric);
```

This line is for changing the Voigt notation to Kelvin or vice versa. Herein, since we represent it in Kelvin notation, we do not change anything.

```
C[1 .. 3, 4 .. 6] := C[1 .. 3, 4 .. 6];
C[4 .. 6, 4 .. 6] := C[4 .. 6, 4 .. 6];
```

Introducing the parameters of elasticity matrix.

```
c := Matrix(6, 6, {(1, 1) = 42.03357978, (1, 2) = 32.49305220,
(1, 3) = 26.42291512, (1, 4) = 5.799531000, (1, 5) = 9.938160420,
(1, 6) = 21.33549018, (2, 1) = 32.49305219, (2, 2) = 36.72218489,
(2, 3) = 34.84774953, (2, 4) = -5.221667422, (2, 5) = -35.36967653,
(2, 6) = -23.60019509, (3, 1) = 26.42291511, (3, 2) = 34.84774954,
(3, 3) = 31.71680164, (3, 4) = 12.16688779, (3, 5) = 3.767088965,
(3, 6) = 10.24209672, (4, 1) = 5.799531000, (4, 2) = -5.221667442,
(4, 3) = 12.16688780, (4, 4) = 32.84181099, (4, 5) = 20.98631307,
(4, 6) = 2.36291613, (5, 1) = 9.938160440, (5, 2) = -35.36967653,
(5, 3) = 3.767088965, (5, 4) = 20.98631308, (5, 5) = -22.64105584,
(5, 6) = -9.709913499, (6, 1) = 21.33549018, (6, 2) = -23.60019510,
(6, 3) = 10.24209672, (6, 4) = 2.36291613, (6, 5) = -9.709913499,
(6, 6) = 11.32667859});
```

Expressing the elasticity matrix C in all coordinate systems by rotating it with a generic orthogonal transformation that is introduced in the above lines.

```
R := evalf(Transpose(Atilde).C.Atilde);
```

This line evaluates the distance of C to monoclinic along the z-axis of the rotated C:

```
Dist := evalf(2*(R[1, 4]^2+R[1, 5]^2+R[2, 4]^2+R[2, 5]^2+R[3, 4]^2+R[3, 5]^2
+R[4, 6]^2+R[5, 6]^2)):
```

In order to rotate the z-axis of C to the x-axis, we introduce 90° rotation:

```
ninetyx := Matrix([[0, 0, 1], [0, 1, 0], [-1, 0, 0]]);
Ax := A.ninetyx;
```

Expressing the above orthogonal transformation in 6D so that it acts the elasticity tensor

```
Atildex := simplify(Matrix([[Ax[1, 1]^2, Ax[1, 2]^2, Ax[1, 3]^2, sqrt(2)*
Ax[1, 2]*Ax[1, 3], sqrt(2)*Ax[1, 1]*Ax[1, 3], sqrt(2)*Ax[1, 1]*Ax[1, 2]],
[Ax[2, 1]^2, Ax[2, 2]^2, Ax[2, 3]^2, sqrt(2)*Ax[2, 2]*Ax[2, 3], sqrt(2)*
Ax[2, 1]*Ax[2, 3], sqrt(2)*Ax[2, 1]*Ax[2, 2]], [Ax[3, 1]^2, Ax[3, 2]^2,
Ax[3, 3]^2, sqrt(2)*Ax[3, 2]*Ax[3, 3], sqrt(2)*Ax[3, 1]*Ax[3, 3], sqrt(2)*
Ax[3, 1]*Ax[3, 2]], [sqrt(2)*Ax[2, 1]*Ax[3, 1], sqrt(2)*Ax[2, 2]*Ax[3, 2],
sqrt(2)*Ax[2, 3]*Ax[3, 3], Ax[2, 3]*Ax[3, 2]+Ax[2, 2]*Ax[3, 3], Ax[2, 3]*
Ax[3, 1]+Ax[2, 1]*Ax[3, 3], Ax[2, 2]*Ax[3, 1]+Ax[2, 1]*Ax[3, 2]],
[sqrt(2)*Ax[1, 1]*Ax[3, 1], sqrt(2)*Ax[1, 2]*Ax[3, 2], sqrt(2)*Ax[1, 3]*Ax[3, 3],
Ax[1, 3]*Ax[3, 2]+Ax[1, 2]*Ax[3, 3], Ax[1, 3]*Ax[3, 1]+Ax[1, 1]*Ax[3, 3],
Ax[1, 2]*Ax[3, 1]+Ax[1, 1]*Ax[3, 2]], [sqrt(2)*Ax[1, 1]*Ax[2, 1],
sqrt(2)*Ax[1, 2]*Ax[2, 2], sqrt(2)*Ax[1, 3]*Ax[2, 3], Ax[1, 3]*Ax[2, 2]+
Ax[1, 2]*Ax[2, 3], Ax[1, 3]*Ax[2, 1]+Ax[1, 1]*Ax[2, 3], Ax[1, 2]*Ax[2, 1]+
Ax[1, 1]*Ax[2, 2]]])):
```

Atildex acts the elasticity matrix in order to express it in a coordinate system where its new z-axis is the x-axis.

```
Rx := evalf(Transpose(Atildex).C.Atildex);
```

This line evaluates the distance of C to monoclinic along the x-axis of the rotated C:

```
Distx := evalf(2*(Rx[1, 4]^2+Rx[1, 5]^2+Rx[2, 4]^2+Rx[2, 5]^2+
Rx[3, 4]^2+Rx[3, 5]^2+Rx[4, 6]^2+Rx[5, 6]^2)):
```

We repeat the same procedure for the directions which are the normals of a mirror plane of a trigonal medium :

```
sixty := Matrix([[3/4, -(1/4)*sqrt(3), 1/2], [-(1/4)*sqrt(3), 1/4, (1/2)*sqrt(3)],
[-1/2, -(1/2)*sqrt(3), 0]]);
Asixty := A.sixty;
```

```
Atildesixty := simplify(Matrix([[Asixty[1, 1]^2, Asixty[1, 2]^2,
Asixty[1, 3]^2, sqrt(2)*Asixty[1, 2]*Asixty[1, 3], sqrt(2)*Asixty[1, 1]*
Asixty[1, 3], sqrt(2)*Asixty[1, 1]*Asixty[1, 2]], [Asixty[2, 1]^2,
Asixty[2, 2]^2, Asixty[2, 3]^2, sqrt(2)*Asixty[2, 2]*Asixty[2, 3],
sqrt(2)*Asixty[2, 1]*Asixty[2, 3], sqrt(2)*Asixty[2, 1]*Asixty[2, 2]],
[Asixty[3, 1]^2, Asixty[3, 2]^2, Asixty[3, 3]^2, sqrt(2)*Asixty[3, 2]*
Asixty[3, 3], sqrt(2)*Asixty[3, 1]*Asixty[3, 3], sqrt(2)*Asixty[3, 1]*
Asixty[3, 2]], [sqrt(2)*Asixty[2, 1]*Asixty[3, 1], sqrt(2)*Asixty[2, 2]*
Asixty[3, 2], sqrt(2)*Asixty[2, 3]*Asixty[3, 3], Asixty[2, 3]*Asixty[3, 2]+
Asixty[2, 2]*Asixty[3, 3], Asixty[2, 3]*Asixty[3, 1]+Asixty[2, 1]*Asixty[3, 3],
Asixty[2, 2]*Asixty[3, 1]+Asixty[2, 1]*Asixty[3, 2]], [sqrt(2)*Asixty[1, 1]*
Asixty[3, 1], sqrt(2)*Asixty[1, 2]*Asixty[3, 2], sqrt(2)*Asixty[1, 3]*Asixty[3, 3],
Asixty[1, 3]*Asixty[3, 2]+Asixty[1, 2]*Asixty[3, 3], Asixty[1, 3]*Asixty[3, 1]+
Asixty[1, 1]*Asixty[3, 3], Asixty[1, 2]*Asixty[3, 1]+Asixty[1, 1]*Asixty[3, 2]],
[sqrt(2)*Asixty[1, 1]*Asixty[2, 1], sqrt(2)*Asixty[1, 2]*Asixty[2, 2], sqrt(2)*
Asixty[1, 3]*Asixty[2, 3], Asixty[1, 3]*Asixty[2, 2]+Asixty[1, 2]*Asixty[2, 3],
Asixty[1, 3]*Asixty[2, 1]+Asixty[1, 1]*Asixty[2, 3], Asixty[1, 2]*Asixty[2, 1]+
Asixty[1, 1]*Asixty[2, 2]]])):

Rsixty := evalf(Transpose(Atildesixty.C.Atildesixty));

Distsixty := evalf(2*(Rsixty[1, 4]^2+Rsixty[1, 5]^2+Rsixty[2, 4]^2
+Rsixty[2, 5]^2+Rsixty[3, 4]^2+Rsixty[3, 5]^2+Rsixty[4, 6]^2+
Rsixty[5, 6]^2)):

htwenty := Matrix([[3/4, (1/4)*sqrt(3), -1/2], [(1/4)*sqrt(3), 1/4, (1/2)*sqrt(3)],
 [1/2, -(1/2)*sqrt(3), 0]]);
Ahtwenty := A.htwenty;

Atildehtwenty := simplify(Matrix([[Ahtwenty[1, 1]^2, Ahtwenty[1, 2]^2,
Ahtwenty[1, 3]^2, sqrt(2)*Ahtwenty[1, 2]*Ahtwenty[1, 3],
sqrt(2)*Ahtwenty[1, 1]*Ahtwenty[1, 3], sqrt(2)*Ahtwenty[1, 1]*
Ahtwenty[1, 2]], [Ahtwenty[2, 1]^2, Ahtwenty[2, 2]^2, Ahtwenty[2, 3]^2,
sqrt(2)*Ahtwenty[2, 2]*Ahtwenty[2, 3], sqrt(2)*Ahtwenty[2, 1]*
```

```
Ahtwenty[2, 3], sqrt(2)*Ahtwenty[2, 1]*Ahtwenty[2, 2]], [Ahtwenty[3, 1]^2,
Ahtwenty[3, 2]^2, Ahtwenty[3, 3]^2, sqrt(2)*Ahtwenty[3, 2]*
Ahtwenty[3, 3], sqrt(2)*Ahtwenty[3, 1]*Ahtwenty[3, 3], sqrt(2)*Ahtwenty[3, 1]*
Ahtwenty[3, 2]], [sqrt(2)*Ahtwenty[2, 1]*Ahtwenty[3, 1], sqrt(2)*
Ahtwenty[2, 2]*Ahtwenty[3, 2], sqrt(2)*Ahtwenty[2, 3]*Ahtwenty[3, 3],
Ahtwenty[2, 3]*Ahtwenty[3, 2]+Ahtwenty[2, 2]*Ahtwenty[3, 3],
Ahtwenty[2, 3]*Ahtwenty[3, 1]+Ahtwenty[2, 1]*Ahtwenty[3, 3],
Ahtwenty[2, 2]*Ahtwenty[3, 1]+Ahtwenty[2, 1]*Ahtwenty[3, 2]],
[sqrt(2)*Ahtwenty[1, 1]*Ahtwenty[3, 1], sqrt(2)*Ahtwenty[1, 2]*
Ahtwenty[3, 2], sqrt(2)*Ahtwenty[1, 3]*Ahtwenty[3, 3], Ahtwenty[1, 3]*
Ahtwenty[3, 2]+Ahtwenty[1, 2]*Ahtwenty[3, 3], Ahtwenty[1, 3]*
Ahtwenty[3, 1]+Ahtwenty[1, 1]*Ahtwenty[3, 3], Ahtwenty[1, 2]*
Ahtwenty[3, 1]+Ahtwenty[1, 1]*Ahtwenty[3, 2]], [sqrt(2)*Ahtwenty[1, 1]*
Ahtwenty[2, 1], sqrt(2)*Ahtwenty[1, 2]*Ahtwenty[2, 2], sqrt(2)*
Ahtwenty[1, 3]*Ahtwenty[2, 3], Ahtwenty[1, 3]*Ahtwenty[2, 2]+
Ahtwenty[1, 2]*Ahtwenty[2, 3], Ahtwenty[1, 3]*Ahtwenty[2, 1]+
Ahtwenty[1, 1]*Ahtwenty[2, 3], Ahtwenty[1, 2]*Ahtwenty[2, 1]+
Ahtwenty[1, 1]*Ahtwenty[2, 2]]]):


Rhtwenty := evalf(Transpose(Atildehtwenty.C.Atildehtwenty));

Disthtwenty := evalf(2*(Rhtwenty[1, 4]^2+Rhtwenty[1, 5]^2+
Rhtwenty[2, 4]^2+Rhtwenty[2, 5]^2+Rhtwenty[3, 4]^2+Rhtwenty[3, 5]^2
+Rhtwenty[4, 6]^2+Rhtwenty[5, 6]^2)):
```

Evaluating the sum of monoclinic-distance functions along the normals of mirror planes of tetragonal symmetry:

```
Distall :=Distx+Distsixty+Disthtwenty:
```

For minimizing the Distall function around some restricted region

```
Mindata := Minimize(Distall, phi= 0. .. 10*(1/180)*Pi,
psi = (1/2)*Pi .. 2*Pi+(1/2)*Pi, theta = 0 .. 2*Pi):
```

Finding the velocities of P- and S-waves in the mirror plane of a monoclinic elasticity tensor

```
restart:
with(LinearAlgebra):
with(Student[LinearAlgebra]):
```

The direction of the wave vector

```
n := proc (theta, phi):
Matrix([[cos((1/180)*Pi*theta)*sin((1/180)*Pi*phi), 0, 0], [sin((1/180)*Pi*theta)
*sin((1/180)*Pi*phi), 0, 0], [cos((1/180)*Pi*phi), 0, 0], [0, cos((1/180)*Pi*theta)
*sin((1/180)*Pi*phi), 0], [0, sin((1/180)*Pi*theta)*sin((1/180)*Pi*phi), 0],
[0, cos((1/180)*Pi*phi), 0], [0, 0, cos((1/180)*Pi*theta)*sin((1/180)*Pi*phi)],
[0, 0, sin((1/180)*Pi*theta)*sin((1/180)*Pi*phi)], [0, 0, cos((1/180)*Pi*phi)]]):
end proc:
```

Introducing the elasticity matrix C in its general form.

```
C := Matrix(6, symbol = c, shape = symmetric);
```

This line is for changing the Voigt notation to Kelvin or vice versa. Since in the formulation of the Christofell matrix Voigt notation is used, we change the Kelvin notation to Voigt

```
C[1 .. 3, 4 .. 6] := C[1 .. 3, 4 .. 6]/sqrt{2};
C[4 .. 6, 4 .. 6] :=  C[4 .. 6, 4 .. 6]/2;
```

Introducing the parameters of a monoclinic elasticity matrix expressed in Equation 4.9. Note that the below matrix is expressed in the natural coordinate system of monoclinic symmetry. Thus, its parameters are not equal to the parameters of the tensor expressed in Equation 4.9. However, the tensors are the same.

```
c := Matrix(6, 6, {(1, 1) = 91.50, (1, 2) = 23.88,
(1, 3) = 32.88, (1, 4) = 0, (1, 5) = 0,
(1, 6) = -5.10, (2, 1) = 23.88, (2, 2) = 69.72,
(2, 3) = 26.91, (2, 4) = 0, (2, 5) = 0,
```

```
(2, 6) = -6.59, (3, 1) = 32.88, (3, 2) = 26.91,
(3, 3) = 107.27, (3, 4) = 0, (3, 5) = 0,
(3, 6) = -3.04, (4, 1) = 0, (4, 2) = 0,
(4, 3) = 0, (4, 4) = 46.65, (4, 5) = -3.06,
(4, 6) = 0, (5, 1) = 0, (5, 2) = 0,
(5, 3) = 0, (5, 4) = -3.06, (5, 5) = 65.16,
(5, 6) = 0, (6, 1) = -5.10, (6, 2) = -6.59,
(6, 3) = -3.04, (6, 4) = 0, (6, 5) = 0,
(6, 6) = 42.81});
```

Introducing the Christofell matrix

```
with(linalg);
M := Matrix(1 .. 9, 1 .. 9, shape = symmetric);
M[1, 1] := C[1, 1]; M[2, 2] := C[6, 6]:
M[3, 3] := C[5, 5]; M[4, 4] := C[6, 6]; M[5, 5] := C[2, 2];
M[6, 6] := C[4, 4]; M[7, 7] := C[5, 5]; M[8, 8] := C[4, 4];
M[9, 9] := C[3, 3]; M[1, 2] := C[1, 6]; M[1, 3] := C[1, 5];
M[1, 4] := C[1, 6]; M[1, 5] := C[1, 2]; M[1, 6] := C[1, 4];
M[1, 7] := C[1, 5]; M[1, 8] := C[1, 4]; M[1, 9] := C[1, 3]:
M[2, 3] := C[5, 6]; M[2, 4] := C[6, 6]; M[2, 5] := C[2, 6];
M[2, 6] := C[4, 6]; M[2, 7] := C[5, 6]; M[2, 8] := C[4, 6];
M[2, 9] := C[3, 6]; M[3, 4] := C[5, 6]; M[3, 5] := C[2, 5];
M[3, 6] := C[4, 5]; M[3, 7] := C[5, 5]; M[3, 8] := C[4, 5];
M[3, 9] := C[3, 5]; M[4, 5] := C[2, 6]; M[4, 6] := C[4, 6];
M[4, 7] := C[5, 6]; M[4, 8] := C[4, 6]; M[4, 9] := C[3, 6];
M[5, 6] := C[2, 4]; M[5, 7] := C[2, 5]; M[5, 8] := C[2, 4];
M[5, 9] := C[2, 3]; M[6, 7] := C[4, 5]; M[6, 8] := C[4, 4];
M[6, 9] := C[3, 4]; M[7, 8] := C[4, 5]; M[7, 9] := C[3, 5];
M[8, 9] := C[3, 4]:

ch := proc (theta, phi):
evalf(Matrix(MatrixMatrixMultiply(MatrixMatrixMultiply
(Transpose(n(theta, phi)), M), n(theta, phi))))
```

```
end proc:
```

Evaluating the eigenvectors and eigenvalues of the Christofell matrix to find the velocities and polarizations of the P- and S-waves propagating along the direction **n**

```
Evect := proc (theta, phi);
evalf(Eigenvectors(ch(theta, phi), output = 'list'))
end proc:

Digits := 7; phi := 90;
for theta from 0 by 2 to 180 do;
print(theta, phi);
print(ch(theta, phi));
print(Evect(theta, phi));
end do:
```

Bibliography

Bibliography

[1] V. Arsigny, P. Fillard, X. Pennec, and N. Ayache. Fast and simple calculus on tensors in the Log-Euclidean framework. In J. Duncan and G. Gerig, editors, Proc. 8th Int. Conf. on Medical Image Computing and Computer-Assisted Intervention - MICCAI 2005, Part I, **3749** of LNCS, pages 115-122, Palm Springs, CA, 2005. Springer Verlag.

[2] Arts, R. J., Helbig, K., Rasolofosaon, N.J.P., General anisotropic elastic tensor in rocks- approximation, invariants, and particular direction. 61st SEG meeting in Houston, Expanded abstracts, ST 2.4 (1991)

[3] Babushka V. and Caro M., 1992, Seismic anisotropy in the Earth, Modern Approaches to Geophysics. 10, Kluwer Acad. Publ.,Dordrecht.

[4] Backus, G.: A geometrical picture of anisotropic elastic tensors. Rev. Geophys. Space Phys. **8(3)**, 633-671 (1970)

[5] Baerheim, R.: Coordinate free representation of the hierarchically symmetric tensor of rank 4 in determination of symmetry. Ph.D. thesis. Geologica Ultraiectina, **159** (1998)

[6] Boehler, J.P., Kirilov Jr., A.A., Onat, E.T.: On the polynomial invariants of elasticity tensor. J. Elast. **34**, 97-110 (1994)

[7] Bóna A., Bucataru I., Slawinski, M.A: Material symmetries versus wavefront symmetries. The Quarterly Journal of Mechanics and Applied Mathematics 2007, **60** (2), pp. 73-84.

[8] Bóna A., Bucataru I., Slawinski, M.A: Coordinate-Free Characterization of the Symmetry Classes of Elasticity Tensors. Journal of Elasticity **87**, 109-132 (2007).

[9] Bóna A., Bucataru I., Slawinski, M.A: Material Symmetries of Elasticity Tensor. Q. J. Mech. Appl. Math. **54**(4) 584-598 (2004).

[10] J. T. Browaeys and S. Chevrot. Decomposition of the elastic tensor and geophysical applications. Geophys. J. Int., **159**:667-678, 2004.

[11] M. S. T. Bukowinski, Annu. Rev. Earth Planet. Sci., 1994, **22**: 167-205

[12] Chadwick, P., Vianello, M., Cowin, S.C. : A New Proof that the Number of Linear Elastic Symmetries is Eight. J. Mech. Phys. Solids **49**, 2471-2492 (2001).

[13] Cowin, S.C., Mehrabadi, M.M: On the identification of material symmetry for anisotropic elastic materials. Q.J. Mech. Appl. Math. **40**, 451-476 (1987)

[14] Cowin, S.C., Properties of the anisotropic elasticity tensor. Quarterly Journal of Mechanics and Applied Mathematics **42(2)** 1989, 249-266.

[15] Cowin, S.C., Mehrabadi, M.M.: The structure of the linear anisotropic elastic symmetries. J. Mech. Phys. Solids **40(7)**, 1459-1471 (1992)

[16] Crampin, S., Effective anisotropic elastic constants for wave propagation through cracked solids, Geophys. J. R. Astr. Soc., 1984, **76**, 135-145

[17] Dellinger, J., Computing the optimal transversely isotropic approximation of a general elastic tensor. Geophysics **70(5)** 2005, 1-10.

[18] Dewangan, P., Grechka, V., Inversion of multicomponent, multiazimuth, walkaway VSP data for the stiffness tensor, Geophysics. **68**, No. 3 2003, 1022-1031

[19] F. I. Fedorov. Theory of Elastic Waves in Crystals. Plenum Press, New York, 1968.

[20] Forte, S., Vianello, M.: Symmetry Classes for Elasticity Tensors. Journal of Elasticity **43(2)**, 81-108 (1996).

[21] Forte, S., Vianello, M.: Symmetry classes and harmonic decomposition for photoelasticity tensors. Int. J. Eng. Sci. **35(14)**, 1317-1326 (1997)

[22] A. F. Gangi. Fourth-order elastic-moduli tensors by inspection. In L. Ikelle and A. F. Gangi, editors, Anisotropy 2000: Fractures, converted waves and case studies. Proc. 9th International Workshop on Seismic Anisotropy (9IWSA), pages 1-10, Tulsa, OK, 2000. Society of Exploration Geophysicists.

[23] Gazis, D.C., Tadjbakhsh, I., Toupin, R.A., The elastic tensor of given symmetry nearest to an anisotropic elastic tensor. Acta Crystal logr. **16**(1963), 917-922

[24] Green, D.J.: An introduction to the mechanical properties of ceramics. Cambridge University Press, Cambridge, UK (1998)

[25] Helbig, K.: The Structure of the Elastic Tensor. Research Report Magma (2005)

[26] Helbig, K.: Foundations of Anisotropy for Exploration Seismics. Pergamon, New York (1994)

[27] K. Helbig. Representation and approximation of elastic tensors. In Sixth International Workshop on Seismic Anisotropy (Trondheim, 1994), ExpandedAbstracts, pages 37-75, 1995.

[28] Herman, B.: Some theorems of the theory of anisotropic media. Comptes rendues (Doklady) delAcadmie des Sciences dc l-URSS. **48(2)**, 89-92 (1945)

[29] Hudson, J., A., Wave speeds and attenuation of elastic waves in material containing cracks, Geophys. J. R. Astr. Soc., 1981, **64**, 133-150

[30] Hudson, J., A., Overall properties of a cracked solid, Math. Proc. Camb. Phil. Soc., 1982, **88**, 371-384

[31] Huo, Y.Z., Del Piero, G.: On the completeness of the crystallographic symmetries in the description of the symmetries of the elasticity tensor. J. Elasticity **25**(1991)203-246.

[32] Kochetov, M., Slawinski, M.A., On obtaining effective transversely isotropic elastcity tensors. J. Elast. **94** (2009) 130..

[33] Kochetov, M., Slawinski, M.A., On obtaining effective orthotropic elasticity tensors. Q. Jl Mech. Appl. Math, **62**. No. 2.

[34] Lord Kelvin (Thompson, W.): On six principal strains of an elastic solid. Phil. Trans. R. Soc. **166**, 495-498 (1856)

[35] Love, A.E.H.: A Treatise on the Mathematical Theory of Elasticity. Cambridge University Press, Cambridge, UK (1927)

[36] Mehrabadi, M.M., Cowin, S.C.: Eigentensors of linear anisotropic elastic materials. Q. J. Mech. Appl. Math. **43(1)**, 15-41 (1990)

[37] Moakher, M., Norris, A.N., The closest elastic tensor of arbitrary symmetry to an elastic tensor of lower symmetry. Journal of Elasticity. **85(3)**(2006), 215-263.

[38] M. Moakher. On the averaging of symmetric positive-definite tensors. J. Elasticity **82**: 273-296 (2006).

[39] Newnham, R.E.: Properties of materials: Anisotropy, symmetry, structure. Oxford University Press, USA (2004)

[40] Norris, A. N. : Elastic moduli approximation of higher symmetry for the acoustical properties of an anisotropic material. J Acoust Soc Am. Apr; **119(4)**:2114-21(2006).

[41] Rychlewski, J.: On Hooke's law. Prikl. Mat. Meh. **48(3)**, 303-314 (1984)

[42] Rychlewski, J.: Unconventional approach to linear elasticity. Arch. Mech. **47(2)**, 149-171 (1995)

[43] Rychlewski, J.: A qualitative approach to Hookes tensors. Part I. Arch. Mech. **52(4,5)**, 737-759 (2000)

[44] Slawinski, M.A., Seismic waves and rays in elastic media, Elsevier, 2003.

[45] Sutcliffe, S.: Spectral decomposition of the elasticity tensor. J. Appl. Mech. **59**, 762-773 (1992)

[46] Ting, T. C T. Generalized Cowin-Mehrabadi theorems and a direct proof that the number of linear elastic symmetries is eight. Int. J. Sloids Structures **40**(2003) 7129-7142

[47] Voigt, W.: Lehrbuch der Kristalphysik. Teubner, Leipzig (1928)

[48] Walpole, L.J.: Fourth-rank tensors of the thirty-two crystal classes: multiplication tables. Proc. R. Soc. Lond. A **391**, 149-179 (1984)

[49] Yang, G., Kabel, J., Van Rietbergen, B., Odgaard, A., Huiskes, R., Cowin, S.C.: The anisotropic Hooke's law for cancellous bone and wood. J. Elast. **53**, 125-146 (1999)